COMMUNICATIONS
FROM THE
KONKOLY OBSERVATORY
OF THE
HUNGARIAN ACADEMY OF SCIENCES

MITTEILUNGEN
DER
STERNWARTE
DER UNGARISCHEN AKADEMIE
DER WISSENSCHAFTEN

No. 105

(Vol. 14, Part 1)

RRL2015

High-Precision Studies of RR Lyrae Stars

edited by: L. Szabados, R. Szabó, K. Kinemuchi

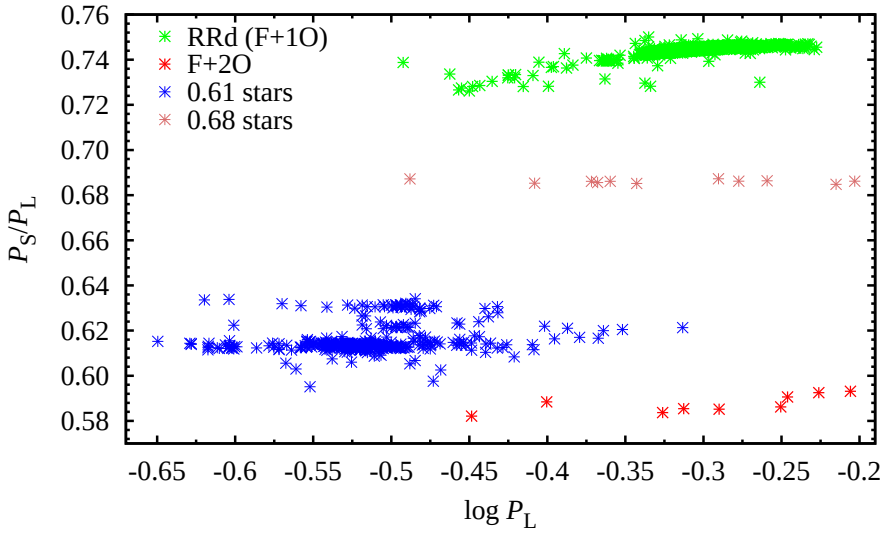

BUDAPEST, 2016

Cover picture: Figure 1 from the paper by Netzel et al.

ISBN 963-8361-56-1
HU ISSN 0238-2091
Felelős kiadó: Kiss L. László

In memoriam László Detre

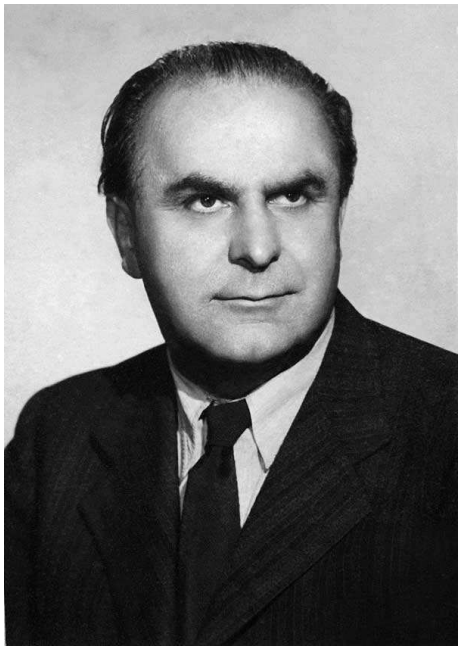

László Detre (1906–1975) was an internationally recognized astronomer, Director of the Konkoly Observatory from 1943 to 1975. He studied in Budapest and in Berlin, where he had famous professors, like Albert Einstein and Max Planck. He established modern astronomy in Hungary and initiated a number of observing projects related to variable stars including pulsating stars, photoelectric photometry and a successful supernova search survey. However, his main research field was RR Lyrae stars. He was trusted to launch the Information Bulletin on Variable Stars in 1961, following an International Astronomical Union decision, edited and published by the Konkoly Observatory ever since. László Detre served as the President of the IAU Commission 27 (Variable Stars) between 1967 and 1970. He established the Piszkés-tető Mountain Station in the Mátra hills, where two of the largest Hungarian telescopes were installed in his era and are still being used.

In memoriam Béla Szeidl

Béla Szeidl (1938–2013) was the Director of the Konkoly Observatory from 1975 to 1996. He had interest in diverse research fields, including RR Lyrae stars, high-amplitude δ Scuti stars, photographic, photoelectric, and later CCD-observations, globular cluster variables, binarity, and in particular the mysterious Blazhko effect. His life-long passion for mathematics led him to study the $O-C$ diagram of pulsating variable stars with the aim at detecting evolutionary effects. One of his most famous discoveries is the 4-year long cycle in the Blazhko-modulation of RR Lyrae, the prototype of its class. He served as the President of the IAU Commission 27 (Variable Stars) between 1985 and 1988.

In memoriam Jean-Robert Buchler

J. Robert Buchler (1942–2012) was a visionary theoretical astrophysicist. He started working on nuclear physics and supernovae, then he switched to pulsating stars. He was particularly interested in nonlinear dynamical phenomena, like resonances, mode selection and chaos. He initiated a long-term project to numerically model radial pulsation including turbulent convection. This work culminated in the success of the Florida-Budapest hydrocode. He authored nearly 250 papers, and supervised several postdocs. He loved teaching physics and worked at the University of Florida for almost four decades. Robert had an extremely broad range of interests including arts, music, acoustic paradoxes, and aviation. He was an avid admirer of beauties of the Nature and a connoisseur of good wines.

In memoriam Janusz Kałużny

Janusz Kałużny (1955–2015) was an accomplished Polish photometrist, one of the founding fathers of the highly successful OGLE survey, founder and leader of the CASE project whose goal was to determine accurate ages and distances of globular clusters based on observations of detached eclipsing binaries. Author of nearly 300 papers, and supervisor of eight PhD students. Recipient of the prestigious award "Mistrz" (Master) from the Foundation for Polish Science (2007). His most important scientific achievements were the resolution of a discrepancy between the cosmological age of the universe and the age of globular clusters, and the discovery of nonradial pulsations in RR Lyrae stars.

Contents

Part 2. Posters

Scientific Organizing Committee

Željko *Ivezić* (University of Washington, USA)
Johanna *Jurcsik* (MTA CSFK, Konkoly Observatory, Hungary)
László *Kiss* (MTA CSFK, Konkoly Observatory, Hungary)
Katrien *Kolenberg* (Harvard-Smithsonian Center for Astrophysics, USA; KU Leuven, Belgium)
Zoltán *Kolláth* (MTA CSFK, Konkoly Observatory, University of West Hungary)
Marcella *Marconi* (INAF-Osservatorio Astronomico di Capodimonte, Naples, Italy)
Paweł *Moskalik* (Copernicus Astronomical Center, Warsaw, Poland)
Marek *Skarka* (Masaryk University, Brno, Czech Republic)
Radosław *Smolec* (Copernicus Astronomical Center, Warsaw, Poland)
Róbert *Szabó*, chair (MTA CSFK, Konkoly Observatory, Hungary)

Local Organizing Committee

Evelin *Bányai* (MTA CSFK, Konkoly Observatory; Loránd Eötvös University)
József *Benkő* (MTA CSFK, Konkoly Observatory)
Zsófia *Bognár* (MTA CSFK, Konkoly Observatory)
Gergely *Dálya* (Loránd Eötvös University)
Aliz *Derekas* (Gothard Observatory, Szombathely; MTA CSFK, Konkoly Observatory)
Ottó *Hanyecz* (Loránd Eötvös University)
László *Molnár* (MTA CSFK, Konkoly Observatory)
Emese *Plachy* (MTA CSFK, Konkoly Observatory)
Ádám *Sódor* (MTA CSFK, Konkoly Observatory)
László *Szabados* (MTA CSFK, Konkoly Observatory)
Róbert *Szabó*, chair (MTA CSFK, Konkoly Observatory)


RRL 2015, Visegrád, Hungary

List of participants

Auer, F. Reinhold	Czech Republic
Balázs, Lajos G.	Hungary
Bányai, Evelin	Hungary
Barentsen, Geert	USA
Bellinger, Earl	Germany
Benkő, József M.	Hungary
Bódi, Attila	Hungary
Bognár, Zsófia	Hungary
Bono, Giuseppe	Italy
Britavskiy, Mikola	Greece
Clement, Christine M.	Canada
Clementini, Gisella	Italy
Csák, Balázs	Hungary
Csányi, István	Hungary
Cseh, Borbála	Hungary
Cusano, Felice	Italy
Dálya, Gergely	Hungary
Derekas, Aliz	Hungary
Deupree, Robert	Canada
Duffau, Sonia	Chile
Dziembowski, Wojciech A.	Poland
Feast, Michael	South Africa
Flewelling, Heather	USA
Guggenberger, Elisabeth	Germany
Hajdu, Gergely	Chile
Hanyecz, Ottó	Hungary
Hernitschek, Nina	Germany
Ivezić, Željko	USA
Jang, Sohee	Korea, South
Jeffery, Elizabeth	USA
Juhász, Áron L.	Hungary
Jurcsik, Johanna	Hungary
Jurković, Monika	Serbia
Kanbur, Shashi M.	USA
Kanev, Evgeny	Russia
Kinemuchi, Karen	USA
Kiss, László L.	Hungary
Kolenberg, Katrien	Belgium
Kolláth, Zoltán	Hungary
Kovács, Géza	Hungary
Liska, Jiři	Czech Republic
Lub, Jan	the Netherlands
Marconi, Marcella	Italy
Martínez-Vázquez, Clara E.	Spain

Medina, Gustavo	Chile
Molnár, László	Hungary
Monelli, Matteo	Spain
Moskalik, Pawel	Poland
Muñoz, Ricardo	Chile
Muthsam, Herbert	Austria
Navarrete, Camila	Chile
Neeley, Jill	USA
Netzel, Henryka	Poland
Ngeow, Chow-Choong	Taiwan
Nuspl, János	Hungary
Pietrukowicz, Pawel	Poland
Plachy, Emese	Hungary
Poretti, Ennio	Italy
Prudil, Zdeněk	Czech Republic
Sesar, Branimir	Germany
Skarka, Marek	Czech Republic
Smolec, Radoslaw	Poland
Sódor, Ádám	Hungary
Szabados, László	Hungary
Szabó, Róbert	Hungary
Udalski, Andrzej	Poland

RRL2015 – High-Precision Studies of RR Lyrae Stars
L. Szabados, R. Szabó, K. Kinemuchi (Eds.) 2016

Preface

Róbert Szabó
Konkoly Observatory, Research Centre for Astronomy and Earth Sciences, Hungarian Academy of Sciences, H-1121, Budapest, Konkoly Thege Miklós út 15-17, Hungary

RR Lyrae stars have been studied in the Konkoly Observatory for decades. Starting from the pioneering investigations of their period variations and the Blazhko effect initiated by László Detre and Béla Szeidl (both of them served as directors for decades) through the Jurcsik and Kovács relations between the light curve parameters and the physical properties of RR Lyrae stars, the Konkoly Blazhko survey led by Johanna Jurcsik, the theoretical studies, numerical modeling, and investigations of dynamical phenomena conducted by Géza Kovács and Zoltán Kolláth, and the accumulated expertise in space photometry of RR Lyrae stars in recent years – it is easy to see that many aspects of this topic have been covered. Therefore it was appropriate to organize a conference dedicated to these fascinating stars here, in Hungary.

The conference titled *High-precision studies of RR Lyrae stars: from dynamical phenomena to mapping the Galactic structure* was a pioneering event at a unique place. It was pioneering, because it was the first major conference dedicated to RR Lyrae stars in recent years. The venue was also special for historical reasons. The small city was once the capital of Hungary, and is famous for the Congress of Visegrád (in 1335) where the meeting of the Hungarian, the Bohemian, and the Polish kings took place. This alliance was renewed in 1991 at the same place, and the Visegrád Countries become an important factor in the European political scenery. The Knights' Tournament and the royal feast made us remember the historical aspects of the venue during the conference – I could not even avoid becoming the King of Visegrád for a while.

As the leaders of Central European kingdoms held an international conference in order to resolve international disputes, so did we, modern day astronomers, discussed interesting topics at a peaceful event. The idea was to bring experts from various fields, such as observers, pulsation theorists, galactic archeologists, experts conducting hydrodynamical modeling and large sky surveys, and have discussions representing the different points of view, while mutually benefiting from the synergies that present and future projects have to offer. We gathered people from different communities, who spoke the same language, and I think this was one of the most important aspects of this conference.

According to the very positive feedback from the community and the participants, the timing of the conference was perfect. These days we enjoy micromagnitude precision light curves from space missions. Our era heralds the advent of multi-dimensional hydrodynamical simulations of pulsation, publicly available light curves of tens of thousands of RR Lyrae stars from ground based surveys, and the discovery of the best candidates for RR Lyrae stars in binary systems.

We all heard about these during the conference, along with the ubiquitous periodicities with a 0.61–0.64 frequency ratio with the first radial overtone mode in seemingly all RRc and RRd stars investigated by space photometric missions. Also, we are eagerly waiting for data from *Gaia*, and also from LSST, to help us to more precisely calibrate the RR Lyrae distance scale and to investigate the structure and history of our Milky Way Galaxy.

I am very proud of the gender balance of the speakers, because we had an almost exactly 1:2 ratio. Male astronomers still gave the majority, but I hope that we are closing the gap and are starting to have a more healthy ratio. On behalf of the SOC, I can say that we tried hard to improve this balance.

I am grateful to the Scientific Organizing Committee and to all the participants for putting together an exciting and balanced program. We have seen exciting and interesting talks, I personally learned a lot and enjoyed every minute of the conference. Many useful conversations took place, and new collaborations arose from the discussions. I thank Katrien Kolenberg for her contribution. Her artworks contributed to the success of the event by lending a specific character to the conference. I'm personally indebted to Katrien to let us use her great works. Special thanks go to the Diamond Congress Ltd. for a smooth service, for perfectly taking care of all our needs, and for proactively troubleshooting any possible problems. I would also like to thank all my colleagues (the Local Organizing Committee) for their help and support. The Proceedings have been printed from the budget of the ESTEC Contract No. 4000106398/12/NL/KML.

The conference held between 19-22 October 2015 was a great chance to bring together the doyens of RR Lyrae research field and young researchers working on the same topic to interact, exchange thoughts, methods, and experiences. Seeing the success of the RRL2015 conference, it is evident that this event should and will be continued, next time again in a Visegrád country, namely in Poland. Thank you for coming to Visegrád and sharing your latest results.

Invited and contributed papers

RRL2015 – High-Precision Studies of RR Lyrae Stars
L. Szabados, R. Szabó, K. Kinemuchi (Eds.) 2016

RR Lyrae stars in the *Gaia* era

Gisella Clementini[1,2]

[1]*INAF-Osservatorio Astronomico di Bologna, via Ranzani 1, 40127, Bologna, Italy*

[2]*Coordination Unit 7, Gaia Data Processing and Analysis Consortium*

Abstract. *Gaia*, the European Space Agency spacecraft successfully launched on 19 December 2013, entered into nominal science operations on 18 July 2014 after a few months of commissioning, and has been scanning the sky to a faint limit of $G = 20.7$ mag since then. *Gaia* is expected to observe more than a hundred thousand RR Lyrae stars in the Galactic halo and bulge (most of which will be new discoveries), and to provide parallax measurements with about 10 μas uncertainty for those brighter than $\langle V \rangle$ ∼12-13 mag.

Status and activities of the spacecraft since launch are briefly reviewed with emphasis on preliminary results obtained for RR Lyrae stars observed in the Large Magellanic Cloud during the first 28 days of science operations spent in Ecliptic Pole scanning mode and in light of the first *Gaia* data release which is scheduled for summer 2016.

1. Introduction

Gaia is the ESA cornerstone astrometry mission building on the heritage of *Hipparcos* (Perryman 2009). It is an unbiased all-sky (∼40,000 deg^2) survey that will enable science with one billion sources by providing μas accuracy astrometry (parallaxes, positions and proper motions) and milli-mag optical spectrophotometry (luminosities and astrophysical parameters) for sources down to a limiting magnitude G[1] = 20.7 mag, as well as spectroscopy (radial velocities and chemistry) for objects brighter than $G = 15.3$-16.2 mag (and $G > 2$ mag).

Key-science topics that *Gaia* will address range from: the study of the Milky Way (MW) structure and dynamics to the Galaxy star formation history (e.g. Cignoni et al. 2006, for a similar study based on *Hipparcos* data), stellar astrophysics to binaries and multiple stars, brown dwarfs and planetary systems to solar system objects, galaxies to quasars and the reference frame, and fundamental physics to general relativity.

The backbones of *Gaia*'s science are also i) the discovery of thousands new variable sources thanks to repeatedly monitoring the whole celestial sphere and, most importantly, ii) the absolute calibration of fundamental standard candles of the cosmic distance ladder such as hundreds/thousands of RR Lyrae stars and Cepheids that will have their parallax (hence distance) measured by *Gaia* at ~ 10 μas accuracy.

[1]G denotes *Gaia* broad-band white-light magnitude.

A better knowledge of the cosmic distance ladder has a profound impact in areas ranging from stellar astrophysics to the cosmological model. With the successful launch of *Gaia* and the release of first astrometric data scheduled for mid-2016, this topic has now become extremely hot and timely.

2. *Gaia*'s payload and instruments

Gaia scans the sky from a Lissajous-type orbit around the L2 Lagrangian point of the Sun and Earth-Moon system, where the spacecraft will remain for its 5-year nominal lifetime and possibly for an additional year, if the mission is extended. The spacecraft features two primary mirrors mounted on a silicon carbide toroidal optical bench, each with $1.7^\circ \times 0.6^\circ$ field of view (FoV). The two mirrors are separated by a basic angle of 106.5° and share a combined focal plane where there are 106 assembled CCDs devoted to different functions: 2 wave-front sensor and 2 basic-angle monitor CCDs; 14 Sky Mapper CCDs with task of detecting sources entering into *Gaia*'s two fields of view; 62 astrometric field CCDs devoted to astrometric measurements and providing integrated white-light (G-band) photometry over the wavelength range: 330-1,050 nm; 7 Blue and 7 Red Photometer (BP and RP) CCDs providing low resolution ($R \sim$20-90) spectrophotometry for each source over the wavelength ranges 320-660 and 650-1,000 nm, respectively; and 12 CCDs for the Radial Velocity Spectrograph (RVS) obtaining $R = 11\,500$ spectra in the Ca triplet (845-872 nm) region for sources brighter than $G \sim$15.3-16.2 mag (and $G > 2$ mag). A more detailed description of *Gaia*'s payload, instruments and focal plane can be found in Prusti (2012) and at http://www.cosmos.esa.int/web/Gaia/spacecraft-instruments.

The way of scanning the sky is due to *Gaia*'s spinning in 6 hours around its axis, which points in a direction 45° away from the Sun, and to the spin axis precessing slowly on the sky (precession period of 63 days and 29 revolutions around solar direction in 5 years). As a result of the precession, the sky seen by the two fields of view every 6 hours changes slowly with time, allowing repeated full sky coverage over the mission lifetime. At the same time, due to the 106.5° separation between the two fields of view, objects transiting FoV_1 at time t_0 will then transit FoV_2 at $t = t_0 + 106.5$ minutes. This will then repeat 6 hours later and then again 10-30 days later. These figures give rise to an optimum nominal scanning law by which over the 5 years *Gaia* will observe each source from 10 to 250 times (the actual number depending on sky position, with maximum frequency at $|\beta| = 45 \pm 10^\circ$) and on average about 70 times in photometry and about 40 times with the RVS. The sky coverage of *Gaia* after 5 years is shown in Fig. 4 of Prusti (2012). Further details on *Gaia*'s scanning law can be found at http://www.cosmos.esa.int/web/Gaia/scanning-law. The scanning law determines the typical cadence of *Gaia* multi-epoch observations and, in turn, bears on the alias patterns we may expect to show up in the power spectrum of *Gaia* time-series data.

Gaia does not send images down to ground. Figure 1 shows a star density map of the sky observed by *Gaia* produced by visualizing the number of stars between $G = 13$ and 18 mag detected per second by *Gaia*'s fields of view. These stars represent only a very small fraction of all detected stars and are used by the attitude control system to ensure that the orientation og *Gaia* is maintained

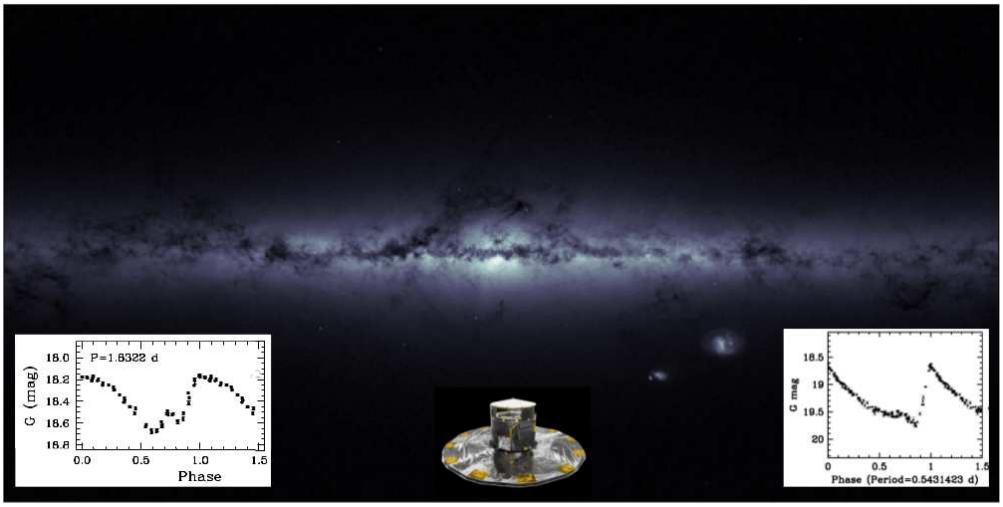

Figure 1. Star density map of the sky produced with *Gaia*'s housekeeping data (Credits: E. Serpell, ESA/Gaia-CC BY-SA 3.0 IGO) showing our Galaxy and the two Magellanic Clouds. The two insets show *Gaia* G-band light curves for a Cepheid on the left (from http://www.cosmos.esa.int/web/Gaia/iow_20150528) and an RR Lyrae star on the right (from http://www.cosmos.esa.int/web/Gaia/iow_20150305) observed by *Gaia* in the Large Magellanic Cloud (LMC) during the first 28 days of science operations in Ecliptic Pole Scanning Law (EPSL).

with the desired precision. The Milky Way and the two Magellanic Clouds are easily recognized.

3. Current status and post-launch performances

After a few months of commissioning, *Gaia* entered into nominal science operations on July 18, 2014. The routine phase started with 28 days in Ecliptic Pole Scanning Law (EPSL), after which *Gaia* went into Nominal Scanning Law (NSL). *Gaia*'s EPSL footprint around the South Ecliptic Pole (SEP) intercepts a portion of the LMC containing a large number of RR Lyrae and Cepheids which were monitored repeatedly during these first days of science operations. Examples of light curves for an RR Lyrae and a Cepheid observed by *Gaia* in the LMC during the EPSL are shown in the two insets of Fig. 1.

Gaia data processing is handled by the Data Processing and Analysis Consortium (DPAC), an ensemble of approximately 450 scientists and software developers from 20 different (primarily European) countries, organized in 6 Data Processing Centers and 9 scientific Coordination Units, each having its own specific tasks. DPAC processing takes place in a cyclic way and with continuous interaction and exchange among different CUs and *Gaia*'s Main Data Base which resides at the European Space Astronomy Centre (ESAC) (see http://www.cosmos.esa.int/web/Gaia/data-processing). Processing of the variable sources observed by *Gaia* is the task of Coordination Unit 7 (CU7) whose main Data Processing Center is at ISDC in Geneva.

Gaia is now fully operational, scanning the sky to a faint limit of $G = 20.7$ mag (and completeness at $G = 20$ mag) since the start of science operations and on average collecting data for 50 million stars per day. For comparison, faint limit and completeness of *Gaia*'s predecessor, *Hipparcos*, are 12 and 7.3-9.0 mag, respectively. Over the first year of operations *Gaia* has collected more than 272 billion astrometric measurements, 54.4 billion BP, RP photometric measurements and 5.4 billion RVS spectra (see http://www.esa.int/Our_Activities/Space_Science/Gaia/Gaia_s_first_year_of_scientific_observations). Current magnitude limits are: $2 < G < 20.7$ mag for photometry and astrometry, and $2 < G \leq 15.3$-16.2 mag for the RVS. Stars brighter than $G = 3$ mag are imaged by the Sky Mapper CCDs (Prusti 2014). DPAC has started the cyclic processing and first tests were made on the EPSL dataset.

Post-launch performances have been derived after conclusion of *Gaia* commissioning and standard errors of the end-of-mission *Gaia* photometry, astrometry and spectroscopy have been re-assessed. Tables and plots showing *Gaia* post-commissioning performances can be found at http://www.cosmos.esa.int/web/Gaia/science-performance.

4. *Gaia*'s RR Lyrae stars

Eyer & Cuypers (2000) predict *Gaia* to observe about 70,000 RR Lyrae stars in the Galactic halo (based on estimates of the RR Lyrae density in the MW halo by Suntzeff et al. 1991) and an additional 15,000-40,000 RR Lyrae stars in the MW bulge (based on MACHO and OGLE detection rates available at the time). However, these might be underestimates, as current ongoing surveys such as OGLE, LINEAR, CATALINA, PanSTARRS, PTF, are constantly reporting new discoveries and increased RR Lyrae densities. In conclusion, likely *Gaia* will significantly revise upward the census of Galactic RR Lyrae stars both in the MW and in some of its close companions. Over a hundred thousand Galactic RR Lyrae are expected to be observed by *Gaia*, compared to *Hipparcos* that observed only 186 such variables, of which only RR Lyrae itself has an accurate enough parallax ($\sigma_\pi/\pi \sim 18\%$). End-of-mission, astrometric standard errors, in units of μas, for position, parallax, and proper motion, as a function of *Gaia* G magnitude, for a G2V star with $(V-I)_0$=0.75 mag and $(V-G)_0$=0.16 mag, are summarized in Table 1 of de Bruijne et al. (2014). According to these estimates all RR Lyraes brighter than $\langle V \rangle$ =12-13 mag will have their parallax measured by *Gaia* to $\sim$ 10 μas, whereas individual accuracies will range between 17 to 140 μas for RR Lyrae stars in Galactic globular clusters with horizontal branch luminosity between $V \sim$14 and 18 mag.

Processing of the variable sources observed by *Gaia* is handled by CU7, that analyzes the calibrated G, BP and RP photometry produced by CU5 to identify variable sources. The CU7 processing chain comprises a number of different modules and work-packages that perform the variability detection, characterize and classify the sources found to vary, and finally produce period, amplitude, mean magnitude, modeled light curves, and stellar parameters that fully typify the confirmed variables. A specific work-package of the CU7 chain is dedicated to the RR Lyrae stars (and the Cepheids) and outputs final attributes for these variable stars, including classification in types according to the pulsation mode

and detection of double-mode pulsation and/or other secondary periodicities. In spring 2015 the CU7 pipeline was tested on data collected by *Gaia* during 28 days of EPSL and 3 days of NSL. About 70 million sources were received from CU5 and processed by CU7. Over twelve hundred RR Lyrae stars were identified, about half of them are new discoveries. Figure 2 shows examples of the G-band light curve for RR Lyrae stars in the LMC observed by *Gaia* during EPSL. *Gaia*'s light curves are folded using periods taken from the OGLE IV catalogue of variable stars in the *Gaia* SEP (Soszynski et al. 2012). OGLE I-band light curves for these stars are also shown for comparison. This figure nicely showcases the excellent quality of *Gaia*'s photometry (median uncertainties of the measurements are around 0.02 mag) at the faint magnitudes of the LMC RR Lyrae stars (typical average apparent magnitudes are $\langle V \rangle \sim 19.5$ mag) and after a first data reduction by CU5 and a first analysis by CU7.

Gaia data have no proprietary rights – they will become public as soon as they have been fully processed and properly validated. Publication of *Gaia*'s final catalogue is currently planned for 2022, however, there will be a number of intermediate data releases, of which the first one is foreseen in 2016. This first release will contain positions and G-band photometry for all-sky single stars, G-band time-series photometry and characterization by CU7 of the RR Lyrae and Cepheids observed during the EPSL, and parallaxes and proper motions for about 2 million stars in common between *Gaia* and the Tycho-2 catalogue based on the Tycho-Gaia Astrometric Solution (TGAS; see Michalik et al. 2015 and http://www.cosmos.esa.int/web/Gaia/iow_20150115 for details).

4.1. Science with *Gaia*'s RR Lyrae stars

Thanks to multi-epoch monitoring of the whole celestial sphere, *Gaia* will discover and measure positions and proper motions of thousands of RR Lyrae stars in the MW and its surroundings down to *Gaia*'s limiting magnitude and will simultaneously determine chemical and dynamical properties for those within reach of the RVS ($G \lesssim 16$ mag). These RR Lyrae will trace the ancient ($t >$ 10 Gyr) stellar component all the way through from the Galactic bulge, to the disk, to the halo and have the potential to unveil streams, faint satellites, stellar overdensities, and remnants left over by past interactions and accretions of the MW assembling process. As an example of *Gaia*'s potential in this area, Table 1 summarizes the estimated number of transits per year at the position of classical and ultra-faint Local Group galaxies with RR Lyrae stars within *Gaia*'s reach.

Gaia's complete census of the Galactic RR Lyrae will definitely increase our understanding of the MW structure and formation. However, even more dramatic is the impact *Gaia* will have on the RR Lyrae (and Cepheid) foundations of the cosmic distance ladder. Both the optical luminosity-metallicity ($M_V - [\mathrm{Fe/H}]$) relation and the near/mid-infrared period-luminosity (PLZ) relation of RR Lyrae as well as the period-luminosity and period-Wesenheit relations of Cepheids need an accurate determination of their zero points in order to reliably calibrate secondary distance indicators, and be able to probe cosmologically relevant distances ($D \geq 100$ Mpc). At present, an accurate parallax is available only for a handful RR Lyrae stars. *Hipparcos* measured the parallax for more than a hundred RR Lyrae stars in the solar neighborhood, but errors are larger than 30%. Only for RR Lyr itself ($\langle V \rangle \sim$7.8 mag) is the *Hipparcos*

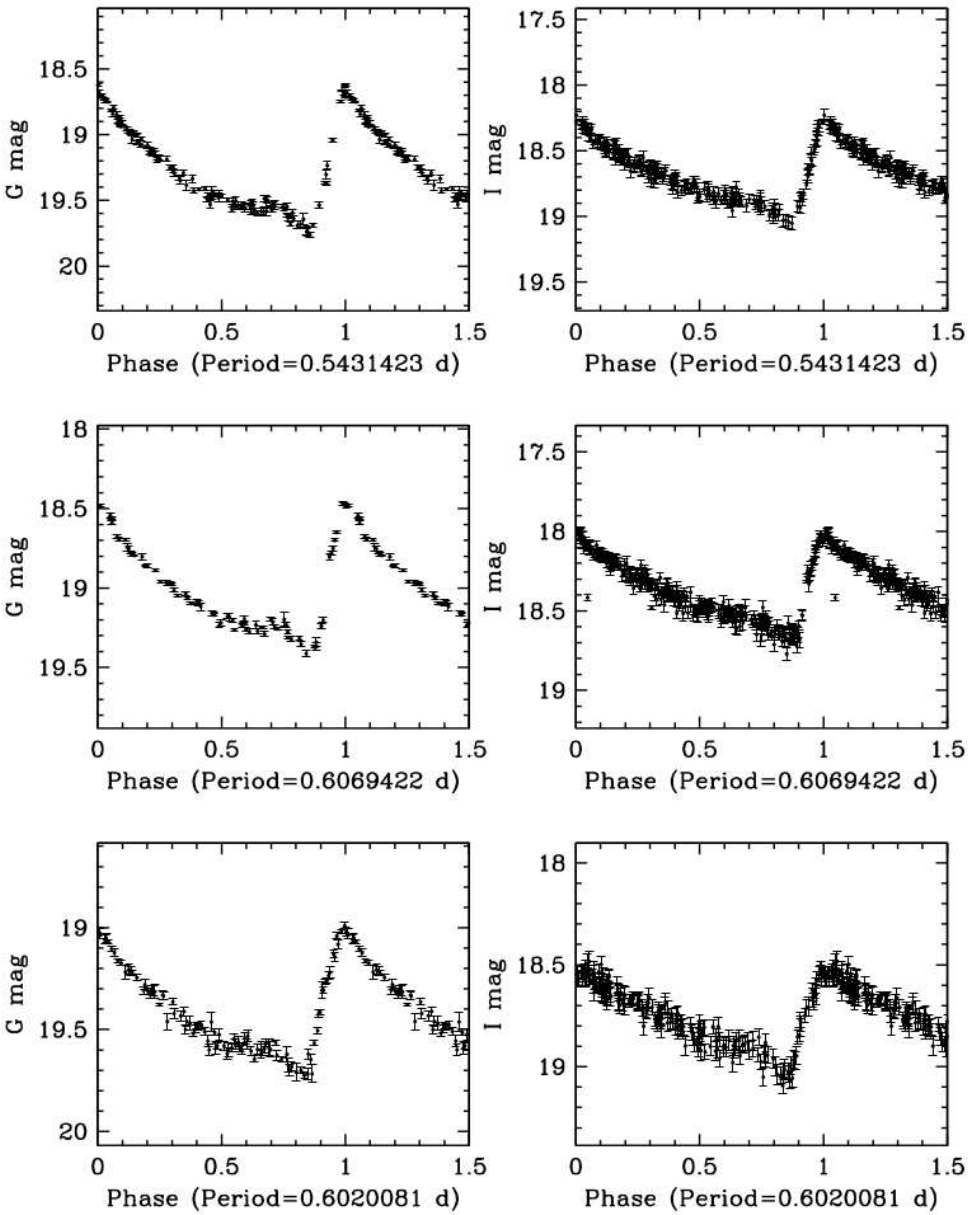

Figure 2. Left panels: *G*-band light curves of fundamental-mode RR Lyrae stars in the LMC observed by *Gaia* during the 28 days of EPSL. Right panels: *I*-band light curves obtained for the same stars by the OGLE IV survey. From http://www.cosmos.esa.int/web/Gaia/iow_20150305.

Table 1. Estimated number of *Gaia*'s transits per year at the position of known close by Local Group galaxies

Name	RA (deg)	Dec (deg)	D[a] (kpc)	Year of mission 1	2^b	3^b	4^b	5^b
MW center	266.41	−29.0	–	10	18	34	47	54
Canis Major	108.14	−27.66	7	22	49	72	98	121
Segue 1	51.76	16.081	23	10	20	29	50	59
Sagittarius dSph	283.83	−30.54	26	11	20	32	44	58
Ursa Major II	132.88	63.13	32	19	51	73	138	160
Segue 2	38.416	20.175	35	9	17	26	43	53
Willman 1	162.33	51.058	38	26	53	74	85	97
Bootes II	209.5	12.85	42	10	30	56	77	84
Coma Berenices	186.74	23.403	44	15	33	42	49	61
Bootes III	209.3	26.8	47	15	34	85	107	114
LMC[c]	80.893	−69.75	51	14	28	47	63	81
SMC	13.186	−72.82	64	20	39	54	73	87
Bootes I	210.02	14.5	66	8	23	49	68	77
Draco	260.05	57.915	76	18	36	50	66	84
Ursa Minor	227.28	67.222	76	18	33	46	64	78
Sculptor	15.0375	−33.709	86	21	35	48	65	120
Sextans	153.26	−1.614	86	11	20	27	58	66

[a] Distances are from McConnachie (2012)
[b] Cumulative numbers
[c] Estimates for the LMC do not include the EPSL transits.

error in the parallax smaller than ∼18%. At present, the zero points of the RR Lyrae relations are anchored on only 5 Galactic RR Lyrae with *HST* parallax measured by Benedict et al. (2011). However, *Hipparcos* parallax of RR Lyr ($\pi_H = 3.46 \pm 0.64$ mas, van Leeuwen 2007) differs from the *HST* parallax (π_{HST} = 3.77± 0.13 mas, Benedict et al. 2011) by an amount corresponding to a 10% difference in distance, although the two values are not totally inconsistent given the large error of *Hipparcos* estimate. On the other hand, use of Benedict et al. (2011)'s parallaxes is not without concern (see, e.g., Section 3.2.2 in Muraveva et al. 2015). *Gaia* will provide individual distances from parallaxes measured to ~ 10 μas for all RR Lyrae brighter than $V \sim 12$ mag (see Table 1 in de Bruijne et al. 2014) and RVS metallicity for those brighter than $V \lesssim 16$ mag. Hence, in a few years from now ~ 10 μas accuracy parallaxes will become available for 100-150 Galactic RR Lyrae spanning a large enough metallicity range to measure both the zero point and slope of the M_V−[Fe/H] and PLZ relations directly from these parallax-calibrated sources. Accuracies quoted in de Bruijne et al. (2014) are end-of-mission estimates. However, parallaxes with sub-milliarcsecond accuracy for RR Lyrae brighter than $\langle V \rangle \sim 12$ mag may already be included in the TGAS catalogue published with *Gaia*'s first data release in 2016.

In summary, the unprecedented precision and accuracy of *Gaia* parallax for the local RR Lyrae (and Cepheids) with allow (i) the absolute calibration via parallaxes of these "primary" standard candles, (ii) a test of the metallicity effects through simultaneous abundance measurements, (iii) a re-calibration of the "secondary" distance indicators and (iv) to set up a homogeneous distance ladder in and beyond the Local Group, and finally producing a total re-assessment

of the whole cosmic distance ladder. This will in turn significantly improve our knowledge of the Hubble constant (H_0). Furthermore, by combining *Gaia*'s photometry, parallax, metallicity and radial velocity information it will be possible to better constrain the physical parameters of RR Lyrae stars, test the pulsation models and their input physics, better determine, for instance, the p-factor used to convert radial to pulsation velocity in Baade-Wesselink studies, better understand double-mode pulsation and the Blazhko effect and many more other phenomena occurring in RR Lyrae stars. This will further improve their use as standard candles and stellar population tracers.

Finally, synergy between *Gaia* and past, ongoing and future surveys covering the full wavelength range from near-UV to the mid-IR, such as OGLE, EROS, LINEAR, CATALINA, PTF, ASAS, PanSTARRS, LSST, 2MASS, VVV, VMC from the ground, and CRRP, SMHASH, CCHPII from space, along with use of upcoming multiplex facilities such as WEAVE, MOONS, 4MOST to complement the RVS spectroscopy, will allow a further quantum leap in the science achievable with RR Lyrae stars in the *Gaia* era.

Acknowledgments

This paper extensively uses information publicly available at the ESA web pages (http://www.cosmos.esa.int/web/Gaia), whose creation and maintenance is gratefully acknowledged. A special thanks goes to the DPAC CU7 members at INAF-OACn, to all of the CU7 team, to CU5 for providing the processed time-series photometry, and to all DPAC members. Support is acknowledged from PRIN-INAF2014, "EXCALIBUR'S" (P.I. G. Clementini) and from the Agenzia Spaziale Italiana (ASI) through grants ASI I/058/10/0 and ASI 2014-025-R.1.2015.

References

Benedict, G. F., McArthur, B. E., Feast, M. W., et al. 2011, AJ, 142:187
Cignoni, M., Degl'Innocenti, S., Prada Moroni, P. G., et al. 2006, A&A, 459, 783
de Bruijne, J. H. J., Rygl, K. L. J., Antoja, T. 2014, EAS, 67, 23
Eyer, L., Cuypers, J. 2000, IAU Coll. 176, The Impact of Large Surveys on Pulsating Stars Research, 203, 71
McConnachie, A. W. 2012, AJ, 144:4
Michalik, D., Lindegren, L., Hobbs, D. 2015, A&A, 574, A115
Muraveva, T., Palmer, M., Clementini, G., et al. 2015, ApJ, 807:127
Perryman, M. A. C. 2009, Astronomical Applications of Astrometry: Ten Years of Exploitation of the Hipparcos Satellite Data, Cambridge University Press, Cambridge, UK
Prusti, T. 2012, Astron. Nachr., 333, 453
Prusti, T. 2014, EAS Publ., 67, 15
Soszynski, I., Udalski, A., Poleski, R., et al. 2012, AcA, 62, 219
Suntzeff, N. B., Kinman, T. D., Kraft, R. P. 1991, ApJ, 367, 528
van Leeuwen, F. 2007, Hipparcos, the New Reduction of the Raw Data, Astrophysics and Space Science Library, Vol. 350

RRL2015 – High-Precision Studies of RR Lyrae Stars
L. Szabados, R. Szabó, K. Kinemuchi (Eds.) 2016

The first decade of RR Lyrae space photometric observations

László Molnár

Konkoly Observatory, Research Centre for Astronomy and Earth Sciences, Hungarian Academy of Sciences, H-1121, Budapest, Konkoly Thege Miklós út 15-17, Hungary

Abstract. Space-based photometric telescopes stirred up stellar astrophysics in the last decade, and RR Lyrae stars have not been an exception from that either. The long, quasi-continuous, high-precision data from *MOST, CoRoT* and *Kepler* revealed a wealth of new insights about this well-known variable class. One of the most surprising mysteries turned out to be the apparent omnipresence of a common additional mode in all RRd and RRc stars. Moreover, fundamental-mode stars seem to populate two distinct classes, one of which is characterized by the presence of additional modes and/or modulation, and another limited to strict single-mode pulsation. The presence of additional modes and multiple modulations in RRab stars allowed us to construct Petersen diagrams for these parameters: while the pulsation modes show clear structures according to period ratios, there seems to be no relation between the modulation periods themselves.

1. Double-mode stars and the rise of the f_X mode

The era of space-based photometry of RR Lyrae stars started a decade ago, when the *MOST* space telescope observed the double-mode star AQ Leo (Gruberbauer et al. 2007). Since the space photometric revolution started with an RRd star, it is fitting to start this review with the classical double-mode stars. Given that the double-mode region of the instability strip is very narrow (see, e.g. Szabó et al. 2004), RRd stars are inherently rare, and only a few have been observed from space so far. *MOST* and *CoRoT* observed one each: Gruberbauer et al. (2007) and Chadid (2012) both identified various additional modes in AQ Leo and CoRoT ID 0101368812, respectively.

The original *Kepler* field did not contain any known RRd stars, but the first *K2* campaigns already presented us with three targets (Kurtz et al. 2016; Molnár et al. 2015a). Despite the diverse notations used in these papers for the additional modes, the comparison of the frequency content of these stars reveal a strikingly similar pattern. Instead of a collection of various additional modes, all five stars exhibit the same f_X or $f_{0.61}$ mode that was originally identified in first-overtone Cepheids and RR Lyrae stars (Moskalik et al. 2014a, and references therein). Although the space-based RRd sample is still small, the data so far indicate that the f_X mode and thus the triple-mode state is common (and quite possibly universal) within this subclass.

2. First-overtone stars: the new double-mode class

The mysterious f_X mode was identified in almost all first-overtone stars observed from space, with the notable exception of the modulated star CSS J235742.1–015022 (Szabó et al. 2014; Molnár et al. 2015a; Moskalik et al. 2015). Although the space-based sample is also small for RRc stars, with only 4 *Kepler*, 4 *K2*, and 2 *CoRoT* targets published so far, other observations also point towards the ubiquity of this additional mode. Notably, the ground-based data from the OGLE surveys and an intensive monitoring of M3 provided us with a large variety of high-precision RRc light curves (Jurcsik et al. 2015; Netzel et al. 2015a,c). These studies revealed that the f_X mode splits into three sequences between period ratios $P_X/P_1 \sim 0.60$–0.64, similarly to the three sequences observed in Cepheids. Half-integer frequencies at $n/2$ f_X values often appear, and all these frequency components show strong amplitude and phase variations on various time scales. Half-integer peaks may indicate that the mode is period-doubled, e.g. two cycles with different amplitudes (or shapes) alternate in time. Both effects can be observed in the phase diagram of an f_X mode shown in Figure 1.

The origin of this (or these) mode(s) is still an open question. If we accept f_X as the intrinsic pulsation frequency, the corresponding nonradial modes in this regime experience either very strong damping or very strong cancellation due to high spherical degrees required (up to $\ell \sim 40 - 50$), or both. An alternative hypothesis is that the pulsation frequency is in fact $f_X/2$, originating from $\ell = 8$ and 9 modes and then all the other peaks are simply the nf_ℓ harmonics (Dziembowski & Smolec, in preparation, also Dziembowski in these proceedings). In that case, period doubling does not occur, but a mode geometry is required where the observed amplitude of the $f_X = 2f_\ell$ can be much higher than that of f_ℓ.

Space-based photometry also revealed that not only the f_X mode but the first overtone itself may exhibit temporal variations. The four *Kepler* targets showed fluctuations in amplitude and phase on very different time scales, but interestingly these time scales are the same for f_1 and f_X for any given star, indicating some connection, such as mode interaction between them (Moskalik et al. 2015). We note that these variations have small amplitudes and show irregularities, so they appear to be different from the Blazhko effect observed in RRc stars.

Finally, not all RRc stars are limited to the first overtone and one or more f_X-type mode. Yet another mode was discovered in one of the *Kepler* stars and later in some OGLE targets (Moskalik et al. 2014a; Netzel et al. 2015b). This mode has a period ratio of $P_1/P_{0.68} = 0.686$, e.g. the mode period is longer than the first overtone, and even longer than the scaled period of the fundamental mode with $P_0/P_{0.68} \sim 0.92$. At the moment the origin of this mode is even less clear than that of the $f_{0.61}$ mode.

3. RRab stars: a group of two classes

Most of the RR Lyrae stars pulsate in the fundamental mode, so naturally most of the targets of space photometric missions were RRab stars as well. These included the eponym, RR Lyr, that was being observed for almost four years

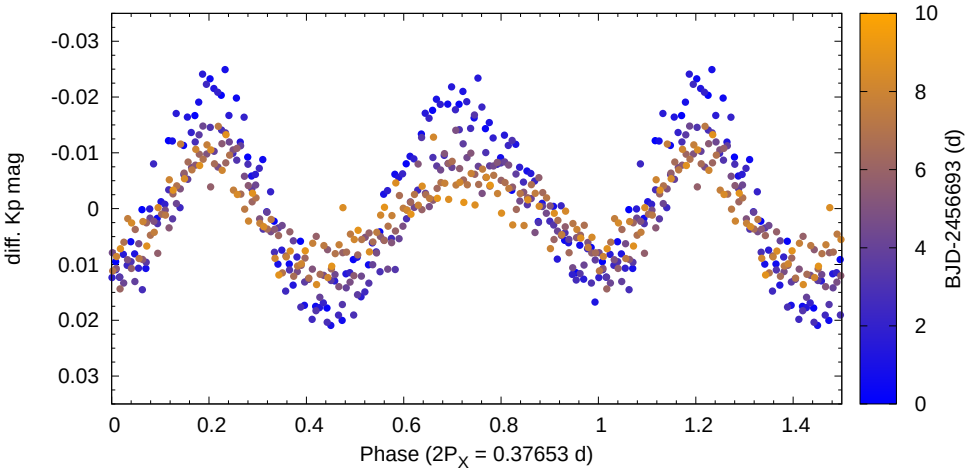

Figure 1. The phase diagram of the disentangled f_X mode in the RRc star EPIC 60018224 (Molnár et al. 2015a). The frequency components of the first overtone and the combination terms were removed. The data are folded with $P = 2/f_X = 1/f_\ell$. The color coding shows the temporal evolution of the mode. The amplitude decreased significantly even during the short *K2*-E2 run. Also note that the two minima are not equidistant from each other.

continuously (Kolenberg et al. 2011). One expectation about RR Lyr was that the *Kepler* data would reveal the details of the suspected four-year cycle and the associated modulation phase shift in the star (Detre & Szeidl 1973). What transpired, instead, was that the levels of both amplitude and phase modulations were decreasing steadily over the four years. Although the amplitude modulation seemed to recover towards the end of the data, the phase variation continued to decrease even afterwards, according to ground-based measurements (Le Borgne et al. 2014).

Although *Kepler* did not find the 4-year cycle, it revealed other, very important details about RR Lyr, and the entire variable class, with the discovery of period doubling and the presence of additional modes (Kolenberg et al. 2010; Szabó et al. 2010). Since then, these additional modes were found in several other RRab stars, although the amplitudes rarely exceed a few mmag. A Petersen diagram (e.g. mode period ratios versus the period of the fundamental mode) of these new frequency components is presented in Figure 2. This plot shows all peaks found between f_0 and $2f_0$, including the ones close to $3/2f_0$ half-integer peak (HIF). This component itself does not indicate a separate mode, just the presence of period doubling, but it often splits into a forest of peaks, with the dominant one shifted from the exact $3/2f_0$ value (see, e.g. Benkő et al. 2010). The shift can be attributed to the facts that both the fundamental mode and period doubling itself is variable in time: this effect was also observed in BL Her hydrodynamic models (Smolec & Moskalik 2012). However, the diagram indicates that the distinction between HIFs and nearby, bona-fide additional modes (or related peaks) towards the first overtone can be indeed subtle. In

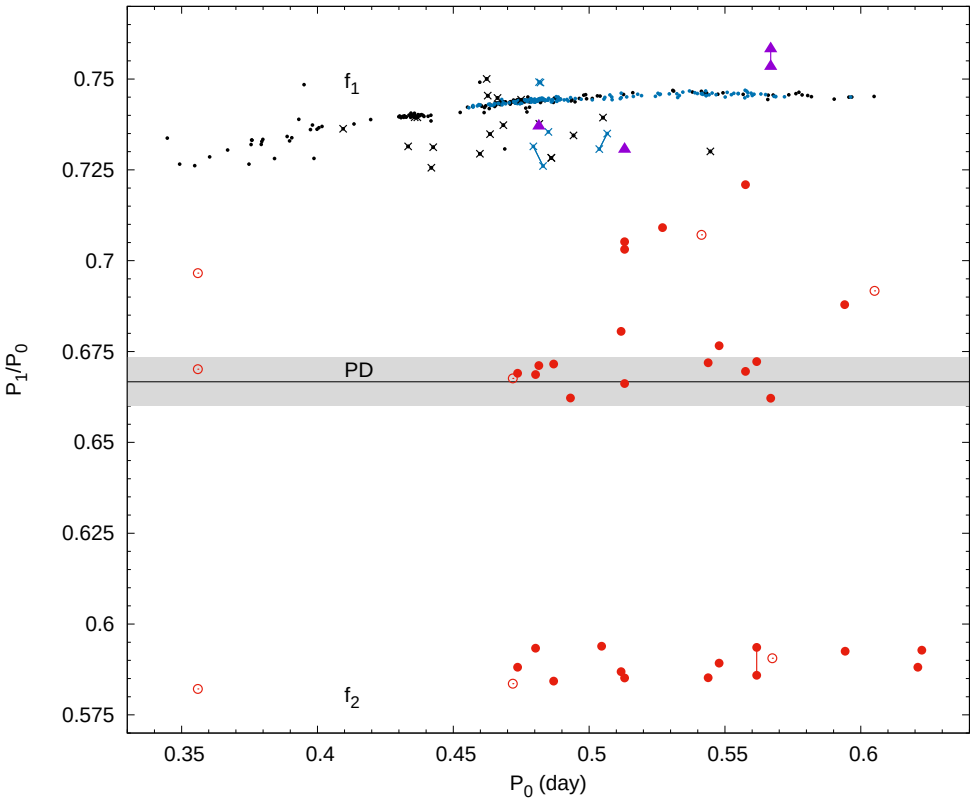

Figure 2. Petersen diagram of the low-amplitude additional modes observed in the *CoRoT* (open symbols) and *Kepler/K2* (filled symbols) RRab stars. Triangles correspond the three instances where the first overtone was potentially detected. Black and blue dots mark the position of classical RRd stars from the OGLE and CSS catalogs. Black crosses indicate the modulated or mode-switching bulge RRd stars, while blue crosses are the modulated RRd stars in M3. The black horizontal line marks the $P_1/P_0 = 2/3$ ratio, the grey area is the $< \pm 1\%$ difference.

contrast, the f_2 mode below clearly separates from the rest of the peaks, and only appears at period ratios between $0.580 < P/P_0 < 0.595$.

The diagram also shows that the first overtone rarely occurs in RRab stars as an additional mode. The three examples so far are RR Lyr itself, V445 Lyr (KIC 6186029), and EPIC 206280713 (Guggenberger et al. 2012; Molnár et al. 2012; Juhász et al., in these proceedings). If we compare the period ratios of these stars to the classical double-mode stars, we can see that RR Lyr is very peculiar, with a ratio of $P_1/P_0 > 0.75$. Interestingly, although the other two stars lie outside the main double-mode ridge as well, they perfectly overlap with the non-standard RRd stars such as modulated and mode-switching objects (Soszyński et al. 2014; Jurcsik et al. 2015; Smolec et al. 2015a,b). This further suggests that we indeed observe the first radial overtone is these stars. One of the great advantages of the step-and-stare approach of the *K2* mission is

that this Petersen diagram is going to be populated with at least one order of magnitude more objects that may reveal more structures and could help us to identify the various additional modes modulated RRab stars exhibit. Another important addition to this sample will be the OGLE data that certainly holds several examples of RRab stars with additional modes.

Apart from these additional modes, there is at least one indication that RRab stars may also exhibit modes with (apparent) periods longer than the fundamental mode. A low-amplitude signal was tentatively identified at $P/P_0 = 0.695$ in EPIC 60018644 (Molnár et al. 2015a). Although that detection was based only the short *K2* Engineering data set, the star will fall on silicon during Campaign 12 of the *K2* mission, making a much longer follow-up study possible.

Space-based photometric observations also revealed a striking dichotomy among the fundamental-mode stars: those that are not modulated, do not contain additional modes either. Therefore non-Blazhko RRab stars seem to be the one and only subclass among the RR Lyraes that are truly monoperiodic (Szabó et al. 2015). This dichotomy was further supported by Benkő & Szabó (2015), who discovered low-level modulations in two *Kepler* stars that initially appeared to have additional modes without the Blazhko effect. The existence of years-long, sub-mmag level modulation, as in the case of KIC 7021124, represents an important challenge in the analysis of the shorter *K2* and *TESS* observations. The findings from *CoRoT* and *Kepler* suggest that in ambiguous cases the presence of additional modes or period doubling can be considered as a proxy for the presence of a long-term and/or low-amplitude Blazhko effect.

4. The Blazhko effect: new insights, new models

Beside these important details of the pulsation, the long-term, continuous coverage of the space missions also showed us the bigger picture: the true shape of the Blazhko effect. The long observations of the original *Kepler* mission were especially useful to investigate the temporal behavior of the modulation. Benkő et al. (2014) found that most of the Blazhko RRab stars in that sample show either multiperiodic or irregular modulation. Together with the rest of the known multiperiodic Blazhko stars, a Petersen diagram of modulation periods can be constructed. In Figure 3, I plotted all stars that have both modulation periods determined, and assigned the two as $P_{\rm BL1} > P_{\rm BL2}$, regardless of the amplitude ratios. Properties of Blazhko stars are collected in the database of Skarka (2013)[1]. The connected circles represent CZ Lac that changed both of its modulation periods over time (Sódor et al. 2011). The figure, at least with the current sample, does not suggest any particular structure or relation between the modulation periods.

5. Classification considerations

The new, intriguing details that space-based photometry have been providing us with may prompt us to redefine, or at least reconsider the old Bailey-type

[1] `http://www.physics.muni.cz/~blasgalf/`

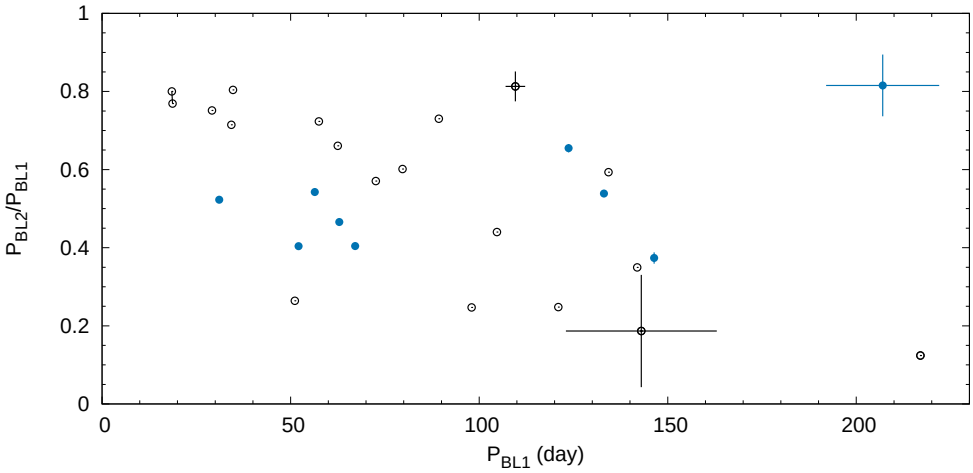

Figure 3. Petersen diagram of the Blazhko-RRab stars where two modulation periods can be determined. Filled points represent the *Kepler* data, empty circles are ground-based measurements.

classification scheme. The picture that has emerged in the last few years can be summarized as follows:

- **RRd class:** stars where both the fundamental mode and the first overtone pulsate with large amplitudes (few tenths of a magnitude) and a low-amplitude f_X-type mode is also present. Blazhko subtype exists, both the fundamental mode and the first overtone can be modulated.
- **RRc class:** stars where the first overtone pulsates with large amplitude (few tenths of a magnitude) and a low-amplitude f_X-type mode is also present. Blazhko subtype exists.
- **Blazhko RRab stars:** stars where the fundamental mode pulsates with large amplitudes (few tenths of a magnitude) and displays quasi- or multi-periodic modulation. Other low-amplitude modes and/or period doubling are usually present.
- **Non-Blazhko RRab stars:** stars where only the fundamental mode pulsates and it has a constant amplitude.

6. Future prospects

In the coming years, space-based photometry is going to provide us with an increasing amount of data about RR Lyrae stars. The *K2* mission is expected to observe a few thousand targets, including a few hundred stars in the Sagittarius stream and the Galactic bulge in various campaigns (Plachy et al., in these proceedings). Later on, the *TESS* space telescope will also cover at least hundreds, but possibly thousands of the nearby, brighter population of RR Lyraes. These

observations will allow us to sample all various subtypes, and promise to fill up the Petersen diagram of RRab stars, for example. Data from various populations, such as the Sagittarius stream, can also reveal incidence rate differences in the Blazhko effect, at least for short-period modulations (Kovács, in these proceedings).

Beside the new observations, the existing data sets still contain valuable information that can be extracted with various methods. The *CoRoT* data set is still not fully analyzed and it may contain additional RR Lyrae stars (Klagyivik et al. 2015). The *Kepler* field, in comparison, is much more thoroughly explored but ingenious methods may allow us to extract even more. The smear measurements, an ancillary engineering data produced by the CCD modules allows us to recover the light variations of the brightest stars in the field of view (Pope et al. 2016). One result of this method is that the light curve of RR Lyr itself can be recovered for quarters Q3 and Q4 when the star was not part of the observing program (Kolenberg et al. 2011). With the smear data, the photometry of RR Lyr now spans the whole mission from Q1 to Q17. Although smear is not very important for the generally fainter RR Lyraes, it will allow us to observe bright Cepheids, such as Y Sgr or V350 Sgr in the future with *K2*, without assigning a large number of pixels to them.

Another important source is the recently released RR Lyrae catalog of the PanSTARSS 3π survey (Hernitschek et al. 2015, also in these proceedings). Asteroid surveys like the Catalina and LINEAR sky surveys have avoided the vicinity of the Galactic plane, so we have had no reliable sources for fainter RR Lyraes in those areas. With the 3π catalog we will be able to search for variables in the existing *Kepler* and *K2* observations as well. The original *Kepler* field included two superstamps covering the two open clusters NGC 6791 and NGC 6819, where faint, previously unknown RR Lyraes may still hide. The large superstamps of the *K2* mission, as well as the generous target pixel masks of the early campaigns are also prime targets for such a follow-up search, and could verify the purity measures of the catalog in various Galactic directions. The 3π RR Lyrae catalog extends to about 21.5^{th} mag in the PanSTARSS r band. As the photometry of the variables in the galaxy Leo IV showed, *Kepler* is perfectly capable to recover stars this faint during the span of one campaign (Molnár et al. 2015b).

The increasing influx of high-precision data presents new challenges for theoretical studies as well. The golden sample of space-based photometry, together with the large ground-based catalogs, can give important constraints on the structure and evolution of the Milky Way. Pulsation theory also faces new challenges with the appearance of the additional modes. While progress has been made for some of those, especially the origin of period doubling and related modes in RRab stars, and the new developments about the f_X mode are also promising, several open questions remain. These include the rest of the additional modes, such as the origin of the f_2 mode in RRab stars, the nature of the long-period modes, the explanation for the mode-switching stars, and so on. And let us hope that the answers to these questions may also lead us closer to the solution of the Blazhko effect itself.

Acknowledgements

L.M. was supported by the János Bolyai Research Scholarship of the Hungarian Academy of Sciences. This research has been supported by the Lendület-2009 and LP2014-17 Program of the Hungarian Academy of Sciences, and by the NKFIH PD-116175 grant of the Hungarian National Research, Development and Innovation Office. The research leading to these results has received funding from the European Community's Seventh Framework Programme (FP7/2007-2013) under grant agreements no. 269194 (IRSES/ASK) and no. 312844 (SPACEINN).

References

Benkő, J. M., Kolenberg, K., Szabó, R., et al. 2010, MNRAS, 409, 1585
Benkő, J. M., Plachy, E., Szabó, R., et al. 2014, ApJS, 213:31
Benkő, J. M., Szabó, R. 2015, ApJ, 809:L19
Chadid, M. 2012, A&A, 540, 68
Detre, L., Szeidl, B. 1973, IBVS, 764, 1
Gruberbauer, M., Kolenberg, K., Rowe, J. R., et al. 2007, MNRAS, 379, 1498
Guggenberger, E., Kolenberg, K., Nemec, J. M., et al. 2012, MNRAS, 424, 649
Hernitschek, N., Schlafly, E. F., Sesar, B., et al. 2016, ApJ, 817:73
Jurcsik, J., Smitola, P., Hajdu, G., et al. 2015, ApJS, 219:25
Klagyivik, P., Csizmadia, Sz., Pasternacki, T., et al. 2015, AJ, accepted, arXiv: 1510.01936
Kolenberg, K., Szabó, R., Kurtz, D. W., et al. 2010, ApJ, 713, L198
Kolenberg, K., Bryson, S., Szabó, R., et al. 2011, MNRAS 411, 878
Kurtz, D. W., Bowman, D. M., Ebo, S. J., et al. 2016, MNRAS, 455, 1237
Le Borgne, J. F., Poretti, E., Klotz, A., et al. 2014, MNRAS, 441, 1435
Molnár, L., Kolláth, Z., Szabó, R., et al. 2012, ApJ, 757:L13
Molnár, L., Szabó, R., Moskalik, P., et al. 2015a, MNRAS, 452, 4283
Molnár, L., Pál, A., Plachy, E., et al. 2015b, ApJ, 812:2
Moskalik, P. 2014, IAUS, 301, 249
Moskalik, P., Smolec, R., Kolenberg, K., et al. 2015, MNRAS, 447, 2348
Netzel, H., Smolec, R., Moskalik, P. 2015a, MNRAS, 447, 1173
Netzel, H., Smolec, R., Dziembowski, W. 2015b, MNRAS, 451, L25
Netzel, H., Smolec, R., Moskalik, P. 2015c, MNRAS, 453, 2022
Pope, B. J. S., White, T. R., Huber, D., et al. 2016, MNRAS, 455, 36
Skarka, M. 2013, A&A, 549, 101
Smolec, R., Moskalik, P. 2012, MNRAS, 426, 108
Smolec, R., Soszyński, I., Udalski, A., et al. 2015a, MNRAS, 447, 3756
Smolec, R., Soszyński, I., Udalski, A., et al. 2015b, MNRAS, 447, 3847
Sódor, Á., Jurcsik, J, Szeidl, B., et al. 2011, MNRAS, 411, 1585
Soszyński, I., Udalski, A., Szymański, M. K., et al. 2014, AcA, 64, 177
Szabó, R., Kolláth, Z., Buchler, J. R. 2004, A&A, 425, 627
Szabó, R., Kolláth, Z., Molnár, L., et al. 2010, MNRAS, 409, 1244
Szabó, R., Benkő, J. M., Paparó, M., et al. 2014, A&A, 570, 100
Szabó, R., Benkő, J. M., Paparó, M., et al. 2015, EPJ WoC, 101, 01003

RRL2015 – High-Precision Studies of RR Lyrae Stars
L. Szabados, R. Szabó, K. Kinemuchi (Eds.) 2016

Target selection of classical pulsating variables for space-based photometry

E. Plachy[1], L. Molnár[1], R. Szabó[1], K. Kolenberg[2,3,4], & E. Bányai[5]

[1]*Konkoly Observatory, Research Centre for Astronomy and Earth Sciences, Hungarian Academy of Sciences, H-1121, Budapest, Konkoly Thege Miklós út 15-17, Hungary*
[2]*Instituut voor Sterrenkunde, Leuven, Belgium*
[3]*Harvard-Smithsonian Center for Astrophysics, Cambridge, USA*
[4]*University of Antwerp, Antwerp, Belgium*
[5]*Eötvös Loránd University, Budapest, Hungary*

Abstract. In a few years the *Kepler* and *TESS* missions will provide ultra-precise photometry for thousands of RR Lyrae and hundreds of Cepheid stars. In the extended *Kepler* mission all targets are proposed in the Guest Observer (GO) Program, while the *TESS* space telescope will work with full frame images and a ∼15-16th mag brightness limit with the possibility of short cadence measurements for a limited number of pre-selected objects. This paper highlights some details of the enormous and important work of the target selection process made by the members of Working Group 7 (WG#7) of the *Kepler* and *TESS* Asteroseismic Science Consortium.

1. *K2* target selection and proposals

The new era of space-based photometry has already begun. The reaction wheel failure of *Kepler* space telescope opened a great possibility to build up a golden sample for many types of variable stars. In the *K2* mission, *Kepler* observes the ecliptic plane and changes its field of view in every ∼80 days (Howell et al. 2014). The mission started in March of 2014 with Campaign 0 (C0) and is planned to end in April of 2018 with Campaign 17 (C17). The invitation to the scientific community to propose targets for ultra-precise measurements in the GO Program motivates many astronomers to come forward with new ideas. Working Group 7 (WG#7) is interested in RR Lyrae and Cepheid stars, and it is responsible for the proposals of these objects for each campaign.

WG#7 has submitted altogether 22 proposals, listed in Table 1, at the time of writing this article. According to the initial concept, proposals were separated by variability types and cadence type (30 or 1 min). We dedicated proposals to dwarf galaxies and globular clusters as well. After C1, joint proposals were submitted for two or three fields. We typically submitted four proposals for each of the first four campaigns. Afterwards the calls were made through the 2-step process of the NASA proposal system. Since then, we have submitted united proposals for short and long cadence targets for the RR Lyrae and Cepheid stars.

The main goal of the proposals is to obtain all RR Lyrae and Cepheid targets that fall on the *K2* fields. To build up a golden sample, it is crucial to calibrate the classification and analysis methods. Our scientific justifications focus on the

Table 1. RR Lyrae and Cepheid proposals in the *K2* mission.

Campaign	Proposal Number	PI	Topic
C0	GO0051	Molnár	Long cadence Cepheid targets
	GO0053	Plachy	Short cadence Cepheid targets
	GO0055	Szabó	Long cadence RR Lyrae targets
	GO0124	Kolenberg	Short cadence RR Lyrae targets
C1	GO1018	Plachy	Long cadence RR Lyrae targets
	GO1019	Molnár	RR Lyrae in the dwarf galaxy Leo IV
	GO1021	Molnár	Long cadence Cepheid targets
	GO1067	Kolenberg	Short cadence RR Lyrae targets
C2 & C3	GO2027 & GO3027	Plachy	Short cadence RR Lyrae targets
	GO2039	Molnár	Pulsating variables in M4 and M80
	GO2040 & GO3040	Molnár	Long cadence RR Lyrae targets
	GO2041 & GO3041	Molnár	Type I and II Cepheids
C4 & C5	GO4066 & GO5066	Molnár	Type I and II Cepheids
	GO4069 & GO5069	Szabó	Exploiting RR Lyrae stars
C6 & C7	GO6082 & GO7082	Kolenberg	RR Lyrae stars from different populations
	GO7014	Molnár	Sampling the Cepheid instability strip
C8 & C10	GO3-0039	Szabó	Pulsation dynamics and Galactic structure of RR Lyrae stars
	GO3-0041	Molnár	Extragalactic Cepheids in IC 1613
C9	DDT	Smolec	RR Lyrae stars in the Galactic bulge
	DDT	Plachy	Classical and Type II Cepheids in the Bulge
C11, C12 & C13	GO4-0070	Plachy	Cepheids throughout the Galaxy
	GO4-0111	Molnár	The grand *K2* RR Lyrae survey

most pressing questions raised recently: the origin of dynamical phenomena, the low amplitude additional modes and the mysterious period ratios. The existence of nonradial modes and the explanation of the Blazhko effect are still open questions. The *K2* mission also provides the opportunity for population and Galactic structure studies as well as statistical analysis of various phenomena. A limited number of targets is observed with 1 minute sampling. We select the most interesting or rare type of targets to propose for short cadence mode (Molnár, Plachy & Szabó 2014).

Our target selection process was first used for the Two-Wheel Concept Engineering Test that led to a detailed analysis of 33 RR Lyrae stars (Molnár et al. 2014). First, we collect all known RR Lyrae and Cepheid candidates from the SIMBAD and VSX databases. Several sky surveys provide semi-automated variability catalogues and downloadable light curves as well. We found the Catalina Sky Survey (Drake et al. 2014), Lincoln Near Earth Asteroid Research (Sesar et al. 2013), All Sky Automated Survey (Pojmanski 2002), Northern Sky Variability Survey (Woźniak et al. 2004) extremely useful for the target selection. The next step is to select the stars that fall on silicon. We use the `K2FoV`[1] tool that has been developed by the Kepler GO Office for this purpose. The sky surveys overlap, so we have to do the cross-identification of the different cata-

[1] http://keplerscience.arc.nasa.gov/software.html, https://github.com/KeplerGO/K2fov

logues. Because of the relatively high uncertainty in the coordinates of certain objects, we found this step to be more reliable if done manually. The last and the most important step is to check of the folded light curves of the targets. The visual inspection can reveal misclassified objects, erroneous published periods and potential short cadence targets as well.

Table 2. Number of proposed and accepted RR Lyrae and Cepheid targets.

Campaign	RR Lyrae targets			Cepheid targets		
	Proposed	Accepted	Success rate	Proposed	Accepted	Success rate
C0	68	10	**∼15%**	54	13	**∼24%**
C1	136	18	**∼13%**	4	4	**100%**
C2	86	61	**∼71%**	8	8	**100%**
C3	117	82	**∼70%**	1	1	**100%**
C4	86	83	**∼97%**	7	7	**100%**
C5	89	88	**∼99%**	4	4	**100%**
C6	206	206	**100%**	-	-	-
C7	528	528	**100%**	10	9	**90%**
C8	85	85	**100%**	190	190	**100%**
C9	200	N/A	N/A	184	N/A	N/A
C10	224	N/A	N/A	2	N/A	N/A
C11	1629	N/A	N/A	164	N/A	N/A
C12	181	N/A	N/A	6	N/A	N/A
C13	94	N/A	N/A	10	N/A	N/A

Table 2 summarizes the number of targets proposed and accepted in each field so far. The success rate of the proposals is quite high. The reason for the initial low percentages is mostly technical: the lack of `K2FoV` tool in C0 or the 5 degree roll of the field of view in C3. In some cases, targets fell near the edge of the CCD, and in one case, the target was too bright to be measured. We note that the number of RR Lyrae and Cepheid stars measured in *K2* are not identical to the numbers of Table 2. Several additional targets are located in the superstamps of the globular clusters (C2) and the Galactic bulge (C9). Moreover, we predict a significant fraction of misclassified objects among the RRc, RRd and Cepheid candidates, but we also expect new findings among the pre-classified binaries.

2. *TESS* target selection

TESS will observe almost the entire sky and will download full frame images with a 30-minute cadence (Ricker et al. 2014). A few hundred thousand targets will be selected for 2-minute sampling. Most of these are exoplanet candidates, but 5 percent will be devoted to asteroseismic targets proposed by the *TESS* Asteroseismic Science Consortium. The target selection of these objects need the same careful process that we use in *K2* mission. The major difference will be in the brightness limit that is expected to be ∼12th mag for the short cadence objects, which reduces the number of the potential targets. In Figure 1, we plotted the continuous viewing zones of *TESS* around the ecliptic poles. 8 (18) RR Lyrae and 3 (35) Cepheid short cadence candidates around the North (South) Ecliptic Poles are marked with black circles and diamonds, respectively.

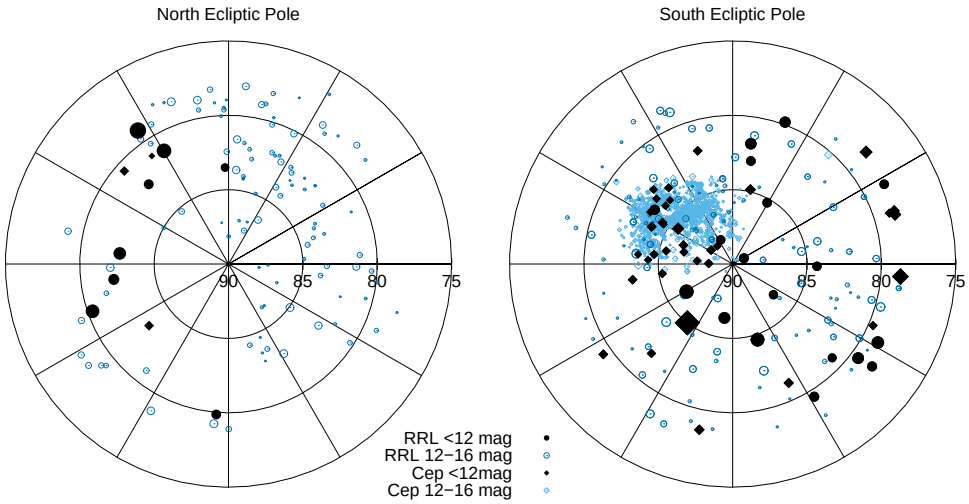

Figure 1. RR Lyrae and Cepheid stars in the *TESS* continuous viewing zone.

Acknowledgements

This research has been supported by the LP2014-17 Program of the Hungarian Academy of Sciences, by the NKFIH K-115709, the OTKA NN-114560 and the PD-116175 grants of the Hungarian National Research, Development and Innovation Office. The research leading to these results has received funding from the European Community's Seventh Framework Programme (FP7/2007-2013) under grant agreements no. 269194 (IRSES/ASK), no. 312844 (SPACEINN) and ESA PECS Contract No. 4000110889/14/NL/NDe. K.K. is grateful for the support of Marie Curie IOF grant 255267 SASRRL (FP7). L.M. was supported by the János Bolyai Research Scholarship of the Hungarian Academy of Sciences. This research has made use of the SIMBAD database, operated at CDS, Strasbourg, France, and the International Variable Star Index (VSX) database, operated at AAVSO, Cambridge, Massachusetts, USA.

References

Drake, A. J., Graham, M. J., Djorgovski, S. G., et al. 2014, ApJS, 213:9
Howell S. B., Sobeck, C., Haas, M., et al. 2014, PASP, 126, 398
Molnár L., Plachy E., Szabó R. 2014, IBVS, 6108, 1
Molnár L., Szabó R., Moskalik, P. A., et al. 2015, MNRAS, 452, 4283
Pojmanski, G. 2002, AcA, 52, 397
Ricker G. R., Winn, J. R., Vanderspek, R., et al. 2014, Proc. SPIE, 9143, E20
Sesar, B., Ivezić, Ž., Stuart, J. S., et al. 2013, AJ, 146:21
Woźniak, P. R., Vestrand, W. T., Akerlof, C. W., et al. 2004, AJ, 127, 2436

RRL2015 – High-Precision Studies of RR Lyrae Stars
L. Szabados, R. Szabó, K. Kinemuchi (Eds.) 2016

Nonradial oscillations in classical pulsating stars. Predictions and discoveries

Wojciech A. Dziembowski[1,2]

[1] *Nicolaus Copernicus Astronomical Center, ul. Bartycka 18, 00-716 Warszawa,*
[2] *Warsaw University Observatory, Aleje Ujazdowskie 4, 00-478 Warszawa, Poland*

Abstract. After a brief historical introduction and recalling basic concepts of stellar oscillation theory, I focus my review on interpretation of secondary periodicities found in RR Lyrae stars and Cepheids as a manifestation of nonradial mode excitation.

1. Introduction

Even after Ledoux's (1951) seminal paper on nonradial oscillations in β Canis Majoris, the idea that such oscillation may be spontaneously excited in stars was not generally accepted. The paradigm of radial pulsation was too deeply rooted. When I (Dziembowski 1971) found that in the radiative cores of evolved stars all nonradial modes become gravity waves of very short wavelength, which leads to a large energy loss, I thought that this explained why Cepheids and RR Lyrae stars excite radial modes only. However, I soon became sceptical about it.

Few years later, independently Osaki (1977) and myself (Dziembowski 1977) showed that models of classical pulsators are unstable to excitation of not only radial but also certain nonradial modes beginning from some moderate degrees. The instability was found for an unfitted envelope upon assuming certain boundary conditions, which each of us derived in different ways and there was an unessential difference in its form.

Complete stellar models are needed to study low degree modes. First survey of low degree modes in an RR star model by Van Hoolst et al. (1998) revealed very dense spectra of unstable modes in the instability range of radial modes but their growth rates were much lower. The authors believed that the dipolar modes, which reach growth rate maxima very close to radial modes, may be excited and cause the Blazhko effect.

2. Nonradial oscillation driven by the opacity mechanism

In Figure 1 I show an example of the two types of unstable modes in the model of RR Lyrae star. All modes shown in this figure owe their instability to the same effect but its efficiency, measured by the driving rate, depends on the relative amplitude in the driving zone; the zone is localized in the outer part of a star. Therefore, the high driving rates are found for modes that are best trapped in

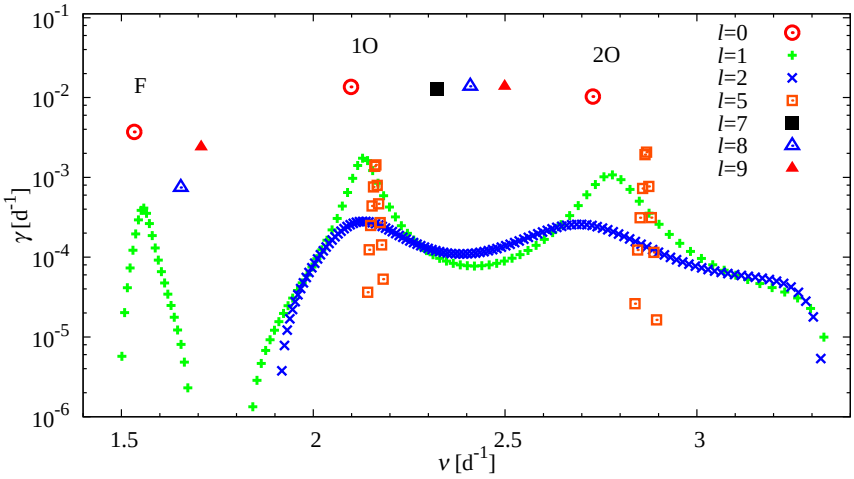

Figure 1. Driving rates of unstable modes in an RR Lyrae star model. The model was selected from the evolutionary track starting from ZAHB with the parameters $M = 0.67 M_\odot$, $Y_{\rm surf} = 0.23$, $Z_{\rm surf} = 0.001$, and $\alpha_{\rm MLT} = 1.99$. The current model parameters are $X_{\rm c} = 0.687$, $\log(L/L_\odot) = 1.717$, $\log T_{\rm eff} = 3.805$.

the outer (acoustic) cavity, which extends down to the place where

$$\max(\mathcal{N}, \mathcal{L}_\ell) = \omega.$$

I adopted here the standard notation for the angular frequency of mode, $\omega = 2\pi\nu$, for the Brunt-Väisälä frequency

$$\mathcal{N} = \sqrt{g\left(\frac{1}{\Gamma_1}\frac{{\rm d}\log P}{{\rm d}r} - \frac{{\rm d}\log\rho}{{\rm d}r}\right)},$$

and the Lamb frequency

$$\mathcal{L}_\ell = \sqrt{\ell(\ell+1)}\frac{c}{r}.$$

There is no inner (gravity wave) cavity for radial modes. For nonradial modes, its top and the bottom are determined by the equality

$$\min(\mathcal{N}, \mathcal{L}_\ell) = \omega.$$

The layer between the two cavities, called evanescent zone, determines the strength of trapping. It is the weakest at $\ell = 2$ and 3 because the two critical frequencies are close to each other but further increase of ℓ results in stronger trapping.

At $\ell = 5$, the modes have still the mixed character. We see in Fig. 1 few unstable modes which are partially trapped in the outer cavity. Their frequencies depend on the properties of the two cavities. Already at $\ell = 7$ there is only one unstable mode associated with the radial mode. For them we will use the $f, p_1, ...$ notation adopted in nonradial oscillation theory. The general category of such

modes was termed by Van Hoolst et al. (1998) the Strongly Trapped Unstable (STU) modes.

In the gravity-wave cavity, the $\mathcal{N}/\omega$ ratio reaches very high values that allows to represent the eigenfunctions of the solution as a superposition of the running wave carrying the energy upward and downward. The neglect of the former leads to the boundary condition which may be safely used only for unstable modes. This is why the letter U is essential in the acronym STU.

3. Why may it be easier to detect nonradial modes at the harmonic than at mode frequencies?

So far efforts to identify the nature of the periodicity in the $(0.6-0.65)P_{1\mathrm{O}}$ range in Cepheids and in RR Lyrae stars (hitherto called P_{x}) were made under the assumption that they are due to individual mode periods. Here I will show that they are likely to be due to harmonics.

Let us consider oscillations in a slowly rotating star written in the inertial spherical coordinate system $(r,\,\theta,\,\phi)$ centered in the star with polar axis aligned with the rotation axis. Then the relative perturbation of the surface radius caused by modes of the angular degree, ℓ, and the azimuthal order $m \le 0$ (these two numbers will be given only when needed) may be written as follows,

$$\frac{\delta R}{R} = \epsilon_z \tilde{P}_\ell^0 \cos(\alpha_z - \omega t) + \tilde{P}_\ell^m[\epsilon_p \cos(\psi_p - \omega t) + \epsilon_r \cos(\psi_r - \omega t)],$$

where the subscripts z, p and r, refer to zonal, prograde and retrograde modes, respectively, $\tilde{P}_\ell^m$ are proportional to the usual associated Legendre functions, except that they are normalized so that each ϵ represents the rms value of $\delta R/R$. For the compactness, I defined

$$\psi_p = \alpha_p + m[\phi - (1-C)\Omega], \quad \text{and } \psi_r = \alpha_r - m[\phi - (1-C)\Omega],$$

where C is the Ledoux constant. $\alpha_{r,\ell}^m$ and $\epsilon_{r,\ell}^m$ denote phases and the rms amplitudes, which are arbitrary in linear theory. Then, the approximate expression for the observable photometric amplitude in the specified passband (here I) is

$$A_{\mathrm{I,obs}}(i) = \epsilon |b_{\ell,\mathrm{I}} \tilde{P}_\ell^m(\cos\theta_{\mathrm{obs}})| \sqrt{(B_T|f|)^2 - 2B_T B_R |f| \cos(\arg f) + B_R^2}, \qquad (1)$$

where $i = \theta_{\mathrm{obs}}$,

$$b_{\ell,\mathrm{I}} = \int_0^1 h_{\mathrm{I}} P_\ell \mu d\mu, \quad \text{with } h_{\mathrm{I}} \text{ being the limb darkening coefficient,}$$

$$B_T = \frac{1}{4}\frac{\partial \log F_I}{\partial \log T_{\mathrm{eff}}}, \quad \text{and} \quad B_R = (\ell-1)(\ell+2).$$

f is complex coefficient that connects the local radiative flux perturbation to the radius perturbation. The b_ℓ coefficient describes cancellation of contributions from various parts of the stellar disc. Its behaviour for low degree modes is plotted in Fig. 2. We observe that even at moderate ℓ it drops by 2 to 3 orders of magnitude as compared to radial mode.

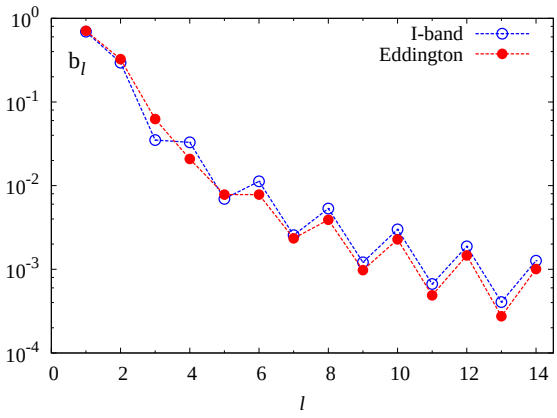

Figure 2. Cancellation factor with two versions of limb darkening law.

The most obvious and likely dominant effect contributing to peaks at the harmonic is the nonlinearity of the $\delta F(\delta R)$ dependence. These peaks arise first from the terms that are proportional to $(\delta R/R)^2$. If we square the expression for $\delta R/R$, because of orthogonality of the associated Legendre functions, only squared functions survive the integration over $\cos\theta$. The only ϕ-dependent coefficients that survive the integration over the azimuth angle are constant terms and terms with $2\omega t$ dependence. The squares of the associated Legendre functions may be put in the form of the following series,

$$(\tilde{P}_\ell^m)^2 = \sum_{k=0}^{2\ell} a_k \tilde{P}_{2k}^{2m}.$$

In view of the steep decline of b_ℓ, it is justified to neglect all higher order terms. Then, using $a_0 = 2 - \delta_{m,0}$, we obtain the following expression for $(\delta R/R)^2$:

$$\left(\frac{\delta R}{R}\right)^2 = \frac{1}{2}\left[\epsilon_z^2 \cos(2\alpha_z - 2\omega t) + 2\epsilon_p\epsilon_r \cos(\alpha_p + \alpha_r - 2\omega t)\right]. \qquad (2)$$

We have only harmonic time-dependence and no cancellation, which for the peaks at individual frequencies is described by the b_ℓ factor. This is why we may have high amplitude at the harmonic and, in addition, all components of the multiplet contribute to 2ω. Let's note that in the linear approximation all the components contribute at different frequencies. Therefore we can expect much simpler structure in the frequency spectrum near 2ω than at ω. Further, we expect much less variability connected with individual frequencies at around 2ω than at ω where complex interaction within the multiplet occurs, even for the simple dipole case as shown by Buchler et al. (1995).

4. Interpretation of the $P_{\mathbf{x}}$ periodicity in 1O Cepheids

Models used for comparison with data in Fig. 3 are the same as in Dziembowski (2012). In particular, the adopted mass-luminosity relation is $\log L/L_\odot = 3.05+$

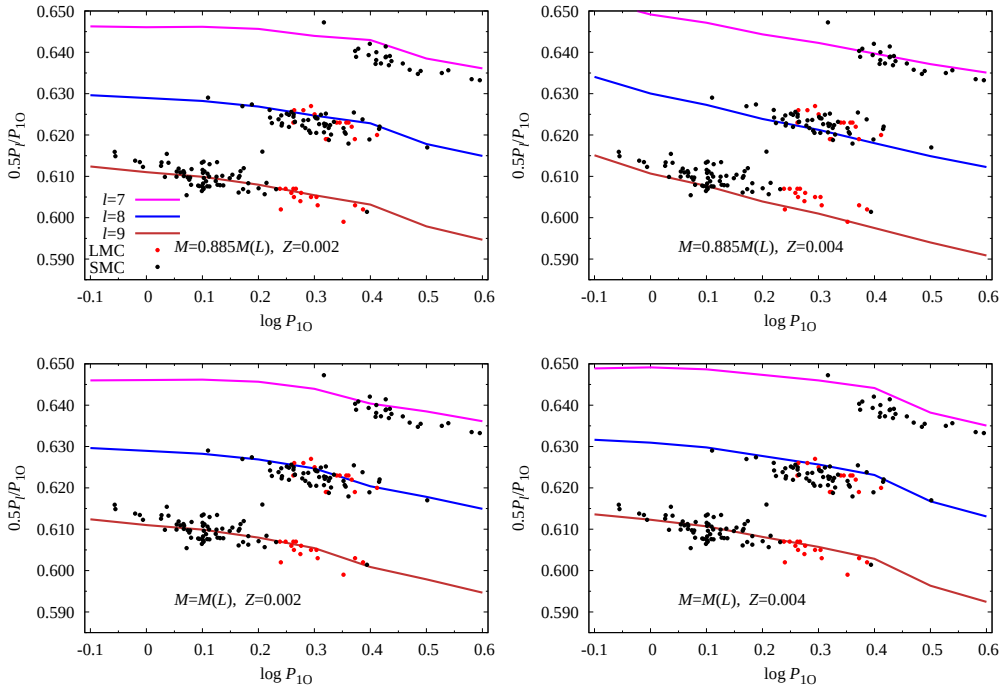

Figure 3. OGLE-III data on $P_{\rm x}$ periods (black dots – SMC, red dots – LMC) confronted in the Petersen diagram with the values of the $0.5P_\ell/P_{1\rm O}$ ratios calculated for stellar envelope models. The lines connect the interpolated ratios at the eight selected values of $\log P_{1\rm O}$ within the instability strip.

$3.6\cdot(\log M/M_\odot - 0.602)$. The observational data are also the same. The difference is in association of the three sequences in the Petersen diagram well visible in OGLE-III data for Cepheids in the Magellanic Clouds (Soszyński et al. 2008, 2010), with oscillation modes. In my 2012 paper, if $P_{\rm x}$ corresponds to unstable modes then the only possibility are f-modes at $\ell = 42, 46$, and 50. There is a number of difficulties for such identification. For instance, while the absence of odd degrees may be blamed to the visibility pattern shown in Fig. 2, the conspicuous lack of $\ell = 44$ and 48 seems impossible to explain. Moreover, there is a good deal of uncertainty in claiming instability of the invoked high degree modes. The *bona fide* driving operates solely in the H-ionization zone, in which convective flux dominates and calculations are notoriously not credible.

In the new picture, the top sequence is due to excitation of the $\ell = 7$ in stars with $\log L/L_\odot \in [3.15, 3.45]$ and $M/M_\odot \in [4.7, 5.2]$, if $Z = 0.002$. The range of luminosity is similar at higher metal abundance but implied masses are lower. At $\ell = 7$ instability occurs only at $\log P_{1\rm O} \gtrsim 0.4$, which corresponds to $\log L/L_\odot \gtrsim 3.1$. The remaining two sequences are well accounted for with unstable $\ell = 8$ and 9 modes in models satisfying adopted mass-luminosity relation at $Z = 0.002$. It is of some interest that this relatively low Z fits to both the SMC and LMC objects, which is well below value of 0.008 usually adopted for massive stars in the LMC. This may explain the much lower incidence rate of

P_x periodicity in this galaxy. The sequence formed by the $\ell = 9$ modes extends from $\log P_{1O} = -0.05$ to 0.4, which corresponds to $\log L/L_\odot \in [2.63, 3.3]$ and $M/M_\odot \in [3.05, 4.7]$. Let us notice that the LMC stars occupy the long period part of the sequence.

With the new interpretation of the P_x periodicity the three sequences seen in the data may be identified with the first three STU f-modes. In the outer part of stellar envelopes, in the driving layers, these modes are similar to radial F-modes. Thus, what we see in the 1O/X stars may be regarded as a form of double-mode pulsation, not much different from the F/1O pulsations and presumably arising in similar circumstances.

5. Interpretation of the P_x periodicity in RRc stars

The P_x periodicity was first discovered in RRc stars. However, only after Netzel et al. (2015b,c) analysis of the OGLE-IV data on RRc stars in the Galactic bulge, we have a sufficiently large sample for studying general properties of RRc stars exhibiting the P_x periodicity.

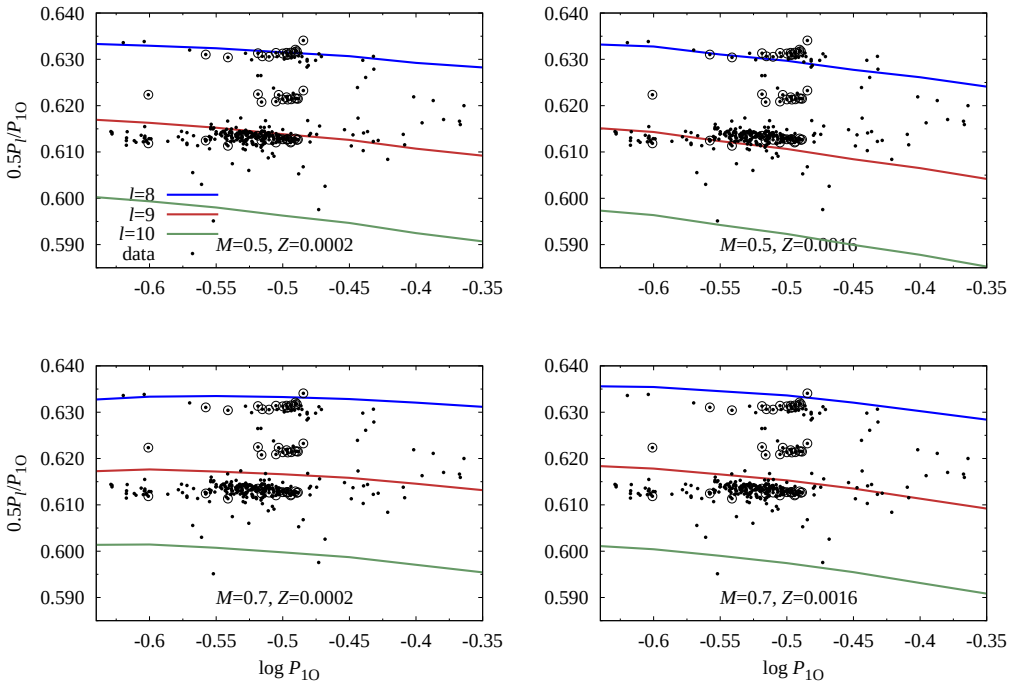

Figure 4. Similar to Fig. 3 but for data for the Galactic bulge RRc stars and suitable envelope models. The encircled dots refer to multiple P_x peaks present in one object

In Fig. 4, like in Fig. 3, we also see three sequences. Within the adopted interpretation of the P_x, the bottom and top sequences may only be associated with $\ell = 9$ and 8 modes, respectively. Then the intermediate sequence may be associated with the corresponding combination peaks. This is consistent with

large fraction of peaks that have partners in one or both surrounding sequences (encircled stars in Fig. 4).

As we may see in Fig. 4, the lower mass models fit to the sequences better. At the long period end, the best fit is achieved for the lower values of Z and $\log(L/L_\odot) \approx 1.65$. At the opposite end, where the fit is better for the higher Z, $\log(L/L_\odot) \approx 1.55$. This is consistent with the known trend of the metallicity-luminosity dependence in RR Lyrae stars.

6. Problems with the long periodicity

Recently, Netzel et al. (2015a) found in the OGLE-IV Galactic bulge photometric data 11 objects classified as RRc showing hitherto unknown periodicity, close to $1.458P_{1O}$. Periods of F-modes in RR Lyrae stars are always shorter. Thus, if this periodicity is to be associated with an oscillation mode, it is most likely stable. A possible exception to consider are dipolar modes, which as we see in Fig. 1, may stay unstable at periods longer than P_F. However, it seems impossible to explain why the modes located far from the driving rate maximum should always be selected.

Stellar envelope models with $1.458P_{1O} = P_F$, that is, $P_S/P_L \approx 0.686$, may be constructed if these objects are not RRc stars but stripped giants similar to OGLE-BLG-RRLYR-02792 (Pietrzyński et al. 2012). Such models may reproduce positions of these objects in a standard Petersen diagram, as shown in Fig. 5. This is an attractive alternative to the interpretation of the $1.458P_{1O}$ periodicity in terms of nonradial modes. Unfortunately, it is not supported by data for the *Kepler* object KIC 9453114 where this periodicity coexists with that at $0.614P_{1O}$ (Moskalik et al. 2015). The latter, more significant, is fully consistent with the positions occupied by the $\ell = 9$ modes in the low mass RRc stars and it would be at about half distance between the $\ell = 9$ and 8 (or 10) if the masses are as low as required with the stripped giant interpretation. On the other hand, interpretation of the $1.458P_{1O}$ periodicity in KIC 9453114 as a consequence of nonradial mode excitation has also unacceptable implications.

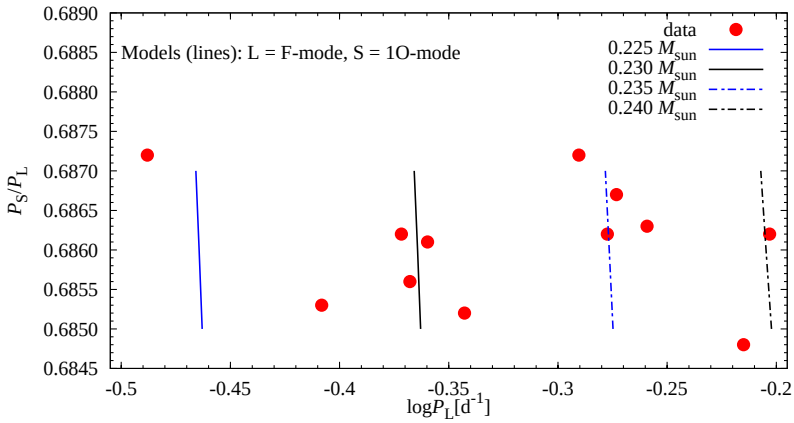

Figure 5. Low-mass giant models in the Petersen diagram.

7. Conclusions

Nearly forty years after the first results from linear nonadiabatic calculation for models of Cepheids and RR Lyrae stars, showing that there are unstable modes in the models, we finally have a convincing evidence that such modes are indeed excited in stars of both types. The evidence is based on the interpretation of periodicity $(0.6 - 0.65)P_{1O}$ (named P_x) found in 1O Cepheids and RRc stars. In the new interpretation, this periodicity arises from harmonics of nonradial f-modes effectively trapped in the outer part of envelope and, as shown in 1977, are driven by the opacity mechanism with a similar rate as the radial F-mode. In Cepheids the modes have angular degrees from $\ell = 7$ to 9, in RR Lyrae only 8 and 9 but, in addition, the signature of the 8+9 combination peak is visible.

The signals at $2P_x$, originally interpreted as subharmonic, are now attributed to mode frequencies. The signatures extend over a broad range, because in fact there are $2\ell+1$ components corresponding to different m-values. Since Cepheids and RR Lyrae stars are slow rotators, we cannot expect the components to be resolved, as the frequency peaks are wide and variable. This variability may arise from resonant interaction between $m = 0$ and the $\pm m$ pairs. Reliable central frequencies are best obtained from P_x, because all components contribute to the peak at 2ω only. It remains to be seen whether they provide useful constraints on stellar global parameters.

The nature of the $1.458P_{1O}$ periodicity in RRc stars is still a puzzle. It could be attributed to P_{1O}/P_F period ratio if the objects are low-mass stripped giants rather than RRc stars. However, data from one star observed with *Kepler* contradict such interpretation, but they cannot be used to support the interpretation invoking the nonradial mode either.

Acknowledgements

This paper is based on materials included in part in the joint publication, coauthored by Radek Smolec, to be published soon. I would like to thank Radek Smolec and my wife Anna for their help in preparing the manuscript. My research is supported by the Polish National Science Centre through grant DEC-2012/05/B/ST9/03932.

References

Buchler, J.R., Goupil, M.-J., Serre, T. 1995, A&A, 296, 405
Dziembowski, W. 1971, Acta Astron., 21, 289
Dziembowski, W. 1977, Acta Astron., 27, 95
Dziembowski, W. A. 2012, Acta Astron., 62, 323
Ledoux P. 1951, ApJ, 114, 373
Moskalik, P., Smolec, R., Kolenberg, K. 2015, MNRAS, 447, 2348
Netzel, H., Smolec, R., Dziembowski, W. 2015a, MNRAS, 451, L25
Netzel, H., Smolec, R., Moskalik, P. 2015b, MNRAS, 447, 1173
Netzel, H., Smolec, R., Moskalik, P. 2015c, MNRAS, 453, 2022
Osaki, Y. 1977, Publ. Astron. Soc. Japan, 29, 235
Pietrzyński G., Thompson, I. B., Gieren, W., et al. 2012, Nature, 484, 75
Soszyński, I., Poleski, R., Udalski, A., et al. 2008, Acta Astron., 58, 163
Soszyński, I., Poleski, R., Udalski, A., et al. 2010, Acta Astron., 60, 17
Van Hoolst, T., Dziembowski, W. A., Kawaler, S. D. 1998, MNRAS, 297, 536

RRL2015 – High-Precision Studies of RR Lyrae Stars
L. Szabados, R. Szabó, K. Kinemuchi (Eds.) 2016

Nonradial modes in RR Lyrae stars from the OGLE Collection of Variable Stars

Henryka Netzel[1], Radosław Smolec[2], & Paweł Moskalik[2]

[1] *Warsaw University Astronomical Observatory, Warsaw, Poland*
[2] *Nicolaus Copernicus Astronomical Center, Warsaw, Poland*

Abstract. The Optical Gravitational Lensing Experiment (OGLE) is a great source of top-quality photometry of classical pulsators. A collection of variable stars from the fourth part of the project contains more than 38 000 RR Lyrae stars. These stars pulsate mostly in the radial fundamental mode (RRab), in radial first overtone (RRc) or in both modes simultaneously (RRd). Analysis of the OGLE data allowed to detect additional nonradial modes in RRc and in RRd stars. We have found more than 260 double-mode stars with characteristic period ratio of the additional (shorter) period to first overtone period around 0.61, increasing the number of known stars of this type by a factor of 10. Stars from the OGLE sample form three nearly parallel sequences in the Petersen diagram. Some stars show more than one nonradial mode simultaneously. These modes belong to different sequences.

1. Introduction

RR Lyrae stars are classical pulsating stars. They are known to pulsate mostly in the radial fundamental mode (RRab) or in the first overtone (RRc). Among RR Lyrae stars there are also double-mode pulsators which pulsate in the fundamental mode and the first overtone simultaneously (RRd, green asterisks in Fig. 1) or in the fundamental mode and the second overtone (red triangles in Fig. 1). The latter group was discovered mostly thanks to excellent space observations. Observations also revealed a group of RR Lyrae stars in which an additional nonradial mode is excited. These stars pulsate in the radial first overtone (RRc or RRd stars) and in an additional mode with shorter period, P_X. The period ratio of the additional mode to the first overtone is in the range of $0.60 - 0.64$ (blue circles in Fig. 1). The most typical value is around 0.61. Such period ratio cannot correspond to two radial modes (Moskalik et al. 2015). Hence, the additional mode (0.61 mode in the following) must be nonradial. This type of pulsations was discovered in 23 RR Lyrae stars, based both on ground- and space-based observations (for a summary see Moskalik et al. 2015) and recently in 18 RR Lyrae stars in M3 (Jurcsik et al. 2015).

2. Data analysis

This 0.61 mode has always a very low amplitude in the millimagnitude regime. Almost all stars observed with space telescopes showed this nonradial mode (Chadid 2012; Molnár et al. 2015; Moskalik et al. 2015; Szabó et al. 2014). The

low amplitude of this mode makes it very difficult to detect it in the ground-based observations. We decided to search for the 0.61 mode in RR Lyrae stars of the Galactic bulge observed by the OGLE project (Udalski et al. 2015; Soszyński et al. 2014). Although the quality of ground-based photometry is lower than of the space-based photometry, the number of observed stars is much higher in ground observations.

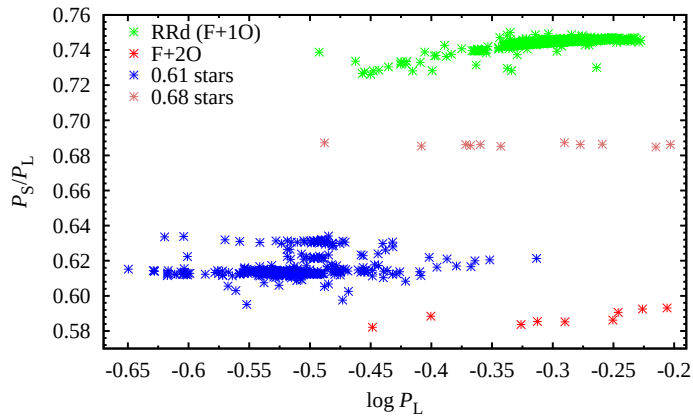

Figure 1. Multi-mode pulsations of RR Lyrae stars in the Petersen diagram.

For the analysis we chose all stars available from the OGLE-III (Soszyński et al. 2011) pulsating in the first overtone. Our input sample consists of 4989 RRc stars and 91 RRd stars. RRc stars were analysed with an automatic method using dedicated software (for details see Netzel et al. 2015a) and the 91 RRd stars were analysed manually. It resulted in a detection of 147 stars with the 0.61 mode (3% of the sample).

In OGLE-IV there are more than 10 000 RRc stars. Because our analysis was focused on a search for low amplitude signals, we decided to choose only the most frequently observed stars. These are located in OGLE fields 501 and 505 (see the position of observational fields in Fig. 15 in Udalski et al. 2015). The input sample consists of 485 RRc stars, which were analysed manually. The rest of stars observed during the fourth phase will be analysed automatically. We detected 131 RRc stars, of which 115 are new discoveries (Netzel et al. 2015b). With the best quality data the 0.61 mode is found in 27% of stars. We also detected another group of double-mode radial–nonradial RR Lyrae stars (magenta crosses in Fig. 1, Netzel et al. 2015c).

3. Results

The Petersen diagram for multi-mode RR Lyrae stars is presented in Fig. 1. All known 0.61 stars are marked with blue asterisks. Thanks to the OGLE data we know altogether 303 0.61 stars, compared to 41 previously known. With such a numerous sample we can see for the first time three sequences in the Petersen diagram. The lowest sequence, around period ratio 0.61, is the most populated. The highest sequence is less populated and is located around period ratio 0.63. Between these two, there is a third, less-populated sequence but well separated

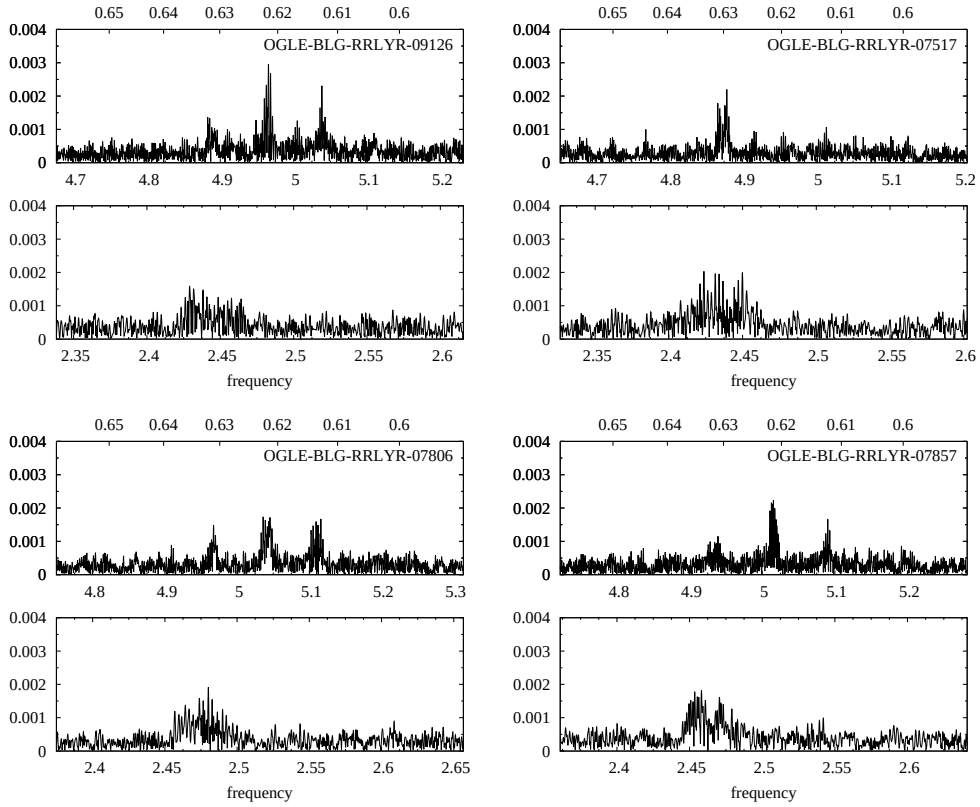

Figure 2. Frequency spectra centered at the frequency range characteristic of the additional mode (top panels) and its 1/2 subharmonic (bottom panels) for a sample of 0.61 stars. Directly underneath a signal with frequency f (top panel) its subharmonic with frequency $1/2f$ is located (the bottom panel). The period ratio of the additional mode (top panels) to first overtone is indicated above the top panel.

from the other two; it is clustered around period ratio 0.62. The structures we detect in the power spectra of the stars are very broad (see Fig. 3 in Netzel et al. 2015b). In the time-domain, it corresponds to variability of the amplitude and the phase of the signal. This behaviour of 0.61 mode is confirmed by other studies both from ground-based (e.g. Jurcsik et al. 2015) and space-based observations (e.g. Moskalik et al. 2015; Molnár et al. 2015; Szabó et al. 2014). The most exciting result is the discovery of stars which have three signals in the power spectrum corresponding to the three sequences in the Petersen diagram. Power spectra of 6 stars such as these are presented in Fig. 5 in Netzel et al. (2015b).

Another common property of 0.61 stars is the occurrence of subharmonics of the additional mode, both 1/2 f_X and 3/2 f_X. We detected signal at a subharmonic frequency in 26 stars, which constitute 20% of the OGLE-IV 0.61 stars. Additional modes and their subharmonic are shown in Fig. 2 for selected stars (see also Fig. 11 in Netzel et al. 2015b). The structures of the subharmonics are very complex. They appear in the power spectra as wide bands of excess power.

Before our analysis of the OGLE data, subharmonics were detected only in space observations. Typically, the presence of a subharmonic frequency indicates the period doubling of the parent mode (see e.g. Smolec et al. 2012). However, there is another possibility proposed by Dziembowski (these proceedings). The signal around 1/2 f_X can be a real mode present in a star, while the signal at f_X is its harmonic.

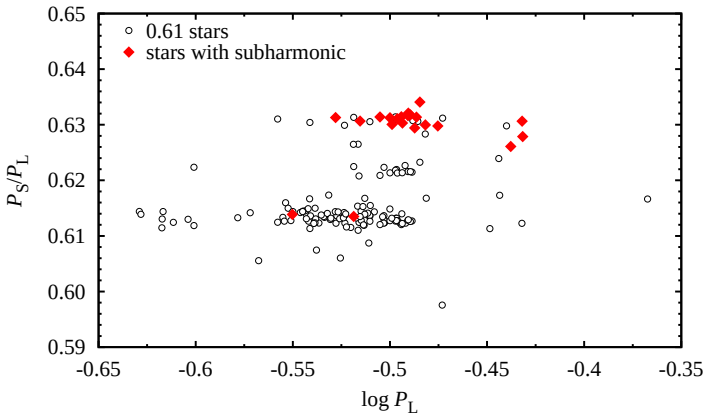

Figure 3. The Petersen diagram of 0.61 stars. Stars found in the OGLE data are marked with black circles. Stars which have frequency at the subharmonic are marked with red diamonds (only stars which show significant signal at f_X *and simultaneously* at around 1/2 f_X are marked).

The majority of the signals at the subharmonic frequency range, 75%, correspond to the 0.63 sequence. In Figure 3 we present the Petersen diagram for 0.61 stars from the OGLE data. With red diamonds we marked stars for which signal at the subharmonic is detected. The majority of these stars occupy the highest sequence. This finding supports the model proposed by Dziembowski (these proceedings).

Acknowledgement

This research is supported by the Polish National Science Centre through grant DEC-2012/05/B/ST9/03932.

References

Chadid, M., 2012, A&A, 540, A68
Jurcsik, J., Smitola, P., Hajdu, G., et al. 2015, ApJS, 219:26
Molnár L., Szabó, R., Moskalik, P. A., et al. 2015, MNRAS, 452, 4283
Moskalik, P., Smolec R., Kolenberg, K. et al. 2015, MNRAS, 447, 2348
Netzel, H., Smolec, R., Dziembowski, W. 2015c, MNRAS, 451, L25
Netzel, H., Smolec, R., Moskalik, P. 2015a, MNRAS, 447, 1173
Netzel, H., Smolec, R., Moskalik, P. 2015b, MNRAS, 453, 2022
Smolec, R., Soszyński, I., Moskalik, P., et al. 2012, MNRAS, 419, 2407
Soszyński, I., Dziembowski, W. A., Udalski, A., et al. 2011, Acta Astron., 61, 1
Soszyński, I., Udalski, A., Szymański, M. K., et al. 2014, Acta Astron., 64, 177
Szabó R., Benkő J. M., Paparó M. 2014, A&A, 570, A100
Udalski, A., Szymański, M. K., Szymański, G. 2015, Acta Astron., 65, 1

RRL2015 – High-Precision Studies of RR Lyrae Stars
L. Szabados, R. Szabó, K. Kinemuchi (Eds.) 2016

The unique dynamical system underlying RR Lyrae pulsations

Zoltán Kolláth[1,2]

[1] *Konkoly Observatory, Research Centre for Astronomy and Earth Sciences, Hungarian Academy of Sciences, H-1121, Budapest, Konkoly Thege Miklós út 15-17, Hungary*
[2] *University of West Hungary, Szombathely, Hungary*

Abstract. Hydrodynamic models of RR Lyrae pulsation display a very rich behaviour. Contrary to earlier expectations, high order resonances play a crucial role in the nonlinear dynamics representing the interacting modes. Chaotic attractors can be found at different time scales: both in the pulsation itself and in the amplitude equations shaping the possible modulation of the oscillations. Although there is no one-to-one connection between the nonlinear features found in the numerical models and the observed behaviour, the richness of the found phenomena suggests that the interaction of modes should be taken seriously in the study of the still unsolved puzzle of Blazhko effect. One of the main lessons of this complex system is that we should rethink the simple interpretation of the observed effect of resonances.

1. Introduction

Recent space- and ground-based observations of RR Lyrae stars have resulted in a golden age of stellar pulsation studies. A new level of complexity is uncovered; new pieces of the great puzzle of RR Lyrae variability have been found: e.g. unexpected pulsation modes and resonances. One of the most interesting features among the new findings is the period doubling visible in most of the Blazhko modulated stars (Szabó et al. 2010). Furthermore this effect is clearly the consequence of a high order (9:2) resonance of the fundamental mode with a strange 9th overtone (Kolláth et al. 2011).

In addition, observations and hydrodynamic models suggest that a third mode may play an important role in the dynamics. Considering that the interaction of two modes leads to a rare and unique dynamical system, the interaction of the base system with additional modes may produce even more interesting behaviour.

The final question remains still unsolved: whether the very complex interaction of modes can solve the mystery of the Blazhko effect. Anyway, the dynamics of RR Lyrae pulsations provide useful lessons in general in relation to nonlinear processes in nature. In this paper we concentrate only one aspect of the complex dynamical system underlying RR Lyrae pulsation: how the resonance appears in modulated solutions. This question is investigated both for the amplitude equations and hydrodynamic calculations.

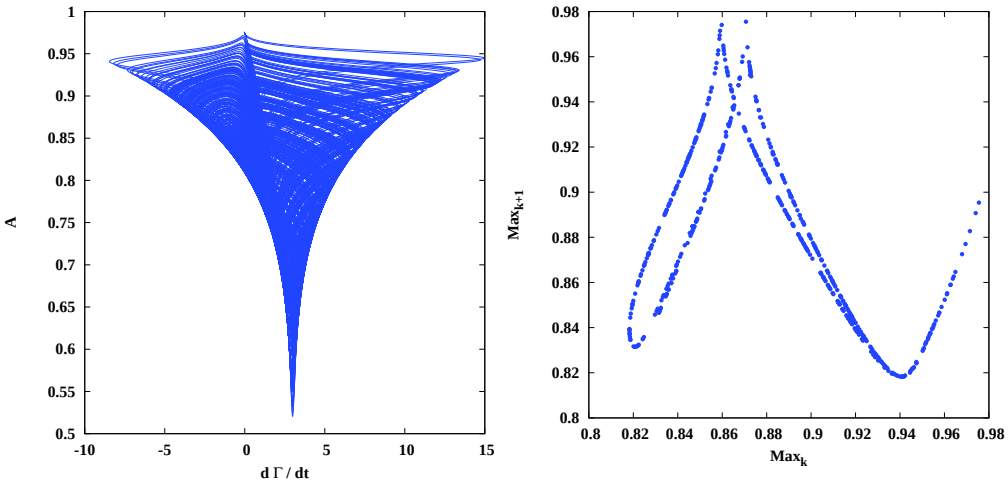

Figure 1. The chaotic attractor of the resonant amplitude equations (left) and corresponding first return map (right).

2. A rare chaotic attractor related to the 9:2 resonance

The period doubling bifurcation found in the hydrodynamic models is a consequence of the resonant interaction of the 9th overtone with the fundamental mode. This effect can be understood by a simplified model of pulsations: if the solution of the amplitude equations with half-integer resonances is a nonzero fixed point (i.e. the amplitudes of both modes are constant) this system provides a natural description of period doubling. Buchler & Kolláth (2001) demonstrated, that the same amplitude equations have solutions that may explain the modulation of RR Lyrae stars, furthermore this modulation can be chaotic. In this paper we use a simplified version of the resonant amplitude equations which is capable to present the major properties of the system:

$$\begin{aligned} \frac{dA_0}{dt} &= \left(1 - A_0^2 - rA_9^2\right)A_0 + cA_0^8 A_9^2 \cos(\Gamma) \\ \frac{dA_9}{dt} &= \left(\kappa - A_9^2 - sA_0^2\right)A_9 + bA_0^9 A_9 \cos(\Gamma) \\ \frac{d\Gamma}{dt} &= 2\Delta - 9cA_0^7 A_9^2 \sin(\Gamma) - 2bA_0^9 \sin(\Gamma), \end{aligned} \tag{1}$$

where A_0, A_9 are the amplitudes of the fundamental mode and the 9th overtone; c, b, r, s and κ are constant parameters. Γ is the phase differences of the modes, its derivative gives the instantaneous frequency difference from the resonance: $d\Gamma/dt = 2\omega_0 - 9\omega_9$. The constant term which forces the system to deviate from the resonance is given by Δ. Please note that we reduced the number of coefficients by setting the time scale to the growth rate of the fundamental mode and by normalizing the amplitudes.

The strange attractor of the system and the first return map calculated from the maxima of the fundamental mode amplitude variation are displayed in Fig. 1.

The parameters used for the figure are the following: $c = 1.5$, $b = 10$, $r = s = 1.0$, $\kappa = -0.1$ and $\Delta = 1.5$. This chaotic attractor represents a very rare type of dynamics: a double cusp map, where the two leaves of the attractor do not superpose exactly. The only known system of this type is the one proposed by Rössler & Ortoleva (1978). It is remarkable that the interaction of two modes results in such a rich dynamical phenomena.

We have to note that modulated solutions of the amplitude equations exist only for non-zero values of the offset parameter Δ. When Δ is small, the resonance locks and a clean period doubled state is obtained. One of the most important pieces of information one can learn from Fig. 1 is that $d\Gamma/dt$ has a non zero mean and a wide distribution. It clearly demonstrates that in the Fourier spectra of such systems, broader and offset structures are expected at the half-integer frequencies instead of single peaks.

3. Modulation and resonances in hydrodynamic models

There exist period doubled solutions in RR Lyrae hydrodynamic models, but no model has been found with Blazhko-like modulation. However, Smolec & Moskalik (2012) found both phenomena in BL Herculis models, indicating that such behaviour is expected in hydrodynamic calculations. Moreover, it has been already demonstrated by Plachy et al. (2013) that period doubling coexists with chaotic and multimode pulsations in RR Lyrae models.

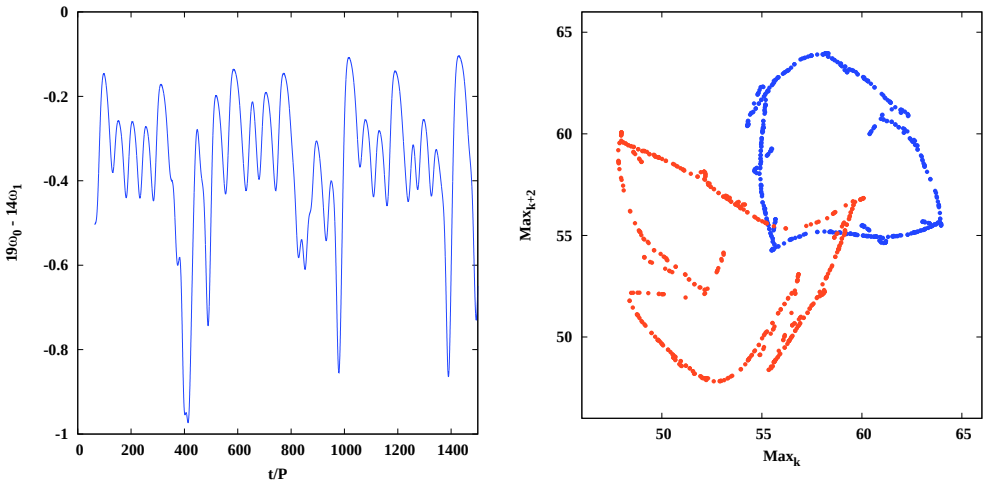

Figure 2. The variation of the relative phase in a hydrodynamic model close to a 14:19 resonance (left) and the corresponding first return map of the radius maxima (right).

When a third mode appears in the interplay of oscillations, the number of possible solutions is increased. For example the interaction of the fundamental mode with the strange mode alters the stability properties of the fundamental mode and makes it more sensitive to other pulsation modes, e.g. our model calculations demonstrated that the period doubled version of the same oscillation now may lose its stability with respect to the first overtone. While in normal double mode scenario of the fundamental mode and the first overtone there is

only one possible solution where both modes coexist, in the presence of the 9th overtone there is a possibility for additional solutions with a double mode character. Figure 2 in Plachy et al. (2013) displays the first return maps calculated from the radius variation of models representing this kind of behaviour.

The right panel in Figure 2 in this paper displays a similar model. By plotting the maxima against the second previous maximum values, the period-doubling structure can be easily recognized (the two branches representing period doubling are plotted with different colours). The substructure of the individual branches is related to the effect of the first overtone which is in a close 14:19 resonance with the fundamental mode. The agglomerations (7 in both branches) in the otherwise smooth return maps are the signs of the still active resonant interaction. In exact resonance the diagram reduces to 14 points in the plot. The instantaneous frequencies are calculated from the radius variation, and the offset from the resonance centre is plotted in the left panel of the figure. Similarly to the 9:2 resonant amplitude equations, an even higher order resonance can play a role in shaping the light variation. And more importantly, an offset from the resonance center results in a slight modulation of the fundamental mode amplitude and a nonzero mean in the $19\omega_0 - 14\omega_1$ off-resonance frequency difference.

4. Conclusion

It is demonstrated that high order resonances play an important role in the dynamics of RR Lyrae model pulsations. However, the exact, phase locked resonance is just one of the possible solutions. In general, when modulation emerges in a resonant system, the behaviour of the dynamics is significantly changed. The main characteristics of these systems are:

- If the frequency offset from the resonance reaches a specific level, the phases are not locked to each other. Even then, fingerprints of the resonance are still observable in the resulting variations.
- The peaks in the Fourier transform of modulated resonant systems do not coincide exactly with the resonant frequencies (e.g. the half integer ones), but there is an offset compared to the resonance centre.
- Broad structures dominate the spectrum instead of single resonant peaks.

Acknowledgments

This research has been supported by the NKFIH K-115709 grant and the European Community's FP7/2007-2013 Programme under grant agreements no. 269194 (IRSES/ASK) and no. 312844 (SPACEINN).

References

Buchler, J. R., Kolláth, Z. 2011, ApJ, 731:24
Kolláth, Z., Molnár, L., Szabó, R. 2011, MNRAS, 414, 1111
Plachy, E., Kolláth, Z., Molnár, L. 2013, MNRAS, 433, 3590
Rössler, O. E., Ortoleva, P. J. 1978, Lecture Notes in Biomathematics, 21, 67
Smolec, R., Moskalik, P. A. 2012, MNRAS, 426, 108
Szabó, R., Kolláth, Z., Molnár, L., et al. 2010, MNRAS, 409, 1244

RRL2015 – High-Precision Studies of RR Lyrae Stars
L. Szabados, R. Szabó, K. Kinemuchi (Eds.) 2016

$K - \log P$ is that all?

J. Lub

Sterrewacht Leiden, Leiden University, Leiden, the Netherlands

Abstract. We investigate the derivation of the $K-\log P$ relation for RR Lyrae stars based upon the simplest possible theoretical pulsation equation. Making use of recent theoretical advances due to Marconi et al. (2015) this leads to a direct determination of M_V for individual stars, but at the same time we rediscover a simple method using the reddening free and metallicity independent combination $W(B,V) = V-3.06(B-V)$ to do the same. We discuss the relation between the two approaches and compare with other determinations in the literature. A consistent distance of the LMC is derived directly from measurements of its RR Lyrae stars.

1. Introduction

Whereas period-luminosity relations abound for their high-mass Population I counterparts, the 'Classical Cepheids', such relations were up till recently of little use for RR Lyrae stars. That is, until it was proven that such relations occur naturally and have a very simple explanation in the near-IR and beyond.

Here we investigate these relations in the light of the recently published 'Framework' by Marconi et al. (2015) and surprisingly resurrect an old suggestion by Fernie (1965) as well. Optical B and V photometric measurements could well be as useful as near-IR data to derive distances. We confront these two approaches with each other.

We have made use of catalogues published by Dambis et al. (2013), Klein et al. (2014)(*WISE*), the reddening maps from *WMAP* by Schlegel et al. (1998) and Schlafly & Finkbeiner (2011), and a variety of data collected by myself from the literature (see below).

Finally we confront our results with other determinations of the RR Lyrae absolute magnitude M_V: globular cluster horizontal branches and relative astrometric parallaxes from *HST* by Benedict et al. (2011) and apply our results to derive the distance to the LMC from the work of Di Fabrizio et al. (2006).

2. $K - \log P$ relation(s)

In a remarkable paper Hertzsprung (1913) calibrated the period-luminosity relation for Cepheids, newly discovered in the SMC by Henrietta Leavitt, see Leavitt & Pickering (1912), by the method of statistical parallax and then went on to determine for the first time the extragalactic distance to the SMC. Less well known is probably that at the same time he addressed the case of RR Lyrae, whose high reduced proper motion showed that it belonged probably to a different population of stars 'more like the Sun', i.e. not to the supergiants.

It is well known now that RR Lyrae stars belong to the old population of our Galaxy and rather than obeying a period-luminosity relation their M_V is on average dependent on metallicity.

Longmore et al. (1990) showed that in the infrared linear $K - \log P$ relations for RR Lyrae stars on the horizontal branches of globular clusters are ubiquitous. One of the most striking examples is the beautiful diagram in the globular cluster Reticulum close to the LMC published by Dall'Ora et al. (2004).

There are indeed many very good reasons to move to the near-IR (e.g. K at 2.2 μm), viz.:

1. Reddening and colour excess are small in K ($E(V-K) = 0.12A_V$).
2. Low amplitude of the light variations ($0\overset{\text{m}}{.}30 - 0\overset{\text{m}}{.}35$), effectively given by the radius variations.
3. Simple (?) theory based upon the van Albada-Baker (vA-B) pulsation relation, colour transformations and bolometric corrections.
4. But ... abundance effects?

Van Albada & Baker (1971) remarked that the scaling relations for a set of (self) similar stellar models gives rise to a relation between P (days), L, $\mathcal{M}$ and $T_{\rm eff}$. Ever since these days, this relation has been standard and every self-respecting theoretician has given his/her own vA-B relation, most recently Marconi et al. (2015), in their 'Framework' paper:

$$\log P = -11.347 + 0.860 \log L - 0.58 \log \mathcal{M} - 3.43 \log T_{\rm eff} + 0.024 \log Z.$$

It is striking that the coefficients of $\log L$ and $\log T_{\rm eff}$ are in the ratio 1:4, so the relation is really much simpler: it is in essence a P-$\mathcal{M}$-R relation. This brings back the fact that it all started with Ritter's $P\sqrt{\rho} = Q$ relation long ago. And seemingly we have now reduced the number of unknowns from 3 to 2, for whatever it is worth.

Stobie (1969) in his survey of the pulsation of helium core burning stars gives a simple relation which fits such models within a few percent. We have adopted this for our purpose as follows:

$$P(\text{days}) = 0.026 \mathcal{M}^{-2/3} R^{5/3}.$$

Now we can demonstrate in a very simple way the origin of the $K - \log P$ relation avoiding all pitfalls of colour transformations, bolometric corrections and the like. For the Sun we have $V_\odot = 4.82$ and $(V-K)_\odot = 1.53$. The IR flux scales as $R^2 T_{\rm eff}$ so:

$$K - K_\odot = -2.5 \log T_{\rm eff} - 5 \log R = -3.5 \log R - 0.625 \log L,$$
$$2.25 \log P = -3.57 + 3.5 \log R - 1.5 \log \mathcal{M},$$

to find finally:

$$K + 2.25 \log P = -0.29 - 0.625 \log L - 1.5 \log \mathcal{M}.$$

What does this give rise to? Taking standard values like $\log L = 1.68$ at [Fe/H] $= -1.3$ and $\log \mathcal{M} = -0.19$:

$K + 2.25 \log P = -1.06$ at [Fe/H] $= -1.3$.

Here we have our $K - \log P$ relation for the metal poor RR Lyrae stars. This is to be compared with the theoretical relation from the Framework which we have adapted to our zero point:

$$K + 2.25 \log P = -0.82 - 2.25 \log P + 0.18[\text{Fe/H}] \ (!)$$

The interesting point here is that our derivation gives in a natural way insight into the dependence of the right hand side of the equation on the stellar parameters. Indeed we find from the selection of horizontal branch models used

in the Framework paper on L, $\mathcal{M}$ and metallicity that this slope is about 0.17. However we will start by assuming first that this dependence is zero.

Finally we would like to remark that nothing is gained by going even further into the infrared. The slope of the period-luminosity relations does not change anymore, the same goes for the Cepheids.

3. Distance moduli from $K - \log P$

In order to proceed we disregard the [Fe/H] dependence for a start and calculate the K-band distance modulus (K-band photometric parallax) as:

$$(m - M)_{K,0} = K_{\rm obs} - 0.12A_V + 2.25 \log P + 1.06 \text{ and:}$$
$$M_V = \langle V \rangle_{\rm int} - A_V - (m - M)_{K,0}.$$

This gives us a consistent set of RR Lyrae absolute magnitudes for a sample of stars with high quality photometric data produced almost 25 years ago, which we compiled from the literature. These data in $UBVRI$ and K were especially acquired for Baade-Wesselink studies of RR Lyrae, they can be found in or are summarized in: Liu & Janes (1989), Carney et al. (1992), Skillen et al. (1993), and Cacciari et al. (1992).

Unavoidably almost the full amount of interstellar absorption has to be corrected for in the final result. Therefore one has to proceed cautiously: one has to check especially at low latitudes or with stars projected against the Magellanic Clouds, that the absorption correction from *WMAP* is not in conflict with (even rather rough) existing photometry.

Our sample has a median [Fe/H] value of -1.36, $N = 45$ stars. Some stars are in common, this is of interest to estimate the achieved precision.

We find $K - \log P$ without metallicity correction:
median absolute magnitude $M_V = 0.604(\pm 0.089)$.

Idem with the theoretical metallicity correction term of 0.18[Fe/H]:
median absolute magnitude $M_V = 0.586(\pm 0.166)$.

We shall mainly make use of the median to characterize our results. The errors quoted will normally be the mean deviation for a single measurement, without correction for the sample size. Note that the small rms in the first case is by construction: we assumed no metallicity dependence and thus artificially reduced the range of M_V. The next Section will provide us with an independent determination and then we will study the metallicity dependence further.

4. Distance moduli from B, V and $\log P$

Fernie (1965) published a short paper titled 'A short method for determining the distances of RR Lyrae stars', giving a period-luminosity-colour relation of the form:

$$M_V = -0.83 - 2.50 \log P + 2.96(B - V)_0.$$

In his Fig. 1 he illustrates this by showing the behaviour of the observed quantity $V - 2.96(B - V)$ as a function of phase for RR Lyrae itself, taken from the original measurements of RR Lyrae by Hardie (1955). He notes:

a. The combination is independent of interstellar reddening and absorption.

b. It follows the temperature variation over the cycle (except not surprisingly, around minimum light, where only the radius changes).

c. Consequently it is rather phase insensitive ...

With an assumed distance modulus of 6.9 this relation did fit the photometry. Unfortunately the basis on which this was derived: a period dependence upon the square of the radius was incorrect and the paper was forgotten.

Nowadays we immediately recognize this quantity as one of many possible W-functions. Upon reading the 'Framework', I was surprised to see that of the many possible combinations of photometric bands the combination $W(B,V) = V - 3.06(B-V)$ is particularly attractive: it has no dependence on metallicity (or mass?) and has all the same advantages as mentioned above.

$$W(B,V)_{\rm theo} = -1.06 - 2.49 \log P.$$

In this relation we combine the intensity mean magnitude $\langle V \rangle_{\rm int}$, which as is well known is equivalent to $V(\phi = 0.3)$ with the value of $(B-V)$ at this phase, which is actually very close to the magnitude mean colour $\langle (B-V)_{\rm mag} \rangle$. A large body of useful and sometimes very accurate photometry exists already. So now we can calculate the visual photometric parallax (distance modulus), which is reddening free, directly as:

$(m-M)_0 = W(B,V)_{\rm obs} - W(B,V)_{\rm theo}$ and consequently

$M_V = V - (m-M)_0 - A_V$ where $A_V = 3.06E(B-V)$ from *WMAP*.

We can now study the dependence of these absolute magnitudes on metallicity and compare them with the results from the previous Section.

Median M_V from $W(B,V)$ 0.595($\pm$0.175) at [Fe/H] = -0.134.

Correlation with [Fe/H]: 0.927 with a slope of 0.34.

We can compare this with the result from the previous Section. It is of interest to determine the residuals between M_V as determined from $K - \log P$ without metallicity correction and M_V from $W(B,V)$: median residual is found as: 0.015($\pm$0.114) with a correlation of 0.919 and a slope of 0.18, fortuitously close to the Framework prediction (!). As a check after applying this metallicity correction: correlating both determinations give a slope of 0.96 with a correlation coefficient of 0.972, making them essentially identical.

One also notes that the mean deviations over the sample are almost equal, reflecting the metallicity dependence. The conclusion is that indeed the theoretical metallicity correction in $K - \log P$ is needed. So now we have two relations to derive RR Lyrae distances rather than the one we started with.

As a final note: Kovács & Walker (2001) and Kovács (2003) related $W(B,V)$ to light curve parameters (P, A_1 and ϕ_{31}) also in an attempt to derive absolute magnitudes.

5. Applications

How do our two methods compare to previous distance determinations? In order to investigate this we took the archetypal globular cluster M3. K-band data are from Longmore et al. (1990), and for the same set of stars we took B and V from Cacciari et al. (2005). We find $(m-M) = 15.05$ and 15.08, respectively from K and $W(B,V)$ and $M_V = 0.55$ and 0.54, this is completely in line with

the data in the Harris (1996) catalogue (edition 2010), viz 15.07. Note: using the old data (Sandage & Roberts, 1954) the result would have been 14.97, this is explained by the fact that $(B-V)$ has been transformed from $C.I.$ and is too red by 0.03.

It is fundamental to compare to astrometric determinations. We will not address here the case of the statistical parallax solutions, but concentrate on the relative astrometric parallaxes from *HST* by Benedict et al. (2011). Whereas they took great care to avoid any bias due to the photometric parallaxes from the background stars before being able to use their results, it proved necessary to rediscuss them.

1. No Lutz-Kelker corrections must be applied to single stars. We removed this bias.

2. The photometry used in the paper is not always of the best quality. The reddening of XZ Cyg is only $E(B-V) = 0.04$, the RZ Cep photometry is uncertain.

3. The RRc star RZ Cep is a problem: in the text and the tables, different values of the parallax are quoted. The final choice $M_V = 0.28$ is incompatible with the pulsation equation. In correspondence with Dr. Benedict I found out that actually there were 2 possible solutions. For a lack of better solution, we took the average. It has also the highest reddening $E(B-V) = 0.25$, but this appears correct apart from any 'variations' in the reddening law average.

Giving RR Lyrae double weight, we find a predicted median M_V from this source of $0.54(\pm 0.05)$ whereas the application of our two methods to the photometry of these 5 stars would give: from K (with abundance term) $0.55(\pm 0.05)$ and from $W(B,V)$ $0.51(\pm 0.06)$. This is summarized in Table 1.

Table 1. Summary comparison of three discussed distance moduli

Name	$\log P_F$	$\langle V \rangle$ int	$B-V$ mean	A_V	$m-M$ *HST*	$m-M$ $W(BV)$	$m-M$ $K \log P$	M_V mean
RR Lyr	−0.247	7.76	0.35	0.10	7.12	7.15	7.02	0.56
SU Dra	−0.184	9.80	0.33	0.03	9.41	9.24	9.29	0.46
UV Oct	−0.266	9.52	0.39	0.26	8.84	8.74	8.75	0.48
XZ Cyg	−0.331	9.68	0.33	0.13	8.89	8.92	9.04	0.60
RZ Cep	−0.383	9.44	0.46	0.78	8.16	8.18	8.11	0.53

Notes:
[1]RZ Cep, the various sources of photometry are in conflict: errors of $0\overset{m}{.}02$ assumed
[2]All other errors of basic observational data are $0\overset{m}{.}01$, combined errors can easily reach $0\overset{m}{.}05$

Finally out of curiosity, we took the data from the 2 LMC fields studied by Di Fabrizio et al. (2005). They discussed in depth the quality of the various sources of RR Lyrae photometry in the LMC. Both fields A and B give the same distance modulus on average: 18.51.

In conclusion, one can say that it appears that we have reached a consistent framework within which RR Lyrae stars can be used for distance determinations.

6. Conclusions and prospects

Lub (1985) reviewed the status of the determination of the physical parameters of field RR Lyrae at the Los Alamos Conference to honour John Cox. In that paper much emphasis was put on the precise derivation of the mean or equilibrium $T_{\rm eff}$. In contrast, here I have tried to avoid any explicit use of temperatures, with rewarding results. Honestly I am surprised by the results I found.

However, there is no apparent solution as yet for the discrepancy of $0\overset{\rm m}{.}10$ with the determinations of M_V from statistical parallax. In addition we seem to have returned to a slightly higher dependence of M_V upon [Fe/H], more in line with the value advocated by Sandage on many occasions in the past, e.g. Sandage (1993). Maybe we should wait for the soon-to-be available first results from *Gaia* to look for an answer.

What are the prospects of the light of this? If it works:

a. RR Lyrae stars can give precise (and consistent) parallaxes to large distances.

b. RR Lyrae stars may help in the study of reddening law variations: R_V.

c. Study of the systematics of RR Lyrae pulsation from precise luminosities.

Acknowledgements

Alexei Dambis and Christopher Klein have been very helpful in giving me access to their data tables in advance of publication. The organizers of the conference deserve to be acknowledged for their support and providing such a relaxed environment for RR Lyraes.

References

Benedict, G. F., McArthur, B. E., Feast, M. W., et al. 2011, AJ, 142:187
Cacciari, C., Clementini, G., Fernley, J. A. 1992, ApJ, 396, 219
Cacciari, C., Corwin, T. M., Carney, T. W. 2005, AJ, 129, 267
Carney, B. W., Storm, J., Jones, R. V. 1992, ApJ, 386, 663
Dall'Ora, M., Storm, J., Bono, G., et al. 2004, ApJ, 610, 269
Dambis, A. K., Berdnikov, L. N., Kniazev, A. Y., et al. 2013, MNRAS, 435, 230
Di Fabrizio, L., Clementini, G., Maio, M., et al. 2005, A&A, 430, 603
Fernie, J. D. 1965, ApJ, 141, 1411
Hardie, R. H. 1955, ApJ, 122, 256
Harris, W. E. 1996, AJ, 112, 487
Hertzsprung, E. 1913, AN, 196, 201
Klein, C. R., Richards, J. W., Butler, N. R., Bloom, J. S. 2014, MNRAS, 440, L96
Kovács, G. 2003, MNRAS, 342, L48
Kovács, G., Walker, A. S. 2001, A&A, 371, 579
Leavitt, H. S., Pickering, E. C. 1912, HarCi, 173
Liu, T., Janes, K. A. 1989, ApJS, 69, 593
Longmore, A. J., Dixon, R., Skillen, I., et al. 1990, MNRAS, 247, 684
Lub, J. 1987, in Stellar Pulsation, Eds: A. N. Cox, W. M. Sparks & S. G. Starrfield, Lecture Notes in Physics, 274, 218
Marconi, M., Coppola, G., Bono, G., et al. 2015, ApJ, 808:50
Sandage, A. R. 1993, AJ, 106, 703
Sandage, A. R., Roberts, M. S. 1954, AJ, 59, 190
Schlafly, E. M., Finkbeiner, D. S. 2011, ApJ, 737:310
Schlegel, D. J., Finkbeiner, D. S., Davis, M. 1998, ApJ, 500, 525
Skillen, I. S., Fernley, J. A., Stobie, R. S., et al. 1993, MNRAS, 265, 301
Stobie, R. S. 1969, MNRAS, 144, 511
van Albada, T. S., Baker, N. H. 1971, ApJ, 169, 311

RRL2015 – High-Precision Studies of RR Lyrae Stars
L. Szabados, R. Szabó, K. Kinemuchi (Eds.) 2016

RR Lyrae stars in ω Centauri: Near-IR properties and period-luminosity relations

Camila Navarrete[1,2], Márcio Catelan[1,2], Rodrigo Contreras Ramos[2,1], Felipe Gran[1,2], & Javier Alonso-García[3,2]

[1] *Institute of Astrophysics, Pontificia Universidad Católica, Chile*
[2] *Millennium Institute of Astrophysics, Chile*
[3] *Unidad de Astronomía, Universidad de Antofagasta, Chile*

Abstract. Omega Centauri (ω Cen) contains a rich harvest of variable stars. Here we report on a deep, wide-field, near-infrared (IR) variability survey for this cluster, carried out using ESO's 4.1 m VISTA telescope. Our time-series data includes more than 180 RR Lyrae light curves in both J and K_s, allowing us to derive an unprecedented homogeneous and complete near-IR catalog of RR Lyrae in the field of ω Cen. Near-IR period-luminosity relations are derived and used to determine an updated (pulsational) distance modulus for the cluster.

1. Introduction

Near-IR observations of RR Lyrae (RRL) stars have some advantages when compared to the optical bands: *(i)* RRL stars follow well-defined near-IR period-luminosity (P-L) relations, that allow to derive precise distances (see e.g., Catelan et al. 2004); *(ii)* the interstellar extinction is one tenth of the one in the visible, enabling to observe RRL in highly-reddened regions, such as the Galactic bulge; *(iii)* the amplitudes in the near-IR are smaller than in the visible, allowing accurate estimates of the mean magnitude with a smaller number of epochs.

Despite these advantages, few well-sampled RRL light curves in the near-IR have been collected so far in the literature (see Table 1 of Angeloni et al. 2014). In this context, ω Cen appears as a suitable target to study the near-IR properties (e.g., amplitudes, mean magnitudes, light curve shapes) of a large sample of RRLs, which had been previously studied in detail in optical bands (Kaluzny et al. 2004; Weldrake et al. 2007).

2. Near-IR RR Lyrae light curves

Our observations were performed using the VISTA 4.1 m telescope and comprises on average 42 epochs in J and 100 epochs in K_s for all the RRL members of the cluster. The first results of this work were published in Navarrete et al. (2015, from now on N15), where the number of RRL cluster members, amplitudes, Bailey diagrams, and Oosterhoff types were already discussed.

2.1. Light curve shape

Optical light curves for most of the RRL stars in the field of ω Cen were collected by Kaluzny et al. (2004), as part of the observations of the OGLE project. Using our near-IR data set, the light curve shape in the optical and in the near-IR wavelengths can be directly compared. Figure 1 shows the light curves of one RRab and one RRc variables of ω Cen in V (top panels), J (middle panels), and K_s (bottom panels).

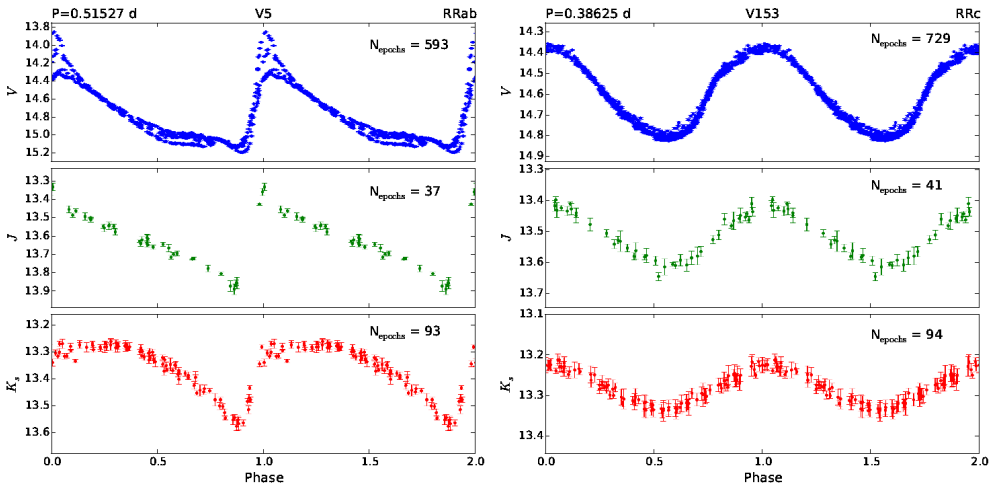

Figure 1. Optical and near-IR light curves for two RRLs in ω Cen. *Left*: V5, an ab-type RRL, which presents a marked Blazhko effect in the V-band light curve. *Right*: the c-type V153, with a visual amplitude of 0.42 mag.

Near-IR light curves of RRL, for both ab- and c-type, have more sinusoidal and symmetric shapes than in the V-band. Because of this, the light curve shapes, both in J and K_s, have less prominent features and are more difficult to classify, especially the RRc type, in massive near-IR variability surveys (see Angeloni et al. 2014; Alonso-García et al. 2015).

Another important difference is that the mean amplitudes decrease as the wavelength increases, with the variations in K_s magnitudes being smaller than 0.4 and 0.15 mag for ab- and c-type RRLs, respectively (see the Bailey diagrams in N15). The smaller near-IR amplitudes are also reflected in the Blazhko effect: the top left panel of Figure 1 shows the light curve of V5, which presents the well-known Blazhko effect. However, its near-IR counterparts do not show the same degree of amplitude modulation. The same occurs for all the other RRab variables in the cluster with well documented Blazhko effect.

2.2. Mean magnitudes

N15 derived empirical relations between the amplitudes in the optical and in the near-IR bands, as well as a relation between J and K_s amplitudes for RRab stars (see their eqs. 3, 4 and 5). The latter relation allows one to estimate the mean

magnitude of a variable with poorly sampled light curve or even single-epoch observation in one of the two near-IR bands.

In this context, another useful empirical relation arises from the intensity-average magnitudes in J and $K_{\rm s}$. Figure 2 shows the (intensity-average) J and $K_{\rm s}$ magnitudes for 79 RRab stars, members of the cluster.

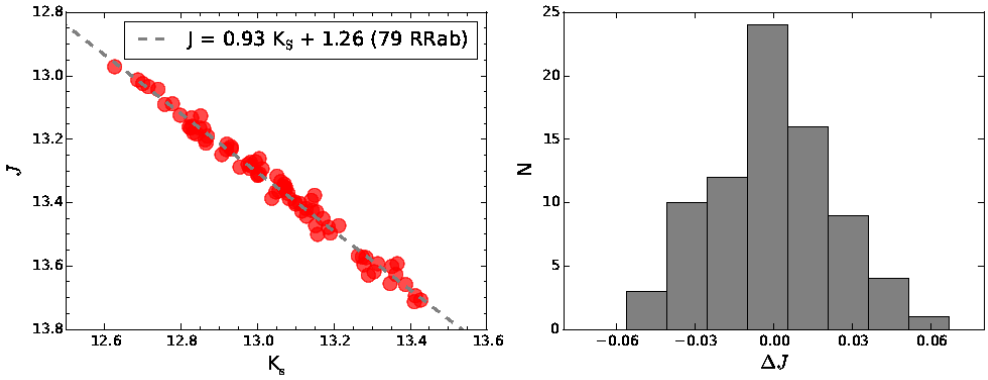

Figure 2. *Left*: Intensity-average J and $K_{\rm S}$ magnitudes of RRab stars in ω Cen. *Right*: Difference between the fit and the observed J magnitudes.

The least-squares linear fit to the data gives

$$J = (0.93 \pm 0.01)K_{\rm s} + (1.26 \pm 0.10),$$

with $\sigma = 0.03$ mag. This relation is useful to estimate J-magnitudes in the case of not well-sampled light curves, which is frequently the case in other near-IR variability surveys, such as VVV (Minniti et al. 2010). In fact, this has been used to determine the color excess and distance for ∼1000 new RRab stars detected in the Galactic bulge (Gran et al., submitted; see also Gran et al. 2015).

3. Pulsational distance modulus

Using the magnitude-calibrated P-L relations for RRLs in J and $K_{\rm s}$ derived by Alonso-García et al. (2015) for the VISTA filter system, and assuming a constant extinction value of $E(B-V) = 0.12$ mag (from the 2010 edition of the Harris' (1996) catalogue), distances for the RRL stars which have spectroscopically derived metallicities (Rey et al. 2000; Sollima et al. 2006) have been obtained.

Figure 3 shows the distribution of true distance moduli obtained in this way. The dashed line shows the values obtained using the metallicities of Rey et al. (2000) for 68 ab- and 55 c-type RRLs, in J and $K_{\rm s}$, while the solid line corresponds to the values derived when the metallicities of Sollima et al. (2006) are used (for 34 ab- and 35 c-type RRLs). For comparison, the distance modulus obtained using the seven Type II Cepheids (and the calibrated relations of Matsunaga et al. 2006) of the cluster are shown as solid bars (amplified by a factor of four, for clarity).

The distributions in Figure 3 are peaked around ∼13.73 mag. However, when the errors are taken into consideration, the weighted-average true distance modulus of the cluster is $\mu = 13.70 \pm 0.03$ mag (weighted-standard deviation). This value is in good agreement with previous estimations in the literature (see Table 2 of Del Principe et al. 2006).

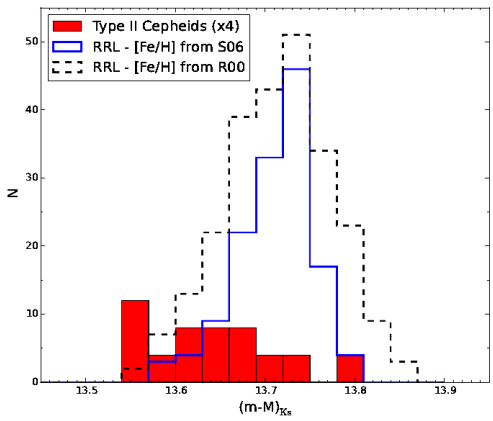

Figure 3. Distribution of the values of distance modulus obtained using different metallicity catalogs for RRL stars in ω Cen. See the text for details.

The true distance modulus obtained based on the Type II Cepheids is slightly smaller than the values obtained using RRL stars. The origin of this discrepancy is still not identified, but could be originated in offsets between the zero points of the *P*-*L* relations used for RRLs and Type II Cepheids.

Acknowledgments

This project is supported by CONICYT through the Ministry for the Economy, Development, and Tourism's Iniciativa Científica Milenio through grant IC 120009, awarded to the Millennium Institute of Astrophysics; by Proyecto Fondecyt Regular #1141141; and by Proyecto Basal PFB-06/2007. Additional support was provided by CONICYT's PCI program through grant DPI20140066. J.A.G. also acknowledges support from the FCI-R Fund, allocated to the project 30321072, and from Fondecyt Iniciación 1150916. C. N. and F. G. acknowledge support from CONICYT-PCHA grants 2015-21151643 (Doctorado Nacional) and 2014-22141509 (Magíster Nacional), respectively.

References

Alonso-García, J., Dékány, I., Catelan, M., et al. 2015, AJ, 149:99
Angeloni, R., Contreras Ramos, R., Catelan, M., et al. 2014, A&A, 567, A100
Catelan, M., Pritzl, B. J., Smith, H. A. 2004, ApJS, 154, 633
Del Principe, M., Piersimoni, A. M., Storm, J., et al. 2006, ApJ, 652, 362
Gran, F., Minniti, D., Saito, R. K., et al. 2015, A&A, 575, A114
Harris, W. E. 1996, AJ, 112, 1487
Kaluzny, J., Olech, A., Thompson, I. B., et al. 2004, A&A, 424, 1101
Matsunaga, N., Fukushi, H., Nakada, Y., et al. 2006, MNRAS, 370, 1979
Minniti, D., Lucas, P. W., Emerson, J. P., et al. 2010, NewA, 15, 433
Navarrete, C., Contreras Ramos, R., Catelan, M., et al. 2015, A&A, 577, A99
Rey, S.-C., Lee, Y.-W., Joo, J.-M., et al. 2000, AJ, 119, 1824
Sollima, A., Borissova, J., Catelan, M., et al. 2006, ApJ, 640, 43
Weldrake, D. T. F., Sackett, P. D., Bridges, T. J. 2007, AJ, 133, 1447

RRL2015 – High-Precision Studies of RR Lyrae Stars
L. Szabados, R. Szabó, K. Kinemuchi (Eds.) 2016

Determining a mid-infrared period-luminosity relation for Galactic globular cluster RR Lyrae stars

Jillian Neeley[1], Massimo Marengo[1], Giuseppe Bono[2,3], Vittorio Braga[2,3], Massimo Dall'Ora[4], and the CRRP team

[1]*Iowa State University, Ames, IA, USA*
[2]*Università di Roma Tor Vergata, Rome, Italy*
[3]*INAF-Osservatorio Astronomico di Roma, Monte Porzio Catone, Italy*
[4]*INAF-Osservatorio Astronomico di Capodimonte, Naples, Italy*

Abstract. We present new RR Lyrae variable period-luminosity (P-L) relations at mid-infrared wavelengths. Accurate photometry was obtained for 37 RR Lyrae variables in the globular cluster M4 (NGC 6121) using the Infrared Array Camera onboard the *Spitzer* Space Telescope. We obtained a very tight MIR P-L relation with 0.056 mag dispersion and 0.007 mag zero point dispersion. The P-L relation was calibrated by five Galactic RR Lyrae stars with parallaxes from *HST*. The resulting band averaged distance modulus for M4 is $\mu = 11.399 \pm 0.007$(statistical) $\pm$ 0.080(systematic) $\pm$ 0.015(calibration) $\pm$ 0.020(extinction).

1. Introduction

RR Lyrae (RRL) variables have long been known to be valuable standard candles, but only recently has a well-defined period-luminosity (P-L) relation been identified at infrared wavelengths. The Carnegie RR Lyrae Program (CRRP) aims to take advantage of this relation to provide an independent Population II calibration of the extragalactic distance scale with better than 2% accuracy. As part of this program, we have observed 31 halo and bulge globular clusters during the warm mission of *Spitzer* Space Telescope using the Infrared Array Camera (IRAC) (Werner et al. 2004; Fazio et al. 2004). The clusters span a wide range of metallicity, allowing us to test for systematic effects in the P-L relation. While recent works have provided P-L relations for the K band (Cacciari & Clementini 2003; Dall'Ora et al. 2004), moving to the mid-infrared offers a lower extinction and lower intrinsic scatter in the P-L relation (Madore & Freedman 2012; Bono 2003). *Spitzer* Space Telescope also allows us to observe with a cadence that covers at least one full pulsation cycle of most RRL. In this paper we will discuss the first results from this project, for the globular cluster M4.

2. Observations

Our observations of M4 were executed on 2013 June 2 - 3 as part of the warm *Spitzer* Space Telescope Cycle 9 (PID 90088). The cluster was observed at 3.6 and 4.5 μm bands at 12 equally spaced epochs over about 14 hours. PSF-fitting

photometry was performed using the most recent version of the DAOPHOT/ ALLSTAR/ALLFRAME suite of programs for crowded-field stellar photometry (Stetson 1987, 1994). In order to reduce blending in the photometry of the M4 crowded field, we used an input source catalog derived by the higher angular resolution optical and NIR images described in Stetson et al. (2014). High order geometric corrections were used to match this catalog to the *Spitzer* data. The photometry was calibrated to standard IRAC Vega magnitudes using aperture photometry on mosaic images. The stars we selected for the photometric zero-point calibration were far from the center of the cluster to reduce blending.

The period and epoch of maximum for every RRL was determined from the optical and NIR data (Stetson et al. 2014). The MIR light curves were then phased and fit using a Gaussian local estimation (GLOESS) algorithm as explained in Madore et al. (2013). The mean magnitude for all stars was determined from the smoothed light curve, and are published in Neeley et al. (2015).

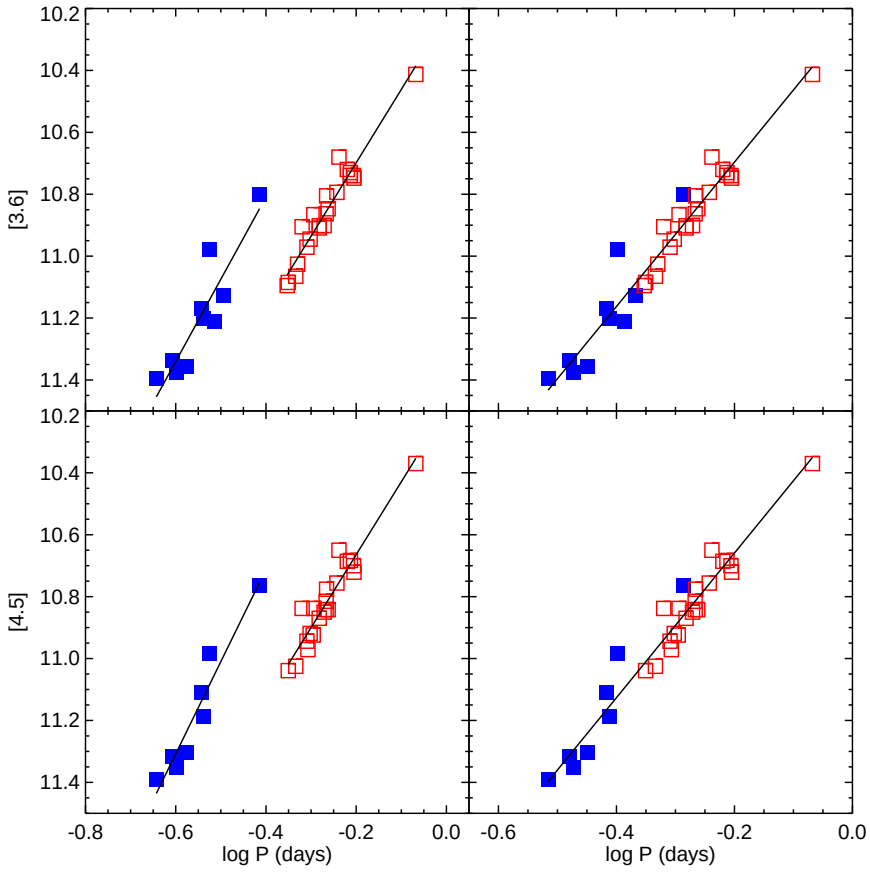

Figure 1. IRAC period-luminosity relations for M4 RRL. *Left* — RRc (blue filled squares) and RRab (red open squares) variables are fit independently (black solid lines). *Right* — single fit with fundamentalized RRc stars. All magnitudes are corrected for extinction. Random uncertainties in the average magnitudes of all variables are smaller than the symbols used, and are not shown.

3. Analysis

The left panels of Figure 1 show the IRAC P-L relation for RRc (first overtone pulsators; filled blue squares) and RRab (fundamental mode; open red squares) RRL in M4. The right panels show the fundamentalized relations. The statistical uncertainties of the mean magnitudes are smaller than the size of the plotted symbols, and are not shown. Two stars were deemed to be blends and not included in the fit.

For the calibrated P-L relation, we adopted the slope measured from the fundamentalized cluster variables. The zero point of the PL relation was fixed using five field RRL with parallaxes measured with *HST* Fine Guidance Sensor shown in Figure 2 (Benedict et al. 2011). We obtain the following P-L relations for the two IRAC bands:

$$M_{[3.6]} = -2.332(\pm 0.106)\log(P) - 1.176(\pm 0.080)$$
$$M_{[4.5]} = -2.336(\pm 0.105)\log(P) - 1.199(\pm 0.080)$$

From the calibrated P-L relation, we can derive the true distance modulus of M4 for each band:

$$\mu_{[3.6]} = 11.406 \pm 0.010\,(\mathrm{stat}) \pm 0.080\,(\mathrm{syst}) \pm 0.015\,(\mathrm{cal}) \pm 0.020\,(\mathrm{ext})$$
$$\mu_{[4.5]} = 11.391 \pm 0.010\,(\mathrm{stat}) \pm 0.080\,(\mathrm{syst}) \pm 0.013\,(\mathrm{cal}) \pm 0.016\,(\mathrm{ext})$$

The error on the distance modulus comes from four sources. The statistical error is the uncertainty in the zero point of the cluster P-L relation, and is derived from the least squares fit to the IRAC data. The systematic error is the uncertainty in the calibrated P-L zero point. The calibration error is the dispersion in our photometric zero point calibration to standard IRAC Vega magnitudes. The extinction error is derived from the uncertainty due to differential reddening. The statistical, calibration, and extinction errors will be reduced as we analyze more clusters, and the systematic error will be reduced when parallaxes from the *Gaia* mission become available. Our distance modulus also agrees with the values obtained from optical and NIR data in Braga et al. (2015).

4. Conclusions

We have presented new RRL MIR P-L relations for the nearby globular cluster M4. Accurate IRAC photometry allows us to reduce the error in the MIR P-L slope by a factor of at least two from previous works using *WISE* data (Madore et al. 2013; Klein et al. 2014). We calibrated the zero point of the MIR P-L relations with five Galactic RRL stars with known distances. The uncertainty in their distances is the largest source of error, and we will be able to provide a much more precise calibration using upcoming results from the *Gaia* mission. Future work will include analysis of the remaining globular clusters as well as 45 additional Galactic RRLs in the CRRP program in order to provide a comprehensive calibration of the RRL P-L relation. This relation can then be used to calibrate other Population II distance indicators, such as the tip of the Red Giant Branch.

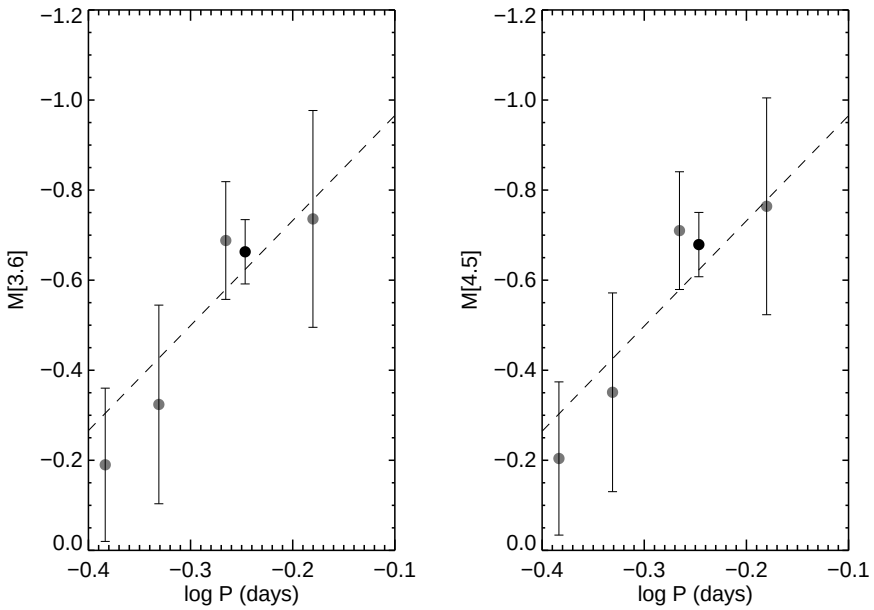

Figure 2. The calibrated IRAC RRL *P-L* relation. The filled circles represent the absolute magnitudes of five Galactic RRL (Neeley et al. 2015). In order of increasing period: RZ Cep, XZ Cyg, UV Oct, RR Lyr (black point), and SU Dra. The period of RZ Cep has been fundamentalized with the same relationship adopted for the M4 RRc stars. The *P-L* relations are shown by the dashed lines, with a slope determined by the M4 cluster data.

References

Benedict, G. F., McArthur, B. E., Feast, M. W., et al. 2011, AJ, 142:187
Bono, G. 2003, in Stellar Candles for the Extragalactic Distance Scale, eds. D. Alloin & W. Gieren, LNP 635, (Springer) 85
Braga, V. F., Dall'Ora, M., Bono, G., et al. 2015, ApJ, 799:165
Cacciari, C., Clementini, G. 2003, in Stellar Candles for the Extragalactic Distance Scale, eds. D. Alloin & W. Gieren, LNP 635, (Springer) 105
Dall'Ora, M., Storm, J., Bono, G., et al. 2004, ApJ, 610, 269
Fazio, G. B., Hora, J. L., Allen, L. E., et al. 2004, ApJS, 154, 10
Klein, C. R., Richards, J. W., Butler, N. R., et al. 2014, MNRAS, 440, L96
Madore, B. F., Freedman, W. L. 2012, ApJ, 744:132
Madore, B. F., Hoffman, D., Freedman, W. L., et al. 2013, AJ, 117:135
Neeley, J. R., Marengo, M., Bono, G., et al. 2015, ApJ, 808:11
Stetson, P. B. 1987, PASP, 99, 191
Stetson, P. B. 1994, PASP, 106, 250
Stetson, P. B., Braga, V. F., Dall'Ora, M., et al. 2014, PASP, 126, 52
Werner, M. W, Roellig, T. L., Low, F. J., et al. 2004, ApJS, 154, 1

RRL2015 – High-Precision Studies of RR Lyrae Stars
L. Szabados, R. Szabó, K. Kinemuchi (Eds.) 2016

A new ϕ_{31}-period-metallicity relation for RR Lyrae stars

C. E. Martínez-Vázquez,[1,2] M. Monelli [1,2], G. Bono[3,4], P. B. Stetson[5], C. Gallart[1,2], E. J. Bernard[6,7], G. Fiorentino[8], & M. Dall'Ora[9]

[1] *IAC-Instituto de Astrofísica de Canarias, Tenerife, Spain*
[2] *Universidad de La Laguna, Tenerife, Spain*
[3] *Università di Roma Tor Vergata, Roma, Italy*
[4] *INAF-Osservatorio Astronomico di Roma, Monte Porzio Catone, Italy*
[5] *Dominion Astrophysical Observatory, Victoria, Canada*
[6] *Royal Observatory of Edinburgh, UK*
[7] *Observatoire de la Côte d'Azur, Nice, France*
[8] *INAF-Osservatorio Astronomico di Bologna, Bologna, Italy*
[9] *INAF-Osservatorio Astronomico di Capodimonte, Napoli, Italy*

Abstract. We present a new calibration of the ϕ_{31}-period-metallicity relation based on cluster instead of field RR Lyrae stars. The novel approach relies on mean Fourier decomposition parameters of their optical light curves, mean periods and metal abundances rooted on a solid metallicity scale. The key advantage when compared with similar relations in the literature is that individual cluster samples cover a broad range in periods, and therefore the opportunity to fully characterize, at fixed metal content, their pulsational behaviour.

To accomplish this goal, we used data for seven globular clusters hosting at least 20 RR Lyrae stars and covering a broad range in metallicity (from −2.3 to −1.1 dex). To further extend the metallicity range, we also included field RR Lyrae stars with a good sampling of the light curve (ASAS, Catalina), and for which iron measurements based on high-resolution spectra are available.

We applied the new calibration to 167 fundamental RR Lyrae in the Sculptor dSph and we found a considerable spread in metallicity, thus confirming the fast early chemical evolution of this galaxy (Martínez-Vázquez et al. 2015).

1. Introduction

The metallicity of RR Lyrae (RRL) stars is a fundamental parameter to constrain the chemical enrichment history of old (> 10 Gyr) stellar populations. This means that they can be used to trace the early formation and evolution of the host galaxies. Local Group (LG) galaxies are a fundamental laboratory to constrain galaxy formation models (Tolstoy et al. 2009), since they can be resolved into stars and detailed metallicity distributions based on high-resolution (HR) spectroscopy of RGB stars are available. However, RGB stars are a mixed bag of old and intermediate-age stars, due to the degeneracy between age and metallicity (Fabrizio et al. 2015). The RRLs provide the unique opportunity to specifically target the old stellar populations.

Metal abundances of RRLs in LG galaxies based on HR spectroscopy are at the limit of the current 8-10 m class telescopes. Indeed, long exposure times imply changes in atmospheric dynamics affecting intrinsic parameter estimates

and, in turn, in the abundances (Sneden et al. 2011, Pancino et al. 2015). This is the reason why detailed spectroscopic investigations are lagging. On the other hand, the shape of the light curve can shed light on the metal content of the RRLs. Based on the technique of the Fourier decomposition, the shape of the light curve can be quantified by low order coefficients of the fit (Simon 1988). Among the studied Fourier parameters, ϕ_{31}, which is defined as $\phi_{31} = \phi_3 - 3 \cdot \phi_1$, has been shown to be a reliable metallicity indicator. The early investigations were provided by Jurcsik & Kovacs (1996), who proposed the first ϕ_{31}-period-[Fe/H] relation, as a linear dependence among them. More recently, Nemec et al. (2013) proposed a non-linear relation among these three parameters.

These studies have shown that Fourier parameters are a promising approach to estimate metal abundances of individual RRL stars. However, solid estimates of Fourier parameters do require accurate photometry and well sampled light curves.

2. The new calibration

We attack the problem by using only calibrators for which metallicities based on HR spectroscopy are available, and covering a wide range in metallicity (Table 1). Selected globular clusters (GCs) cover the range –2.33 and –1.07 dex, while field RRL stars are used to extend the range into the more metal-poor and the more metal-rich regimes ([Fe/H] $\sim$ –3.00 and $\sim$ 0.20). Concerning the cluster variables we have used a novel approach: for each cluster, the RRab stars were divided in period bins of 0.05 days between 0.4 and 0.9 days. Then for every bin we computed the mean period, ϕ_{31}, and V-band amplitude. This means that the new relation is, for the first time, based on average instead of individual properties. Note that we took advantage of GCs hosting sizable samples of at least 20 RRL stars.

Figure 1 shows the mean ϕ_{31} as a function of the mean period of every period bins for the GCs in our sample. Data plotted in this figure bring forward three interesting findings: a) The ϕ_{31} attains, at fixed period, systematically larger values when moving from metal-poor (bluer colors) to metal-rich (redder colors) GCs. b) The ϕ_{31} of individual GCs steadily decreases when moving from shorter to longer periods. This trend is expected since the ϕ_{31} mainly depends on the luminosity amplitude. c) The field RRL stars (open circles with their metallicity labelled) show the same behaviour, except two stars –2MASS J14375130+0617448, 2MASS J17073392+5850598– which are peculiar and need further investigation.

We performed a linear fit similar to that of Jurcsik & Kovacs (1996) using both GCs and field RRL stars. We found:
$[\mathrm{Fe/H}] = -1.26(0.08) - 6.36(0.77) \cdot (P - 0.6) + 1.21(0.19) \cdot (\phi_{31} - 5.5)$ ($\sigma_{\mathrm{fit}} = 0.386$), where the numbers in parentheses indicate the sigma value of each coefficient. The *rms residual* for the binned points is 0.23, while it is 0.70 for the individual stars. This relation provides metallicities in Carretta et al. (2009) scale.

Note that these are preliminary results; we are now in the process of collecting a larger, high quality dataset, to address the following questions: *What is the optimal analytical relation? Are the Fourier parameters the most robust parameters to estimate individual metallicities?*

Table 1. Characteristics of our selected field and GCs RRab stars.

Field RRL stars	[Fe/H][a]	Source[b]	Sampling[c]
V445 Oph	0.18	ASAS	411
DX Del	−0.35	ASAS	180
VW Scl	−1.24	ASAS	493
RR Leo	−1.28	ASAS	299
X Ari	−2.55	ASAS	354
2MASS J22093541−4025512	−2.77	Catalina	267
2MASS J14375130+0617448	−2.87	Catalina	369
2MASS J17073392+5850598	−3.01	Catalina	179
Clusters[d]	**[Fe/H][e]**	**RRab stars[f]**	**Sampling[c]**
NGC 6362	−1.07	18 (18)	80
NGC 5904 (M5)	−1.37	90 (67)	87
NGC 5271 (M3)	−1.50	177 (175)	167
NGC 5286	−1.70	30 (25)	111
NGC 4833	−1.89	11 (11)	72
NGC 4590 (M68)	−2.27	14 (13)	41
NGC 7078 (M15)	−2.33	64 (64)	223

Notes:

[a] Metallicities in the Carretta et al. (2009) metallicity scale (Bono et al. 2016, in preparation).

[b] Light curves of field RRL stars collected by ASAS (All Sky Automated Survey, Pojmanski 2002) and Catalina Sky Survey (Drake et al. 2014).

[c] Typical number of phase points per V-band light curve.

[d] Data from the homogeneous photometric data base of P. B. Stetson (http://www3.cadc-ccda.hia-iha.nrc-cnrc.gc.ca/en/community/STETSON/homogeneous/).

[e] Metallicities from Carretta et al. (2009)

[f] Total number of RRab stars in each GC according to the Clement's catalog: http://www.astro.utoronto.ca/∼cclement/read.html.
In parentheses we list the number of RRab stars available in our photometry.

3. A new spin on the metallicity distribution of RRLs in Sculptor

In Martínez-Vázquez et al. (2015), we analysed 536 RRL stars in the Sculptor dSph, which increased by more than a factor of two the number of known RRLs in this galaxy (Kaluzny et al. 1995). A zoom-in on the RRL stars in the colour-magnitude diagram of this galaxy revealed a large luminosity spread. We found that this spread could not be explained by the evolution off the ZAHB of a mono-metallic population. Adopting the distance modulus obtained from the RRL metal-independent period-Wesenheit relation and using a theoretical period-luminosity-metallicity (PLM) relation (Marconi et al. 2015), we found that their metallicity distribution ranges from –2.3 to –1.5 dex (Martínez-Vázquez et al. 2015).

Applying the new ϕ_{31}-period-[Fe/H] relation derived above to Sculptor RRab stars, we obtained a metallicity distribution which broadly agrees with results based on low resolution spectroscopy for RRL stars in Sculptor (Clementini et al.

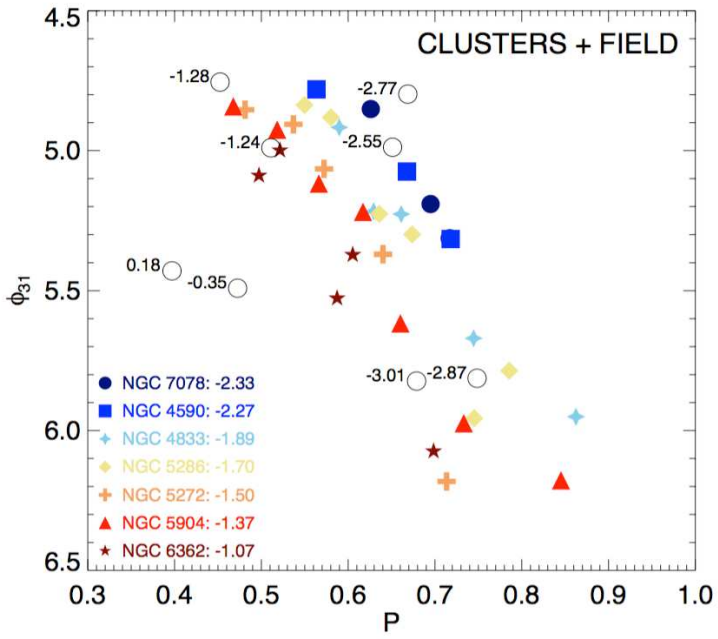

Figure 1. Period-ϕ_{31} diagram for the GCs and field RRL stars used in this work. For cluster RRLs we plot $\langle P \rangle$ and $\langle \phi_{31} \rangle$ for every period bin. The more metal-rich (metal-poor) clusters are represented with redder (bluer) colours. Open circles display field RRLs and their metallicities are labelled.

2005). The derived distribution is also consistent with the one obtained with the PLM, thus strongly supporting our previous findings (Martínez-Vázquez et al. 2015).

References

Carretta, E., Bragaglia, A., Gratton, R., et al. 2009, A&A, 508, 695
Clementini, G., Ripepi, V., Bragaglia, A., et al. 2005, MNRAS, 363, 734
Drake, A. J., Graham, M. J., Djorgovski, S. G., et al. 2014, ApJS, 213:9
Fabrizio, M., Nonino, M., Bono, G., et al. 2015, A&A, 580, A18
Jurcsik, J., Kovacs, G. 1996, A&A, 312, 111
Kaluzny, J., Kubiak, M., Szymanski, M., et al. 1995, A&AS, 112, 407
Marconi, M., Coppola, G., Bono, G., et al. 2015, ApJ, 808:50
Martínez-Vázquez, C. E., Monelli, M., Bono, G., et al. 2015, MNRAS, 454, 1509
Nemec, J. M., Cohen, J. G., Ripepi, V., et al. 2013, ApJ, 773:181
Pancino, E., Britavskiy, N., Romano, D., et al. 2015, MNRAS, 447, 2404
Pojmanski, G. 2002, Acta Astronomica, 52, 397
Simon, N. R. 1988, ApJ, 328, 747
Sneden, C., For, B.-Q., Preston, G. W. 2011, in RR Lyrae Stars, Metal-Poor Stars, and the Galaxy, ed. A. McWilliam, p. 196, arXiv:1108.5162
Tolstoy, E., Hill, V., Tosi, M. 2009, ARA&A, 47, 371

RRL2015 – High-Precision Studies of RR Lyrae Stars
L. Szabados, R. Szabó, K. Kinemuchi (Eds.) 2016

Period-color and amplitude-color relations for RR Lyrae stars

Shashi Kanbur[1], Anupam Bhardwaj[2], H. P. Singh[2], & C. C. Ngeow[3]

[1]*SUNY Oswego, NY, USA 13126*
[2]*University of Delhi, India*
[3]*National Central University, Taiwan*

Abstract. We use published OGLE LMC/SMC data to present comprehensive period-color (PC) and amplitude-color (AC) relations for both fundamental and overtone stars. For fundamental mode stars, we confirm earlier work that the minimum light extinction corrected PC relation in $V-I$ has a shallow slope but with considerable scatter (LMC: $[0.093 \pm 0.019]$ with a standard deviation about this line of 0.116, SMC: $[0.055 \pm 0.058]$ with a standard deviation about this line of 0.099). We note the high scatter about this line for both the LMC and SMC: either there is some source of uncertainty in extinction or some other physical parameter is responsible for this dispersion. We compare with previous results and discuss some possible causes for this scatter. In contrast, RRc overtone stars do not obey a flat PC relation at minimum light (LMC: $[0.604 \pm 0.041]$ with a standard deviation about this line of 0.109, SMC: $[0.472 \pm 0.265]$ with a standard deviation about this line of 0.091). The fact that fundamental mode RR Lyrae stars obey a flat relation at minimum light and overtone RR Lyrae stars do not is consistent with the interaction of the stellar photosphere and hydrogen ionization front. We compare these results with PC relations for fundamental mode and first overtone Cepheids. The fact that the PC relations change significantly as a function of phase indicates strongly that Cepheid and RR Lyrae relations can only be understood at mean light when their properties as a function of phase are determined.

1. Introduction

RR Lyrae stars are very important objects because knowledge of their mean absolute magnitudes leads to a population II age and distance scale. Their spatial distribution provides a way to map galaxy structure and hence constrain theories of galaxy formation. Here we study period-color (PC) and amplitude-color (AC) relations as a function of phase. Applying the Stefan-Boltzmann law at the phases of maximum/minimum light we find

$$\log L_{\max} - \log L_{\min} \approx 4 \log T_{\max} - 4 \log T_{\min}, \tag{1}$$

where we make the assumption that radius fluctuations during a pulsation cycle are small, a reasonable assumption for Cepheids and RR Lyraes (Cox 1980).

Equation (1) implies that if $T_{\max}/T_{\min}$ does not vary with period, then there will be a relationship between period and $T_{\min}/T_{\max}$ and between amplitude and $T_{\min}/T_{\max}$. We note that the observational counterpart of temperature is color. Theoretical relations supporting a flat PC relation at *minimum* light for fundamental mode (FU) RR Lyraes are provided in Kanbur (1995) and Kanbur & Phillips (1996).

The hydrogen ionization front (HIF) and stellar photosphere (SP) are not co-moving as the star pulsates. In certain situations they can be engaged with the SP lying at the base of the HIF. Then the color of the star is the temperature at which hydrogen ionizes. The SP cannot go further inside the mass distribution of the star because of the large opacity associated with hydrogen ionization. When the SP and HIF are engaged in certain envelope temperature/density ranges, the temperature at which hydrogen ionizes and hence the color of the star is somewhat independent of global stellar parameters such as period. This engagement varies with stellar period/pulsation phase and metallicity. For example, first overtone (FO) RR Lyraes are generally hotter than FU stars. This increased temperature means that the temperature at which hydrogen ionizes depends more strongly on period. Thus even though the SP and HIF are engaged, the color of the star depends more strongly on period at minimum light than is the case for FU stars. These same considerations imply that FO RR Lyraes should not follow a flat PC relation at minimum light because such stars are hotter than FU stars.

2. Results

Figures 1 and 2 are adapted from B14 and present results for FU (Fig. 1)/ FO (Fig. 2) LMC (top panels)/SMC (bottom panels) RR Lyraes observed by OGLE III (Soszyński et al., 2008). The left/right panels are PC/AC relations. Minimum/maximum light are represented by blue/red points, respectively. The data were corrected for reddening and extinction using Haschke et al. (2011) maps. Tables 1 and 2 present these results quantitatively.

For FU stars, we clearly see a flat or flatter PC relation at minimum light with a significant relation at maximum. We also see that RRc stars do not follow a flat relation at minimum light. These observations are consistent with the ideas presented in Kanbur & Phillips (1996). The AC relations are also broadly consistent with these ideas.

Table 1. Slope and intercept for PC/AC relations at maximum/minimum light for FU stars.

	Phase	Slope(RRab)	Intercept(RRab)	σ(RRab)
		LMC		
PC	max	1.505 ± 0.018	0.654 ± 0.004	0.116
	min	0.093 ± 0.019	0.716 ± 0.005	0.116
AC	max	-0.361 ± 0.003	0.392 ± 0.002	0.091
	min	0.049 ± 0.003	0.631 ± 0.003	0.114
		SMC		
PC	max	1.768 ± 0.053	0.705 ± 0.012	0.097
	min	0.055 ± 0.058	0.725 ± 0.013	0.099
AC	max	-0.370 ± 0.007	0.594 ± 0.006	0.074
	min	0.067 ± 0.010	0.660 ± 0.008	0.098

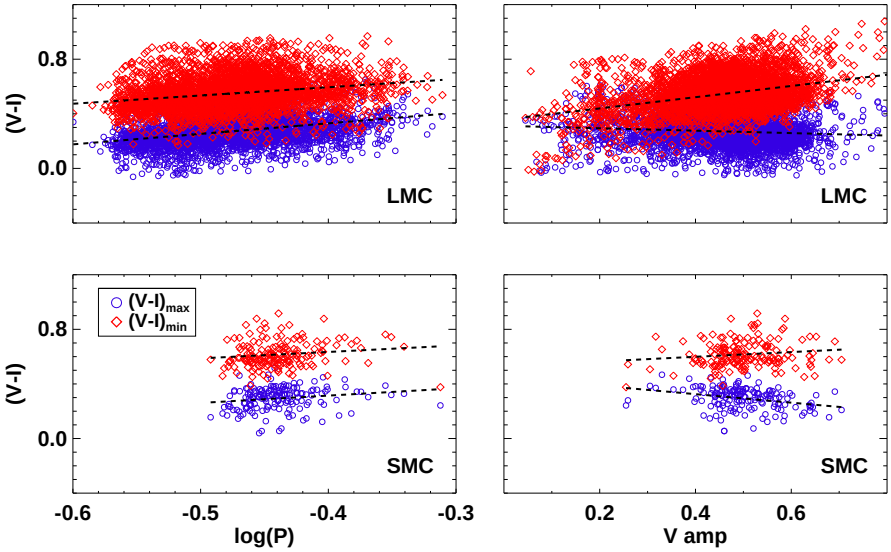

Figure 1. RR Lyrae fundamental mode PC/AC relations at maximum light (blue circles) and minimum light (red diamonds) for the SMC and LMC.

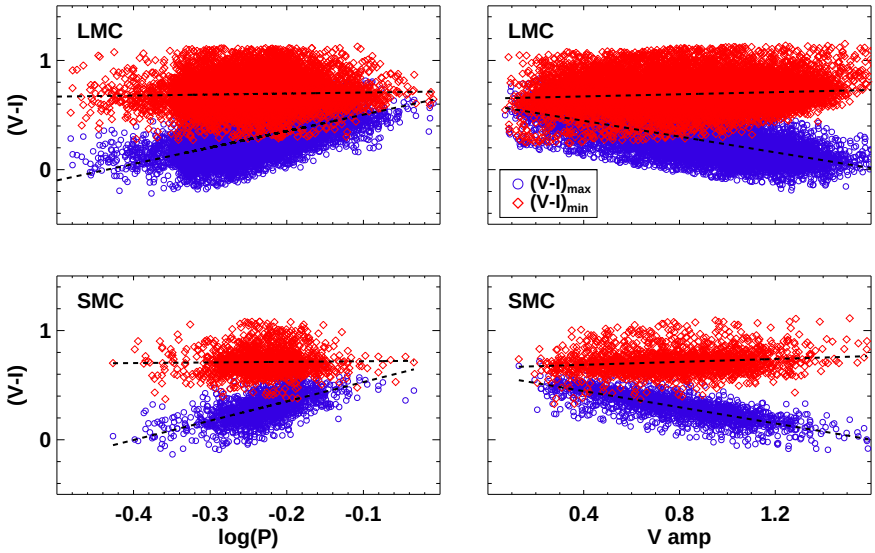

Figure 2. RR Lyrae first overtone PC/AC relations at maximum light (blue circles) and minimum light (red diamonds) for the SMC and LMC.

3. Conclusion

Our results are to be compared with those for Cepheids (B14 and references therein) that display a flat PC relation at *maximum* light. Because Cepheids are cooler, the HIF lies further inside the mass distribution and hence the SP and HIF are only engaged at maximum light.

Table 2. Slope and intercept for PC/AC relations at maximum/minimum light for FO stars.

	Phase	Slope(RRc)	Intercept(RRc)	σ(RRc)
		LMC		
PC	max	0.770 ± 0.032	0.638 ± 0.015	0.084
	min	0.604 ± 0.041	0.836 ± 0.020	0.109
AC	max	-0.089 ± 0.014	0.312 ± 0.007	0.091
	min	0.411 ± 0.017	0.357 ± 0.008	0.111
		SMC		
PC	max	0.536 ± 0.228	0.529 ± 0.228	0.079
	min	0.472 ± 0.265	0.823 ± 0.116	0.091
AC	max	-0.312 ± 0.078	0.450 ± 0.030	0.074
	min	0.172 ± 0.098	0.530 ± 0.050	0.094

The broader implication is that Cepheid and RR Lyrae pulsation properties such as period-luminosity, period-Wesenheit, and period-color relations are always quoted at mean light. However, Figs. 1 and 2 clearly demonstrate that such relations change as a function of pulsation phase: mean light relations are obtained by averaging over the corresponding relations at different phases. We suggest that a deeper understanding of Cepheid and RR Lyrae pulsation will only occur if these relations are studied as a function of pulsation phase.

Acknowledgments

This work was supported by a grant from the Indo-US Science and Technology Forum and by a travel grant from SUNY Oswego.

References

Bhardwaj, A., Kanbur, S. M., Singh, H. P., Ngeow, C. C. 2014, MNRAS, 445, 2655
Cox, J. P. 1980, Theory of Stellar Pulsation, Princeton University Press
Haschke R., Grebel, E., Duffau, S. 2011, AJ, 141:158
Kanbur, S. M. 1995, A&A, 297, L91
Kanbur, S. M., Phillips, P. 1996, A&A, 314, 514
Soszyński, I., Poleski, R., Udalski, A., et al. 2008, Acta Astronomica, 58, 153

RRL2015 – High-Precision Studies of RR Lyrae Stars
L. Szabados, R. Szabó, K. Kinemuchi (Eds.) 2016

The Blazhko phenomenon

Géza Kovács
Konkoly Observatory, Research Centre for Astronomy and Earth Sciences, Hungarian Academy of Sciences, H-1121, Budapest, Konkoly Thege Miklós út 15-17, Hungary

Abstract. In spite of the accumulating high quality data on RR Lyrae stars, the underlying cause of the (quasi)periodic light curve modulation (the so-called Blazhko effect) of these objects remains as mysterious as it was more than hundred years ago when the first RR Lyrae observations were made. In this review we briefly summarize the current observational status of the Blazhko stars, discuss the failure of all currently available ideas attempting to explain the Blazhko effect and finally, we contemplate on various avenues, including massive 2-3D modeling to make progress. Somewhat unconventionally to a review, we present some new results, including the estimate of the true incidence rate of the fundamental mode Blazhko stars in the Large Magellanic Cloud, and tests concerning the effect of the aspect angle on the observed distribution of the modulation amplitudes for Blazhko models involving nonradial modes.

1. Introduction

Cepheids and RR Lyrae stars have always played an invaluable role in mapping the Universe and tracing the kinematical and physical properties of various stellar populations. With the advance of the *Gaia* mission, in a few years' time we will be able to fix the zero points of the period-luminosity-color or period - near infrared magnitude relations with an error lower than 0.01 mag (Windmark et al. 2011) and thereby measure distances in the nearby Universe with an unprecedented accuracy. Although the physics behind the basic properties (such as their self-excitation mechanism) of these vital objects are well known for more than half of a century, there is a nearly complete lack of understanding two, well-populated subgroups of these variables. These subgroups are those of the double-mode pulsators (both among Cepheids and RR Lyrae stars) and the Blazhko variables (characteristically among RR Lyrae stars). Although the modes occurring in the 'classical' double-mode variables are well-identified with the low-order modes from the linear theory[1], the clear cause of the sustained double-mode state is still unknown and nonlinear modeling is controversial (see Kolláth et al. 2002 vs. Smolec & Moskalik 2010). The situation with the Blazhko stars (RR Lyrae variables showing periodic amplitude and phase modulations) is even worse. As of this writing, *we do not have a clue* why many RR Lyrae stars vary their amplitudes that leads in some cases nearly ceasing pulsation in the low-amplitude states. This is not just a minute wrinkle spoiling the classi-

[1] Although this statement is true for the fundamental/first overtone pulsators, the nature of the newly discovered class with period ratios of ~ 0.60–0.64 is a mystery (see Netzel et al. 2015, and references therein).

cal and simple picture on these old stars. On the opposite, with no physically justified and testable idea/model we miss some basic ingredient not just in the pulsation models but most likely in the evolutionary models, too.

No detailed accounts are to be given in this summary on the observational properties and failed modeling of these objects. On these we refer to the review by Kovács (2009) from the pre-*Kepler* era and those by Kolenberg (2011) and Szabó (2014) more recently, already incorporating the results of the *Kepler* mission. We list some obvious (but strenuous) avenues for future works, including detailed spectroscopic studies and higher dimension hydrodynamical surveys of RR Lyrae models. Unconventionally, we present some new results concerning the simple consequences of the observed distributions of modulation amplitudes.

2. How many are they?

Here we focus on the fundamental mode (RRab) variables, since their considerably larger number and higher amplitudes yield statistically more reliable samples than those available for the first overtone stars. The basic rates and related data are summarized in Table 1.

Table 1. Current incidence rates for RRab BL stars

System	Rate	# stars	Note
Galactic field	5%	1435	ASAS; Szczygiel & Fabrycky (2007)[a]
	47%	30	ground-based; Jurcsik et al. (2009)
	39%	44	*Kepler*; Szabó (2014)[b]
	60%	13	*CoRoT*; Szabó et al. (2014)
	34%	268	ASAS & WASP; Skarka (2014)
Galactic bulge	23%	215	OGLE-I; Moskalik & Poretti (2003)
	25%	1942	OGLE-II; Mizerski (2003)
	30%	11756	OGLE-III; Soszynski et al. (2011)[c]
M3	50%	200	ground-based; Jurcsik et al. (2014)
LMC	12%	6135	MACHO; Alcock et al. (2003)
	8%	478	OGLE-III; Chen et al. (2013)[d]
	20%	17693	OGLE-III; Soszynski et al. (2009)[c]
SMC	22%	1933	OGLE-III; Soszynski et al. (2010)[c]

Notes:
[a] The low incidence rate is most probably accounted for by the lower sampling rate and the higher noise in the then available release of the ASAS data base.
[b] See Benkő et al. (2014) for a slightly lower incidence rate.
[c] No details are given.
[d] Strange low incidence rate in spite of the high-quality data selection.

What is clear from this table is that Blazhko (BL) stars are numerous in various stellar populations and the actual figures suggest internal differences among them (e.g., LMC vs. Galactic field). It is interesting that traditional ground-based surveys yield rates close to the ones derived by the orders of magnitude more accurate space missions.[2] This suggests that *the relative number of BL*

[2]Note that the Konkoly BL survey by Jurcsik and co-workers was based on the observations made by a 60 cm telescope, whereas wide-field transit/variability surveys operate $\sim$ 10–20 cm-class telescopes.

stars with low modulation amplitudes is small. Indeed, from the 15 BL stars of the *Kepler* sample discussed by Benkő et al. (2014) only two show modulation amplitudes lower than 0.01 mag. This is a remarkable property, indicating the existence of some lower floor of the amplitude modulation and suggesting that reliable statistics can be derived also from the today's ground-based surveys capable of hitting the detection limit for sinusoidal signals with amplitudes of ~ 0.005–0.01 mag.

2.1. The debiased incidence rate in the LMC

We see from Table 1 that the incidence rates in both Magellanic Clouds are systematically lower that those derived in the Galactic bulge and, especially, in the Galactic field (GF). There is also a significant difference between the MACHO and OGLE rates. Since both rates are based on fairly large samples, we suspect that the difference is due to the higher accuracy of the OGLE data as they evolved over the years after the MACHO project was abandoned. In the following we correct the MACHO statistics for the lower detection rates and examine if it leads to an agreement with the OGLE rates.

First we compute the Cumulative Distribution Function (CDF) of the maximum Fourier side lobes available from the published data (Alcock et al. 2003 [LMC]; Jurcsik et al. 2014 [M3] and Skarka 2014 [GF]). Recall that CDF denotes the probability that the modulation amplitude is smaller than a given value, i.e., $\mathrm{CDF}(\mathrm{MAX_{sidelobe}}) = \mathrm{P}(A < \mathrm{MAX_{sidelobe}})$. Figure 1 shows the resulting CDFs, clearly indicating a want of the low-amplitude BL stars in the LMC sample. With similar observational noise, the BL stars in M3 and in the GF seem to follow the same distribution (we do not deal with the small differences at this stage).

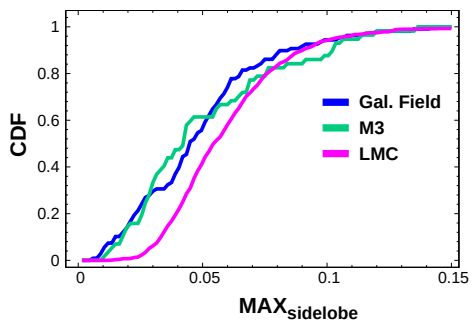

Figure 1. Cumulative distribution functions of the largest sidelobes of the Fourier spectra for fundamental mode Blazhko stars in three different stellar populations.

We test the hypothesis that BL stars both in the LMC and in the GF follow the same intrinsic CDF and the difference is entirely attributed to the lower detection efficiency on the more noisy MACHO data. In a simple approach the test can be performed by injecting sinusoidal signals in the time series consisting the Gaussian noise, generated according to the standard deviations of the residuals (particular to each star) in the single mode RR Lyrae sample. Instead of generating and then analyzing these time series, we estimate the signal-to-noise ratio (SNR) of a sinusoidal component with amplitude A, data point number N and noise standard deviation σ

$$\mathrm{SNR} = \frac{A\sqrt{N/2}}{\sigma} \quad . \tag{1}$$

We tested the applicability of this formula by comparing the above parameter with the S/N of the frequency spectra. We found good correlation, and set the lower limit of SNR to 5.5 to fix the detection rate equal to the one obtained directly from the frequency spectra.

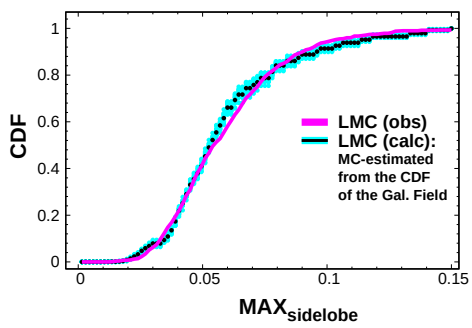

Figure 2. *Light dots:* Monte Carlo-based cumulative distribution function of the modulation amplitudes for the LMC, following the noise properties of the MACHO data base with the priors given by the observed distribution of the Galactic field Blazhko stars; *Black dots:* Averages of these realizations; *Continuous line:* Observed CDF of the RRab BL stars in the LMC.

After generating amplitudes following the CDF of the GF BL stars, many realizations are tested by using the standard deviations of the residuals in some 2000 monoperiodic stars from the MACHO LMC sample. Each star is checked for the detection criterion of SNR > 5.5 and flagged as 'detected' or 'not detected' accordingly. Since the amplitudes are known, we are able to construct the CDF for the detected cases. The result is shown in Fig. 2. We see that using the noise properties of the MACHO data on the CDF of the GF BL stars, the resulting CDF becomes very similar to the observed CDF of the LMC. This suggests that *the distribution of the modulation amplitudes is likely the same in the two populations.*

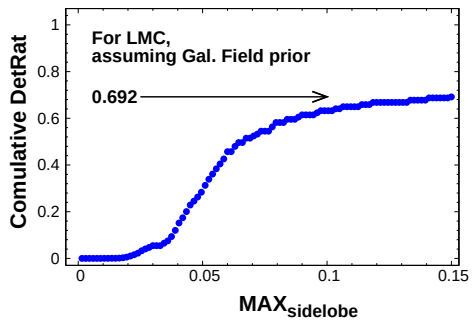

Figure 3. Cumulative detection rate of sinusoidal signals on the MACHO/LMC data with the prior amplitude distribution as given by the Galactic field stars.

The true incidence rate for the LMC can be calculated from the unnormalized version of the CDF based on the amplitude distribution of the GF (black dots in Fig. 2). This cumulative detection rate (see Fig. 3) yields a factor of 0.69 for the total detection rate. This, with the observed rate of 12% of Alcock et al. (2003) results in an unbiased incidence rate of 17%. Considering the values listed in Table 1, we see a better (though not perfect) agreement with the values obtained from the more accurate OGLE data for both Clouds. This test supports the idea that *the lower incidence rate in the Magellanic Clouds is real and that there is a likely population dependence of the occurrence of BL stars.*

2.2. Modeling the distribution of the modulation amplitudes

With the recent sample of the GF BL stars by Skarka (2014) and the already existing large amount of data on the Magellanic Clouds, we are in a position to test a simple BL model involving the $(l, m) = (1, \pm 1)$ nonradial components. We recall that in the basic model of the BL effect this nonradial mode is the one that is most viable for a 1 : 1 resonant interaction with the fundamental radial mode (see Van Hoolst et al. 1998). The coupling gives rise to a steady (constant amplitude) triple-mode pulsation with the $l = 0$ radial fundamental, and the $l = 1$, $m = -1$ and $m = +1$ nonradial modes (see Nowakowski & Dziembowski 2001). The interaction leads to a phase-locked, that is single-period pulsation. The amplitude modulation is due to the changing sky-projected area with the nonradial component of the rotating star. Although in this simple form this model is unable to explain asymmetric modulation side lobes, it is still interesting how the observed distribution of the modulation amplitudes look like if the above mode pattern played some role in the BL phenomenon.

Following Dziembowski (1977), the observed luminosity variation of a nonradially pulsating star can be written in the following form (the abbreviated form of his Eq. 6)

$$\Delta M_{\rm bol} = A_l^m P_l^m(\cos\theta_0) \sin(\omega_l^m t + \phi_l^m) \ . \qquad (2)$$

Here A_l^m, ω_l^m and ϕ_l^m are, respectively, the surface amplitude, frequency and phase of the nonradial mode. The factor $P_l^m(\cos\theta_0)$ is the associated Legendre polynomial, depending on the mode order, degree and the inclination angle $i = \theta_0 + \pi/2$ ($\theta_0 = 0$ if the rotational axis is perpendicular to the line of sight). In the simple case of the $(l, m) = (1, \pm 1)$ mode, this factor is just a sine function. Below we examine the effect of this factor on the observed distribution of the amplitude modulation, assuming different priors for the distributions of the underlying nonradial mode amplitudes and a uniform prior for inclination angle.

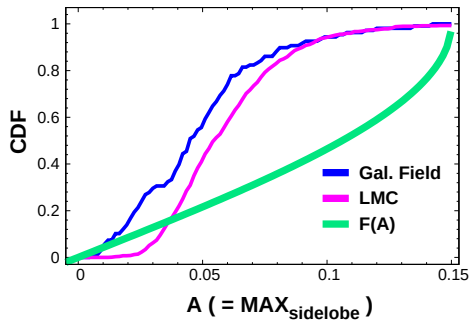

Figure 4. Predicted CDF of the observed modulation amplitudes assuming Dirac delta prior (i.e., the same value) for the ($l = 1$, $|m| = 1$) nonradial component in all BL stars. The theoretical CDF can be computed analytically in this case, yielding $F(A) = \frac{2}{\pi} \arcsin(\frac{A}{A_{\rm max}})$, where $A_{\rm max} = 0.15$.

First we assume that all BL stars have the same modulation amplitude and the observed amplitude is merely affected by the aspect angle. This admittedly not too likely scenario leads to the theoretical CDF shown in Fig. 4. It is comforting that we can clearly exclude the extreme mechanism that might lead to such a particular amplitude distribution. Next, we consider the physically more likely setting, when all amplitudes in $[0, A_{\rm max}]$ occur with the same probability (here $A_{\rm max}$ is the maximum possible modulation amplitude – which, as noted earlier, we take as the maximum sidelobe in the Fourier spectra). As shown in Fig. 5, this is a better-fitting model but still shows characteristic deviations by under/overestimating the observed distribution at high/low modulation amplitudes.

Finally, we assume that low/high modulation amplitudes are intrinsically of low probability. This situation is modeled by a Gaussian distribution peaked at $A = 0.07$. We see on the right panel of Fig. 5 that this assumption yields a considerably better fit, although the high-amplitude part of the distribution is now overestimated. From these results we conclude that even if the BL phenomenon is affected by an aspect-dependence, there should exist some mechanism that prefers mid-size modulations and makes low/high modulations much less likely.

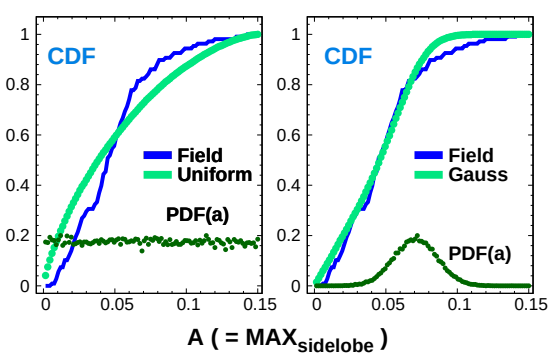

Figure 5. *Left:* Predicted CDF (thick line) of the modulation amplitude, assuming uniform priors for the ($l = 1$, $|m| = 1$) nonradial component. For reference, the probability density (arbitrarily shifted) of these amplitudes generated in the Monte Carlo simulations are shown by the points labelled as PDF(a). *Right:* As on the left but for a Gaussian prior, chosen to fit better the observed distribution.

3. Properties to be explained and the failure to do so

There are many intriguing properties of the BL stars and it is obviously impossible to list them all here. What might perhaps still be useful is to focus on the more general, robust properties, that are inescapable to deal with in any future modeling. We list these properties in Table 2 with some sort of ranking based on a mixture of the size and/or the commonality of the given property. We do not know which feature will finally unveil the secret of the BL phenomenon but at this stage our preference goes to those ideas/models that offer some solution to reproduce the first three/four properties.

For the currently available models/ideas, here is a brief summary of the main reasons of their failure in their present forms.[3]

■ *Magnetic oblique rotator/pulsator:* Shibahashi (2000): symmetric sidelobes only, lack of strong magnetic field.

■ *Nonresonant radial/nonradial double-mode pulsator:* Cox (2013): questions about the strength of the excitation of the nonradial mode and about the reasons why the close radial and nonradial modes are not phase-locked, leading to monoperiodic pulsation.

■ *Resonant nonradial rotator/pulsator:* Nowakowski & Dziembowski (2001): symmetric sidelobes only, questions concerning the current forms of amplitude equations in the case of nonradial modes in RR Lyrae models (Nowakowski & Dziembowski 2003).

■ *Radial mode resonance of 9:2 :* Buchler & Kolláth (2011): lack of modulation in the RR Lyrae nonlinear hydrodynamical models.

[3]We list only the most striking deficiencies of the models/ideas and refer to earlier reviews for a more extended discussion.

Table 2. Basic properties of the RRab BL stars

#	Property	Reference[a]
1	High (20–50%) incidence rate	these proceedings
2	Cases of high modulations ($A_{\rm mod}/A_{\rm puls} > 0.5$)	Sódor et al. (2012)
3	High rates of strongly asymmetric side lobes[b]	Alcock et al. (2003)
4	Range of modulation time scales ($\sim$ 5–1000 d)	Benkő et al. (2014)
5	Intermittent amplitude alternation[c]	Szabó et al. (2010)
6	Role of the 1st overtone and multimodality	Smolec et al. (2015)
7	Occurrence of multiperiodic modulations	Skarka (2013)
8	Chaotic/stochastic effects?	Plachy et al. (2014)

Notes:
[a] The references are not complete. They are merely shown for guidance.
[b] By the loose term 'strongly asymmetric' we mean those cases when one of the side lobes is close to the noise level. The number of these stars may also depend on the stellar population (i.e., for the LMC this ratio is 50%, whereas for the GF it is 40% – see Skarka 2014). At lower noise level they may exhibit both side lobes but they remain quite different.
[c] The phenomenon is commonly called in the RR Lyrae community as 'period doubling'. We think that unless it can be clearly related to the first step on the route of bifurcation to chaos, it is more appropriate to call 'amplitude alternation', since the expression 'period doubling' is specifically attached to the process mentioned (Feigenbaum 1983). We also note the systematic frequency displacements at the positions of the expected half integer resonances in some well-studied cases (Bryant 2015) are also atypical of period doubling.

■ *Magnetic dynamo-driven convection:* Stothers (2011): lack of mathematical/physical rigor and any modeling[4].

■ *Periodic energy dissipation driven by shock wave dynamics:* Gillet (2013): the idea is based on the analysis of standard 1D hydrodynamical models showing no amplitude modulation, therefore it is unclear what kind of mechanism could be deciphered from these models that might be relevant for future modeling.

4. Future progress: Can further observations or 3D modeling help?

Because of the lack of any physically sound idea, it is hard to point toward any direction in which progress can be made. Nevertheless, we can mention two areas that are still not investigated with the depth required for getting useful information for model building. From the side of the observations, it would be vital to find out if there is any nonradial component. If yes, then does its size correlate with the amplitude of the Blazhko effect? It is a hard observational project (faint objects, long-term data acquisition, need for high-dispersion spectroscopy, difficulties in disentangling the nonradial component in the presence of the large radial, time-dependent component, etc.). From the side of modeling – again, due to the lack of any better guidance – one may try to conduct some expensive survey of the already existing 2D/3D hydrodynamical models (e.g., Mundprecht et al. 2015 and Geroux & Deupree 2015), and investigate the effect of better modeled convection or that of the rotation. Of course, due to the well-known attribute of serendipity of scientific discoveries, it might well be that we

[4]See Smolec et al. (2011) and Molnár et al. (2012) for some negative hydrodynamical tests of this idea.

find something completely unexpected in the course of other studies that will finally lead to the long-waited understanding of this exceptional hydrodynamical phenomenon.

Acknowledgements

My life-long appreciation and gratitude go out to my mentor and long-time friend Wojtek who introduced me into the exciting field of nonlinear stellar pulsations and gave me his support and encouragement over the years.

References

Alcock, C., Alves, D. R., Becker, A., et al. 2003, ApJ, 598, 597
Benkő, J. M., Plachy, E., Szabó, R., et al. 2014, ApJS, 213:31
Bryant, P. H. 2015, arXiv1501.06485
Buchler, J. R., Kolláth, Z. 2011, ApJ, 731:24
Chen, B.-Q., Jiang, B.-W., Yang, M. 2013, Res. in Astron. & Astroph., 13, 290
Cox, A. N. 2013, ASSP, 31, 77
Dziembowski, W. 1977, AcA, 27, 203
Feigenbaum, M. J. 1983, Physica D, Vol. 7, Issues 1-3, p. 16
Geroux, C. M., Deupree, R. G. 2015, ApJ, 800:35
Gillet, D. 2013, A&A, 554, 46
Jurcsik, J., Sódor, Á., Szeidl, B., et al. 2009, MNRAS, 400, 1006
Jurcsik, J., Smitola, P., Hajdu, G., et al. 2014, ApJ, 797:L3
Kolenberg, K. 2011, RR Lyrae Stars, Metal-Poor Stars, and the Galaxy, Ed. Andrew McWilliam, Carnegie Observatories Astrophysics Series, Vol. 5., p.100
Kolláth, Z., Buchler, J. R., Szabó, R., et al. 2002, A&A, 385, 932
Kovács, G. 2009, AIPC, 1170, 261
Mizerski, T. 2003, AcA, 53, 307
Molnár, L., Kolláth, Z., Szabó, R. 2012, MNRAS, 424, 31
Moskalik, P., Poretti, E. 2003, A&A, 398, 213
Mundprecht, E., Muthsam, H. J., Kupka, F. 2015, MNRAS, 449, 2539
Netzel, H., Smolec, R., Moskalik, P. 2015, MNRAS, 453, 2022
Nowakowski, R. M., Dziembowski, W. A. 2001, AcA, 51, 5
Nowakowski, R. M., Dziembowski, W. A. 2003, Ap&SS, 284, 273
Plachy, E., Benkő, J. M., Kolláth, Z., et al. 2014, MNRAS, 445, 2810
Shibahashi, H. 2000, ASPC, 203, 299
Skarka, M. 2013, A&A, 549, 101
Skarka, M. 2014, A&A, 562, 90
Smolec, R., Moskalik, P. 2010, A&A, 524, 40
Smolec, R., Moskalik, P., Kolenberg, K., et al. 2011, MNRAS, 414, 2950
Smolec, R., Soszynski, I., Udalski, A., et al. 2015, MNRAS, 447, 3756
Sódor, Á, Jurcsik, J., Molnár, L., et al. 2012, ASPC, 462, 228
Soszynski, I., Udalski, A., Szymanski, M. K., et al. 2009, AcA, 59, 1
Soszynski, I., Udalski, A., Szymanski, M. K., et al. 2010, AcA, 60, 165
Soszynski, I., Dziembowski, W. A., Udalski, A., et al. 2011, AcA, 61, 1
Stothers, R. B. 2011, PASP, 123, 127
Szabó, R. 2014, IAUS, 301, 241
Szabó, R., Kolláth, Z., Molnár, L., et al. 2010, MNRAS, 409, 1244
Szabó, R., Benkő, J. M., Paparó, M., et al. 2014, A&A, 570, A100
Szczygiel, D. M., Fabrycky, D. C. 2007, MNRAS, 377, 1263
Van Hoolst, T., Dziembowski, W. A., Kawaler, S. D. 1998, MNRAS, 297, 536
Windmark, F., Lindegren, L., Hobbs, D. 2011, A&A, 530, 76

RRL2015 – High-Precision Studies of RR Lyrae Stars
L. Szabados, R. Szabó, K. Kinemuchi (Eds.) 2016

On period ratios in modulated double-mode RR Lyrae stars

Radosław Smolec

Nicolaus Copernicus Astronomical Center, PAS, Warsaw, Poland

Abstract. With the help of linear pulsation models we briefly discuss the peculiar period ratios characteristic of modulated double-mode RR Lyrae stars.

In about fifty per cent of the fundamental mode RR Lyrae stars (RRab), we observe a quasi-periodic modulation of pulsation amplitude and phase – the Blazhko effect. It is also observed in single-mode first overtone stars (RRc), in which the occurrence rate is smaller. The origin of the Blazhko modulation remains a puzzle. For a review see e.g. Szabó (2014) and Kovács (these proceedings). Precise space observations significantly increased our knowledge about the Blazhko effect. The most interesting discoveries are the detection of period doubling at some phases of the Blazhko cycle (Kolenberg et al. 2010; Szabó et al. 2010) and detection of additional radial modes of very low amplitude, mostly of the second overtone, and rarely of the first overtone (Benkő et al. 2010, 2014) (see also Smolec & Bąkowska, these proceedings).

Until recently modulation was not observed in double-mode RR Lyrae stars (RRd stars), pulsating simultaneously in the radial fundamental and radial first overtone modes (with large amplitude of the two). This rare form of pulsation was detected only recently in top-quality ground-based observations collected by the Optical Gravitational Lensing Experiment (OGLE; Udalski et al. 2015) in the direction of Galactic bulge (15 stars; Soszyński et al. 2014; Smolec et al. 2015) and in observations of the globular cluster M3 (4 stars; Jurcsik et al. 2014). The most peculiar feature of these stars is a somewhat atypical period ratio of the two radial modes. This is illustrated with the help of the Petersen diagram displayed in Fig. 1. The majority of RRd stars in this diagram form a rather tight and curved progression; the period ratio increases with the increasing fundamental mode period, up to $P_0 \approx 0.52\,\mathrm{d}$, and then, a mild decline is observed as period increases further. The period ratio is a well known indicator of the star's metallicity; in particular the short-period tail of the RRd sequence is formed by Galactic bulge stars of relatively high metallicity (Soszyński et al. 2011). Modulated RRd stars, except two, do not follow the described progression. Their period ratio is either too low, or too high, as compared to other RRd stars of similar fundamental mode period. Why their period ratios are atypical remains an open question.

With the help of linear pulsation codes, we can check whether the period ratios in modulated stars can be reproduced assuming physical parameters typical of RR Lyrae stars. Results of model calculations are presented in Fig. 2. We used pulsation codes of Smolec & Moskalik (2008), assumed three different masses, 0.5 $\mathrm{M}_\odot$, 0.6 $\mathrm{M}_\odot$ and 0.7 $\mathrm{M}_\odot$ (top, middle and bottom panels, respectively), four different luminosity levels, 30 $\mathrm{L}_\odot$ (circles), 40 $\mathrm{L}_\odot$ (squares), 50 $\mathrm{L}_\odot$ (triangles)

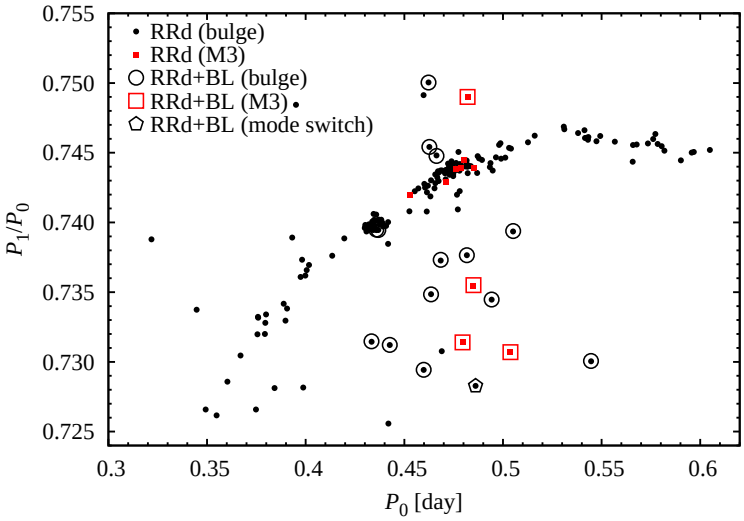

Figure 1. Petersen diagram for RRd stars of the Galactic bulge (Soszyński et al. 2014; Smolec et al. 2015) and globular cluster M3 (Jurcsik et al. 2014, 2015).

and 60 $L_\odot$ (diamonds), and a range of metallicities (plotted with different colors and labelled in Fig. 2). For a given M and L our model sequences are horizontal and computed with 100 K step in effective temperature. Only the models in which both the fundamental mode and the first overtone are linearly unstable are plotted. This is a parameter study; parameters of our models cover the range expected for RR Lyrae stars, but these are not evolutionary models.

First, we focus our attention on typical, non-modulated RRd stars that form the curved sequence in the Petersen diagram. As already mentioned, the period ratio is a good indicator of metallicity. The shortest period Galactic bulge RRd stars have higher metallicity and lower luminosities, as is expected from evolutionary calculations. The other striking feature is that models predict simultaneous instability of the two radial modes over the entire Petersen diagram. Some extreme combinations of M, L, and Z are likely not allowed by evolutionary calculations, but it is clear that non-modulated RRd stars occupy a much narrower band than allowed by the pulsation models. In the Hertzsprung-Russell diagram, the domain in which double-mode pulsation is present, is narrower than the domain in which the two radial modes are simultaneously unstable. This is a manifestation of a well known and difficult, non-linear problem of mode selection (Smolec 2014). Simultaneous instability of the two radial modes is only necessary, but insufficient condition for the (non-resonant) double-mode pulsation. The other factors are not known. Since the majority of the non-modulated RRd stars follow the same and continuous progression in the Petersen diagram we may conclude that most likely mode selection mechanism is the same for these stars.

Now we turn to modulated RRd stars. The majority of these stars have an atypical period ratio. From Fig. 2 it is obvious that such period ratios present no difficulty for the pulsation theory. We observe that the lower the period ratio the higher the metallicity. Also, the lower the luminosity, the shorter the period

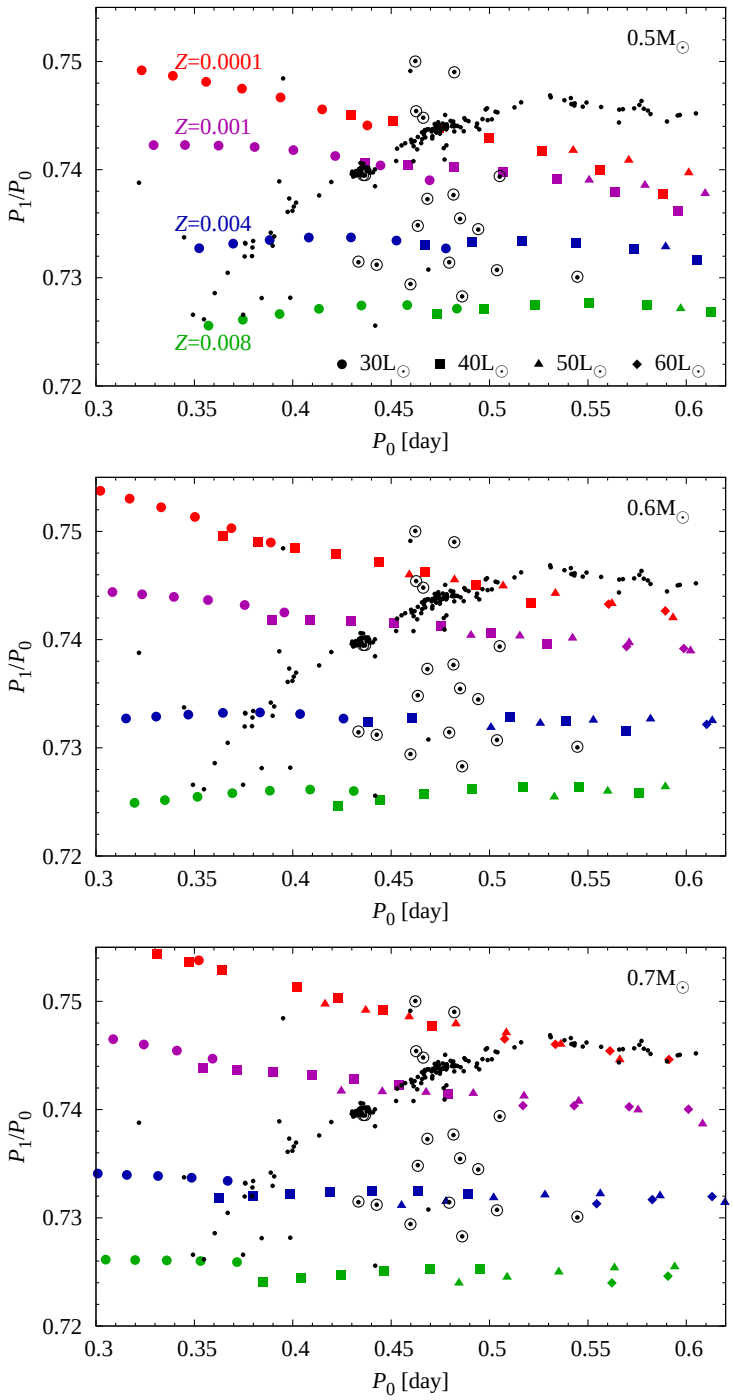

Figure 2. Linear period ratios for RR Lyr models of different masses, luminosities and metallicities. RRd stars from the Galactic bulge and M3 are marked with small black dots; modulated stars are encircled.

at which the domain of simultaneous instability of the two radial modes start. For each considered mass the modulated RRd stars are easily reproduced with luminosities $\sim 40 - 50$ $L_\odot$ and a range of metallicities. It seems that there is no need to invoke any atypical masses or luminosities to explain their period ratios. Linear pulsation theory cannot help further; in particular, we cannot conclude about mode selection mechanism in these stars. This is a difficult and non-linear problem, and the tools we have to tackle it are insufficient (Smolec 2014).

The origin of the Blazhko effect in RRd stars and the origin of atypical period ratios remains a mystery. One of the modulated stars (marked with pentagon in Fig. 1) switched the pulsation mode recently from RRab to RRd (Soszyński et al. 2014). In Smolec et al. (2015) we hypothesize that the modulation and mode-switching may be connected. Properties of the modulated RRd stars are strongly non-stationary, amplitudes and phases of the radial modes vary on a time scale of few hundred days. Long-term monitoring of these stars, and RR Lyrae stars in general, is needed to check whether the mode-switching and modulation are indeed connected.

Acknowledgement

This research is supported by the Polish National Science Centre through grant DEC-2012/05/B/ST9/03932.

References

Benkő, J. M., Kolenberg, K., Szabó, R., et al. 2010, MNRAS, 409, 1585
Benkő, J. M., Plachy, E., Szabó, R., et al. 2014, ApJS, 213:131
Jurcsik, J., Smitola, P., Hajdu, G., et al. 2014, ApJ, 797:L3
Jurcsik, J., Smitola, P., Hajdu, G., et al. 2015, ApJS, 219:25
Kolenberg, K., Szabó, R., Kurtz D.W., et al. 2010, ApJ, 713, L198
Smolec, R., 2014, IAU Symp., 301, 265
Smolec, R., Moskalik, P. 2008, Acta Astron., 58, 193
Smolec, R., Soszyński, I., Udalski, A., et al. 2015, MNRAS, 447, 3756
Soszyński, I., Dziembowski, W.A., Udalski, A., et al. 2011, Acta Astron., 61, 1
Soszyński, I., Udalski, A., Szymański, M.K., et al. 2014, Acta Astron., 64, 177
Szabó, R. 2014, IAU Symp., 301, 241
Szabó, R., Kolláth, Z., Molnár, L., et al. 2010, MNRAS, 409, 1244
Udalski, A., Szymański, M. K., Szymański, G. 2015, Acta Astron., 65, 1

RRL2015 – High-Precision Studies of RR Lyrae Stars
L. Szabados, R. Szabó, K. Kinemuchi (Eds.) 2016

The magnificent past of RR Lyrae variables

Ennio Poretti[1,2,3,4], Jean-Francois Le Borgne[2,3,4], Alain Klotz[2,3,4], Maurice Audejean[5], & Kenji Hirosawa[6]

[1] *INAF-Osservatorio Astronomico di Brera, Merate (LC), Italy*
[2] *Université de Toulouse, UPS-OMP, IRAP, Toulouse, France*
[3] *CNRS, IRAP, Toulouse, France*
[4] *GEOS, Groupe Européen d'Observations Stellaires, France*
[5] *Observatoire de Chinon, Astronomie en Chinonais, Chinon, France*
[6] *Variable Star Observers League (VSOLJ), Matsushiro, Japan*

Abstract. We briefly review the results obtained by using the times of maximum brightness of RR Lyrae variables. They cover more than 120 years and have been used to study the evolutionary changes of the pulsational periods, the different shapes of the Blazhko effect among Galactic RRab stars, and the interplay between pulsational and Blazhko periods in the eponym of the class, RR Lyr. The data are stored in the GEOS database, continuously fed by contributions from professional and amateur astronomers.

1. Introduction

The history of the observations of RR Lyrae variables started in the 19$^{\rm th}$ century, more than 120 years ago. The variability of RR Lyr itself was discovered on the photographic plates of the *Henry Draper Memorial* by Mrs. Williamina P. Fleming (Pickering et al. 1901). The first measurement dates back to July 20, 1899, and the first time of maximum brightness ($T_{\rm max}$) to September 23, 1899. The list of $T_{\rm max}$ recorded from 1906 July 15 to August 25 on RW Dra clearly shows variations of amplitude and phase (Blazhko 1907). Shapley (1916) noted the same variations in the data of RR Lyr itself: this phenomenon was later named *Blazhko effect* in the astronomical literature.

The very long time-baseline of available data combined with the short period of RR Lyrae variables offer an unique opportunity to look at their past as a treasure of valuable information. At this purpose, the amateur/professional association Groupe Européen d'Observations Stellaires (GEOS) has built a database aimed at gathering all the published $T_{\rm max}$ values (Le Borgne et al. 2007). It also promotes the regular monitoring of RR Lyrae variables by means of self-made instruments and observing time at robotic telescopes.

2. Evolutionary changes

The long time baseline allowed us to study period changes due to stellar evolution (Le Borgne et al. 2007). Most of the 123 scrutinized RRab stars do not show any significant period variation. This reflects the fact that the rapid evo-

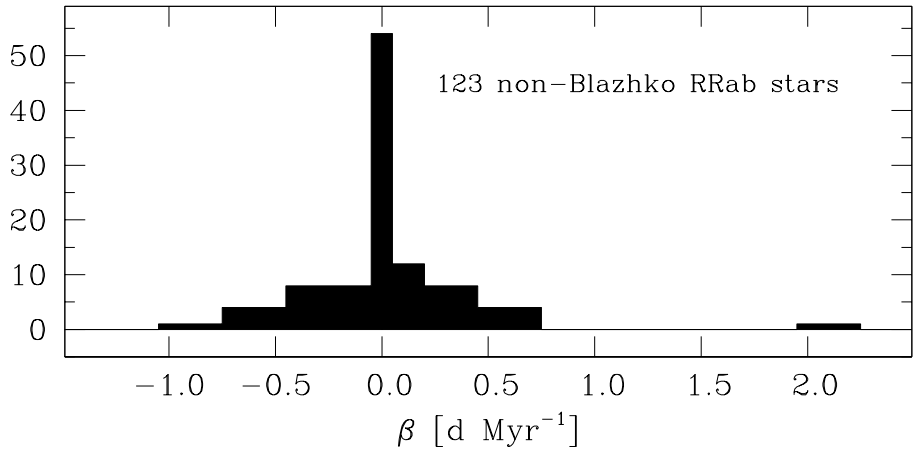

Figure 1. Distribution of the rates of period changes. The extreme positive value is that of SV Eri.

lution is confined to short evolutionary phases. Notwithstanding this, we could put in evidence period increases in 27 stars and decreases in 21 (Fig. 1). The median values of the rates are $+0.14 \cdot 10^{-6}$ d yr^{-1} and $-0.20 \cdot 10^{-6}$ d yr^{-1}, respectively. The order of magnitude of these rates is that expected from evolutionary models and being common to a large number of stars it strongly supports the evolutionary origin.

To study the evolutionary changes, we used stars not showing the Blazhko effect, or at least not showing an appreciable effect from the ground-based observations. Indeed, nowadays space-based time series are detecting very small Blazhko effects, as in the case of V350 Lyr (Benkő & Szabó 2015). Even if present in our sample, these small effects are not able to mask the large amplitude evolutionary changes. Several cases of erratic changes were observed, both increasing and decreasing the period. They should be the result of particular temporary instabilities rather than to be considered as representative of a particular evolutionary stage. A slight excess of RR Lyrae stars showing period decreases (i.e., stars on blueward evolutionary tracks) was also noticed. However, further studies on a larger sample suggested that the excess was mainly due to the limited statistics (Vanderbroere et al. 2014).

3. The different shapes of the Blazhko effect

We used the GEOS database to study the Blazhko effect of Galactic RRab stars (Le Borgne et al. 2012). The closed curves representing the Blazhko effect are constructed by plotting the magnitudes at maximum ($V_{\max}$) vs. the $O - C$ (*observed* minus *calculated*) $T_{\max}$ values. We could emphasize some clear observational facts: *i)* the same value of the Blazhko period is observed at different values of the pulsation periods; *ii)* different values of the Blazhko periods are observed at the same value of the pulsation period; *iii)* the closed curves describing the Blazhko cycles have different shapes. These curves have often the

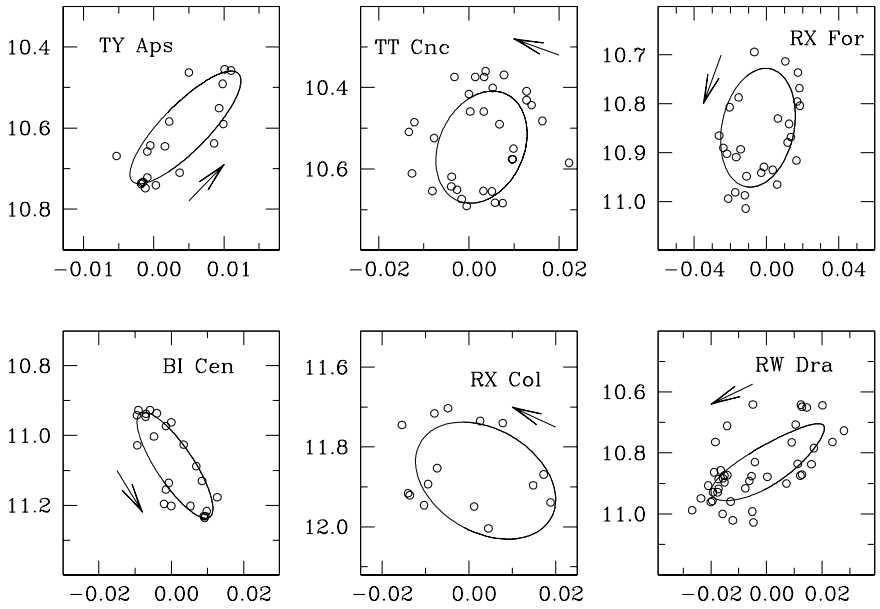

Figure 2. Stars for which the closed curves in the $O-C$ (abscissa, in days) vs. $V_{\max}$ (ordinate) plot run counterclockwise.

shape of a potato, but other exotic contours are observed; *iv)* both clockwise and counterclockwise rotations are possible for closed curves with similar shapes.

All these facts lead to a variegated group of behaviours. For instance, the brightest maximum could correspond to the most negative phase shift in some stars and to the most positive one in others. We could observe a full rotation of the *Blazhko potato* in the sample of Galactic RRab stars. Figure 2 shows the case of stars running counterclockwise. The regular survey of RRab stars is undergoing using both amateurs' observatories and the robotic TAROT telescopes (Klotz et al. 2008, 2009; Le Borgne et al. 2012).

4. Vanishing of the Blazhko effect of RR Lyr

The analysis of the $T_{\max}$ epochs listed in the GEOS database allowed us to reconstruct the changes in the pulsational period of RR Lyr. We could establish the existence of two states characterized by the pulsation over a "long" period (longer than 0.56684 d) and over a "short" one (shorter than 0.56682 d). We also determined the Blazhko period in several time intervals since 1910 and we verified how it changed while the two states alternated. The variations in the pulsation and Blazhko periods appeared completely decoupled, since the Blazhko period had just one sudden decrease from 40.8 d to 39.0 d in 1975 (Le Borgne et al. 2014). The current period is the shortest ever measured, i.e., less than 0.5668 d.

Some years ago, two of us (J. F. Le Borgne and A. Klotz) planned and realized small, autonomous and transportable photometric instruments to make the

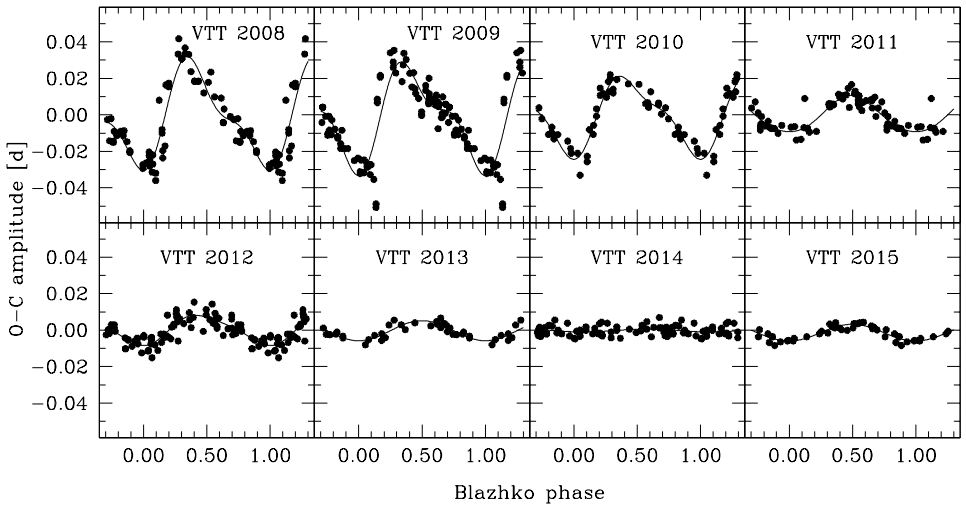

Figure 3. $O-C$ values of RR Lyr folded with the Blazhko period

ground-based survey of RR Lyr as effective as possible. They assembled a commercial equatorial mount (Sky-Watcher HEQ5 Pro Goto), an AUDINE CCD camera (512×768 kaf400 chip) and a photographic 135-mm, f/2.8 lens with a field of view of $2^\circ \times 3^\circ$. They gave them the nickname VTTs for "Very Tiny Telescopes". The regular recording of $T_{\max}$ values of RR Lyr started in 2008. Data from VTTs and *Kepler* have been extensively used to record the monotonic long-term decrease in the amplitude of the Blazhko effect. As a matter of fact, the Blazhko effect was hardly detected by looking at the maxima collected in 2014 only. However, the new $T_{\max}$ collected with the VTTs in 2015 seem to show a slight increase in the amplitude of the $O-C$ values (Fig. 3), a sign that the still unknown Blazhko mechanism is back at work.

Acknowledgments

The projects exploiting the GEOS database have been developed during some visits of E. Poretti at the *Institut de Recherche en Astrophysique et Planétologie* in Toulouse. Supports from this Institute are gratefully acknowledged.

References

Benkő, J. M., Szabó, R. 2015, ApJ, 809:L19
Blazhko, S. 1907, AN, 175, 325
Klotz, A., Boër, M., Atteia, J. L., Gendre, B. 2009, AJ, 137, 4100
Klotz, A., Vachier, F., Boër, M. 2008, Astron. Nachr., 329, 275
Le Borgne, J.-F., Klotz, A., Poretti, E., et al. 2012, AJ, 144:39
Le Borgne, J.-F., Paschke, A., Vandenbroere, J., et al. 2007, A&A, 476, 307
Le Borgne, J.-F., Poretti, E., Klotz, A., et al. 2014, MNRAS, 441, 1435
Pickering, E. C., Colson, H. R., Fleming, W. P., Wells, L. D. 1901, ApJ, 13, 226
Shapley, H. 1916, ApJ, 43, 217
Vandenbroere, J., Le Borgne, J. F., Boninsegna, R. 2014, Geos Circular RR53

RRL2015 – High-Precision Studies of RR Lyrae Stars
L. Szabados, R. Szabó, K. Kinemuchi (Eds.) 2016

Periodic variable star searches in the Pan-STARRS1 Medium Deep Fields

Heather Flewelling

Institute for Astronomy, University of Hawaii at Manoa, Honolulu, HI, USA

Abstract. Pan-STARRS1 (PS1) is a 1.8 m survey telescope located at the summit of Haleakala, Hawaii. PS1 is equipped with a 1.4 gigapixel camera, 0.256 arcsec/pixels pixel scale, and a 7 square degree field of view. Between 2009 and 2014, 25% of the observing time was used to collect images in 10 fields called the Medium Deep (MD) fields, in 6 filters ($g_{\rm P1}$, $r_{\rm P1}$, $i_{\rm P1}$, $z_{\rm P1}$, $y_{\rm P1}$, $w_{\rm P1}$), with a focus on searching for supernovae. The observing strategy consisted of observing multiple MD fields per night, in a couple of filters each night, usually in sets of 8 consecutive exposures per filter, per MD field. This cadence is perfect for searching for periodic variable stars. To do the variable star search, I constructed 2.5 million light curves, each with between 200 and 4500 epochs, and ran the Lomb-Scargle algorithm on each to determine the likelihood of periodicity as well as the most prominent period. I then picked out interesting candidates and classified them. Comparisons with Vizier, for field MD02, suggest that we recover all the variables that are known in Vizier for that patch of sky, and which are in the correct magnitude range to be visible in PS1. We are also able to determine periods for those variables in Vizier which were classified as variable but had provided no period information. This is just a small fraction of the variables that are detected by PS1 – it saturates at approximately 15th magnitude, and single exposures go down to below $24^{\rm th}$ magnitude. Finally, I will highlight some of the more interesting variables discovered by Pan-STARRS1.

1. Introduction

There are now a number of surveys (such as *Kepler*, OGLE and others) with thousands of epochs of observations spanning many years that enable high precision studies of RR Lyrae. With more data, it is clear that RR Lyrae and other periodic variable stars are not as simple as previously thought.

Pan-STARRS offers 2 unique surveys that will be of much use in the future. One survey, the 3π Survey, has precise photometry and astrometry for 3/4 of the sky, in 5 ($g_{\rm P1}$, $r_{\rm P1}$, $i_{\rm P1}$, $z_{\rm P1}$, $y_{\rm P1}$) filters. Hernitschek et al. (2015) uses the 3π survey to find ∼150,000 RR Lyraes. The other survey, the Medium Deep Survey, offers a much smaller area of sky (70 square degrees), but with ~ 4000 epochs in 5 filters. This allows for extremely well sampled periodic variable star light curves in 5 filters. There will be a forthcoming catalog of periodic variable stars from the Medium Deep Survey.

The structure of this article is as follows. We start with a brief description of the Pan-STARRS telescopes and the surveys that have been conducted in the past as well as ongoing and future surveys. Next, a discussion of the Pan-STARRS Public Data Release, which will happen in 2016, and provide a very

precise static sky survey covering 3/4 of the sky in $g_{\rm P1}$, $r_{\rm P1}$, $i_{\rm P1}$, $z_{\rm P1}$, $y_{\rm P1}$, as well as a smaller Medium Deep survey which primarily focuses on time domain astronomy. Then, I will discuss my searches for periodic variable stars within the Medium Deep Fields.

2. Pan-STARRS telescopes

Pan-STARRS1 (PS1) is a 1.8 meter telescope with a 1.4 gigapixel camera and is located on the summit of Haleakala, Hawaii. The telescope has 6 filters $g_{\rm P1}$, $r_{\rm P1}$, $i_{\rm P1}$, $z_{\rm P1}$, $y_{\rm P1}$, and $w_{\rm P1}$, (see Tonry et al. 2012b for an overview of the filter system), a pixel scale of 0.256 arcsecond per pixel, and a 7 square degree field of view. A view of the PS1 telescope and an example raw image of M31 can be seen in Figure 1. Pan-STARRS2 (PS2) is nearly identical to Pan-STARRS1, and it is located next to Pan-STARRS1 and shares the support building. It is still in commissioning, but so far we have already detected a number of Near Earth Objects (NEOs) as well as a comet.

The Pan-STARRS telescopes are survey telescopes. The first set of surveys were collected by PS1 between 2009 and 2014. These surveys were defined by and funded by the PS1 Science Consortium (PS1SC). The data from the first set of surveys will be publicly released in 2016 and will be available as pixel data products and as a queryable photometric and astrometric catalog.

The current ongoing survey, which uses the PS1 telescope and the PS2 telescope, is called the NEO Survey, and is funded by NASA. It covers 26,000 square degrees excluding the Galactic plane and ecliptic poles, and will take observations in $w_{\rm P1}$ from 2014 to 2017. Since 2012, PS1 found most of the potentially hazardous asteroids[1] and finds the majority of near Earth asteroids since 2014[2]. Pan-STARRS is currently looking for new consortium members for a certain percentage of time during the NEO Survey, as well as after the NEO Survey. Consortium members can influence the surveys observed by Pan-STARRS.

3. Pan-STARRS public data release

There will soon be a public data release of Pan-STARRS1 data. During the PS1SC survey, data for several different surveys were collected. The two that will be released very soon are the 3π and the Medium Deep (MD) Survey, and they will be available via MAST and STScI.

The 3π Survey is the largest survey within Pan-STARRS with 58% of the observing time dedicated to it. The 3π Survey covers 3/4 of the sky, in $g_{\rm P1}$, $r_{\rm P1}$, $i_{\rm P1}$, $z_{\rm P1}$, and $y_{\rm P1}$ filters, observing everything with a declination larger than $-30°$. Each area of sky is observed more than 60 times, or at least 12 visits per filter. Each exposure is between 30-45 s in duration. Details about the analysis of a small area of the survey, including information on the magnitude depths, can be found in Farrow et al. (2014), which is fairly representative

[1] http://www.minorplanetcenter.net/iau/lists/YearlyBreakdown.html

[2] http://neo.jpl.nasa.gov/stats/

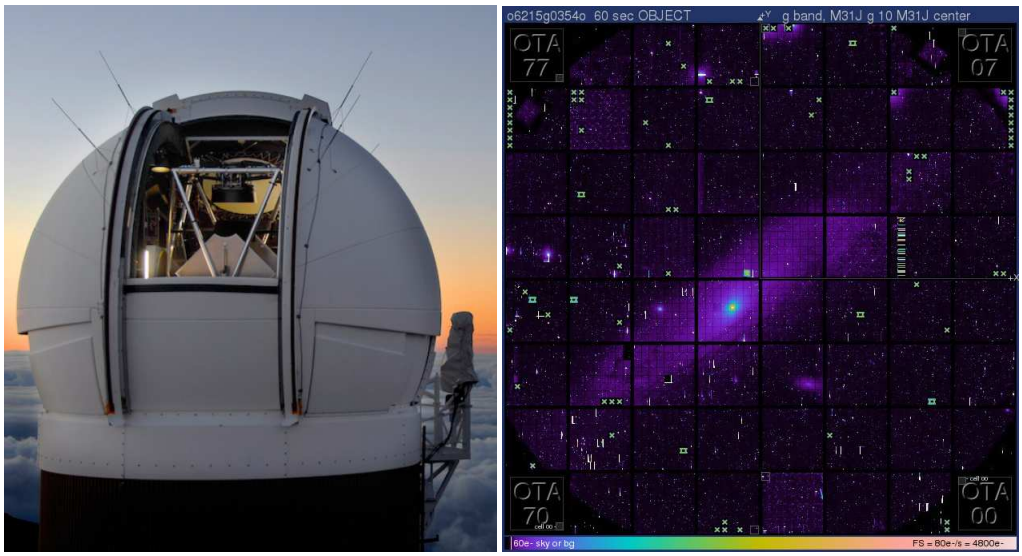

Figure 1. *Left:* Pan-STARRS1, located on the summit of Haleakala, in Maui. *Right:* A single 60 s $g_{\rm P1}$ raw exposure of M31, to demonstrate the large field of view of the Pan-STARRS1 telescope.

of the 3π survey. There are more than 75 billion detections and more than 3 billion astronomical objects in the 3π survey. There are precise astrometric and photometric calibrations of PanSTARRS data, described in Magnier et al. (2013) and Schlafly et al. (2012) for the first 1.5 years of the survey, these show that Pan-STARRS photometry and astrometry are better than 1%.

The Medium Deep (MD) is the second largest survey that is part of the PS1 science mission. It used 25% of the observing time, and it is focused on transient science, such as searches for supernovae. There are 10 fields, totaling 70 square degrees, which are described in Table 1, and plotted on the sky in Figure 2. These fields are chosen to be far from the Galactic plane, but also to overlap with other well observed fields such as the COSMOS fields. The observations were taken in sets of 8 dithered, consecutive exposures per filter, per field, with a few filters per field, per night, usually a few fields per night. For example, during the night of 2015-08-16, MD01, MD09 and MD10 were each observed in filters g and z, 8 exposures per filter per MD, for a total of 48 MD exposures that night. This results in around 4000 epochs per MD field, as seen in Figure 3.

One of the types of data products that will be made available are the processed pixels, for both the 3π and the MD survey. These will include processed images, warped to have 0.25 arcsecond pixels, and rotated to have RA/DEC on each axis, available as single "warp" skycells and as stacked skycells (a brief description is provided in Tonry et al. 2012a). An example of a warp and stack skycell is seen in Figure 4. M16 coincidentally fits exactly in the center of that skycell.

The other type of data product that will be made available is a queryable database, similar to SDSS's CasJOBS[3], for both the 3π and MD surveys. From this database, it is possible to get photometric and astrometric information for the mean properties of the astronomical objects, as well as for single exposures, stack exposures, and difference images. We expect to have more than 3 billion objects, each object can be easily queried to create a time-series light curve.

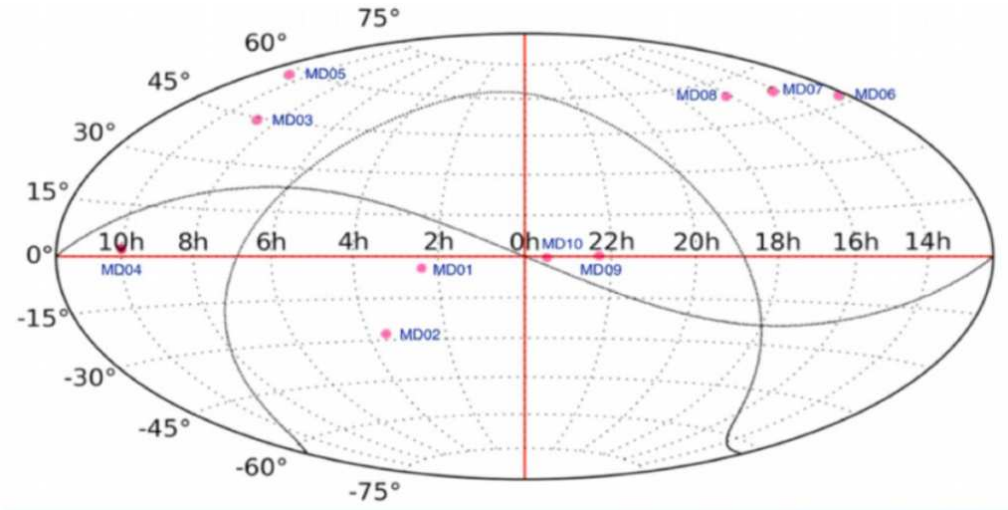

Figure 2. The locations of the Medium Deep fields, plotted to see their positions with respect to the ecliptic (sine wave), and the Galactic plane (Ω line).

4. Pan-STARRS Medium Deep Field variable star searches

Although the Medium Deep fields only consist of 70 square degrees, there are many features that make them ideal for searching periodic variable stars. The MD fields and observing strategy were chosen primarily to search for supernovae, and was quite successful at this (Rest et al. 2014). Tonry et al. (2012a) have more details about the MD Fields, as well as proper motions studies using the MD fields. The MD fields have a depth limit of $\sim 24^{\rm th}$ mag for nightly stacks, for all bands, are observed in 5 filters ($g_{\rm P1}$, $r_{\rm P1}$, $i_{\rm P1}$, $z_{\rm P1}$, $y_{\rm P1}$), and have a high cadence of observations (8 112-240 s exposures taken consecutively per filter, per field), spanning 4 years of observations with $\sim$ 4000 epochs per object in each MD field.

Within the MD fields, there are 2.5 million objects with more than 200 detections. I ran Lomb-Scargle on all 2.5 million of these objects, and am in the process of sorting through the periodograms to find periodic variable star candidates. Some of the analysis was done for MD02. There are 197,077 objects in MD02 with more than 200 detections. I only filtered out those detections which

[3]http://skyserver.sdss.org/casjobs/

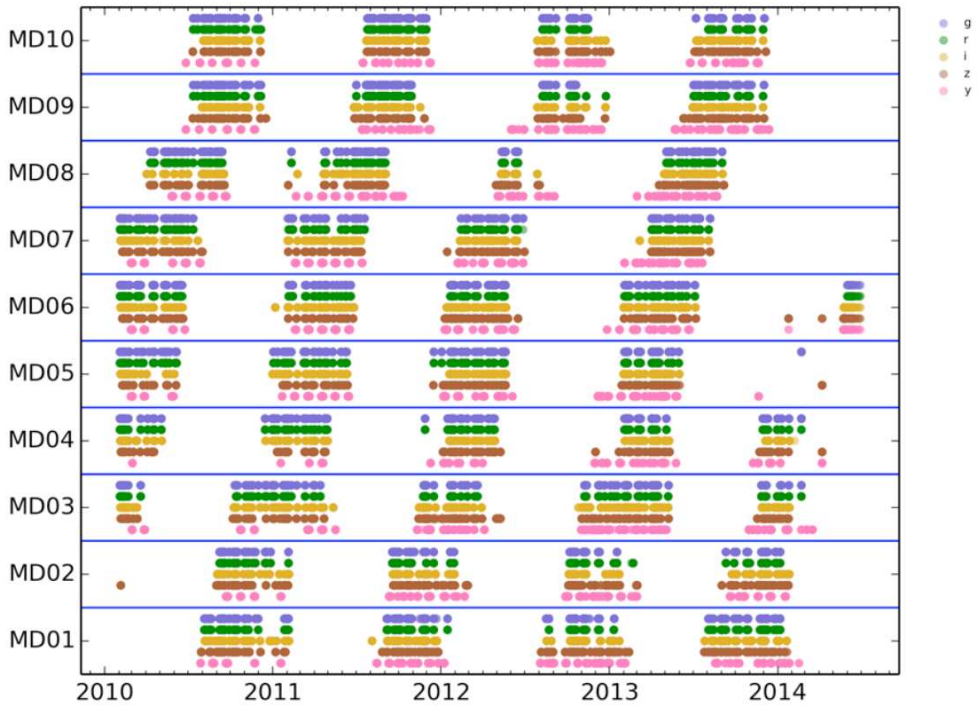

Figure 3. A plot of the observation cadence of each of the MD fields, sorted by filter. The gaps that are present are due to bad weather or miscellaneous hardware issues.

Table 1. These are the 10 Medium Deep fields, their names and their locations in the sky. Each field is 7 square degrees. (The coordinates are in given in degrees.)

MD field	Name	RA (J2000)	Dec (J2000)
MD01	XMM-LSS-DXS/VVDS-02h	036.2074	−04.5833
MD02	CDFS/GOODS/GEMS	053.1000	−28.1333
MD03	IFA/Lynx	130.5917	+44.3167
MD04	COSMOS	150.0000	+02.2000
MD05	Lockman-DXS	161.9167	+58.0833
MD06	NGC 4258	185.0000	+47.1167
MD07	DEEP2 Field 1	213.7051	+53.0834
MD08	ElliasN1-DXS	242.7875	+54.9500
MD09	SA22-DXS/VVDS-22h	334.1875	+00.2833
MD10	DEEP2-Field3	352.3125	−00.4333

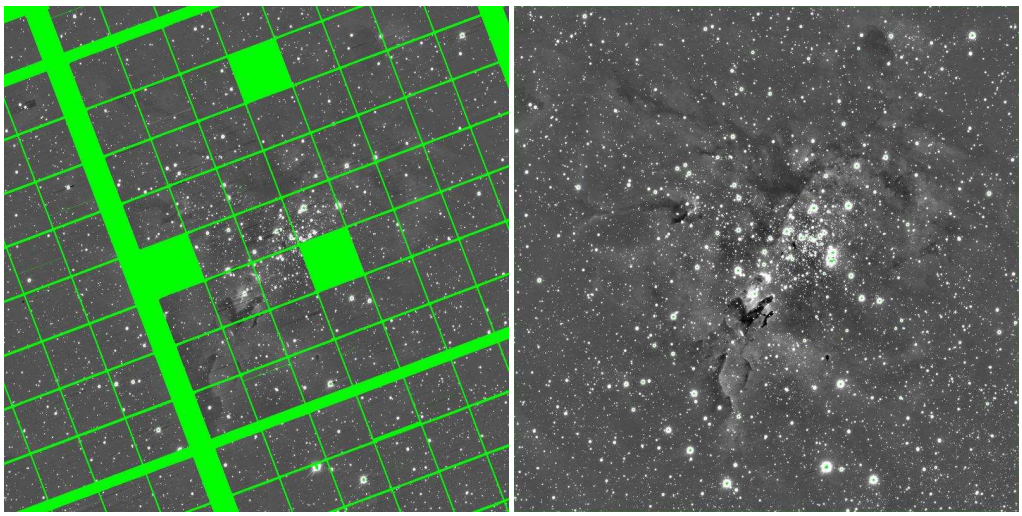

Figure 4. *Left:* A single exposure, called a warp, in $z_{\rm P1}$, taken by PS1 of M16 – this is a 30 second exposure *Right:* A stack of 14 exposures taken by PS1 in $z_{\rm P1}$, of M16. These are examples of the 2 different pixel data products available in 2016.

were saturated, and no other cuts were made, as I used a very preliminary set of PS1 data. For each object, I calculated the median $g_{\rm P1}$, $r_{\rm P1}$, $i_{\rm P1}$, $z_{\rm P1}$, $y_{\rm P1}$ magnitudes, then subtracted this from the light curve to produce a multi-wavelength light curve with a median magnitude of 0. I then calculated a Lomb-Scargle periodogram for each of the 197,077 objects. Lomb-Scargle gives a most likely frequency as well as the probability the signal is a false alarm. Plotting the most likely period vs the probability the signal is a false alarm, we can easily select out the most interesting candidates to visually inspect. These candidates have an extremely low probability of being a false alarm as well as having a most likely period between 0.03 and 1 day. There are significant problems with aliasing, as this has to do with the observation strategy.

There are 77 of these candidates, and many thousands more that are also interesting, but with lower probability of being periodic, or with a period < 0.03 days or a period > 1 day, which will be investigated later. Of those 77 candidates, all show signs of variability, and 30 are very clearly periodic with a well defined period. Some of the more dramatic light curves from the MD fields can be seen in Figure 5. For example, it is possible to find very short period, well sampled objects with periods of $\sim$0.03 days and faint RR Lyraes. The magnitude range for Pan-STARRS MD periodic variable stars is from $\sim$14.5 to nearly $\sim 23^{\rm rd}$ for $g_{\rm P1}$.

A comparison of MD02 to Vizier's and AAVSO's catalogs yielded the following. There are 17 variable stars in the MD02 field from other known catalogs. Of those 17, two were not found in the Pan-STARRS data – there were no nearby neighbors, so we suspect bad coordinates in Vizier's catalog.

There were 5 that were too bright for Pan-STARRS and were discarded. Of the 10 remaining known variable stars, all are present and detected in the Pan-

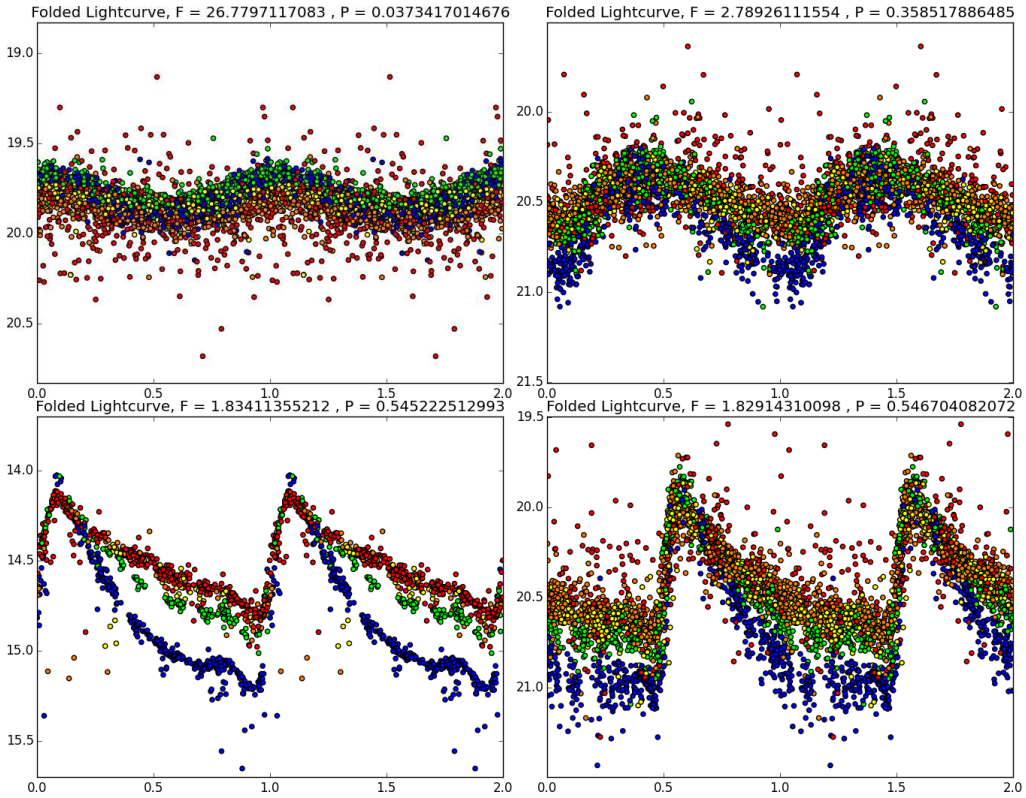

Figure 5. Examples of folded light curves. *Upper left:* a δ Scuti variable; *Upper right:* an RRc; *Lower left:* an RRab; *Lower right:* an RRab. The colors represent the filters, red = $y_{\rm P1}$, orange = $z_{\rm P1}$, yellow = $i_{\rm P1}$, green = $r_{\rm P1}$, blue = $g_{\rm P1}$. These are from single exposures, only saturated detections have been removed, no other outliers have been removed. Error bars are not included in order to see better the density of the points.

STARRS data: 3 are periodic, with a defined period, which Pan-STARRS also confirms; 3 are listed as variable but with an unknown period, Pan-STARRS is able to find the period; and 4 are variable, but no defined period, and Pan-STARRS is also unable to find a period. This leaves at least 23 (30 found in Pan-STARRS1 MD02, but 7 were known in Vizier) new periodic variable stars with well-defined periods that Pan-STARRS has discovered, and this is just from the easy and extremely dramatic candidates within 1 of the 10 fields in our set of data.

5. Conclusion

Pan-STARRS has two unique sets of data, which will soon be publicly released. The 3π is very large (3/4 of the sky), has shorter exposures (30-45 s) and has very precise calibrations, but not many ($\sim$60) epochs, while the Medium Deep

Survey is very small (70 square degrees), has longer exposures (112-240 s), and ∼4000 epochs, and is very useful for time-domain astronomy.

Preliminary searches for variable stars within the Medium Deep fields recovers previously known periodic variable stars, and a much larger number of unknown periodic variable stars. Work is ongoing to find, categorize, and catalog the periodic variable stars.

Once the 3π data are publicly released, the author will have more time to continue work on the Medium Deep periodic variable star searches, and hopes to soon release a catalog of the periodic variable stars within the Medium Deep fields, including multi-band light curves.

Acknowledgments

The Pan-STARRS1 Surveys (PS1) have been made possible through contributions of the Institute for Astronomy, the University of Hawaii, the Pan-STARRS Project Office, the Max-Planck Society and its participating institutes, the Max Planck Institute for Astronomy, Heidelberg and the Max Planck Institute for Extraterrestrial Physics, Garching, The Johns Hopkins University, Durham University, the University of Edinburgh, Queen's University Belfast, the Harvard-Smithsonian Center for Astrophysics, the Las Cumbres Observatory Global Telescope Network Incorporated, the National Central University of Taiwan, the Space Telescope Science Institute, the National Aeronautics and Space Administration under Grant No. NNX08AR22G issued through the Planetary Science Division of the NASA Science Mission Directorate, the National Science Foundation under Grant No. AST-1238877, the University of Maryland, the Eötvös Loránd University (ELTE) and the Los Alamos National Laboratory.

HF is very grateful for the invitation to attend the RRL2015 conference, and appreciates the opportunity to learn a lot about RR Lyrae. Thank you!

References

Farrow, D. J., Cole, S., Metcalfe, N., et al. 2014, MNRAS, 437, 748
Hernitschek, N., Schlafly, E. F, Sesar, B., et al. 2016, ApJ, 817:73
Magnier, E. A., Schlafly, E., Finkbeiner, D., et al. 2013, ApJS, 205:20
Rest, A., Scolnic, D., Foley, R. J., et al. 2014, ApJ, 795:44
Schlafly, E., Finkbeiner, D. P., Jurić, M., et al. 2012, ApJ, 756:158
Tonry, J. L., Stubbs, C. W., Kilic, M., et al. 2012a, ApJ, 745:42
Tonry, J. L., Stubbs, C. W., Lykke, K. R., et al. 2012b, ApJ, 750:99

RRL2015 – High-Precision Studies of RR Lyrae Stars
L. Szabados, R. Szabó, K. Kinemuchi (Eds.) 2016

Finding, characterizing and classifying variable sources in multi-epoch sky surveys: QSOs and RR Lyraes in PS1 3π

Nina Hernitschek[1], Edward F. Schlafly[1], Branimir Sesar[1], Hans-Walter Rix[1], David W. Hogg[1,2,3], Željko Ivezić[4], & Eva K. Grebel[5]

[1] *Max-Planck-Institut für Astronomie, Königstuhl 17, 69117 Heidelberg, Germany*
[2] *Center for Cosmology and Particle Physics, Department of Physics, New York University, 4 Washington Place, New York, NY, 10003, USA*
[3] *Center for Data Science, New York University, 726 Broadway, 7th Floor, New York, NY, 10003, USA*
[4] *University of Washington, Dept. of Astronomy, Box 351580, Seattle, WA 98195*
[5] *Astronomisches Rechen-Institut, Zentrum für Astronomie der Universität Heidelberg, Mönchhofstr. 12-14, 69120 Heidelberg, Germany*

Abstract. We develop a new approach for quantifying statistical properties of non-simultaneous, sparse, multi-color light curves through light-curve structure functions. Using PS1 data on SDSS Stripe 82 as "ground truth", a Random Forest Classifier identifies QSOs and RR Lyrae stars based on their variability and mean PS1 and *WISE* colors. We find that, aside from the Galactic plane, QSO and RR Lyrae samples of purity ∼75% and completeness ∼92% can be selected. On this completeness and purity basis we have identified a QSO candidate sample of a million objects, including many at low latitudes. We have assembled an unprecedentedly large and deep sample of 150 000 likely RR Lyrae candidates, with distances from ∼10 kpc to ∼120 kpc. We provide a catalog of 2.6×10^7 likely variable point sources. This work illustrates the power of time-domain surveys to identify variable objects and opens up enormous follow-up possibilities.

1. Introduction

Over the last decade, a number of time-domain, wide-area sky surveys with modern digital detectors have been implemented, making time domain astronomy a promising growth area of astrophysics. In this context, the Pan-STARRS1 survey (PS1) 3π (e.g. Kaiser et al. 2010) offers a unique combination of area, time sampling and depth, and has been extensively used to find and study transient sources. We lay out, develop, test, and apply an approach to characterize variable sources in a survey such as PS1 having multi-band, non-simultaneous observations. We focus on two classes of astrophysical objects: QSOs and RR Lyrae (RRL) stars. The basic approach should also be very relevant to the LSST. Our methodology encompasses identification of sources that clearly vary, characterization of their light curves with a multi-band structure function, and using known variable sources to train an automatic classifier and apply it. We provide a description of this approach in Hernitschek et al. (2015b).

2. Data

Our approach is based on PS1 3π data, supported by time-averaged photometry from the Wide-field Infrared Survey Explorer (WISE) survey. SDSS S82 sources are used as ground truth. Here, we describe the properties of these surveys.

2.1. PS1 3π data

PS1 is a multi-epoch survey over 3/4 of the sky at $\sim$55 epochs between 2010 and 2014 in $g_{\rm P1}, r_{\rm P1}, i_{\rm P1}, z_{\rm P1}, y_{\rm P1}$ (e.g. Kaiser et al. 2010). In each of its bands it has only a few epochs, and the observations in different bands are not taken simultaneously. We use PS1 catalog processing version PV2, where the average number of detections per source is 35 over 3.7 years after rejection of non-photometric data. To process only objects with sufficient signal-to-noise and number of epochs, we select only point sources having (i) $15 < \langle g_{\rm P1}\rangle, \langle r_{\rm P1}\rangle, \langle i_{\rm P1}\rangle < 21.5$, where $\langle\rangle$ denotes the mean magnitude after outlier cleaning, (ii) at least 10 epochs remaining after outlier cleaning. We also remove objects with problematic PS1 detections. This results in more than 3.88×10^8 objects.

2.2. *WISE* data

WISE is a space telescope providing all-sky mid-infrared data. Nikutta et al. (2014) have shown that the color cut $W12 = W1 - W2 > 0.5$ is able to isolate QSOs, as it is an indicator of its hot dust torus. For objects with $\sigma_{W1} < 0.3$ and $\sigma_{W2} < 0.3$, we use $W12$ as parameter for classification. This is the case for 1.46×10^8 out of the 3.88×10^8 selected objects from Section 2.1.

2.3. SDSS S82 sources

The SDSS (York et al. 2000) contains a stripe in the South Galactic Cap, Stripe 82 (S82), scanned multiple times for co-addition of the data and to enable discovery of variable objects. S82 contains nearly 10^4 spectroscopically confirmed quasars (Schneider et al. 2007; Schmidt et al. 2010) as well as 483 RR Lyrae stars (Sesar et al. 2010). Both are used as a ground truth: as training set for classification as well as for testing our classification method (see Sect. 3.).

3. Methodology

In this section we describe the steps we take to identify and characterize variable point sources: first, determine whether sources vary; second, characterize their variability with a structure function; and third, attribute classifications.

3.1. Identifying significantly varying sources

We start with a very generic and non-parametric measure to characterize the significance of variability, defining for an object's total number N of observations across all n bands:

$$\hat{\chi}^2 = \frac{\chi^2_{\rm source} - N_{\rm dof}}{\sqrt{2\,N_{\rm dof}}}, \quad \chi^2_{\rm source} = \sum_{\lambda} \sum_{i=1}^{N} \frac{(m_{\lambda,i} - \langle m_\lambda\rangle)^2}{\sigma^2_{\lambda,i}}. \tag{1}$$

The sum over λ is over the PS1 bands $g_{\rm P1}$,$r_{\rm P1}$,$i_{\rm P1}$,$z_{\rm P1}$,$y_{\rm P1}$, and the degree of freedom (dof) is $N_{\rm dof} = N - n$. Assuming that most of the sources are not variable, we expect the distribution of $\hat{\chi}^2$ to be a unit Gaussian. Varying sources should form a "tail" of higher $\hat{\chi}^2$. The QSOs and RR Lyrae are indeed well separated in the *normalized* distributions. However, there are only 415 RRL

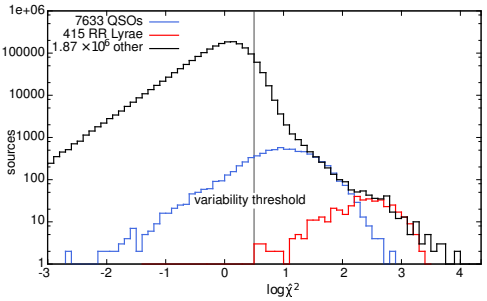

Figure 1. Histograms for $\hat{\chi}^2$ of the training set's sources; PS1 photometry in S82 region, type from SDSS. The histograms are not normalized in order to show how the distribution of "other" sources superimposes the distribution of QSOs and RR Lyrae due to the high number of "other" sources. A threshold of $\log \hat{\chi}^2 > 0.5$ is used later on for production of the catalog.

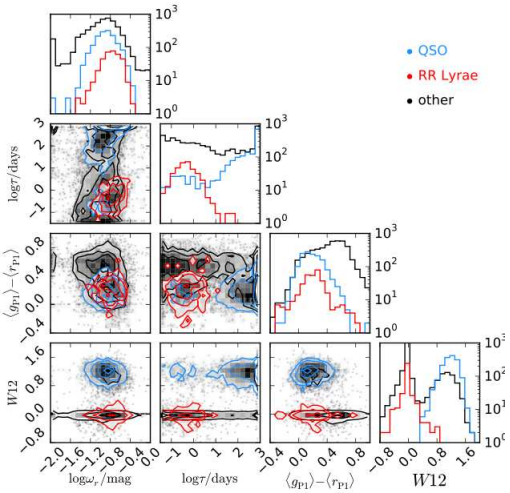

Figure 2. Structure function parameters and colors for a subsample of 2380 QSO (blue), 362 RR Lyrae (red), 5196 "other" objects (black) surviving magnitude cut and $\hat{\chi}^2 > 5$, $\hat{\chi}^2 > 30$ in the stellar locus in S82. The $W12$ color illustrates how powerful *WISE* data are in separating QSOs from other sources. We presume that most "other" sources with $W12 > 0.5$ are indeed QSOs missed by the SDSS classification.

stars and 7630 QSOs, compared to $\sim$1.85 $\times$ 10^6 "other" objects in SDSS S82 cross-matched to PS1 3π. Figure 1 shows how the distribution of "other" sources superimposes the distributions of QSOs and RR Lyrae due to the high number of "other" sources. Therefore, a simple criterion such as $\hat{\chi}^2$ is insufficient to identify QSOs or RR Lyrae variables.

3.2. Non-simultaneous, multi-band structure functions

A well-established tool for characterizing both stochastically varying and periodic variable sources is the structure function (e.g. Kozłowski et al. 2010): It describes the mean squared magnitude difference between pairs of observations of the object's brightness (Δm) as a function of the time lag between the observations (Δt). This can be used to select remarkably pure and complete samples of QSOs and RR Lyrae stars (Schmidt et al. 2010). The cadence of PS1 3π data makes it necessary to extend the usual single-band formalism of this approach for multi-band fitting.

For a given source we have N observations across all bands. For each observation n, we have magnitude m_n, its error σ_n, its epoch t_n and the corresponding bandpass b_n. There are various ways to parameterize a structure function. A common one is the damped random walk (DRW). For a multi-band DRW, the structure function is specified by a variability time scale τ and a band-depending variability amplitude $\omega(b_n)$ for the band of the observation n in case. Analogous to the single-band structure function (e.g. Hernitschek et al. 2015a), the light

curve variability is described by a $N \times N$ covariance matrix C with elements

$$C_{nn'} = \omega(b_n)\,\omega(b_{n'})\,\exp\left[-\frac{|t_n - t_{n'}|}{\tau}\right] + \sigma_n^2\,\delta_{nn'}. \quad (2)$$

To account for wavelength-depending variability amplitudes, we link the $\omega(b_n)$ by a power law with exponent $\alpha = \frac{\log(\omega(b_k)/\omega_r)}{\log(\lambda_k/\lambda_r)}$. This formalism allows for computing the probability of magnitudes m_n given meta data (t_n, b_n, σ_n^2) and parameters ($\omega(b)$, τ and $\mu(b)$), the likelihood function. Using this to predict unobserved data based on observed leads to a fitting method. Using the covariance matrix C as defined in Eq. (2), the probability of the parameters given the data can be computed, which yields a maximum likelihood approach (see Rasmussen & Williams 2006, Eq. (2.45)). The resulting log-likelihood with time-series magnitude predictions $\overrightarrow{\mu}$ is

$$\log \mathcal{L}(\mathbf{m}|\omega_r, \tau, \alpha, \mu) = -0.5\left(\log|C| + \log|C_\mu| + \chi^2\right),$$
$$\chi^2 = (m - \overrightarrow{\mu})^{\mathrm{T}} \cdot C^{-1} \cdot (m - \overrightarrow{\mu}). \quad (3)$$

We calculated the structure function parameters ω_r, τ and mean magnitudes μ from the PS1 photometry of all samples sources within the SDSS S82 area. The distribution is shown in Fig. 2. It illustrates a number of points: first, it shows the power of the *WISE* color $W1 - W2$ to separate QSOs from other sources. Second, it shows that RR Lyrae and QSOs populate different areas of (ω_r, τ) space: RRL stars have typical $\tau \sim 1$ day and QSOs have $\tau \sim 100 - 1000$ days.

3.3. Random Forest Classifier

For classifying objects based on the previously calculated parameters, we use a Random Forest Classifier (RFC). Using a training set with observed object parameter values as well as class labels, it will give the classification probability of a target set's object being of a certain class, p_{QSO} and p_{RRLyrae}. However, we treat them as arbitrary numbers and not as probabilities, and instead calculate purity and completeness of the sample later on. Table 1 summarizes the parameter set for the RFC. Though the mean r band magnitude is helpful in detecting RR Lyraes in general, we do not use it as it introduces a limit in distance.

Table 1. Parameter set for the Random Forest Classifier

Parameter	Description
$\omega_{r,\mathrm{grid}}$,τ_{grid}	best fit structure function parameter on log-spaced grid
$\hat{\chi}^2$	normalized χ^2 statistic, see Eq. (1)
$(g-r)_{\mathrm{P1}}$, $(r-i)_{\mathrm{P1}}$, $(i-z)_{\mathrm{P1}}$, $(z-y)_{\mathrm{P1}}$	colors from dereddened PS1 mean magnitudes
$\langle r \rangle_{\mathrm{P1,deredd}}$	dereddened PS1 mean r_{P1} mag., for calculation of p_{QSO}
$W12$	$W1 - W2$, helps with QSO identification
$i_{\mathrm{P1}} - W1$	RR Lyrae gravity indicator (Vickers et al. 2012).

3.4. Verification of the method using SDSS S82 classification

To quantify purity and completeness of our classifications, a randomly selected 50% of the S82 objects is used for creating the training set, with the other half as the validation set. Figure 3 shows the trade-off between purity and completeness, calculated for sources having all $\langle g_{\rm P1}\rangle$, $\langle r_{\rm P1}\rangle$, $\langle i_{\rm P1}\rangle$ between 15 and 20. We also show the case of all sources as dashed blue lines. At the top horizontal axis we have indicated the relation between completeness and $p_{\rm RRL}$, $p_{\rm QSO}$. Completeness and purity may depend on the brightness of objects under consideration. According to our tests, we assume the purity and completeness for $p_{\rm RRL} \geq 0.2$ to be constant within $15 \leq \langle r_{\rm P1}\rangle \leq 20$.

3.5. Limitations of the method

Our method is subject to several limitations. The most important ones are: (i) mismatch between ground-truth and other regions of sky, (ii) incompleteness of the training set, and (iii) inhomogeneity of the available data over the sky. The application of the classifier to regions other than S82 is only justified when the region has distributions of RRLs, QSOs, and contaminants similar to that on S82. This is the case at high latitudes. At low latitudes, as these regions include very large numbers of disk stars as well as distance depending reddening is present, the relative number of contaminants is much larger than in S82. The second problem is that even in high latitude regions, our adopted training set is imperfect. As the QSO sample from Schmidt et al. (2010) is only complete down to $i_{\rm P1} \lesssim 21.25$, fainter training set objects are labeled as non-QSOs, and our classifier learns to discard these objects. A final concern is that the classification of sources may be relatively uncertain, if they lack specific colors.

4. Results

We applied this variability characterization and subsequent RFC to all sources in PS1 3π, with the selection criteria discussed in Section 2, resulting in a total of more than 3.88×10^8 classified sources. In the following, all "purity" and "completeness" given for a threshold on $p_{\rm QSO}$, $p_{\rm RRL}$ refer to the case having the full parameter set from Table 1 available and making sure the sources fulfilling the criterion of $15 < \langle g_{\rm P1}\rangle, \langle r_{\rm P1}\rangle, \langle i_{\rm P1}\rangle < 20$.

4.1. QSO candidates

The assumption of an isotropic distribution of ∼20 QSOs per deg^2 within $15 <$ mag < 21.5 (Hartwick et al. 1990; Schneider et al. 2007; Shmidt et al. 2010) allows us to test the large scale homogeneity of our classification. We have selected 3.99×10^5 likely QSO candidates over the total PS1 3π area at a level of purity of 82%, completeness of 75%, and 1.6×10^6 possible candidates at a level of purity of 72%, completeness of 98%. The candidate selection is homogeneous to a high degree away from the Galactic plane. Around the plane, the number density of QSO candidates with high $p_{\rm QSO}$ decreases because of dust. Until dust extinction and disk star contamination become severe, we may still get an approximately uniform density of objects with high $p_{\rm QSO}$. The number density at a given minimum $p_{\rm QSO}$ is comparable for all $|b| > 20°$, and comparable to S82. At high latitudes, the increase of candidates with $p_{\rm QSO}$ is similar on and off S82. Around the Galactic anticenter, the number density of sources with low $p_{\rm QSO}$ per deg^2 is much higher than around the Galactic north pole, by a factor

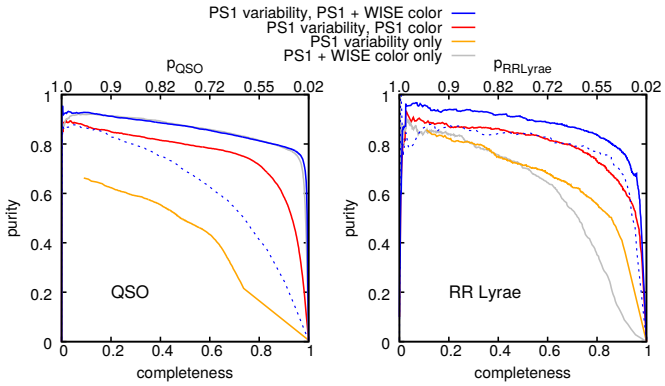

Figure 3. Trade-off between purity and completeness with respect to total cross-matched sources for different pieces of information provided to the RFC. The upper panels show precision-recall curves when PS1 variability and PS1 + *WISE* colors, PS1 variability and colors only, PS1 variability only, PS1 + *WISE* colors are provided. The numbers for purity and completeness are calculated from bright sources in the S82 training set, having $15 < \langle g_{\rm P1}\rangle$, $\langle r_{\rm P1}\rangle$, $\langle i_{\rm P1}\rangle < 20$. Calculating them for all sources ($15 < \langle g_{\rm P1}\rangle$, $\langle r_{\rm P1}\rangle$, $\langle i_{\rm P1}\rangle < 21.5$) produces the dashed blue lines.

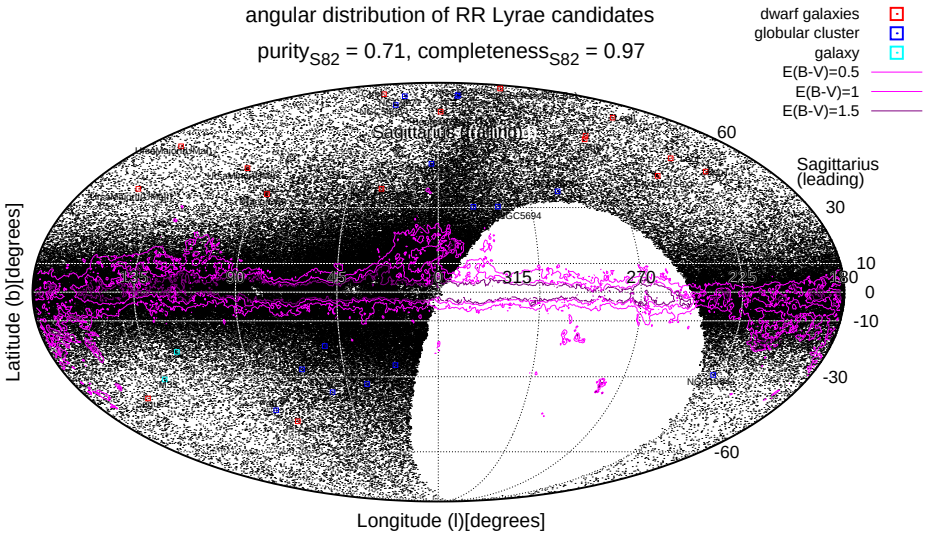

Figure 4. Distribution of likely RRL candidates, shown in Mollweide projection of Galactic coordinates. A contour plot of the reddening-based $E(B-V)$ dust map (Schlafly et al. 2014) is overlaid, as well as identified known objects of the Milky Way spheroid substructure and its neighborhood.

of ∼5. This higher overall source density does not lead to an erroneous increase of the number of candidate objects with a high $p_{\rm QSO}$, but decreases, caused by dust or varying *WISE* depth, to less than 2 objects per deg^2.

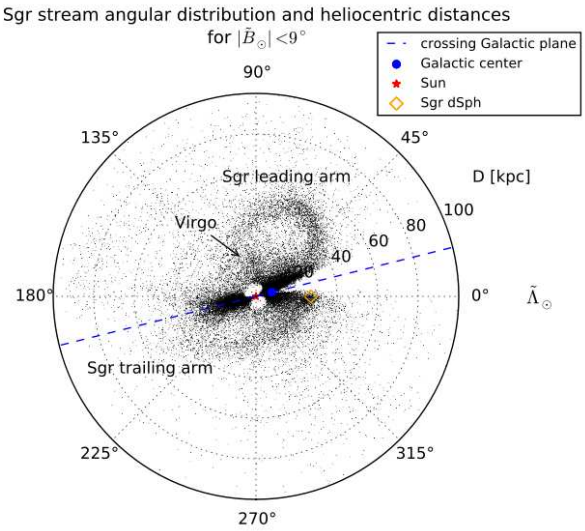

Figure 5. The extent of the Sagittarius tidal stream from the distribution of RRL candidates ($p_{\rm RRL} \geq 0.05$, purity=71%, completeness=97%) within ±9° of the Sagittarius plane, shown in Sagittarius coordinates (Belokurov et al. 2014). The leading and trailing arm of Sagittarius stream can be identified, as well as several substructures up to more than 100 kpc. Distances are from distance modulus of dereddened r band mean magnitude.

4.2. RR Lyrae candidates

Within the complete area covered by PS1 3π, we find 2.5×10^5 possible RR Lyrae candidates and 1.5×10^5 highly likely RR Lyrae candidates. In the Galactic halo, at Galactic latitudes of $|b| > 20°$, we have 60000 candidates with $p_{\rm RRL} \geq 0.05$, some extending to distances as large as ∼140 kpc. We can make use of this to verify our candidate selection. Known halo substructures, clusters and satellite galaxies are labelled in Fig. 4. Using the RR Lyrae candidates in Draco, we show that we get distance precisions of 6% at a distance of ∼80 kpc. A projection of our candidate sample into the orbital plane of the Sagittarius stream reveals the stream morphology. Figure 5, showing the RRL candidates in the Sagittarius plane, provides a striking view of the stream, with its trailing and leading arm to distances of about 100 kpc. We compare our Fig. 5 to Fig. 6 in Belokurov et al. (2014) as well as to Figs. 6 and 17 in Law et al. (2010) that shows the best-fit N-body debris model in a triaxial halo and with observational constraints for the leading and trailing arm. We also compare our results to Ruhland et al. (2011), who traced the Sagittarius stellar stream using BHB stars. From our results, we confirm the extension of the trailing arm at distances of 60 – 80 kpc from the Sun. Furthermore, we find a cloud-like overdensity at $\tilde{\Lambda}_\odot$∼110°, $5 \lesssim D \lesssim 25$ kpc, that can be identified with the Virgo overdensity. Our RR Lyrae candidates show the three-dimensional structure more clearly than in other works (Ruhland et al. 2011; Cole et al. 2008; Newberg et al. 2007).

4.3. The catalog of variable sources in PS1 3π

Out of the processed 3.88×10^8 PS1 3π sources, we provide a catalog of all likely variable point sources in PS1 and of all likely QSOs, a total of $\sim 2.6 \times 10^7$ sources. We include all sources with either $\log \hat{\chi}^2 > 0.5$ (see Fig. 2) or $W12 > 0.5$. The latter criterion ensures that we provide variability statistics for almost all QSOs.

5. Discussion and conclusion

We have set out to identify, characterize and classify variable sources in PS1 3π. We had to develop and implement new methodology for multi-band fitting of structure functions to characterize non-simultaneous multi-band light curves. Over all, this work has resulted in variability parameters and mean magnitudes for more than 3.88×10^8 sources, and a catalog of $\sim 2.6 \times 10^7$ variable sources. The results of variability studies in the Milky Way context offer the possibility for all-sky detection of variable sources and will enable us to use RRLs to precise distance estimates for finding streams and satellites. QSO candidates will provide a reference frame for Milky Way astrometry. Candidates of periodic variables can be processed further to increase their purity. As approaches for period finding are very computational expensive, they need to be applied to pre-selected candidates (see Sesar et al. in prep.; VanderPlas et al. 2015). Promising approaches for detecting periodicity in sparsely sampled multi-band time domain data are the multiband periodogram (VanderPlas et al. 2015) as well as light curve template fitting (Sesar et al. in prep.). The variability parameters also allow classification for other types of variable sources. Looking forward to catalogs of variable stars from LSST and other multi-band all-sky time-domain surveys, our approach meets the constraints of being able to deal with noisy multi-band observations, accompanied by data from other surveys, and is fast enough to provide pure and complete samples for further analysis.

References

Belokurov, V., Koposov, S. E., Evans, N. W., et al. 2014, MNRAS, 437, 116
Cole, N., Newberg, H. J., Magdon-Ismail, M., et al. 2008, ApJ, 683, 750
Hartwick, F. D. A., Schade, D. 1990, ARA&A, 28, 437
Hernitschek, N., Rix, H.-W., Bovy, Jo, et al. 2015a, ApJ, 801:45
Hernitschek, N., Schlafly, E. F., Sesar, B., et al. 2015b, ApJ, 817:73
Kaiser, N., Burgett, W., Chambers, K., et al. 2010, Proc. SPIE, 7733
Kozłowski, S., Kochanek, Ch. S., Udalski, A., et al. 2010, ApJ, 708, 927
Law, David R., Majewski, S. R. 2010, ApJ, 714, 1
Newberg, H. J., Yanny, B., Cole, N., Beers, T. C., et al. 2007, ApJ, 668, 221
Nikutta, R., Hunt-Walker, N., Nenkova, M., et al. 2014, MNRAS, 442, 3361
Rasmussen, C. E., Williams, C. K. I. 2006, Gaussian Processes for Machine Learning, Cambridge, MA: MIT Press
Ruhland, Ch., Bell, E. F., Rix, H.-W., et al. 2011, ApJ, 731:119
Schlafly, E. F., Green, G., Finkbeiner, D. P., et al. 2014, ApJ, 789:15
Schmidt, K. B., Marshall, P. J, Rix, H.-W., et al. 2010, ApJ, 714, 1194
Schneider, D. P., Hall, P. B., Richards, G. T., et al. 2007, AJ, 134, 102
Sesar, B., Ivezić, Ž., Grammer, S. H., 2010, ApJ, 708, 717
VanderPlas, J.T., Ivezić, Ž. 2015, ApJ, 812:18
Vickers, J. J., Grebel, E. K., Huxor, A. P. 2012, AJ, 143:86
York, D. G., Adelman, J., Anderson Jr., J. E., et al. 2000, ApJ, 120, 1579

RRL2015 – High-Precision Studies of RR Lyrae Stars
L. Szabados, R. Szabó, K. Kinemuchi (Eds.) 2016

Searching for distant RR Lyrae stars using the High cadence Transient Survey

Gustavo Medina T.[1], A. Katherina Vivas[2], F. Förster[3,4], & Ricardo R. Muñoz[1]

[1]*Departamento de Astronomía, Universidad de Chile, Santiago, Chile*
[2]*Cerro Tololo Inter-American Observatory, La Serena, Chile*
[3]*Millennium Institute of Astrophysics MAS*
[4]*Center for Mathematical Modelling, Universidad de Chile, Santiago, Chile*

Abstract. The High cadence Transient Survey is a deep optical campaign carried out with the Dark Energy Camera imager at the 4 m telescope on Cerro Tololo, Chile, aimed at detecting early supernova explosions. However, the cadence and survey strategy are well matched for RR Lyrae detection as well, with up to 37 single-band observations. Our goal is to use the data from the survey to find distant RR Lyrae and study their connection with known or undiscovered halo substructures. In the first year of the survey, we have been able to detect new RR Lyrae stars candidates out to at least 100 kpc from the Sun, and preliminary results also show the tantalizing detection of RR Lyrae even farther away.

1. Introduction

One of the most important properties of the RR Lyrae pulsating variable stars is that they can be used as standard candles to measure distances within the Milky Way and its neighborhood. The study of the outer halo of the Milky Way has become particularly interesting in the last decade, with the discovery of many new dwarf spheroidal (dSph) satellite galaxies, and the characterization of several substructures (e.g. stellar streams, tidal debris). RR Lyrae (RRL) stars are excellent tracers of such structures. In fact, it is known that even the least luminous and most metal-poor Milky Way satellites which have been searched for RRL stars, have at least one of such stars (Sesar et al. 2014, and references therein). Thus, finding new distant RRLs, especially in the galaxy outskirts, may help to discover faint, distant halo structures which is fundamental to understand the formation history of our Galaxy.

2. Observations and methodology

We analysed data taken by the Dark Energy Camera (DECam) on the 4 m Blanco telescope at Cerro Tololo Inter-American Observatory, Chile, during the first campaign made by the High cadence Transient Survey (HiTS) in 2014. The main goal of the survey is the detection of very young supernovae and their characterization in real time. The HiTS search strategy consists of observations

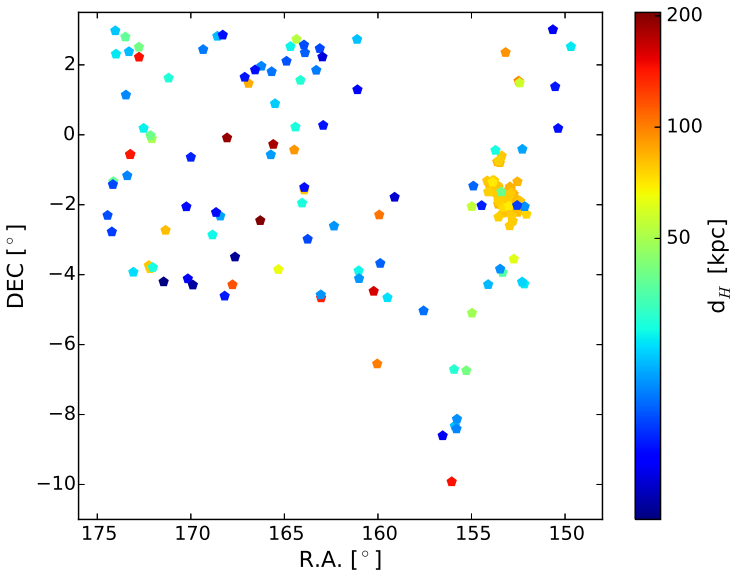

Figure 1. Distribution of our 181 RRL stars in the sky. The color code represents the heliocentric distance.

using the g filter for 40 fields observed with a cadence of two hours, during five consecutive nights, with 160 s exposures. In that sense, the search for very distant RR Lyrae variable stars seems like a natural extension of the HiTS main purpose given the deep and wide field images that DECam is able to provide (each field covers about 3 sq. degrees of the sky). The total area covered in this campaign is $\sim$ 120 sq. degrees.

The extraction of the sources from the images was performed using the photometry software SExtractor. Relative photometry was performed by calculating zero point differences between all images with respect to a reference one. Calibration was performed by comparing with SDSS photometry. For the extinction correction, the recalibrated dust maps by Schlafly & Finkbeiner (2011) were used. We only considered objects with more than five detections and that show signs of variability.

The periods were determined using the generalized Lomb-Scargle periodogram (GLS) technique (Zechmeister & Kürster 2009). Stars with periods of shorter than 0.2 days and longer than 0.9 days were filtered out. Using the statistical significances for the periods found by the astroML python module and the GLS tool (VanderPlas et al. 2012), a filter was performed allowing only objects with a significance level detection better than 8%.

The last filter used was a visual inspection of all candidates, and the requirement that the difference between the brightest and the faintest observation be larger than 0.2 magnitudes.

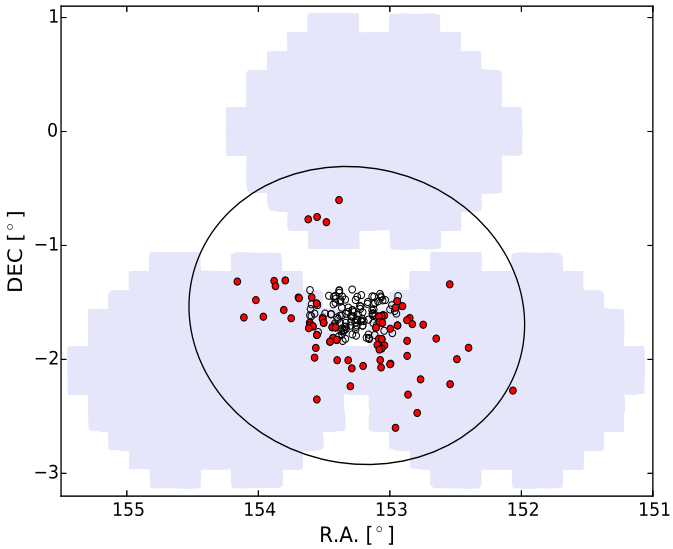

Figure 2. Spatial distribution of the RRL stars near the Sextans dSph galaxy. HiTS fields are shown in grey. The red filled circles are the RRL stars in our sample, and the open circles near the center of Sextans are variable stars in Lee et al. (2003). The dark solid line represents the tidal radius of Sextans (Mateo 1998).

3. Preliminary results

In the observed fields, 181 RRL stars were found, of which the majority seem to be RRab type based on their period, amplitude and shape of the light curve. The distance to these stars ranges from $\sim$ 8 kpc to $\sim$ 150 kpc, as shown in Figure 1. In this figure it is possible to see an overdensity near RA $\sim$ 153 degrees. According to that position and to the distances obtained for those stars (82 ± 5 kpc) we believe they belong to the Sextans dSph (RA $= 153.2512°$, DEC $= -1.6147°$, $d_H = 86 \pm 4$, McConnachie 2012).

In Figure 2 the observed HiTS fields are shown, in addition to our Sextans RRL and some variable star candidates from Lee et al. (2003). The tidal radius of the galaxy (Mateo 1998) is also shown, indicating that HiTS does not cover the center of the galaxy but only its outskirts. Thus, these stars will be valuable for studying the distribution of RRL stars within the galaxy and its possible interaction with the Milky Way. In a preliminary revision, there seems to be no extra-tidal material associated with Sextans.

In Figure 1 it is also possible to observe several RRL candidates with heliocentric distances larger than 90 kpc that do not seem to be part of Sextans. These 15 stars do not follow a clear pattern in the sky and lie in the range from 92 kpc to 204 kpc (approximately). An example of distant RRL light curves with fitted templates is presented in Figure 3. The high quality of the light curves at these faint magnitudes do not leave doubt about the classification of these variables as RRL stars.

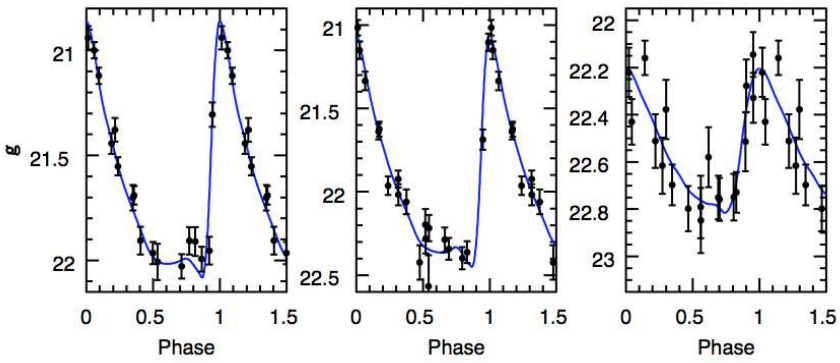

Figure 3. Folded light curves of three of the most remote ab-type RRL stars found in our survey, with $d_H \approx 141$ kpc (left), 146 kpc (middle) and 180 kpc (right). Templates from Sesar et al. (2010) are represented with blue solid lines.

4. Final remarks

Our preliminary results show the detection of more than 100 RR Lyrae candidates in the observed fields (about 120 square degrees in total), and the tantalizing finding of 15 candidates with d_H larger than 90 kpc. The origin of the distant RRL is still unclear, and additional data will be needed to understand their role in the galactic halo.

This study was made using data taken during the first HiTS campaign. We are expecting to use the data from the subsequent years of the survey, which will provide not only additional epochs to the stars in this work but also will cover additional area.

Acknowledgments

F.F. acknowledges support from CONICYT 11130228, CONICYT and NSF DPI 201400090, CONICYT Quimal 140003, and IC20009. Powered@NLHPC: This research was partially supported by the supercomputing infrastructure of the NLHPC (ECM-02). This project used data obtained with the Dark Energy Camera (DECam), which was constructed by the Dark Energy Survey (DES) collaboration.

References

Lee, M. G., Park, H. S., Park, J.-H., et al. 2003, AJ, 126, 2840
Mateo, M. L. 1998, ARA&A, 36, 435
McConnachie, A. W. 2012, AJ, 144:4
Schlafly, E. F., Finkbeiner, D. P. 2011, ApJ, 737:103
Sesar, B., Ivezić, Ž., Grammer, S. H., et al. 2010, ApJ, 708, 717
Sesar, B., Banholzer, S. R., Cohen, J. G., et al. 2014, ApJ, 793:135
VanderPlas, J., Connolly, A. J., Ivezic, Z., Gray, A. 2012, Proceedings of Conference on Intelligent Data Understanding (CIDU), pp. 47-54
Zechmeister, M., Kürster, M. 2009, A&A, 496, 577

RRL2015 – High-Precision Studies of RR Lyrae Stars
L. Szabados, R. Szabó, K. Kinemuchi (Eds.) 2016

Periodograms for multiband astronomical time series

Željko Ivezić[1] & Jacob T. VanderPlas[2]

[1]*Department of Astronomy, University of Washington, USA*
[2]*eScience Institute, University of Washington, USA*

Abstract. We summarize the *multiband periodogram*, a general extension of the well-known Lomb-Scargle approach for detecting periodic signals in time-domain data developed by VanderPlas & Ivezić (2015). A Python implementation of this method is available on GitHub. The multiband periodogram significantly improves period finding for randomly sampled multiband light curves (e.g., Pan-STARRS, DES, and LSST), and can treat non-uniform sampling and heteroscedastic errors. The light curves in each band are modeled as arbitrary truncated Fourier series, with the period and phase shared across all bands. The key aspect is the use of Tikhonov regularization which drives most of the variability into the so-called base model common to all bands, while fits for individual bands describe residuals relative to the base model and typically require lower-order Fourier series. We use simulated light curves and randomly subsampled SDSS Stripe 82 data to demonstrate the superiority of this method compared to other methods from the literature, and find that this method will be able to efficiently determine the correct period in the majority of LSST's bright RR Lyrae stars with as little as six months of LSST data.

1. Introduction

The detection and quantification of periodicity in time-varying signals is an important area of data analysis within modern time-domain astronomical surveys. In most cases, data are either obtained in a single band (e.g., LINEAR, see Sesar et al. 2011), or simultaneously in many bands (e.g., SDSS). For surveys that obtain multiband data one band at a time (e.g., LSST, see Ivezić et al. 2008), it is desirable to have a single estimate of the periodogram which accounts for all observed data in a manner which does not depend on the intrinsic behavior of the object. We recently proposed such a method dubbed the *multiband periodogram* (VanderPlas & Ivezić 2015), and here we summarize its main aspects.

The multiband model contains the following features: 1) an $N_{\rm base}$-term truncated Fourier fit which models a latent parameter, called the "overall variability" and 2) a set of $N_{\rm band}$-term truncated Fourier fits, each of which models the residual of a single band from this overall variability. The total number of parameters for K filters is then $M_K = (2N_{\rm base} + 1) + K(2N_{\rm band} + 1)$. As a result, for each band k we have the following model of the observed magnitudes:

$$\begin{aligned} y_k(t|\omega,\theta) = \quad & \theta_0 + \textstyle\sum_{n=1}^{M_{\rm base}} \left[\theta_{2n-1}\sin(n\omega t) + \theta_{2n}\cos(n\omega t)\right] \quad + \\ & \theta_0^{(k)} + \textstyle\sum_{n=1}^{M_{\rm band}} \left[\theta_{2n-1}^{(k)}\sin(n\omega t) + \theta_{2n}^{(k)}\cos(n\omega t)\right]. \end{aligned} \tag{1}$$

The important feature of this model is that *all bands* share the same base parameters θ, while their offsets $\theta^{(k)}$ are determined individually.

This multiband approach comprises a set of models indexed by their value of $N_{\rm base}$ and $N_{\rm band}$. The most fundamental models have $(N_{\rm base}, N_{\rm band}) = (1, 0)$ and $(0, 1)$, called the *shared-phase* and *multi-phase* models, respectively. In the shared-phase model, all variability is assumed to be shared between the bands, with only the fixed offset between them allowed to float. In the multi-phase model, each band has independent variability around a shared fixed offset. The key aspect of the solution is the use of Tikhonov regularization[1] (for a detailed discussion, see Ivezić et al. 2014), which drives most of the variability into the so-called base model common to all bands ("overall variability"), while fits for individual bands describe residuals relative to the base model and typically require lower-order Fourier series.

This algorithm is available in `gatspy`, an open-source Python package for general astronomical time-series analysis[2]. Along with the periodogram implementation, it also contains code to download all the data used in VanderPlas & Ivezić (2015). Code to reproduce that paper, including all figures, is available in a separate repository[3].

2. The method performance and prospects for LSST

In VanderPlas & Ivezić (2015), we used a simulated LSST cadence in 25 arbitrarily chosen fields that are representative of the anticipated main survey temporal coverage. A set of 50 RR Lyrae stars were simulated with the Sesar et al. (2010) SDSS-based templates, and with a range of apparent magnitudes between $g = 20$ and $g = 24.5$ (corresponding to bright-to-faint range of LSST main-survey observations, for details see Ivezić et al. 2008). The performance of the multiband periodogram and that of the single-band Supersmoother method are compared in Figure 1.

The multiband method outperforms the single-band results; the improvement is most apparent for faint stars, where the greater model flexibility of the Supersmoother causes it to over-fit the noisy data. These results point to much more promising prospects for LSST science with variable stars than previously reported. In particular, even with only six months of LSST data, we can expect to correctly identify the periods for over 60% of stars brighter than $g = 22$; with the first two years of LSST observations, this increases to nearly 100%. Part of this improvement is due to the performance of the shared-phase multiband model with noisy data, and part of this improvement is due to the relaxed period-matching constraints enabled by the hybrid approach of periodogram-based and template-based period determination.

---

[1] Tikhonov regularization (Tikhonov 1963) is also known as *L2 regularization* or *Ridge Regression* (Hoerl & Kennard 1970); it introduces a quadratic penalty term in the model parameters added to the χ^2. Mathematically, it is equivalent in the Bayesian framework to using a zero-mean Gaussian prior on the model parameters.

[2] See http://github.com/jakevdp/gatspy/

[3] See http://github.com/jakevdp/multiband_LS/

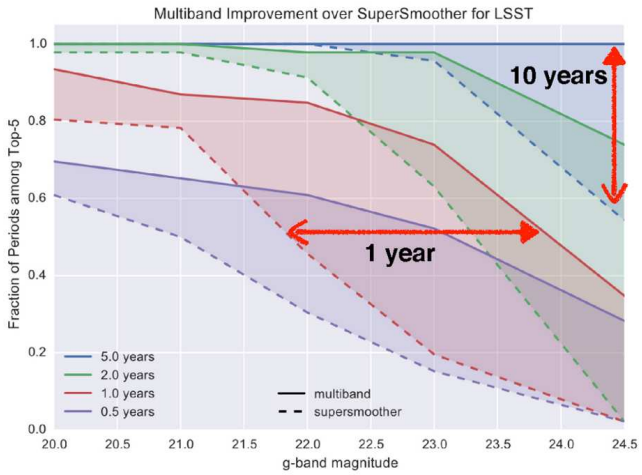

Figure 1. A comparison of the fraction of periods correctly determined for simulated LSST RR Lyrae light curves as a function of the length of the observing season and the mean g-band magnitude for the multiband periodogram approach (method of this work, solid lines) and single-band SuperSmoother approach (method of Oluseyi et al. 2012, dashed lines). The multiband method is superior to the single-band SuperSmoother approach in all cases and especially for the faintest objects. After 1 year of data, the improvement is equivalent to two magnitudes of depth, and after 10 years of data the sample completeness is boosted from ≈60% to ≈100% even at the faint limit of data ($g \approx 24.5$).

3. Discussion

Experiments on several hundred RR Lyrae stars from the SDSS Stripe 82 dataset indicate that a multiband version of the classic Lomb-Scargle method for detecting periodicity in astronomical time-series outperforms methods used previously in the literature, especially for sparsely-sampled light curves with only single bands observed each night. Looking forward to future variable star catalogs from Pan-STARRS, DES, and LSST, there are two important constraints that any analysis method must meet: i) the methods must be able to cope with heterogeneous and noisy observations through multiple band-passes, and ii) the methods must be fast enough to be computable on millions or even billions of objects. The multiband method, through its combination of flexibility and model simplicity, meets the first constraint: in the case of sparsely-sampled noisy multiband data, it outperforms previous approaches to period determination. It also meets the second constraint: it requires the solution of a simple linear model at each frequency, compared to a sliding-window model in the case of Supersmoother, a nonlinear optimization in the case of template-fitting, and a Markov Chain Monte Carlo in the case of CARMA models. In our own benchmarks, we found the multiband method to be several times faster than the single-band supersmoother approach, and several orders of magnitude faster than the template fitting approach.

The strengths and weaknesses of the multiband method suggest a hybrid approach to finding periodicity in sparsely-sampled multiband data: a first pass

with the fast multiband method, followed by a second pass using the more computationally intensive template-fitting method to select among these candidate periods. Despite pessimism in previous studies, our experiments with simulated LSST data lead us to expect such a hybrid approach to successfully identify periods in the vast majority of RR Lyrae stars brighter than $g \sim 22.5$ in the first months of the survey. This finding suggests that the multiband periodogram could have an important role to play in the analysis of variable stars in future multiband surveys.

We note that an interesting alternative method is the multiband generalization of the multiharmonic Analysis of Variance (AoV) period estimation algorithm proposed by Mondrik, Long, & Marshall (2015) (see also Long, Chi & Baraniuk 2014 for related work). They presented two methods, the "Multiband Generalized Lomb-Scargle" which is effectively identical to the $(1, 0)$ multi-phase model here, and the "Penalized Generalized Lomb-Scargle" (PGLS), which is similar in spirit to our $(0, 1)$ shared-phase model. Their regularization terms penalize deviations of the amplitude and phase from a common mean between the bands; in this sense the PGLS model can be considered a conceptual mid-point between our shared-phase and multi-phase models. Given the differences between their and our methods for multiband model regularization, we are currently undertaking a detailed comparison of their performance.

Acknowledgements

ŽI acknowledges support by NSF grant AST-0551161 to LSST for design and development activity. JTV is supported by the University of Washington eScience institute, including grants from the Alfred P. Sloan Foundation, the Gordon and Betty Moore Foundation, and the Washington Research Foundation. The authors thank GitHub for providing free academic accounts which were essential in the development of this work.

References

Hoerl, A. E., Kennard, R. W. 1970, Technometrics, 12, 55
Ivezić, Ž., Tyson, J. A., Abel, B., et al. 2008, arXiv:0805.2366
Ivezić, Ž., Connolly, A., VanderPlas, J., Gray, A. 2014, *Statistics, Data Mining, and Machine Learning in Astronomy: A Practical Python Guide for the Analysis of Survey Data*, Princeton, NJ: Princeton Univ. Press
Long, J. P., Chi, E. C., Baraniuk, R. G. 2014, arXiv:1412.6520
Mondrik, N., Long, J. P., Marshall, J. L. 2015, ApJ, 811:34
Oluseyi, H. M., Becker, A. C., Culliton, C., et al. 2012, AJ, 144:9
Sesar, B., Ivezić, Ž., Grammer, S. H., et al. 2010, ApJ, 708, 717
Sesar, B., Stuart, J. S., Ivezić, Ž., et al. 2011, AJ, 142:190
Tikhonov, A. 1963, Soviet Math. Dokl., 5, 1035
VanderPlas, J. T., Ivezić, Ž. 2015, ApJ, 812:18

RRL2015 – High-Precision Studies of RR Lyrae Stars
L. Szabados, R. Szabó, K. Kinemuchi (Eds.) 2016

Measuring amplitudes of harmonics and combination frequencies in variable stars

Earl P. Bellinger[1,2], Daniel Wysocki[3], & Shashi M. Kanbur[4]

[1]*Max-Planck-Institut für Sonnensystemforschung, Göttingen, Germany*
[2]*Stellar Astrophysics Centre, Aarhus, Denmark*
[3]*Rochester Institute of Technology, NY, USA*
[4]*State University of New York at Oswego, NY, USA*

Abstract. Discoveries of RR Lyrae and Cepheid variable stars with multiple modes of pulsation have increased tremendously in recent years. The Fourier spectra of these stars can be quite complicated due to the large number of combination frequencies that can exist between their modes. As a result, light-curve fits to these stars often suffer from undesirable ringing effects that arise from noisy observations and poor phase coverage. These non-physical overfitting artifacts also occur when fitting the harmonics of single-mode stars. Here we present a new method for fitting light curves that is much more robust against these effects. We prove that the amplitude measurement problem is very difficult (NP-hard) and provide a heuristic algorithm for solving it quickly and accurately.

1. Introduction to the Fourier decomposition

The light curve of a Cepheid or RR Lyrae variable star with one or more modes of pulsation can be represented as a sum of periodic components:

$$m(t;\vec{\omega},\mathbf{A},\mathbf{\Phi}) = \sum_{k_1=-N}^{N} \dots \sum_{k_{|\vec{\omega}|}=-N}^{N} A_{\vec{k}} \sin\left(t\left[\vec{k}\cdot\vec{\omega}\right] + \Phi_{\vec{k}}\right) \tag{1}$$

where t is the time of observation, m is the magnitude, $\vec{k}$ is a vector of wavenumbers, $\vec{\omega}$ is a vector of angular frequencies, $\mathbf{A}$ is a multidimensional array of amplitudes, and $\mathbf{\Phi}$ is a multidimensional array of phases. This equation is known as the *Fourier decomposition* and is especially useful for fitting light curves of stars that have been sampled irregularly in time.

The ordinary approach of measuring the amplitudes and phases in this equation begins by first separating each component into a sum of sines, $\mathbf{S}$, and cosines, $\mathbf{C}$, with

$$A_{\vec{k}} \sin\left(t\left[\vec{k}\cdot\vec{\omega}\right] + \Phi_{\vec{k}}\right) = S_{\vec{k}} \sin\left(t\left[\vec{k}\cdot\vec{\omega}\right]\right) + C_{\vec{k}} \cos\left(t\left[\vec{k}\cdot\vec{\omega}\right]\right). \tag{2}$$

A matrix $\mathbf{X}$ is constructed containing columns for each sine and cosine term and a row for each individual observation. The amplitude of each component of the Fourier fit can then be measured with least squares linear regression, i.e. $\left[\mathbf{S}\ \mathbf{C}\right] = (\mathbf{X}^{\mathrm{T}}\mathbf{X})^{-1}\mathbf{X}^{\mathrm{T}}\vec{m}$, and finally we can obtain

$$A_{\vec{k}} = \sqrt{C_{\vec{k}}^2 + S_{\vec{k}}^2} \quad \text{and} \quad \tan(\Phi_{\vec{k}}) = -S_{\vec{k}}/C_{\vec{k}}. \tag{3}$$

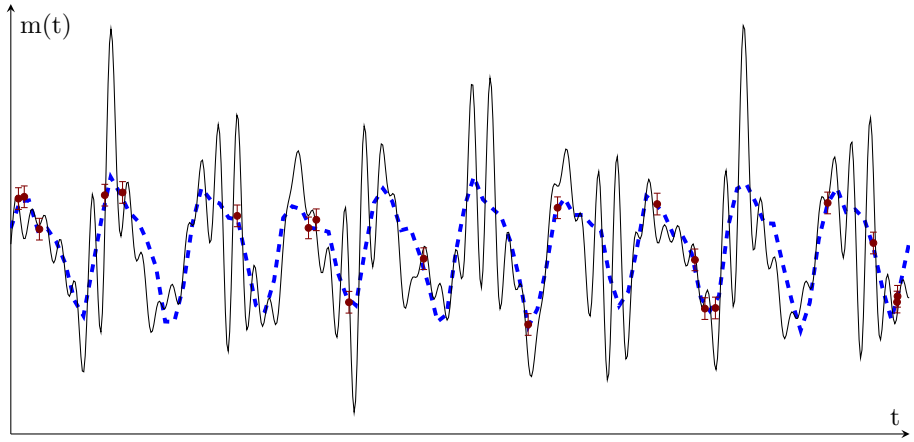

Figure 1. An example of a simulated multi-mode variable star being fit by the least squares Fourier decomposition. The blue dotted line is the true light curve of the star, the red points are the observations, and the solid line is the least squares fit. The fit is very poor and shows strong non-physical ringing effects.

The only thing left to be determined is the order of fit N, that is, the number of components needed to describe the signal. This is commonly achieved by successive prewhitening or with the procedure known as Baart's criterion, which involves iteratively increasing N until the auto-correlation of the residuals are below some threshold (Baart 1982; Petersen 1986).

Unfortunately, these procedures can result in very poor fits to observational data, especially when the data contain outliers or the time series has significant gaps in the phase coverage of the periods. An example of this can be seen in Fig. 1, in which a time series of observations for a simulated multi-mode variable star is fitted using the least squares Fourier decomposition.

2. Improving the Fourier decomposition with regularization

We want to estimate the optimal parameters $\hat{\mathbf{A}}$ and $\hat{\mathbf{\Phi}}$ for a multi-mode oscillator $\hat{m}$ that is best supported by the observed data $\left(\vec{t}, \vec{m}, \vec{\epsilon}\right)$, where $\vec{\epsilon}$ are the uncertainties on the observations. We also want to find the simplest model; that is, the one with the smallest number of components needed to describe everything we witnessed. This is just Occam's razor. And finally, we want to minimize the squared error between our model and the observations with the uncertainty on each observation taken explicitly into account. Putting this all together, we have

$$\left(\hat{\mathbf{A}}, \hat{\mathbf{\Phi}}\right) = \underset{\left(\mathbf{A}, \mathbf{\Phi}\right)}{\arg\min} \left(\|\mathbf{A}\|_0 \, , \left\| \epsilon^{-1} \left[\vec{m} - \hat{m}\left(\vec{t}; \vec{\omega}, \mathbf{A}, \mathbf{\Phi}\right) \right] \right\|_2 \right) . \tag{4}$$

This optimization problem has several aspects that make it very difficult to solve. Not only does it have multiple objectives, but it is also a sparse (ℓ_0-

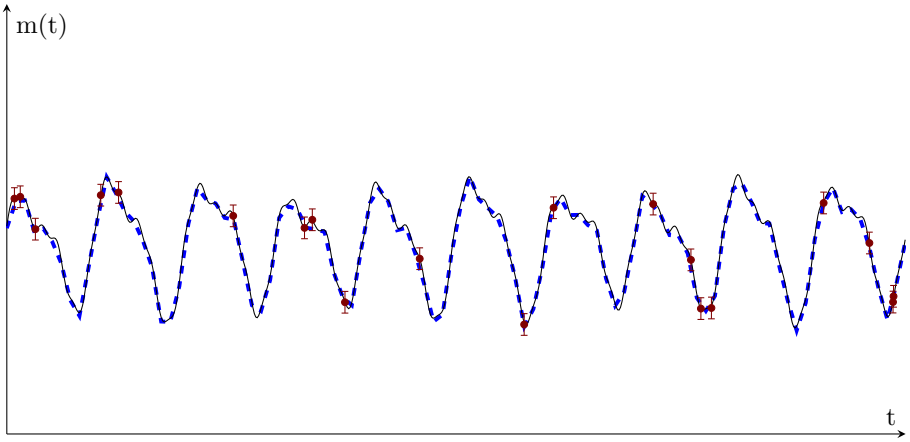

Figure 2. The same data in Fig. 1 being fit with the LASSO method.

norm) minimization problem, which is NP-hard (Natarajan 1995) and therefore it cannot be solved in practice. Hence, we are required to simplify the problem.

If we relax the constraint on the amplitudes to ℓ_1-norm minimization (that is, minimizing $\|\mathbf{A}\|_1$), which encourages sparsity rather than requiring it, then we can make use of the method of Lagrangian multipliers to scalarize the objectives. We can combine the objective functions with a *regularization parameter* that can be chosen either via cross-validation or with an information criterion such as Akaike (1974) or Bayes (Schwarz 1978). This is equivalent to putting Laplacian priors on all of the amplitudes. This simplified problem is known in regression analysis as the Least Absolute Shrinkage and Selection Operator, or *LASSO*, and we can solve it using quadratic programming (Tibshirani 1996), coordinate descent (Fu 1998), or least-angle regression (Efron et al. 2004).

In Fig. 2, we return to the simulated multi-mode variable star and fit it with our LASSO method. It can be seen that the ringing effects have been eliminated. In Fig. 3, we apply this method to a classical RR Lyrae light curve with one period of pulsation. Here it can be seen that the LASSO vastly outperforms the least squares method, especially when there are few data points.

We are developing a free, open source, and easy-to-use code for fitting light curves with the LASSO method. In addition, we are preparing a catalog of LASSO light-curve fits for stars that have been observed by OGLE-III. These will both be released in a future publication. The source codes for producing the figures in this manuscript are available electronically at `https://github.com/earlbellinger/multiperiod` (Bellinger 2015).

Acknowledgements

EPB thanks the ERC grant agreement no. 338251 (StellarAges), the NPSC and NIST for fellowship support, and the Max Planck Society and IMPRS for travel support. The authors thank the IUSSTF for their support of the Joint Center for the Analysis of Variable Star Data that funded collaborative visits. DW thanks SUNY Oswego for support to visit the University of Delhi.

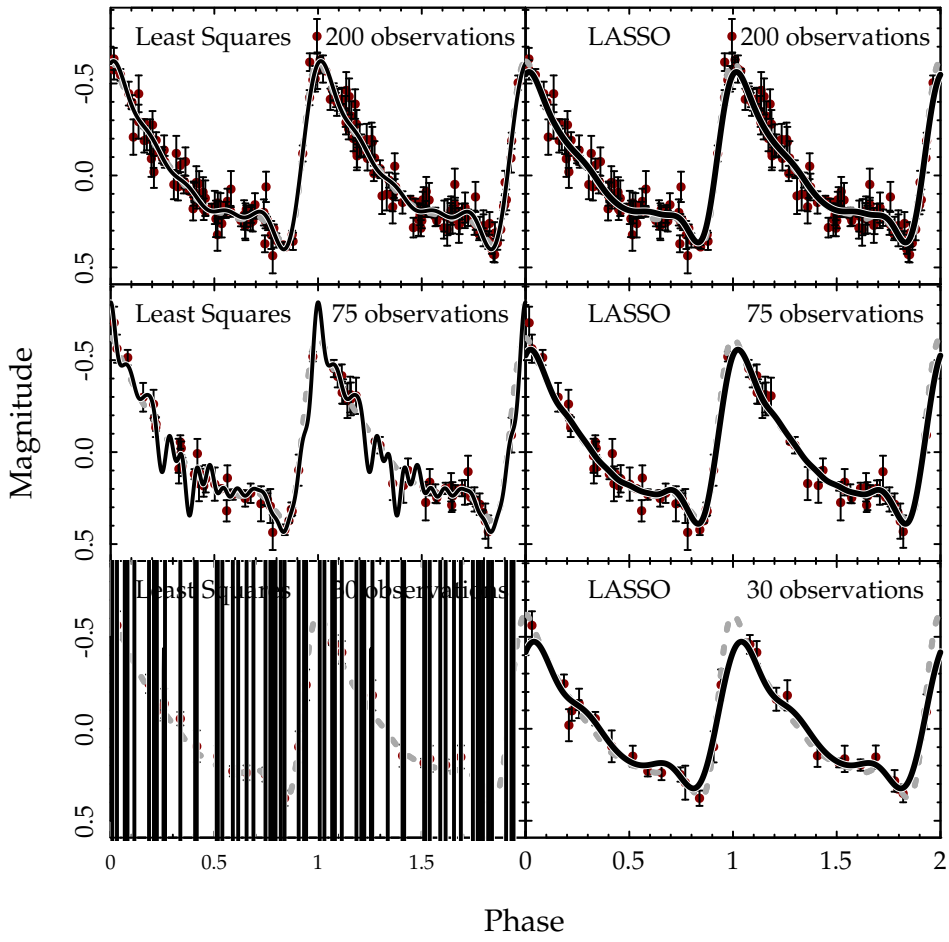

Figure 3. Sensitivity analysis of a simulated RR Lyrae light curve (dashed gray line). When the number of observations (red points) is large (top), both least squares (solid black line, left) and LASSO (solid black line, right) fits perform well. When the number of observations is small (bottom), however, the least squares fit fails catastrophically and only LASSO still works as desired.

References

Akaike, H. 1974, IEEE Transactions on Automatic Control, 19, 716
Baart, M. L. 1982, IMA Journal of Numerical Analysis, 2, 241
Bellinger, E. P. 2015, Zenodo, DOI: 10.5281/zenodo.34418
Efron, B., Hastie, T., Johnstone, I., et al. 2004, Annals of Statistics, 32, 407
Fu, W. J. 1998, Journal of Computational and Graphical Statistics, 7, 397
Natarajan, B. K. 1995, SIAM Journal on Computing, 24, 227
Petersen, J. O. 1986, A&A, 170, 59
Schwarz, H., 1978, Annals of Statistics, 6, 461
Tibshirani, R. 1996, Journal of the Royal Statistical Society B, 267

RRL2015 – High-Precision Studies of RR Lyrae Stars
L. Szabados, R. Szabó, K. Kinemuchi (Eds.) 2016

Method of LSD profile asymmetry for estimating the center of mass velocities of pulsating stars

Nikolay Britavskiy[1,2], Elena Pancino[4], Vadim Tsymbal[5], Donatella Romano[3], Carla Cacciari[3], & Gisella Clementini[3]

[1]*IAASARS, National Observatory of Athens, Athens, Greece*
[2]*Department of Astronomy and Astronomical Observatory, Odessa National University, Odessa, Ukraine*
[3]*INAF-Osservatorio Astronomico di Bologna, Bologna, Italy*
[4]*INAF-Osservatorio Astrofisico di Arcetri, Florence, Italy*
[5]*Crimean Federal University, Simferopol, Crimea*

Abstract. We present radial velocity analysis for 20 solar neighborhood RR Lyrae and 3 Population II Cepheids. High-resolution spectra were observed with either TNG/SARG or VLT/UVES over varying phases. To estimate the center of mass (barycentric) velocities of the program stars, we utilized two independent methods. First, the 'classic' method was employed, which is based on RR Lyrae radial velocity curve templates. Second, we provide the new method that used absorption line profile asymmetry to determine both the pulsation and the barycentric velocities even with a low number of high-resolution spectra and in cases where the phase of the observations is uncertain. This new method is based on a least squares deconvolution (LSD) of the line profiles in order to analyze line asymmetry that occurs in the spectra of pulsating stars. By applying this method to our sample stars we attain accurate measurements ($\pm$ 2 km s^{-1}) of the pulsation component of the radial velocity. This results in determination of the barycentric velocity to within 5 km s^{-1} even with a low number of high-resolution spectra. A detailed investigation of LSD profile asymmetry shows the variable nature of the project factor at different pulsation phases, which should be taken into account in the detailed spectroscopic analysis of pulsating stars.

1. Introduction

RR Lyrae stars are important tracers of galactic dynamics and evolution. Their high luminosity makes them good tracers for investigations of the Galactic halo and of stellar systems outside the Milky Way. Together with the proper motion, the center-of-mass velocity (or barycentric velocity, V_γ) of this type of stars is thus a fundamental parameter that should be derived with the highest possible accuracy. Indeed, the uncertainties associated to the determination of barycentric velocities of RR Lyrae stars constitute a long-standing problem, which also affects the accuracy of RR Lyraes as distance indicators. Several studies have been devoted to the problem (Jeffery et al. 2007; For et al. 2011; Sesar 2012). Briefly, two main methods have been traditionally employed. In the first approach, one relies on a template radial velocity curve, that is shifted and scaled to match the observed radial velocity at a few different phases. This method becomes more accurate when observations covering several phases are available.

Otherwise, the second approach may turn out to be useful: RR Lyraes are observed at a particular phase (usually around 0.5) during a pulsation period, when the observed radial velocity most likely equals the barycentric velocity of the star. However, this solution is not realistically applicable in the case of large surveys, where often there is no possibility to schedule the observations in convenient phases.

In this work, we apply a method which allows to estimate the barycentric velocity of RR Lyrae stars from just a few observations at random phases. The method is based on (i) investigations of the absorption line profile asymmetry that occurs during the radial pulsations and (ii) determination of the absolute value of the pulsation component using line profile bisectors, taking carefully into account limb-darkening effects. We test our method on a sample of solar neighborhood RR Lyraes that was investigated in a previous paper (Pancino et al. 2015) and on densely-spaced observations of RR Lyr (Fossati et al. 2014).

2. Sample of program stars

The analysed sample consists of 20 RR Lyr stars and 3 Population II Cepheids. The stars were observed as part of different observational programs with the SARG echelle spectrograph at the Telescopio Nazionale Galileo (TNG, La Palma, Spain) and with the UVES spectrograph at ESO's Very Large Telescope (VLT, Paranal, Chile). Furthermore, additional archival spectra were retrieved from the ESO archive. The resolving power of the spectra obtained with SARG is $R = \lambda/\delta\lambda \approx 30\,000$ with an average signal-to-noise ratio S/N $\approx$ 50-100 and spectral range from 4000 to 8500 Å. UVES spectra have a higher resolving power, $R \approx 47\,000$, and S/N $\approx$ 70-150 and cover the wavelength range from 4500 to 7500 Å. The observations were performed at random pulsation phases generally three times for each star; however, for some stars we have more observations, or just one. The general information about the program stars are presented in Pancino et al. (2015).

3. Barycentric velocity of pulsating stars

From an observational point of view, the barycentric velocity, V_γ, can be described using the following components:

$$V_\gamma = v_{\rm obs} + v_\odot - v_{\rm puls} \qquad (1)$$

where $v_{\rm obs}$ is the observed velocity of the star along the line of sight, $v_\odot$ is the heliocentric correction, and $v_{\rm puls}$ is the pulsation velocity of the radially pulsating star. We will see in the following sections that the determination of $v_{\rm puls}$ requires a treatment of limb-darkening effects, generally included in the form of a *projection factor*. The sum $v_{\rm obs} + v_\odot$ is the heliocentric radial velocity of the star, $v_{\rm rad}$, at any given phase in the pulsation cycle. In other words, the determination of the barycentric radial velocity of pulsating stars such as RR Lyraes and Cepheids requires — in principle — the determination of two observational quantities: (i) the observed radial velocity (with respect to the heliocentric reference) and (ii) the pulsation component at the moment

of the observation or, better, at the specific pulsation phase of the observations (corrected for limb-darkening effects).

4. Method of bisectors

We propose a method for the determination of the barycentric radial velocity that is based on the asymmetry of line profiles in pulsating stars, which vary along the pulsation cycle and thus can also be used to infer the pulsational component of the barycentric velocity. The method, hereafter referred to as *bisectors method* for brevity, allows for an estimate of the barycentric velocity of pulsating stars with a sparse phase sampling, and it works even with just one observation, albeit with a slightly larger uncertainty.

To determine line profiles, we use the LSD method (least-squares deconvolution, Donati et al. 1997) that derives a very high S/N ratio line profile for each spectrum from the profiles of many observed absorption lines, under the assumption that the vast majority of lines have the same profile, and that different line components add up linearly. Depending on the number of used lines, the reconstructed LSD profile can have an extremely high S/N ratio, rarely attainable with RR Lyrae observations on single lines. The original LSD method by Donati et al. (1997) was modified and extended to different applications by several authors. We used the Tkachenko et al. (2013) implementation, and our workflow can be outlined as follows:

1. We compute the LSD profile of each observed spectrum; this also allows for an independent estimate of $v_{\rm obs}$;
2. We compute a theoretical library of LSD profiles, predicting the line profile asymmetries at each pulsation phase, and we compute the bisectors of each of the profiles; one of the example of such grid is presented on top panel of Fig. 1;
3. We compute the bisector of the observed LSD line profile and compare that to the theoretical ones, to determine which pulsation velocity corresponds to the observed asymmetry of the LSD bisector; in our computation, we implement a full description of limb-darkening effects.

Once the observed and pulsational components are known, the barycentric velocity can be trivially obtained from equation (1). The final radial velocity analysis of programme stars is still in progress and final results will be published later, in this paper we presented only the intermediate results.

5. A test on RR Lyrae

In order to test the method, we applied it to the prototype of the RR Lyrae class: RR Lyrae itself. We used the 56 high-resolution ($R = 60\,000$) and high signal-to-noise (100–300) spectra of RR Lyr taken along the whole pulsation cycle, including Blazhko phases, kindly provided by Fossati et al. (2014, private communication). The good phase sampling allows us to test the method thoroughly along the whole pulsation cycle.

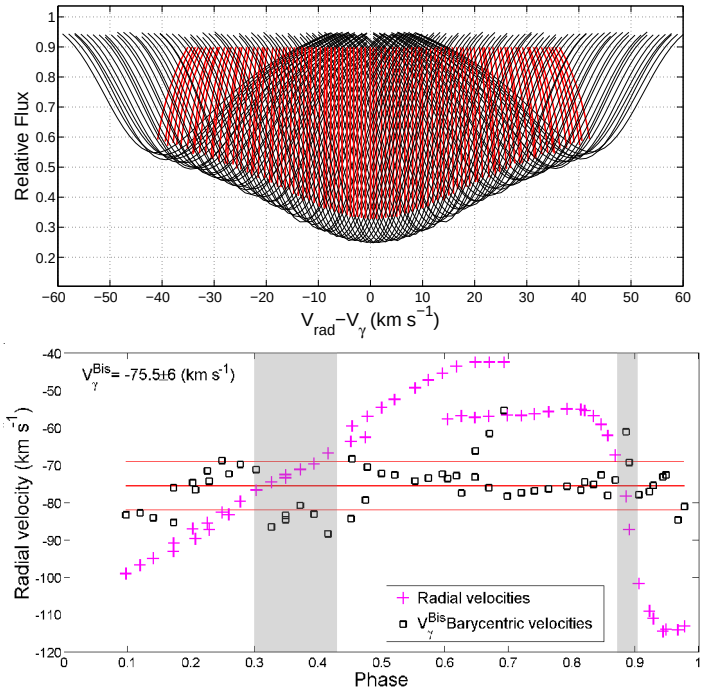

Figure 1. *Top panel:* Example of LSD profiles and bisector computed from model spectra of RR Lyrae with pulsation velocities from −50 to +50 km s^{-1}. *Bottom panel:* Barycentric velocities of RR Lyr (black squares - by using method of bisectors) inferred from radial velocities measurements (magenta crosses) at different phases. Grey regions presumably correspond to the phases with low pulsation velocities, that do not affect the line profile asymmetry.

For each spectrum we computed the LSD-profile and the bisectors, deriving both $v_{\rm rad}$ and $v_{\rm puls}$ with the same method used for our programme stars. The results are presented in bottom panel of Figure 1, where the values of the radial velocity and barycentric velocity at different phases are indicated with magenta crosses and black squares, respectively. We finally derived a mean value of $V_\gamma^{\rm Bis} = -75.5 \pm 6$ km s^{-1}. However, in the phase ranges 0.2–0.3 and 0.85–0.90, deviations up to 15 km s^{-1} were found. The explanation is as follows: in these phase ranges, the pulsational velocity is small, and our method is not very sensitive to $|v_{\rm puls}| < 5$ km s^{-1}, and also, during the shock phase 0.85–0.90 the absorption iron lines are disappearing, that causes difficulties in the correct determination of line profile asymmetries.

References

Donati, J.-F., Semel, M., Carter, B. D., et al. 1997, MNRAS, 291, 658
For, B.-Q., Sneden, C., Preston, G. W. 2011, ApJS, 197:29
Fossati, L., Kolenberg, K., Shulyak, D. V., et al. 2014, MNRAS, 445, 4094
Jeffery, E. J., Barnes, III T. G., Skillen, I., Montemayor, T. J. 2007, ApJS, 171, 512
Pancino, E., Britavskiy, N., Romano, D., et al. 2015, MNRAS, 447, 2404
Sesar, B. 2012, AJ, 144:114
Tkachenko, A., Van Reeth, T., Tsymbal, V., et al. 2013, A&A, 560, A37

RRL2015 – High-Precision Studies of RR Lyrae Stars
L. Szabados, R. Szabó, K. Kinemuchi (Eds.) 2016

Multidimensional hydrodynamic convection in full amplitude RR Lyrae models

Robert Deupree[1] & Christopher Geroux[1,2]

[1] *Saint Mary's University, Halifax, NS, Canada*
[2] *University of Exeter, Exeter, UK*

Abstract. Multidimensional (both 2D and 3D) hydrodynamic calculations have been performed to compute full amplitude RR Lyrae models. The multidimensional nature allows convection to be treated in a more realistic way than simple 1D formulations such as the local mixing length theory. We focus on some aspects of multidimensional calculations and on the model for treating convection.

1. Introduction

The computation of radially pulsating RR Lyrae stars was one of the early successes of 1D hydrodynamic simulations in astrophysics. While these successfully reproduced many features of RR Lyrae stars, they did not produce a red edge to the instability strip. Christy (1966) and Cox et al. (1966) noted that convection was becoming important in models near the red edge and speculated that convection may have a role in quenching the pulsation there. Various simple attempts at treating the time dependence of convection during a pulsation period, specifically leaving the convective flux constant during the pulsation (Tuggle & Iben 1973) and forcing instantaneous adjustment of the convection to current pulsation conditions (Cox et al. 1966), failed to produce a red edge. This led to several mixing length formulations for treating time dependent convection (e.g., Stellingwerf 1982a,b, 1984,a,b,c; Kuhfuss 1986; Xiong 1989). These have been applied with some success (e.g., Gehmeyr 1992a,b, 1993; Bono & Stellingwerf 1994; Bono et al. 1997a,b; Marconi et al. 2003). Calculations using some of these models near the red edge can lead to a red edge, but the agreement with the light curves, specifically near the red edge, is not as satisfactory as desired (Marconi & Degl'Innocenti 2007), and it is generally considered that improvements are required (e.g., Buchler 2009; Marconi 2009).

A different approach was taken by Deupree (1977a,b), who used 2D hydrodynamic simulations with an eddy viscosity model for convection to show how convection quenched pulsation at the red edge. However, these calculations could not be carried to full amplitude for numerical reasons, so that a comparison with the light curves was not possible. More recently other 2D calculations have become available (e.g., Gastine & Dintrans 2008a,b, 2011; Mundprecht et al. 2013, 2015). These have tended to focus on comparatively highly zoned calculations to obtain detailed information about the behavior of convection in this time dependent environment.

At about the same time we felt that computer capabilities had advanced sufficiently for us to attempt to perform both 2D and 3D simulations of full amplitude RR Lyrae stars. We developed a C++ code (SPHERLS) with MPI multiprocessor communication and have completed a number of simulations of RR Lyrae stars (Geroux & Deupree 2013, 2014, 2015) that appear to give reasonable light curves near the red edge as well as the rest of the instability strip. All of the multidimensional calculations taken together appear to give a similar picture of time dependent convection limiting the pulsation effectively by increasing the energy transport in the ionization regions during contraction and decreasing it during expansion from what one gets with convection omitted.

Because other researchers of RR Lyrae stars may not be very familiar with multidimension simulations in general or with multidimensional models for simulating turbulent convection, we shall focus on these aspects of the calculations. Section 2 focuses on how one controls the behavior of the computational mesh with time, and Section 3 discusses some features of the convective treatment. In Section 4 we present the behavior of an RR Lyrae model very near the red edge.

2. Features of multidimensional finite difference techniques

Finite difference techniques are based on computational cells defined by a computational mesh in the appropriate number of dimensions. State quantities are defined at cell midpoints, while velocities and a few other quantities are defined at appropriate cell interfaces. Differentials are computed as differences of the appropriate quantity in adjacent cells. The computational mesh is defined by the user and may change during the calculation according to algorithms also defined by the user. Two specific cases are a Lagrangian mesh, which follows the flow of the material, and an Eulerian mesh, which does not change its location in time as the material flows through it.

Most 1D stellar pulsation simulations use a Lagrangian mesh because it is well adapted to specific features of the pulsation problem. One of these features is that the radius of the model changes by about 20 per cent during the course of a period, and the mesh must provide decent numerical resolution during all pulsation phases. The second feature is that the hydrogen ionization region, which plays a significant role in the pulsation, is very thin and has steep gradients. Again, the mesh must have a computational cell in at least some part of the hydrogen ionization region nearly all the time.

In multiple dimensions the picture becomes more complex. Convectively unstable regions will produce latitudinal and longitudinal flow, while the radial pulsation still occurs. A purely Eulerian mesh would have to contain a large number of radial zones to provide sufficient resolution to capture the hydrogen ionization region at maximum and minimum radius and everywhere in between. A purely Lagrangian mesh would follow the turbulent convective motion as well as the radial pulsation, rapidly becoming so tangled up that expressing differentials as finite differences breaks down. This could, in principle, be fixed by complete rezones of the problem an unknown number of times each pulsation period, but rezones are both time consuming and of limited accuracy. What we believe is desired is a mesh that "flows" with the radial pulsation, but which is essentially Eulerian in the horizontal directions. Deupree (1977a) made an

initial attempt to build such a mesh by forcing the radial interfaces of the mesh to move with the horizontal average of the radial velocity. This worked for up to about 20 periods, but then the computational mesh ceased to capture the hydrogen ionization region reliably through the entire period. It should be noted that the radial resolution of those calculations, while fairly standard for the time, was only about a third of what we use today, so that this algorithm for the radial mesh flow might be more successful now.

We have developed a better algorithm for determining how the radial interfaces move. Because the Lagrangian calculation works so well in 1D, we use this to guide us. A Lagrangian 1D calculation keeps the mass in a given spherical shell constant throughout the calculation. This becomes our criterion, but we must develop it in a multidimensional context. In one dimension, the material remains the same in a given spherical shell throughout the calculation; in multiple dimensions, the requirement becomes that the total amount of material in a given spherical shell (made up of all the horizontal shells in that radial shell) remains the same throughout the calculation (hence the designation "Spherical Lagrangian"). Material can flow into and out of the spherical shell, as well as flowing horizontally, but the radial interfaces move so there is no *net* motion into or out of the spherical shell at any time.

We can see how the algorithm develops by noting that the amount of material flowing out the top of a zone in the mesh (identified by radial zone number i, latitudinal zone number j, and longitudinal zone number k) is given by $\rho_{i+1/2,j,k} d\mathrm{Area}_{i,j,k,\mathrm{top}}(V_{i+1/2,j,k} - V_{0,i+1/2})$. Here, V is the radial velocity and V_0 is the mesh flow velocity at the top of the computational cell. Similarly, the amount of material flowing into the bottom of that same zone is given by $\rho_{i-1/2,j,k} d\mathrm{Area}_{i,j,k,\mathrm{bottom}}(V_{i-1/2,j,k} - V_{0,i-1/2})$. The difference between the inflow and outflow summed over all the horizontal zones in the spherical shell must be zero to keep the mass in the spherical shell constant. The only unknowns are the mesh flow velocity at the top and the mesh flow velocity at the bottom of the spherical shell. However, we require that the radial velocity at the core boundary of the mesh be zero for all time, so that the bottom mesh flow velocity for the radial zone just exterior to the core is also zero. Thus, the mesh velocity at the top of this radial zone represents the only unknown, and one may move to the next spherical shell where now the only unknown is the mesh flow velocity at the top of the second spherical shell. One can thus bootstrap this calculation all the way to the surface.

One final feature arises because our calculations are constrained by the Courant condition, which stipulates that the time step must be sufficiently short that a sound wave does not cross any zone in a time step for the calculation to remain numerically stable. However, we note that $r\Delta\theta$ becomes very small as the inner boundary of the calculation is approached. As well, the sound speed in this region is very high, making the time step unreasonably short. It is fortunate that the convective region does not penetrate this deeply for RR Lyrae stars so that we can actually make this region a purely 1D region. The radial zone at which the transition between the 1D and multidimensional calculations take place is arbitrary with the sole constraint that the convective velocities must be very small as this location is approached.

A cartoon of the computational mesh is shown in Figure 1. The dashed curves denote the boundaries of the problem and the dash-dot curves indicate the 1D region. The radial velocity at the core boundary is zero and the luminosity emerging from the core is constant, the same as in 1D calculations. The horizontal boundaries are periodic, so the flow pattern endless replicates itself in latitude and longitude. The curves defined by given radii move radially as determined by the mesh flow algorithm while the curves defined by given θ or ϕ values remain stationary. Most calculations have 20 zones in each horizontal direction and about 120 radial zones.

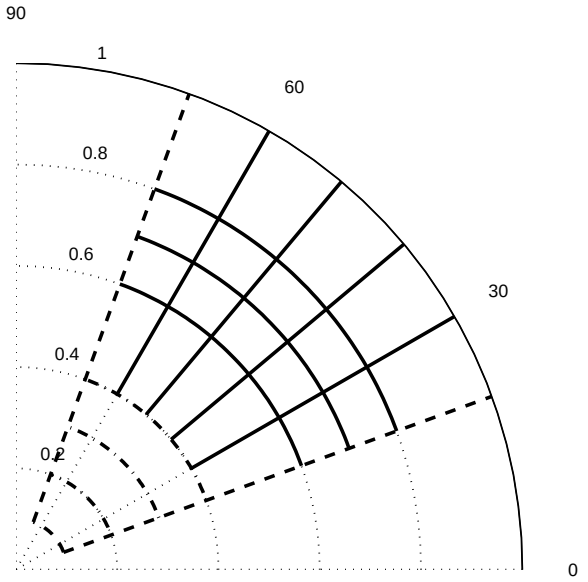

Figure 1. Cartoon of the computational mesh. The horizontal boundary conditions are periodic, and the total horizontal width of the calculation is usually 6 degrees, not the 50 degrees shown here for presentation purposes.

Geroux & Deupree (2011) computed adiabatic radial oscillations along with horizontal motion over about 180 periods and found that this approach has the desired effects and remains both accurate and stable over many periods. The algorithm also works well in nonadiabatic calculations over the several hundred pulsation periods that many models require to reach full amplitude.

3. Basics of the convective model

Our treatment of convection falls under the classification of sub grid scale (SGS) turbulence models, of which there are many variations. The general idea is to divide each dependent variable in a given computational cell into two components: one you can resolve (call it q_r), and one that varies within the computational

cell and you cannot resolve (q_u). Included in the definition is the constraint that the integral of q_u over a single cell is zero.

We substitute this relation for all the dependent variables in the finite difference expressions of the conservation laws, integrate over a cell volume, and divide by the cell volume. The results are the original finite difference expressions of the conservation laws in q_r plus new terms which include products of at least two unresolved components, for example $\langle q_{u1} q_{u2} \rangle$, where $\langle\rangle$ denotes average of the quantities integrated over the inside of the cell.

So far we have managed to generate almost twice as many variables as we have equations for. To proceed, we must either 1) generate new equations for the unresolved variables, 2) write the unresolved variables in terms of the resolved variables, or 3) discard terms. An example of the last is the SGS terms for the radiation flow, assuming the SGS flow does not impact the radiative diffusion as a process (or equivalently assuming that the only impact on radiation is the large scale flow changing the thermal structure). There are SGS turbulence models which do generate new equations for at least some of the unresolved variables, but here we shall replace a number of these terms with expressions which include only the resolved variables.

Many of these terms have an unresolved velocity component (call it u_u) in them. These we will choose to write as

$$\langle u_u q_u \rangle \rightarrow -\frac{\mu_t}{\rho Pr_t} \bigtriangledown_u q_r. \tag{1}$$

Here μ_t is the turbulent viscosity coefficient, $\bigtriangledown_u$ is that part of the gradient in the direction of the velocity component, and Pr_t is the turbulent Prandtl number (or some other nondimensional number depending on the variable q). We choose the algebraic expression for the eddy viscosity coefficient formulated by Smagorinski (1963):

$$\mu_t = C^2 L^2 \rho \left\{ \bigtriangledown u : \left[\bigtriangledown u + (\bigtriangledown u)^T \right] \right\}^{1/2}, \tag{2}$$

C is a free parameter and L is the turbulent length scale. The chief result in our formulation is to add terms to the vector momentum equation which look like a viscosity and to add two terms to the energy equation, one of which represents the SGS transport of internal energy and the other the conversion of SGS kinetic energy into heat. The full equations used are given by Geroux & Deupree (2013).

The net effect of this approach is to elevate the scale on which kinetic energy is converted to heat to the length scale of the computational mesh. Ideally, one would like this to occur on length scales several orders of magnitude smaller than those length scales of the eddies which are transporting the bulk of the energy and momentum, but this is often not possible (and in our case is not done).

There are four free parameters associated with our formulation of the SGS model. Two are C and the turbulent Prandtl number given above. A third (A_t) relates the eddy viscosity coefficient to the SGS kinetic energy density (K):

$$\mu_t = A_t \rho L K^{1/2} \tag{3}$$

and the fourth relates the turbulent length scale to the mesh zone size

$$L = s\left([\Delta r]^2 + [r\Delta\theta]^2\right)^{1/2}. \quad (4)$$

There are two basic procedures for selecting the values of these free parameters. The first is to examine simulations of turbulence experiments and select values for the free parameters based on those experiments. The second argues that there are no Earth-based turbulence experiments which could adequately represent the RR Lyrae conditions and that a large suite of simulations covering a range of values for all the free parameters should be performed with comparison of the theoretical and observed light curves guiding the choice. Partially because of the length of time required to perform such a study, we opt for the first choice and use results from internal combustion engine simulations and data, with the parameter values given by Cloutman (1991).

4. Very near the red edge

As the red edge is approached, the calculations become more time consuming and the results less open to straightforward interpretation. We show an example in Figure 2, where we have plotted the log of the peak of the kinetic energy versus time for a model with $T_{\rm eff} = 5900$ K. After an early, but short lived growth, the peak kinetic energy shows a very long period of erratic behavior showing little or no growth. After about $5 \cdot 10^7$ s, it begins to grow at a rate of about 0.5 per cent per period for the next 600 periods. During the period of erratic behavior, there are clearly many frequencies involved, and the velocity curve shows great variation from period to period. Even after the pulsation starts growing, the velocity curves display more noise than coherent pulsation, although the pulsation is reasonably smooth by the end of the calculation. The pulsation velocity amplitude is about 12 km/s at the end of the calculation, still with some contamination of other frequencies. Clearly, the calculation with this slow a growth rate is going to be difficult to model to full amplitude regardless of how low the final amplitude is.

5. Some other considerations

The code is written in C++ and uses MPI for multiprocessing. Typical multidimensional runs use 12-16 processors, although more work could be done to find the optimum number of processors in 2D and 3D. There is a substantial time performance degradation if all processors are not on the same node. The analysis scripts are written in PYTHON. Results from a suite of calculations such as we performed require several Tbytes of storage.

The understanding of the 3D simulations benefited greatly from visualization with the Compute Canada immersive Data Cave at Saint Mary's University.

The SGS approach to convection is expected to become a better approximation to reality as the zoning resolution (in all dimensions) becomes finer. In particular, one would like the zoning to be significantly smaller than the size of the convective eddies carrying most of the convective flux. Our current best cases ($N_r \approx 120$ and $N_\theta = 80$ in 2D, $N_r \approx 120$, and $N_\theta = N_\phi = 20$ in 3D) fall well short of this criterion. While predicting exactly how much better resolution

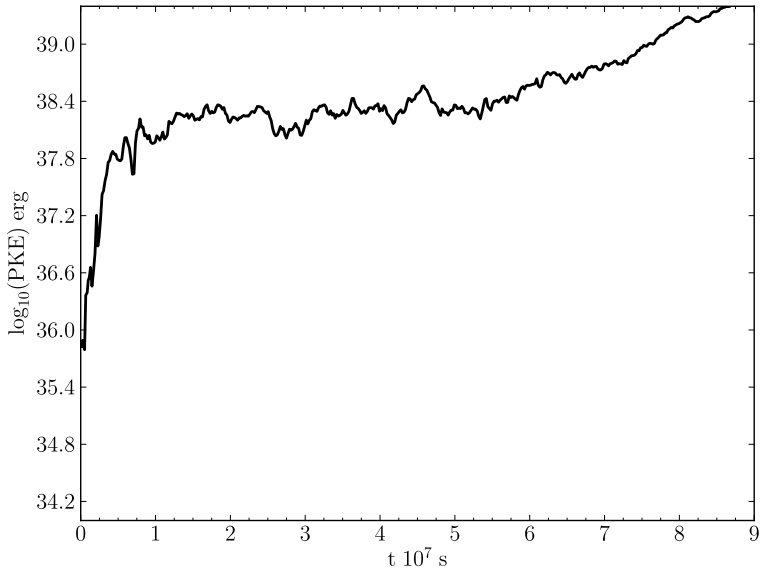

Figure 2. Plot of the peak kinetic energy per period (PKE) as a function of time for a $T_{\rm eff} = 5900$ K model. This model is different from bluer models we have computed because it displays a long time period of about $3.5 \cdot 10^7$ s with little or no growth before beginning to slowly grow again. The peak velocity amplitude after the approximately 1300 fundamental mode periods calculated is about 12 km/s.

will be required is uncertain, it seems that something like another two orders of magnitude in each dimension is highly desirable. As the zoning in each dimension becomes a factor of ten finer, we note that the amount of computer time required increases 10^{n+1}, where n is the number of dimensions. The extra factor of ten comes from the decrease in the time step determined by the Courant condition brought about by the finer zoning. Also, it is not clear how much larger the horizontal extent of the calculations needs to be. Given that current calculations take up to a couple of months (2D), and several months up to about a year (3D) in calendar time, a full suite of calculations with two orders of magnitude better resolution than our current work seems unlikely at the present time. It is not the number of zones that are the problem in 2D (million zone calculations are relatively common), but rather the number of time steps required to reach full amplitude (even if starting at a relatively high amplitude). Now we could possibly perform what was once considered a "once in a lifetime" calculation in 2D, and our past experience has been that what was "once in a lifetime" takes about a decade to become routine. The picture for 3D calculations, of course, is much less optimistic, but even here the number of billion zone calculations that have been done suggest that it is not out of the question in the foreseeable but not immediate future.

Acknowledgments

We wish to thank the Canada Research Chairs program for financial support and the Canada Foundation for Innovation and Compute Canada for supporting the research facilities.

References

Bono, G., Caputo, F., Cassisi, S. 1997a, ApJ, 483, 811
Bono, G., Caputo, F., Castellani, V., et al. 1997b, A&AS, 121, 327
Bono, G., Stellingwerf, R. F. 1994, ApJS, 93, 233
Buchler, R. 2009, Stellar Pulsation: Challenges for Theory and Observation, Eds. J. Guzik & P. Bradley, (New York: American Institute of Physics), p. 51
Christy, R. F. 1966, ARA&A, 4, 350
Cloutman, L. D. 1991, Lawrence Livermore National Laboratory Report, UCRL-ID-107128
Cox, J. P., Cox, A. N., Olsen, K. H., et al. 1966, ApJ, 144, 1038
Deupree, R. G. 1977a, ApJ, 211, 509
Deupree, R. G. 1977b, ApJ, 214, 502
Gastine, T., Dintrans, B. 2008a, A&A, 484, 29
Gastine, T., Dintrans, B. 2008b, A&A, 490, 743
Gastine, T., Dintrans, B. 2011, A&A, 528, A6
Gehmeyr, M. 1992a, ApJ, 399, 265
Gehmeyr, M. 1992b, ApJ, 399, 272
Gehmeyr, M. 1993, ApJ, 412, 341
Geroux, C. M., Deupree, R. G. 2011, ApJ, 731, 18
Geroux, C. M., Deupree, R. G. 2013, ApJ, 771, 113
Geroux, C. M., Deupree, R. G. 2014, ApJ, 783, 107
Geroux, C. M., Deupree, R. G. 2015, ApJ, 800, 35
Kuhfuss, R. 1986, A&A, 160, 116
Marconi, M. 2009, Stellar Pulsation: Challenges for Theory and Observation, Eds. J. Guzik & P. Bradley, (New York: American Institute of Physics), p. 223
Marconi, M., Caputo, F., Di Criscienzo, M., et al. 2003, ApJ, 596, 299
Marconi, M., Degl'Innocenti, S. 2007, A&A, 474, 557
Mundprecht, E, Muthsam, H. J., Kupka, F. 2013, MNRAS, 435, 3191
Mundprecht, E, Muthsam, H. J., Kupka, F. 2015, MNRAS, 449, 2539
Smagorinski, J. 1963, Mon. Weather Rev., 91, 99
Stellingwerf, R. F. 1982a, ApJ, 262, 330
Stellingwerf, R. F. 1982b, ApJ, 262, 339
Stellingwerf, R. F. 1984a, ApJ, 277, 322
Stellingwerf, R. F. 1984b, ApJ, 277, 327
Stellingwerf, R. F. 1984c, ApJ, 284, 712
Tuggle, R. S., Iben, I. 1973, ApJ, 186, 593
Xiong, D. 1989, A&A, 209, 126

RRL2015 – High-Precision Studies of RR Lyrae Stars
L. Szabados, R. Szabó, K. Kinemuchi (Eds.) 2016

Multidimensional modelling of classical pulsating stars

Herbert J. Muthsam & Friedrich Kupka

Faculty of Mathematics, University of Vienna, Austria

Abstract. After an overview of general aspects of modelling the pulsation-convection interaction we present reasons why such simulations (in multidimensions) are needed but, at the same time, pose a considerable challenge. We then discuss, for several topics, what insights multidimensional simulations have either already provided or can be expected to yield in the future. We finally discuss properties of our ANTARES code. Many of these features can be expected to be characteristic of other codes which may possibly be applied to these physical questions in the foreseeable future.

1. Introduction

Numerical modelling RR Lyrae stars and Cepheids[1] has been one of the earliest successes of modern computational stellar physics. Computers becoming available around 1960, say, allowed for the first time to build numerical models which encompass a physically "complete" (in some sense) description of "real" astrophysical objects. It cannot come as a surprise that such early work centered on questions concerning objects which are (or were considered as) planar or spherically symmetric and therefore, in a computational sense, one-dimensional (1D) plus possibly time-dependent. This comprised issues in stellar atmospheres, stellar structure and evolution, but also protostellar collapse, supernova explosions, etc. Modelling pulsating stars fell into that category, and relatively soon after ultimate identification of the basic source of pulsation excitation even nonlinear, time-dependent models became available. An overview of early achievements can be gained by consulting Zhevakin (1963) and Christy (1966a,b). Nonlinear time-dependent calculations proved particularly useful in providing nontrivial properties of, for example, the light curve (departure from the sinusoidal form). That allowed stringent confrontations with and deductions from observations. In a number of cases a mismatch between observations and simulations resulted.

Today's basic source for mismatch is quite likely the pulsation-convection interaction. The crucial role of the interaction between convection and pulsation for a number of observable properties of classical variables has been discussed in the literature for a long time. Examples include the reviews by Buchler (1997, 2009) and Marconi (2009). Of particular interest in this context is the boundary between objects exhibiting large radial pulsations due to the κ-mechanism on the "hotter" or "blue" side of this transition region and stable objects on the "cooler" or "red" side of this famous "red edge" of the pulsational insta-

[1] These classical variables, basically exhibiting *radial* oscillations, will be termed here as "pulsating stars" for the sake of brevity.

bility strip. Other, related observations include the presence of double- or even triple-mode pulsators and their location as a function of effective temperature and luminosity or any observational equivalent and the particular shapes (amplitudes, phase dependence) of light curves observed for these objects. Since for sufficiently low effective temperature the blocking of radiative flux by the partial ionization of hydrogen and its associated increase in opacity becomes very large, deep convection zones have inevitably to form for these objects to take care of energy transport instead of radiation.

The "classical" 1D simulations had by necessity to include the pulsation-convection interaction in a manner compliant with this basic computational setting. Hence, they heavily parameterized this interaction so that multidimensional simulations which *in principle* are capable to fully deal with this issue are warranted. Indeed, on the side of theoretical modelling two grand numerical challenges have been identified in the area of pulsating stars after a critique of the present hydrocodes (Buchler 2009): *Multidimensional simulation of convection in classical pulsating stars* and *Modelling of nonradial pulsation* in such stars[2].

After a very early work (Deupree, 1977 and subsequent papers) on multidimensional modelling of convection in pulsating stars, the topic has been considered anew only in the last few years. Of course, this research greatly benefits from the huge increase in computer power as well as from advances in numerical methods and codes. Still, such work amounts to a great challenge even today.

In the present paper we want to discuss first *why* modelling pulsation-convection interaction in multidimensions poses such large difficulties. We will then turn towards various scientific questions, and the way they have recently been investigated, or which might benefit in the future, with the methods available or within reasonable reach. Since the contribution of Deupree & Geroux (2016) covers what is being done in this group, we will concentrate on such items which are close to our own research and its possible extensions.

A discussion of the limitations of the approach is also warranted in order to draw a realistic pathway of possible future development. We therefore also give room to such considerations. From these discussions it will follow that various questions in this area cannot be directly tackled by multidimensional simulations, and some can be approached this way only at a cost which is prohibitive for everyday work. It is therefore essential that improved convection models are developed which comply with the basic setting of traditional codes (spherically symmetrical and, hence, geometrically 1D). We discuss some basic requirements such models would have to fulfill.

The numerical simulation software is equally important as the enhanced power of computers. For that reason we give an overview of the capabilities of our ANTARES code (Muthsam et al. 2010; Mundprecht et al. 2013) as a guide what will be necessary for other codes which should be applied for these problems in the future.

---

[2]Of course, there are unsolved problems, in particular the Blazhko effect, where even the basic physical cause is not yet known with certainty; hence it is also unknown what precise sort of computational experiments would be required to deal with it.

2. Pulsation-convection interaction in multidimensions: the challenge

From a numerical point of view, already the 1D (radially symmetric) simulations faced the problem of a very steep temperature gradient and small characteristic spatial scales in the hydrogen ionization region. That led to the introduction of adaptive gridding strategies as described by Castor et al. (1977), Dorfi & Feuchtinger (1991), Buchler et al. (1997).

This already explains in part why, with the exception of very early work by Deupree (1977) and some subsequent papers, modelling of pulsating stars has remained in the 1D setting for so long. Only recently has hydrodynamic modelling of pulsating variables gained impetus as is being described by Deupree's contribution to these Proceedings and by the present article.

This late advent of multidimensional models for pulsating stars may appear particularly conspicuous given how advanced 3D modelling of solar granulation, the issue probably best explored in this area, has been already quarter of a century ago (e.g. the review by Nordlund & Stein 1990). One reason for this different pace of progress is the presence of the small spatial scales just mentioned. This makes challenging to model the *atmospheres* of some other types of stars, too. It applies, for example, to ordinary main-sequence A-type stars as extensively discussed in Kupka et al. (2009). Lack of resolution is probably the source of poor agreement between observed and simulated spectral line shapes in such objects (Kochukhov et al. 2007).

The other major reason has to be found in the fact that in pulsating stars the time scales of convection and pulsation are comparable, largely precluding, for example, taking a fixed phase in the sense of pulsation and letting convection develop against this static background. For a fair comparison of the challenges inherent in convection modelling for solar-like and pulsating stars, respectively, it must however be kept in mind that there is more to modelling solar like stars than may be deduced from the considerations above. Modelling of solar granulation is just a part of the task, made relatively easy by the fact that the solar atmosphere is not heavily influenced by what is going on in deeper layers (setting sunspots, etc. aside). Modelling *all* of the solar convection zone is a challenge however due to the huge disparity in time scales (minutes or even a few seconds at the top, and hundred thousands of years at the bottom). As a consequence, two largely disjoint research communities have developed in this area, with focus either on the outer layers and on the interior. For reviews on the state of art in these fields see Miesch et al. (2015). Because of the long time scales, even models of the bulk zone of solar convection (omitting the surface layers), one has to modify physical parameters in order to get manageable relaxation times near the bottom. In pulsating stars this problem may either not exist as in Mundprecht et al. (2015) or render multidimensional simulations unfeasible as in Geroux & Deupree (2013) (even if probably in a less fundamental sense than in the solar case), depending on the model under investigation.

To sum up, modelling *all* of the solar convection zone (setting aside magnetic effects) has to consider

i) huge differences in spatial and time scales at top and bottom (with top, i.e. granulation readily amenable to 3D modelling)

ii) extremely large time scales also at the bottom which request changing parameters to end up with a computable problem even if excluding the top of the convection zone.

As a consequence, there exists no simulation of the solar convection zone which represents both granulation and the bulk of the zone. In pulsating stars, atmospheres may pose a problem even if they were treated in isolation, but, other than in the Sun, they cannot be essentially decoupled from the deeper layers. So, one has to model the whole star. Solar problem ii) may or may not exist in such stars, depending on the star under consideration.

Given these facts we address now achievements of multidimensional models of pulsating stars and we discuss specific points which could be clarified in the foreseeable future by such methods. Such items concern specific questions either immediately, or they might help improve traditional 1D modelling.

3. Multidimensional models: present and future insights

3.1. Testing time dependent convection models

In Mundprecht et al. (2015) the HeII convection zone has been investigated in a 2D Cepheid model. Besides studying mechanical driving and damping such simulations allow to test traditional convection models such as those of Kuhfuß (1986) and Stellingwerf (1982). These time-dependent convection models (TDCs) allow to stay with the 1D nature of classical simulations of pulsating stars in the numerical sense. A calibration factor α_c which gives the ratio between the 1D model flux and the physical flux varies by a factor of ~ 2 during pulsation. Even more worrisome is that α_c, evaluated either in the convection or overshoot zone, varies by a factor of up to 10, the exact numbers depending on details. This results in much too strong an overshoot zone in the 1D models and casts doubts on results which may be sensitive on convective properties. Therefore, further development of TDCs is of paramount importance. We turn to some details now.

3.2. Further development of TDCs

Rather varied models (compliant with the 1D setting) have been proposed to describe how to compute the convective (non-radiative) energy transport in this case and how convection influences the large scale, radial pulsations in these objects. Buchler & Kolláth (2000) give a summary of the models most widely used in this context, in particular those by Kuhfuß and Stellingwerf just mentioned.

In one way or another each of these models provide a prescription to compute ensemble averages of the dynamical variables and quantities of interest which are needed to construct a closed system of predictive equations. The problem with each of these models is that they involve a lot of *ad hoc* reasoning which in turn has been driven by keeping the models as simple as possible. Thus, they usually involve only one time-dependent equation joined by a number algebraic relations and a host of modelling parameters (up to eight) which cannot be determined from within the model and for which there is no reason to assume that they are universal in the sense that once they have been calibrated for one star by

some kind of measurements, they may also be used to model other stars without invoking further changes to those modelling parameters.

Rather than attempting to fit some set of observations with sufficiently many degrees of freedom due to the number of available model parameters, one might "turn the table around" and ask instead: what is the minimum complexity a model has to have in order to describe the physics of convection-pulsation interaction properly? With numerical simulations at hands this is now a question we can hope to provide some answers for. In Mundprecht, Muthsam & Kupka (2015) model of the convective flux — as discussed by Buchler & Kolláth (2000) and as used by many investigators who use either the convection model of Stellingwerf (1982) or that one by Kuhfuß (1986) in their studies of classical variables — was analyzed in detail. It turned out that a proper reproduction of the convective flux computed from the numerical simulation requires a model to a) account for the efficiency of convection as a function of distance to the boundary of the convection zone, b) account for this efficiency to behave completely differently in stable and unstable layers, c) consider the dependence of this efficiency as a function of pulsation phase, d) consider that the ratio of kinetic energy stored in horizontal motions versus that one stored in vertical motions is different inside the convection zone (where vertical flows dominate) and outside of it (where horizontal ones dominate), and e) the convective flow is subject to radiative losses. While the latter is typically accounted for, the success in doing so for the others is either limited or they are ignored altogether.

Reynolds stress models such as those proposed by Canuto (1993, 1997, 1999), Canuto & Dubovikov (1998), or more recently in Canuto (2011), or alternatively Xiong et al. (1997), provide at least the formal framework to take these properties into account. With separate dynamical equations for total and vertical kinetic energy, temperature fluctuations and velocity-temperature cross-correlation (convective flux), and optionally also the dissipation rate of kinetic energy and a coupling to mean structure equations which may even feature a non-zero mean radial velocity, the dependencies of the convective flux observed in the numerical simulations could be obtained from within the model itself. Whether this is indeed the case or how these much more complex models would have to be adjusted to succeed remains an open question. Multidimensional simulations would be an important tool to guide such model development and to ultimately provide test cases.

It goes without saying that such tests would be equally important for physically and algorithmically much simpler models than those of Reynolds stress type such as, for example, presented by Pasetto et al. (2014) where, contrarily to what holds true in Reynolds stress models, effects of compressibility, turbulence and, in its present form, also overshooting are not included quite from the outset.

3.3. The atmospheres

Spectroscopy clearly demonstrates the presence of phase-varying turbulence or radial shocks in many pulsating stars, see e.g. Preston (2011) for RR Lyrae stars. Our simulations for a Cepheid model have shown strong, phase-varying nonradial shocks (Mundprecht et al. 2013). As a consequence, adding this to the peculiarities of the atmospheres we have mentioned previously the atmospheres are a challenging and rewarding object for numerical investigation in multidimensions. They require high resolution so that even 2D simulations

are expensive. 3D simulations would need extremely massive computational resources at least for the objects where we presently have an estimate of the requirements. Since convection in the atmosphere can easily be much more violent than convection in the HeII zone with strong shocks development of faithful TDCs for that purpose may amount to a task even tougher than holds true for the bulk zone.

Determination of basic stellar parameters. Multidimensional atmospheric models would obviously bring about benefits in conjunction with the determination of the basic stellar parameters ($T_{\rm eff}$, $\log g$, abundances,...). Note that with very few exceptions all work in that direction has been based on static, planar model atmospheres if not even resorting to curve-of-growth methodology.

This must provoke concerns already on general grounds given that the interaction of pulsation with atmospheric structure which is known to be strong in a number of cases (see e.g. Preston 2011). There are other hints which point to major effects of pulsation on atmospheric structure and, hence, derived parameters. So, for a Cepheid which at the same time happens to be a member of an eclipsing binary it has been possible to determine the limb darkening coefficient. In that analysis Pilecki et al. (2013) found a much lower limb darkening coefficient for the Cepheid component than would result from a static atmosphere with the same basic parameters. In their paper, Barcza & Benkő (2014) note difficulties when applying their method to determine fundamental parameters, based among others on broad-band colours from ATLAS atmospheres, in particular for one star (DH Peg).

Broad-band investigations. The remarks just made prompt of course the need for assessing the difference between broad-band colours obtained from ATLAS-type and fully dynamic atmospheres. A similar need for studies of the atmosphere arises for the limb darkening coefficient and appropriate determination of the p-factors critical for distance determination of pulsating stars via the Baade-Wesselink method. This factor depends on the physics of the stellar atmosphere in a complicated way (e.g. Nardetto et al. 2014).

A special way of interaction of the hydrogen ionization front with the photosphere of a pulsating star has implications for the relations between period, colour and amplitude, see Kanbur & Ngeow (2006). Due to the inhomogeneous nature of the atmospheres of such stars a multidimensional study is warranted.

Nonradial pulsations? We have observed a tantalizing phenomenon when calculating an annulus containing the HeII convection zone of a Cepheid (no atmosphere) and regions below to fully allow for overshoot (Kupka et al. 2014). This model was developed for 20 pulsations of full amplitude. In that model the convective cells flock together in certain regions as time advances, leaving other places of the same radial distance essentially void. In otherwise similar models with sectors of a "normal" opening angle (10°) we could not observe that phenomenon. One wonders whether in this way nonradial mode can be excited. If so, it would obviously be difficult to model such a phenomenon in the TDC setting since it is highly questionable whether one can properly represent such a genuinely geometrical and collective behaviour of convection cells in a 1D model. It would be of importance to corroborate such an effect by running several multidimensional models.

4. Multidimensional models: code requirements

As it seems, the classical hydrocodes for radial stellar pulsation have been developed with precisely the goal of modelling stellar pulsation in mind. In contrast, our ANTARES code has been developed differently, as a general tool for research in stellar physics or astrophysics with special features added to make is also useful for research in stellar pulsation. Since even a multidimensional code streamlined towards that goal will be quite large, codes used in the future may be derived from (or later on extended to) a general, multipurpose package. Properties of the ANTARES code which we deem to be essential for future codes in this area include

- time-dependent radiation-hydrodynamics in 1D, 2D, 3D
- radiative transfer (grey or nongrey by opacity binning), diffusion approximation in the interior
- high resolution numerical schemes
- polar coordinates[3]
- coordinates moving radially, adapting to pulsation
- grid refinement, at least for logically rectangular patches
- highly parallelizable (in ANTARES based on MPI plus OpenMP for parallelization *within* multicore nodes).

5. Conclusions

We have given a comparison of the difficulties of modelling radial pulsations of convective stars with modelling the solar convection zone, the most advanced topic in stellar convection studies. Multidimensional models show substantial weakness of convection models traditionally applied in 1D. Multidimensional models are capable to tackle a number of specific problems directly. For other questions, they may aid development and testing of TDCs. High quality numerics and a number of advanced code features are necessary for many problems in that area.

Acknowledgements

We are thankful to Eva Mundprecht for long lasting cooperation. This work has benefited directly or indirectly from several Austrian Science Foundation ASF projects (P18224, P21742, P25229).

[3]If, in 3D, a whole spherical shell should be modelled, polar coordinates are unsuited because of the convergence of longitude circles (at constant radius) towards the polar axis. Placing the star in a box may be feasible but leads to extremely serious problems with resolution (or demands very advanced grid-refinement strategies) in the atmosphere for which the box coordinates are ill suited. One way out of that difficulty could be the development and application of curved grid techniques with irregular meshes; see e.g. Grimm-Strele et al. (2014).

References

Barcza, S., Benkő, J. M. 2014, MNRAS, 442, 1863
Buchler, J. R. 1997, in Variable Stars and the Astrophysical Returns of the Microlensing Surveys, Editions Frontières, 181
Buchler, J. R. 2009, American Institute of Physics Conference Series, 1170, 51
Buchler, J. R., Kolláth, Z. 2000, Annals of the New York Academy of Sciences: Astrophysical Turbulence and Convection, vol. 898, 39
Buchler, J. R., Kolláth, Z., Marom, A. 1997, Ap&SS, 253, 139
Canuto V. M. 1993, ApJ, 416, 331
Canuto V. M. 1997, ApJ, 482, 827
Canuto V. M. 1999, ApJ, 524, 311
Canuto V. M. 2011, A&A, 528, A76
Canuto V. M., Dubovikov M. 1998, ApJ, 493, 834
Castor, J., Davis, C. G., Jr., Davison, D. K. 1977, Los Alamos Scientific Laboratory Report LA-6664
Christy, R. F. 1966a, ARA&A, 4, 353
Christy, R. F. 1966b, ApJ, 144, 108
Deupree, R. G. 1977, ApJ, 211, 509
Deupree, R. G., Geroux, C. 2016, these proceedings, p. 109
Dorfi, E. A., Feuchtinger, M. U. 1991, A&A, 249, 417
Geroux, C. M., Deupree, R. G. 2013, ApJ, 771:113
Grimm-Strele, H., Kupka, F., Muthsam, H. J. 2014, Computer Physics Communications, 185, 764
Kanbur, S. M., Ngeow, C.-C. 2006, MNRAS, 369, 705
Kochukhov, O., Freytag, B., Piskunov, N., et al. 2007, IAU Symposium, 239, 68
Kuhfuß, R. 1986, A&A, 160, 116
Kupka, F., Mundprecht, E., Muthsam, H. J. 2014, IAU Symposium, 301, 177
Kupka, F., Ballot, J., Muthsam, H. J. 2009, Communications in Asteroseismology, 160, 30
Marconi, M., 2009, AIPC, 1170, 223
Miesch, M., Matthaeus, W., Brandenburg, A., et al. 2015, Space Sci. Rev., 196, 79
Mundprecht, E., Muthsam, H. J., Kupka, F. 2013, MNRAS, 435, 3191
Mundprecht, E., Muthsam, H. J., Kupka, F. 2015, MNRAS, 449, 2539
Muthsam, H. J., Kupka, F., Löw-Baselli, B., et al. 2010, NewAst, 15, 460
Nardetto, N., Storm, J., Gieren, W., et al. 2014, IAU Symposium, 301, 145
Nordlund, Å., Stein, R. F. 1990, in Solar Photosphere: Structure, Convection, and Magnetic Fields, IAU Symp. 138, 191
Pasetto, S., Chiosi, C., Cropper, M., Grebel, E. K. 2014, MNRAS, 445, 3592
Pilecki, B., Graczyk, D., Pietrzyński, G., et al. 2013, MNRAS, 436, 953
Preston, G. W. 2011, AJ, 141:6
Stellingwerf R. F. 1982, ApJ, 262, 330
Xiong, D. R., Cheng, Q. L., Deng, L. 1997, ApJS, 108, 529
Zhevakin, S. A. 1963, ARA&A, 1, 367

RRL2015 – High-Precision Studies of RR Lyrae Stars
L. Szabados, R. Szabó, K. Kinemuchi (Eds.) 2016

Helium abundance effects on RR Lyrae pulsation properties

Marcella Marconi[1], Giuseppina Coppola[1], Giuseppe Bono[2], Vittorio Braga[2], & Adriano Pietrinferni[3]

[1] *INAF-Osservatorio Astronomico di Capodimonte, Napoli, Italy*
[2] *University of Tor Vergata, Roma, Italy*
[3] *INAF-Osservatorio Astronomico di Collurania, Teramo, Italy*

Abstract. A new set of nonlinear convective pulsation models of RR Lyrae stars has been computed varying both the metallicity and the helium content. To constrain the helium dependence of pulsation observables we adopted, for each metal content, at least three different helium abundances. We provide for the first time a homogeneous evolutionary and pulsation framework covering the entire range of cluster and field variables. The implications for the use of RR Lyrae as stellar population tracers and distance indicators are briefly discussed.

1. Introduction

RR Lyrae stars are important standard candles to evaluate the distance and trace the properties of population II stars (Caputo 2012; Marconi 2012; Marconi et al. 2015). They are the most popular variable stars in globular clusters and the characterization of their properties is crucial not only to date but also to constrain the chemistry and the kinematics of the host systems. In the last decade there has been a growing interest towards the study of globular clusters thanks to the observational evidence of secondary stellar populations in these systems (Piotto et al. 2015). This evidence has been widely interpreted in terms of a helium enhancement in subsequent stellar generations (Renzini 2010; Milone 2015; Nardiello et al. 2015). Helium abundances up to about Y=0.40 (abundance in mass fraction) are often invoked by stellar evolution studies on specific Galactic globular clusters (ω Cen, NGC 6441, NGC 2808, NGC 6352), thus pointing out the need to verify the presence of such an enhancement through independent methods. The RR Lyrae stars play, in this context, a crucial role, since their pulsation properties can be soundly adopted to constrain the occurrence of a helium-enhanced stellar population. We have already computed He-enhanced models for RR Lyrae in ω Cen (Marconi et al. 2011) and the comparison with observations suggested that:

1. The key parameter causing the difference between canonical and He-enhanced observables is the luminosity.

2. The period distribution of He-enhanced models moves to periods that are systematically longer than observed.

3. The fraction of He-enhanced structures in ω Cen cannot be larger than 20%.

However, these models only covered two metal abundances. The extension of the He-effect analysis to the whole metallicity range covered by Galactic and extragalactic RR Lyrae is mandatory in order to properly trace the He enhancement phenomenon through RR Lyrae stars pulsation properties (Marconi et al. in preparation). Here we present some preliminary theoretical results concerning the helium abundance effects on pulsation periods and light curves.

2. The new helium enhanced pulsation models

Starting from the canonical theoretical scenario presented in Marconi et al. (2015), for each selected metal abundance, ranging from $Z = 0.0001$ to $Z = 0.008$, we increased the helium content from the canonical value (ranging from 0.245 for $Z = 0.0001$ to 0.256 for $Z = 0.008$) to $Y = 0.30$ and $Y = 0.40$. Nonlinear convective models with the same physical and numerical assumptions as in Marconi et al. (2015) were computed for the new helium-enhanced chemical compositions. As a result, we computed an extensive and detailed grid of models including 18 chemical compositions and, for each selected Z, Y combination, two different stellar masses and three different luminosity levels. The anchor, for each given chemical composition, is given by the mass and the luminosity predicted by evolutionary models for the Zero Age Horizontal Branch (ZAHB). This set was complemented with a new sequence with the same ZAHB mass, but a luminosity level that is 0.1 dex brighter than the ZAHB luminosity level. This takes account of the off-ZAHB evolution within the instability strip. We also computed a third sequence assuming a stellar mass that is 10% smaller than the ZAHB mass and a luminosity level 0.2 dex brighter than the predicted ZAHB level. This takes account of the spread in mass inside the instability strip.

The luminosity level of the predicted ZAHB increases with the assumed helium content and, at fixed mass and effective temperature, will produce longer predicted pulsation periods, as discussed in the following section.

3. Helium abundance effect on the predicted pulsation period and light-curve morphology

The main effect on the pulsation properties when increasing Y from the canonical value to 0.30 and 0.40 is shown in Figure 1. In this plot the predicted fundamental pulsation periods are shown as a function of the corresponding effective temperatures for the three different assumptions on the helium abundance (see labels). The pulsation periods get significantly longer so that the fundamental minimum period of an RR Lyrae sample is expected to be a crucial observable to disentangle the helium abundance of the underlying stellar population.

The light-curve amplitude and morphology is also affected by the increase in helium content as disclosed in Figure 2. In this plot the bolometric light curve is shown for two fundamental models with $Z = 0.0006$, effective temperature $T_{\rm e} = 6100$ K and a luminosity level $\log L/L_{\odot} = 1.69$, but two different helium abundances (see labels).

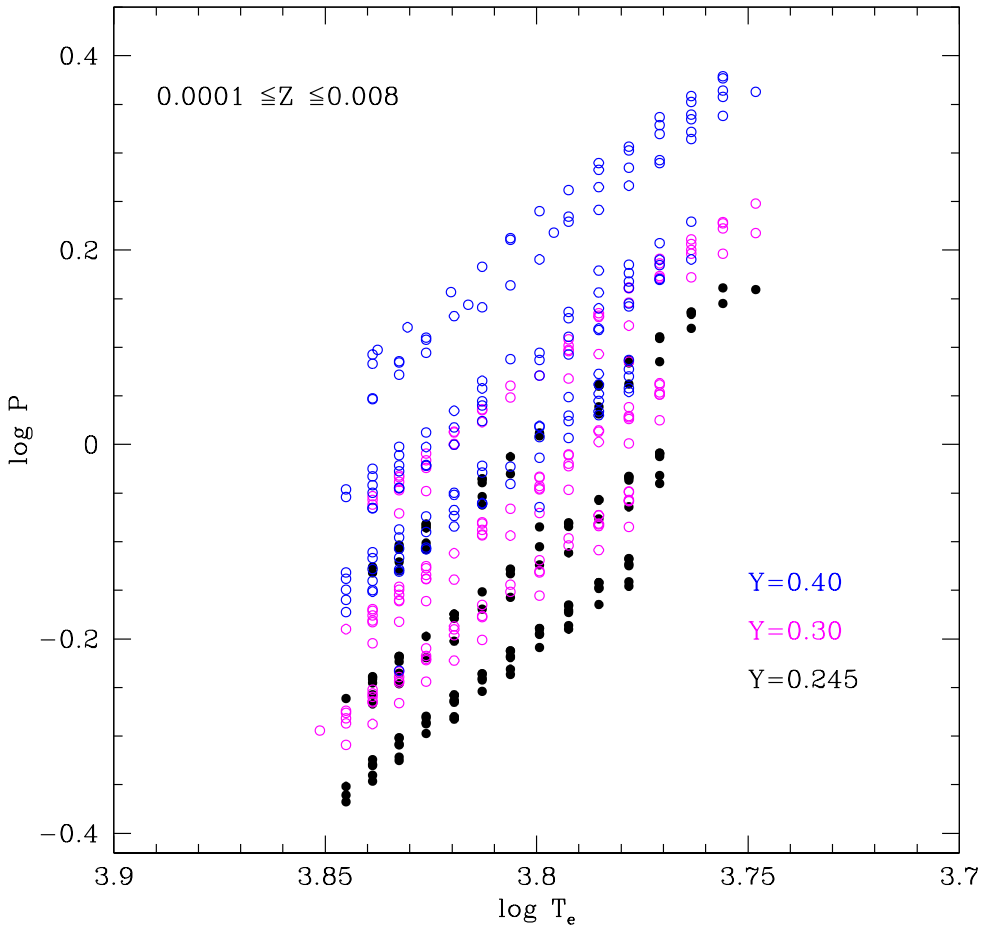

Figure 1. Computed fundamental pulsation periods as a function of the effective temperatures for the canonical helium abundance (black filled circles), $Y = 0.30$ (magenta open circles) and $Y = 0.40$ (blue open circles).

A glance at the models plotted in Figure 2 suggests that the predicted amplitude decreases (and the morphology gets smoother) as the helium content increases, as also confirmed by the fact that the corresponding model for $Y = 0.40$ shows a vanishing amplitude, as it does not pulsate. This occurrence is expected, the increase in helium content causes a decrease in the envelope opacity, and in turn in driving the pulsation.

In spite of the quoted significant effect on the pulsation period, as the evolutionary luminosity levels also increase, the slope and the zero point of the predicted period-luminosity (in the near infrared bands) and multi-filter Wesenheit relations are expected to be barely affected by helium content variations (Marconi et al. in preparation).

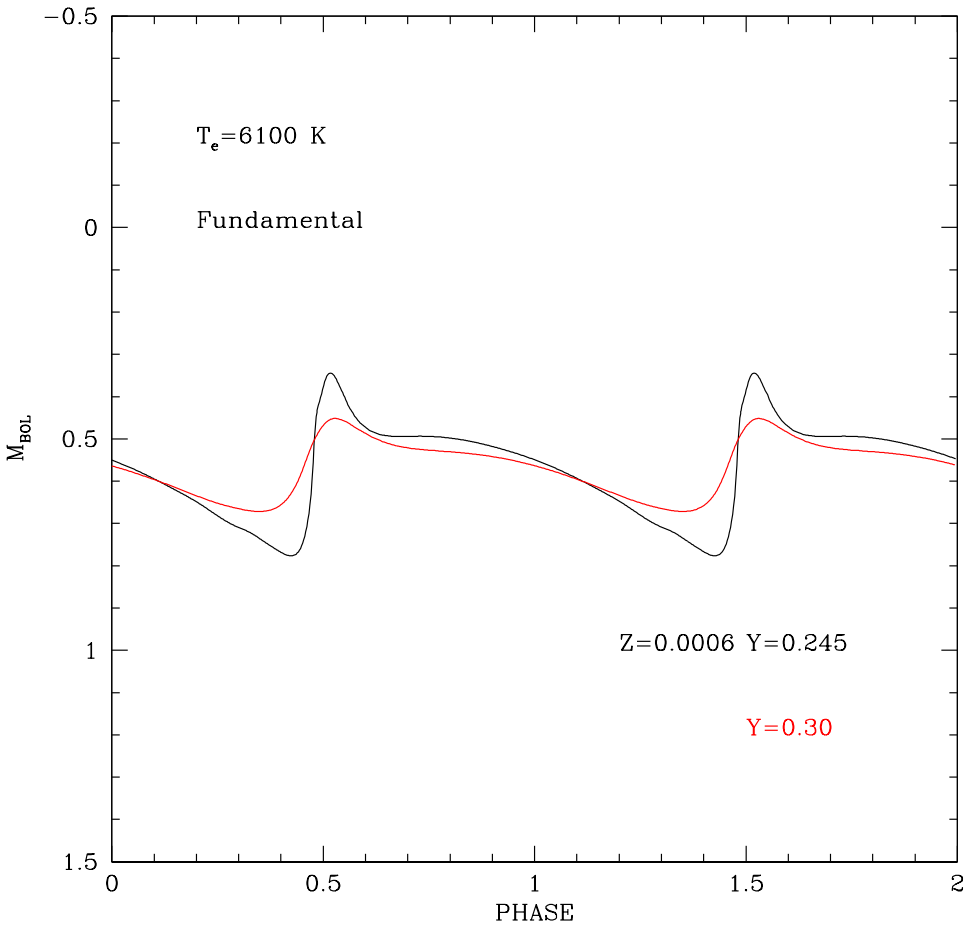

Figure 2. Predicted bolometric light curves of models with the same metallicity ($Z = 0.0006$), effective temperature ($T_e = 6100$ K) and luminosity ($\log L/L_\odot = 1.69$) and two different helium contents (see labels).

References

Caputo, F. 2012, Ap&SS, 341, 77
Marconi, M., Bono, G., Caputo, F., et al. 2011, ApJ, 738:111
Marconi, M. 2012, MSAIS, 19, 138
Marconi, M., Coppola, G., Bono, G., et al. 2015, ApJ, 808:50
Milone, A. P. 2015, MNRAS, 446, 1672
Nardiello, D., Piotto, G., Milone, A. P., et al. 2015, MNRAS, 451, 312
Piotto, G., Milone, A. P., Bedin, L. R., et al. 2015, ApJ, 149:91
Renzini, A. 2010, in The Impact of HST on European Astronomy, Springer, 83

RRL2015 – High-Precision Studies of RR Lyrae Stars
L. Szabados, R. Szabó, K. Kinemuchi (Eds.) 2016

OGLE and pulsating stars

A. Udalski
Warsaw University Observatory, Al. Ujazdowskie 4, 00-478 Warszawa, Poland

Abstract. OGLE-IV is currently one of the largest sky variability surveys worldwide, focused on the densest stellar regions of the sky. The survey covers over 3000 square degrees and monitors regularly over a billion sources. The main targets include the inner Galactic bulge and the Magellanic System. Supplementary shallower Galaxy Variability Survey covers the extended Galactic bulge and 2/3 of the whole Galactic disk. The current status, prospects, and the latest results of the OGLE-IV survey focused on pulsating stars, in particular RR Lyrae variables, are presented.

1. Introduction

The Optical Gravitational Lensing Experiment (OGLE) is a long-term large-scale sky variability survey that has been conducted practically continuously since 1992 (Udalski et al. 2015a). OGLE began its operation as one of the first generation so-called microlensing surveys which started hunting for gravitational microlensing phenomena in the search for dark matter in the early 1990s, following Bohdan Paczyński's idea (Paczyński 1986). These surveys revolutionized modern observational astrophysics due to their novel observing strategy. The very small probability of occurrence of gravitational microlensing events required long term photometric monitoring of as many sources of light (source stars) as possible for successful detection. Thus, the densest stellar sky regions like the Magellanic Clouds and the Galactic center were the natural targets of microlensing programs. These objects are well known astrophysical laboratories containing a large variety of virtually all classes of stars. Therefore, years-long photometric monitoring of these targets provided unique observational material not only for microlensing detection and studies but also for studies of long-term behavior and statistical properties of all kinds of variable and non-variable stars in these astrophysical laboratories. This opened completely unexplored niches of modern astrophysics which led to hundreds of new discoveries in many different fields. The microlensing surveys were in fact precursors of nowadays large-scale optical sky surveys.

2. OGLE-IV – fourth phase of the OGLE survey

The OGLE project has evolved with time – both increasing its observing capabilities as well as widening the range of scientific challenges it undertook – switching from its original form of a microlensing survey to a general sky variability survey. For details see Udalski et al. (2015a). Currently the OGLE project operates in

its fourth phase – OGLE-IV. The observing setup of this phase consists of the dedicated 1.3-m Warsaw Telescope located at the Las Campanas Observatory, Chile, and a CCD mosaic camera filling the entire focal plane of the Warsaw telescope with 32 CCD detectors (E2V 2048×4102 pixel CCDs). The total field of view of the camera is 1.4 square degrees (seven full Moon disks) with the pixel scale of 0.26 arcsec/pixel.

Observations are conducted through the Johnson-Cousins VI filters. The typical cadence of observations varies from 20 minutes for the densest stellar fields in the Galactic center to 3–4 days in the Magellanic System. Photometry of all stellar objects is derived from collected images in almost real time – within a few minutes after the image has been read out. The Difference Image Analysis (DIA) technique (Woźniak 2000) is used by the OGLE photometric data pipeline. The OGLE photometry has been widely recognized as one of the best available from the ground and serves as a "gold standard" for all microlensing studies. The accuracy reaches 4 mmag level for the brightest stars and it is practically photon noise limited down to $I \approx 19 - 21$ mag (depending on the target) in the densest stellar fields of the Galactic center and disk and Magellanic System.

3. OGLE-IV variable sky

The OGLE survey currently monitors about 3000 square degrees in the sky. These fields contain over one billion objects (mostly stars but also a fair number of extragalactic sources) that are regularly observed by OGLE. During the OGLE survey about 800 billion individual photometric measurements were carried out leading to the discovery and characterization of about 500 000 new variable stars and over 50 extrasolar planets. Typically over 2000 gravitational microlensing events are detected annually by the OGLE-IV real time microlensing system – Early Warning System (EWS). Figure 1 presents the current coverage of the sky by the OGLE-IV survey.

The OGLE-IV survey consists of a series of long-term and short-term monitoring programs. The latter are conducted usually for one observing season and have strictly predefined observing goals. The long term surveys are designed to be conducted for several observing seasons and their science goals continuously evolve. Currently three long term variability surveys are conducted by the OGLE-IV project.

The OGLE second generation microlensing survey covers about 130 square degrees in the densest stellar regions of the Galactic bulge. Its main scientific goal is the detection and characterization of large samples of exoplanets discovered with the microlensing technique. The exoplanets discovered with this method are typically located in the very desired regions of their planetary systems – behind the "snow line" where they are supposed to form. Such planets, especially the low mass ones, are not accessible observationally by other detection methods currently in use. Many interesting discoveries of exotic exoplanets were recently reported by OGLE (Gould et al. 2014; Udalski et al. 2015b,c). The microlensing observing strategy predefines the cadence of observations. About 13 square degrees of the central bulge are observed with one hour frequency or higher. The remaining fields are visited from 2-3 times per night to one visit per two nights.

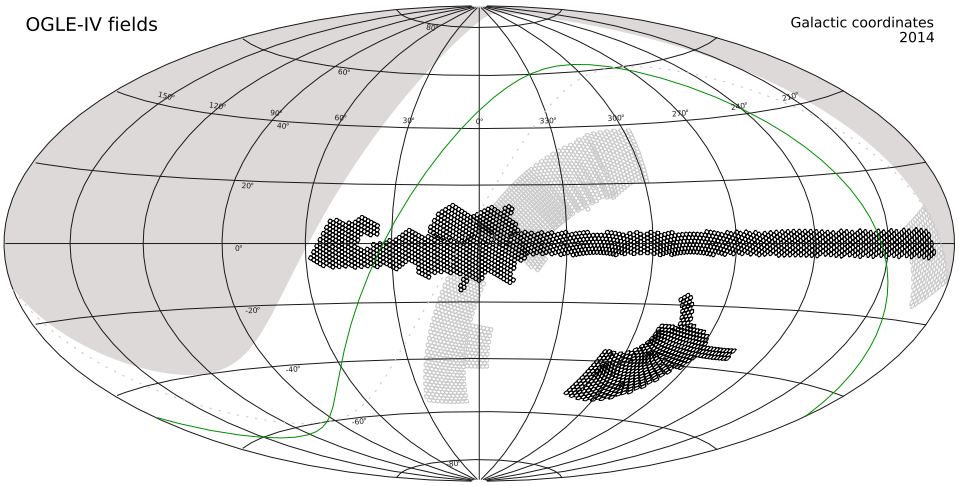

Figure 1. OGLE-IV sky coverage in the Galactic coordinates. Dark squares denote individual OGLE-IV pointings of the long-term surveys (credit: J. Skowron).

The OGLE-IV Magellanic System Survey covers about 650 square degrees around the Magellanic Clouds. The observed regions include the Magellanic Bridge and a large area of the halo of the Magellanic Clouds. The main science goal of this survey is to obtain the full variability census of objects in the Magellanic System. In parallel, the OGLE-IV Transient Survey is conducted based on observations collected by the Magellanic System Survey leading to over 200 supernovae detections per year and several other transient objects (Wyrzykowski et al. 2014).

Finally, the OGLE-IV Galaxy Variability Survey (GVS) covers about 1700 square degrees. This includes a six-degree-wide strip along the whole Galactic plane visible at the Las Campanas Observatory and the large region of the outer Galactic bulge not covered by the OGLE-IV microlensing survey. The main science goal of this survey is to provide a complete variability status of this huge region of the sky. GVS will provide invaluable data for the Galactic structure studies.

The high precision OGLE photometry of millions of stars can be used for solving many astrophysical problems. While the main focus of the OGLE survey is variability, hundreds of millions of non-variable stars with precise OGLE photometry have also been used for a variety of important projects including studies of the structure of the Magellanic Bridge (Skowron et al. 2014), the discovery of the Galactic bar X-shape structure (Nataf et al. 2010) or studies of interstellar reddening (Nataf et al. 2013).

OGLE-IV sky variability studies concentrate on four classes of objects: gravitational microlensing events, variable stars, transient objects and extragalactic variable sources. Here we present the summary of recent OGLE contributions to the variable stars studies focusing mostly on pulsating stars.

The OGLE Collection of Variable Stars contains currently over 465 thousand variable stars discovered by the OGLE survey. It should be stressed that these objects are genuine variable stars with precisely characterized properties. This is possible thanks to the high precision of the OGLE photometry and the large number of collected epochs. The OGLE experience indicates that for a reasonably complete survey of variable objects at least 100 epochs are necessary.

The OGLE Collection of Variable Stars (Soszyński et al. 2014b) is the largest and most uniform dataset of variable objects worldwide. It will be soon significantly increased with the continuous stream of new discoveries from the fourth phase of the OGLE survey.

4. Pulsating stars in the OGLE survey

The pulsating stars were of high interest from the very beginning of the OGLE project. Actually, the first variables detected by the OGLE survey were RR Lyrae stars near the Galactic center (Udalski et al. 1992). Large samples of these variables were discovered in the Sculptor dwarf galaxy and globular clusters (Kaluzny et al. 1995, 1997) during OGLE-I phase. Up to now, the OGLE survey has discovered the largest number of pulsating stars of all types. Figure 2 shows the period-luminosity (P-L) diagram based on OGLE-III phase detected objects showing P-L relations for many different pulsating star classes.

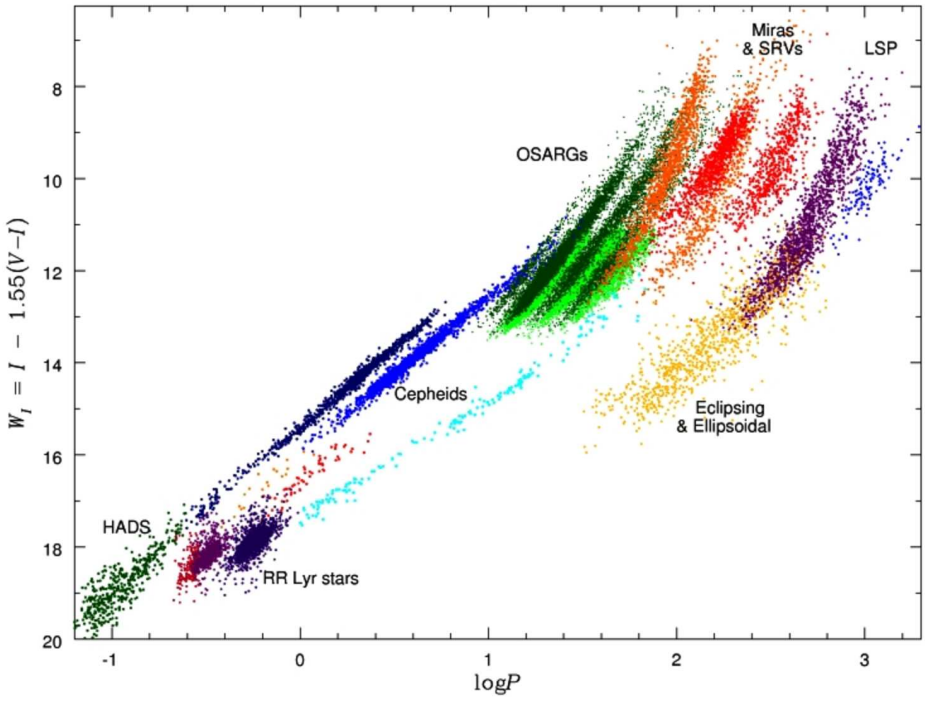

Figure 2. Period–luminosity diagram for pulsating stars discovered during the OGLE-III phase (credit: I. Soszyński).

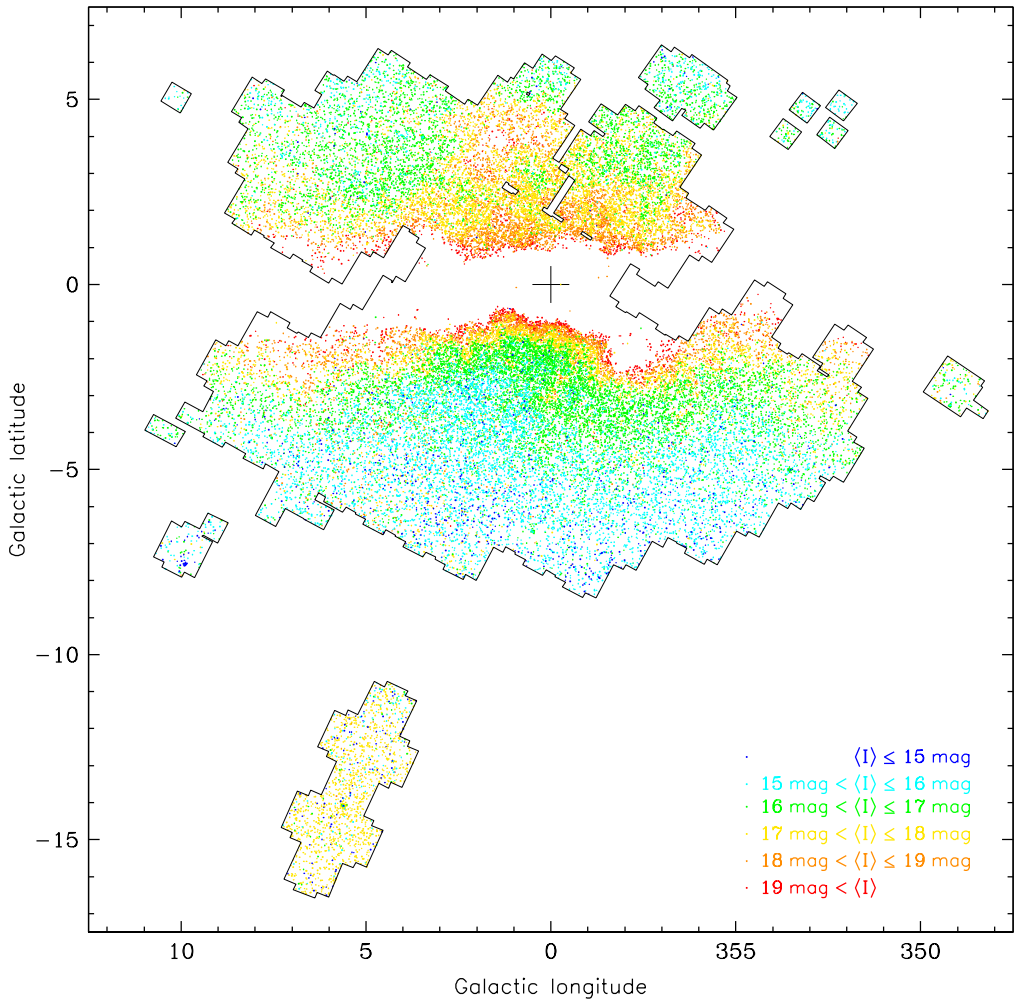

Figure 3. Distribution in the sky of over 38 000 RR Lyrae stars discovered by OGLE in the Galactic bulge (with permission, Acta Astron. 64, 177).

Recently over 38 000 RR Lyrae stars were discovered in the central Galactic bulge monitored during OGLE microlensing survey (Soszyński et al. 2014b). Figure 3 presents their distribution in the sky. A subsample of these stars, namely RRab type variables, were used by Pietrukowicz et al. (2015) for studies of the Galactic structure. A huge sample of the RR Lyrae stars from the Sagittarius dwarf galaxy has also been discovered and used for studies of this dwarf galaxy neighbor (Hamanowicz et al., in preparation). The sample of the Galactic RR Lyrae will be significantly increased in the coming years when OGLE-IV completes the GVS.

Large samples of pulsating stars have also been discovered by OGLE in the Magellanic System. Figure 4 shows the distribution of the OGLE classical Cepheids in the Magellanic System (Soszyński et al. 2015). This is a virtually complete sample of these extremely important variable stars in the Magellanic System. It contains altogether over 9500 objects.

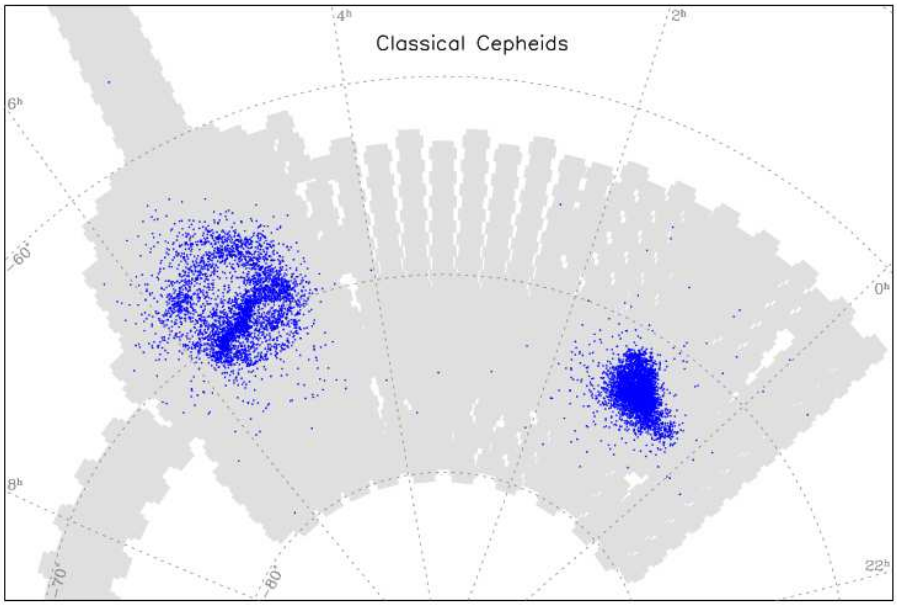

Figure 4. Distribution in the sky of about 9500 classical Cepheids discovered by OGLE in the Magellanic System (with permission: Acta Astron., 65, 297).

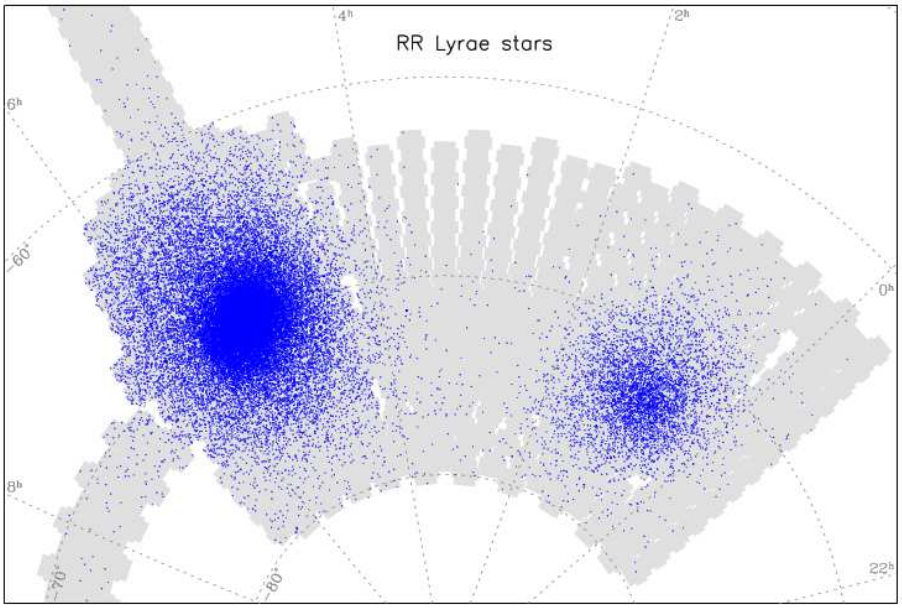

Figure 5. Distribution in the sky of over 45 000 RR Lyrae stars discovered by OGLE in the Magellanic System (credit: I. Soszyński).

A similar plot for RR Lyrae stars is presented in Figure 5. This sample contains over 45 000 objects. When comparing Figs. 4 and 5 one can immediately notice the difference in the distribution of the young and old stars in the Magellanic System. More detailed studies of the Clouds' structure based on these objects are underway.

Pulsating stars form a pulsation laboratory that can provide many important information on the structure of stars, pulsating mechanisms, etc. The most recent discoveries based on the OGLE samples of RR Lyrae stars include: the discovery of the mode switching RR Lyrae stars (Soszyński et al. 2014a), the discovery of the Blazhko effect in RRd type RR Lyrae stars (Soszyński et al. 2014b; Smolec et al.2015a), the discovery of many multiperiodic objects pulsating in radial modes (Soszyński et al. 2014b) as well as in enigmatic modes with the period ratio of 0.60–0.64 and 0.686 (Netzel et al. 2015), the discovery of the triple mode RR Lyrae with period doubling (Smolec et al. 2015b). It was also possible to find numerous samples of stars showing Blazhko effect which hopefully will lead finally to the full explanation of this phenomenon.

One of the most important observational parameters of RR Lyrae stars which has not been yet verified with the theoretical predictions is the mass of RR Lyrae stars. A huge progress occurred in the last few years for the Cepheid variables thanks to the discovery of several Cepheids in wide binary systems by the OGLE survey, which led to precise weighing (accuracy of 1%) of the Cepheid components (Pietrzyński et al. 2010, 2011; Gieren et al. 2015). However, so far only one RR Lyrae candidate star was found in an eclipsing system in spite of the detection of tens of thousands of these pulsating stars. Moreover, the precise characterization of the pulsating component showed that the star has a completely different evolutionary status than regular RR Lyrae stars and only mimics RR Lyrae star behavior (Pietrzyński et al. 2013). Thus, the chance for measuring the RR Lyrae dynamical mass in an eclipsing system remains slim as no promising candidates were found in the OGLE-IV Magellanic System sample. It is, however, possible that OGLE-IV GVS sample of RR Lyrae stars will bring new candidates.

Another possible option for measuring masses of RR Lyrae stars in the Galactic bulge is microlensing. Although the probability of microlensing even in stellar fields as dense as the Galactic center is very low (one star per million is microlensed at any given moment) there exists some possibility that one of the numerous pulsating stars there will participate in an event. Actually, in the huge collection of the OGLE microlensing events (over 17 000 events) one can find microlensing cases with a δ Scuti pulsator or RRc type RR Lyrae star (Soszyński et al. 2014b). In this latter case the RR Lyrae star plays, unfortunately, the role of the lensed star not the lensing one so its mass cannot be derived. Nevertheless, the reverse situation may also happen, and then the lens mass could be in principle directly measured.

OGLE-IV will continue monitoring its main observing targets for the next couple of years bringing new discoveries in the pulsating stars field. With continuously increasing time span of the OGLE light curves, already reaching twenty or more years in some fields, it will be possible to study many long term effects occurring in the pulsating stars.

Acknowledgments

The OGLE project has received funding from the National Science Centre, Poland, grant MAESTRO 2014/14/A/ST9/00121 to AU. This project has been also supported by the Polish Ministry of Science and Higher Education through the program "Ideas Plus" award No. IdP2012 000162 to Igor Soszyński.

References

Gieren, W., Pilecki, B., Pietrzyński, G., et al. 2015, ApJ, 815:28
Gould, A., Udalski, A., Shin, I.-G., et al. 2014, Science, 345, 46
Kaluzny, J., Kubiak, M., Szymanski, M., et al. 1995, A&AS, 112, 407
Kaluzny, J., Kubiak, M., Szymanski, M., et al. 1997, A&AS, 125, 343
Nataf, D.M., Udalski, A., Gould, A., et al. 2010, ApJ, 721, 28
Nataf, D.M., Gould, A., Fouqué, P., et al. 2013, ApJ, 769:88
Netzel, H., Smolec, R., Moskalik, P. 2015, MNRAS, 453, 2022
Paczyński, B. 1986, ApJ, 304, 1
Pietrukowicz, P., Kozłowski, S., Skowron, J., et al. 2015, ApJ, 811:113
Pietrzyński, G., Thompson, I. B., Gieren, W., et al. 2010, Nature, 468, 542
Pietrzyński, G., Thompson, I. B., Graczyk, D., et al. 2011, ApJ, 742:20
Pietrzyński, G., Graczyk, D., Gieren, W., et al. 2013, Nature, 495, 76
Skowron, D. M., Jacyszyn, A. M., Udalski, A., et al. 2014, ApJ, 795:108
Smolec, R., Soszyński, I., Udalski, A., et al. 2015a, MNRAS, 447, 3756
Smolec, R., Soszyński, I., Udalski, A., et al. 2015b, MNRAS, 447, 3873
Soszyński, I., Dziembowski, W. A., Udalski A., et al. 2014a, Acta Astron., 64, 1
Soszyński, I., Udalski A., Szymański, M. K., et al. 2014b, Acta Astron., 64, 177
Soszyński, I., Udalski A., Szymański, M. K., et al. 2015, Acta Astron., 65, 297
Udalski, A., Szymański, M. K., Kaluzny, J., et al. 1992, Acta Astron., 42, 253
Udalski, A., Szymański, M. K., Szymański, G. 2015a, Acta Astron., 65, 1
Udalski, A., Yee, J. C., Gould, A., et al. 2015b, ApJ, 799:237
Udalski, A., Jung, Y. K., Han, C., et al. 2015c, ApJ, 812:47
Woźniak, P. R. 2000, Acta Astron., 50, 421
Wyrzykowski, Ł., Kostrzewa-Rutkowska, Z., Kozłowski, S., et al. 2014, Acta Astron., 64, 197

RRL2015 – High-Precision Studies of RR Lyrae Stars
L. Szabados, R. Szabó, K. Kinemuchi (Eds.) 2016

RR Lyrae binary systems in the Galactic bulge

Gergely Hajdu[1,2], Márcio Catelan[1,2], Johanna Jurcsik[3], István Dékány[2,1], Andrew Drake[4], & Jean-Baptiste Marquette[5]

[1]*Instituto de Astrofísica, Pontificia Universidad Católica de Chile, Santiago, Chile*
[2]*Millennium Institute of Astrophysics, Santiago, Chile*
[3]*Konkoly Observatory, Research Centre for Astronomy and Earth Sciences, Hungarian Academy of Sciences, H-1121, Budapest, Konkoly Thege Miklós út 15-17, Hungary*
[4]*California Institute of Technology, Pasadena, CA, USA*
[5]*Institut d'Astrophysique de Paris, Sorbonne Universités, UPMC Univ Paris 6 et CNRS, Paris, France*

Abstract. The apparent lack of RR Lyrae stars in binary systems has been a mystery for decades. Without such systems, a direct mass determination of these variables has been out of reach, and the modeling of pulsation and evolution of these stars was left without this important constraint. We have searched for such systems using the $O-C$ method in the light curves collected by the OGLE project towards the Galactic bulge. We have identified 20 good candidates out of 1952 investigated stars. We have also derived the first lower limit of such systems of at least 4%.

1. Introduction

Binary stars play a fundamental role in astrophysics: knowledge of the binary elements immediately yields the mass of the components, which is the most basic physical parameter of a star. Unfortunately, up to this point, no such measurement has been made for any RR Lyrae variable. Indeed, until recently, only one RR Lyrae had been known to reside in a binary system with high confidence, TU UMa (Wade et al. 1999), but the long period ($\sim$ 23 yr) of this system made the follow up particularly difficult.

An alternative way of deriving the mass of RR Lyrae stars is utilizing the double-mode nature of RRd variables through the so-called *Petersen diagram* (Petersen 1973). From modeling, it is known that the period ratio has a strong dependence on the mass, and comparing the periods and period ratios to models, the mass can be derived. However, the mass determined in this way is strongly dependent on the assumptions of the modeling, which in itself sorely lacks a constraint on the mass itself.

In order to remedy this situation, we have conducted a search for binary stars utilizing the light curves of RR Lyrae stars collected by the OGLE project[1], and have published our first results in Hajdu et al. (2015).

[1]http://ogle.astrouw.edu.pl/

2. Analysis of variables

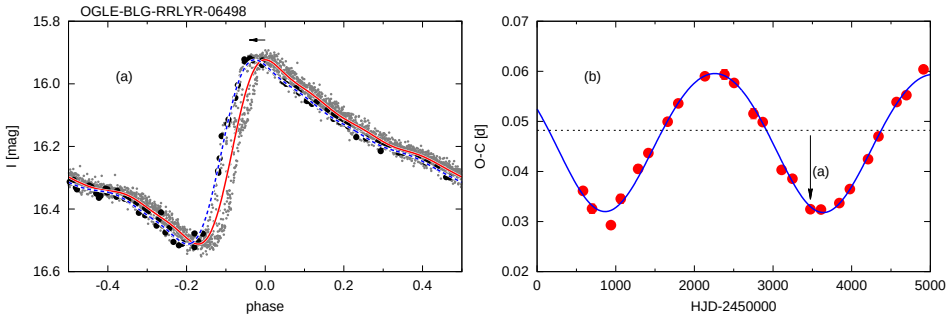

Figure 1. Construction of the $O-C$ diagrams. *Left:* The original light curve (*grey dots*) folded with the period of pulsation. An initial Fourier-series fit (*red line*) is constructed, then it is fitted (*dashed blue line*) to shorter segments of the light curve (*black dots*). *Right:* The constructed $O-C$ diagram. The arrow corresponds to the measurement on the left panel.

We have analyzed 1952 fundamental-mode RR Lyrae (RRab) stars with the most extended OGLE-III light curves (Soszyński et al. 2011), using the $O-C$ diagram method (Sterken 2005). In principle, the $O-C$ diagram reveals the deviation of a variable (pulsating or eclipsing) star from a supposed simple ephemeris with a constant period. Variables in binary systems display a periodic $O-C$ due to the light-time effect (LTE), with a shape heavily dependent on the binary parameters (see, e.g., Irwin 1959).

We measured individual $O-C$ points of the variables with a modified version of Hertzsprung's (1919) method, as shown in Fig. 1. The resulting $O-C$ diagrams were inspected for all 1952 stars, searching for stars with $O-C$ shapes compatible with the LTE. The resulting candidates were further analyzed by inspecting their light curves. In some cases, the long-term cyclic changes were clearly caused by the Blazhko (1907) effect, and these stars were discarded from our sample.

While we were in the process of analyzing the candidates found using the OGLE-III data, the OGLE project published the catalog of RR Lyrae variables observed towards the Galactic bulge in the course of the OGLE-IV phase (Soszyński et al. 2014). We have thus combined the OGLE-III and IV light curves in order to increase the baseline of our $O-C$ diagrams. In a number of RR Lyraes the strictly periodic behavior expected from the LTE did not continue in the OGLE-IV data, while for some other variables the dense OGLE-IV data have revealed low-amplitude Blazhko effect. All of these stars were discarded from further consideration.

We have found in total 20 stars where the cyclic $O-C$ variations are likely to be caused by the LTE. Out of these, 12 stars have data covering long enough a time span so as to disentangle the effect of the intrinsic period change (causing a parabolic $O-C$ shape) from the LTE, and thus allowing us to derive the (partial) binary parameters. Figure 2 illustrates the $O-C$ diagrams of two of these stars, along with the corresponding fits.

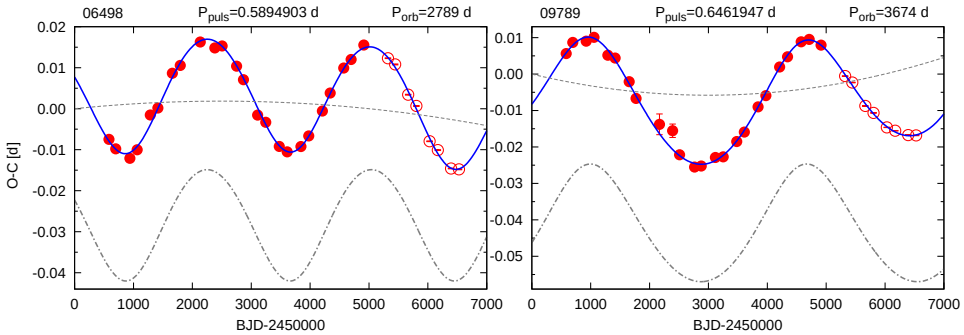

Figure 2. Representative $O-C$ diagrams of the RR Lyrae binary candidates. Each panel shows the measured $O-C$ points (*circles: filled – OGLE-III data; empty – OGLE-IV data*); the light-time effect (*dot-dashed line*), shifted downwards for clarity; the parabolic trend caused by the intrinsic period change of the RR Lyrae (*dashed lines*); and the complete fit of the $O-C$ measurements (*blue line*). For both stars, the name of the variable, the pulsation and orbital periods are indicated on top of the panels.

3. Discussion

We have investigated 1952 RR Lyrae variables, and found 20 binary candidates among them, allowing us for the first time to assess the binary frequency among RR Lyrae stars. A naive statistic implies a 1% rate of binaries among RR Lyrae; however, we know that the detection rate of binary systems in our case is artificially lowered by the presence of the Blazhko effect, which affects $\sim 50\%$ of all RRab stars (Jurcsik et al. 2009; Kolenberg et al. 2010). As we have discarded all stars displaying the Blazhko effect, we must correct our estimate by a factor of two for these variables, increasing the rate to 2%. We have chosen to further increase this ratio by an additional factor of two, in order to correct for other biases that affect the sample (e.g., stars with low quality photometry, undetected binaries due to low LTE amplitude or too long binary periods compared to the baseline of observations, etc.), and regard this 4% as a lower limit of the true incidence rate of RR Lyrae stars in binary systems.

The shortest orbital period we have detected in our sample for an RR Lyrae (OGLE-BLG-RRLYR-07640) is ~ 3.5 yr. Indeed, most of our candidates have periods of 9 to 11 years. As binary systems with shorter periods are common, we suppose that their absence among RR Lyrae is a consequence of the binary evolution of the system: as horizontal branch (HB) stars, RR Lyrae variables have already passed through the red giant branch (RGB) phase of their evolution. In this phase, stars that are situated in close binary systems can easily lose too much mass through Roche-lobe overflow, thus preventing them from becoming a normal HB star within the instability strip; instead, they will become blue HB stars. Finding more RR Lyrae with similar orbital periods, and subsequent modeling of the evolution of RR Lyrae binary systems, could provide an interesting insight into the coevolution of low-mass stellar binaries.

Figure 2 shows the $O-C$ diagrams of two of the most interesting binary candidates: OGLE-BLG-RRLYR-06498 and 09789. They have fairly large expected radial velocity semi-amplitudes (9.2 and 8.4 km s^{-1}, respectively), making follow-up spectroscopy for verification of the binary status relatively easy.

The large amplitude LTE also implies an interesting common property for these systems: regardless of the inclination, the companion objects must be more massive than the RR Lyrae variables themselves. As the stars naturally lose substantial mass during the RGB phase (even without Roche-lobe overflow), an unevolved companion around the main-sequence turnoff point can easily outweigh the RR Lyrae variable. If these stars are indeed near the turn-off point, they might even be bright enough to contribute significantly to the spectra of these systems. However, due to the large differences in magnitude, spectra of S/N > 100 would be required to detect the companions. Due to the faint magnitudes (~ 16.2 and ~ 15.6 in I, respectively), this task will be very challenging.

In absence of eclipses, astrometric observations are needed in order to achieve the first ever reliable dynamical mass derivation of any RR Lyrae. Unfortunately, the projected semi-major axis on the sky is very small (below 0.5 mas) for all of our candidates. Measuring the inclination through the astrometric orbit of the binary candidates will most probably require a dedicated follow-up program with the next-generation VLTI instrument GRAVITY (Gillessen et al. 2010) or the future 30 m class telescopes.

Our study has proven that RR Lyrae binary systems are relatively common, but the orbital periods are fairly long. Currently, the decade-long data from the OGLE survey provide the best opportunity to uncover more of these systems, and indeed, we are currently analyzing the remainder of the OGLE light curves. Long-term photometry of brighter, closer RR Lyrae stars is strongly encouraged, as they might provide better targets for spectroscopic and astrometric follow up.

Acknowledgements

Support for this project is provided by the Ministry for the Economy, Development, and Tourism's Programa Iniciativa Científica Milenio through grant IC 120009, awarded to the Millennium Institute of Astrophysics; by Proyecto Basal PFB-06/2007; by Fondecyt grant #1141141; and by CONICYT's PCI program through grant DPI 20140066. G.H. gratefully acknowledges support from CONICYT-PCHA/Doctorado Nacional grant 2014-63140099, and by CONICYT Anillo grant ACT 1101.

References

Blazhko, S. 1907, AN, 175, 325
Gillessen, S., Eisenhauer, G., Perrin, G., et al. 2010, Proc. SPIE, 7734, 77340Y
Hajdu, G., Catelan, M., Jurcsik, J., et al. 2015, MNRAS, 449, L113
Hertzsprung, E. 1919, AN, 210, 17
Irwin, J. B. 1959, AJ, 64, 149
Jurcsik, J., Sódor, Á., Szeidl, B., et al. 2009, MNRAS, 400, 1006
Kolenberg, K., Szabó, R., Kurtz, D. W., et al. 2010, ApJ, 713, L198
Petersen, J. O. 1973, A&A, 27, 89
Soszyński, I., Dziembowski, W. A., Udalski, A., et al. 2011, AcA, 61, 1
Soszyński, I., Udalski, A., Szymański, M. K., et al. 2014, AcA, 64, 177
Sterken, C. 2005, The Light-Time Effect in Astrophysics, Ed: C. Sterken, (San Francisco: Astronomical Society of the Pacific), p. 3
Wade, R. A., Donley, J., Fride, R., et al. 1999, AJ, 118, 2442

RRL2015 – High-Precision Studies of RR Lyrae Stars
L. Szabados, R. Szabó, K. Kinemuchi (Eds.) 2016

Review of candidates of binary systems with an RR Lyrae component

Marek Skarka[1,2], Jiří Liška[1], Miloslav Zejda[1], & Zdeněk Mikulášek[1]

[1]*Department of Theoretical Physics and Astrophysics, Masaryk University, Brno, Czech Republic*
[2]*Konkoly Observatory, Research Centre for Astronomy and Earth Sciences, Hungarian Academy of Sciences, H-1121, Budapest, Konkoly Thege Miklós út 15-17, Hungary*

Abstract. We present an overview and the current status of research on RR Lyrae stars in binary systems. In recent years the number of binary candidates has steeply increased and it was suggested that the occurrence of multiple stellar systems with an RR Lyrae component is much higher than previously thought. We discuss the probability of their detection using various observing methods, compare recent results regarding selection effects, period distribution, the proposed orbital parameters and the Blazhko effect.

1. Introduction

It is generally assumed that the majority of stars resides in binary or even multiple systems. However, the situation is not so simple, because the estimates of their incidence differ for different stellar populations and stellar types. For example, Sana & Evans (2011) give about 40% of O and B type stars, Duquennoy (1991) give 60–80% of F and G stars, Lada (2006) proposes that 30% of stars of all stellar types are bound in binaries.

Nevertheless, we know that many pulsating stars really orbit around a common center of mass with some kind of companion. There are more than 150 Cepheids and more than 100 δ Sct type stars known in binaries (Szabados 2003; Liakos et al. 2012). The list assembled from the available literature is provided by Zhou (2014).

What is the situation with RR Lyrae stars? There are only 61 candidates known so far[1] (Liška & Skarka 2016), and only one system, in which a pulsating component is not a classical RR Lyrae, has been confirmed (Pietrzyński et al. 2012). Considering the fraction of known to all binary RR Lyrae candidates this is less than 0.1%. The reasons for this unpleasant situation emerge mainly from stellar evolution producing difficulties in detection of binarity.

[1]And several tens of candidates in globular clusters (e.g. Jurcsik et al. 2012) and in the Galactic Bulge (Hajdu et al. 2016).

2. Expected characteristics of binary candidates

A binary system with an RR Lyrae component should be well detached because otherwise mass transfer causing a different evolutionary scenario could take place. Such a wide binary with an orbital period longer than a few hundreds of days will be hardly detectable because of the very low probability of eclipses, and the low amplitude of the radial velocity (hereafter RV) variations vanishing in the RV changes caused by pulsations. Difficulties in the detection are also caused by the necessity of long-term monitoring which is not always available, or possible to do.

If the initial mass of the companion was higher than that of the RR Lyrae component, it would evolve much faster and should presently be in a form of a degenerate remnant – either white dwarf, neutron star, or a black hole. Such binaries would definitely not be detectable as eclipsing, and only spectral lines of the RR Lyrae component would be visible (SB1 type). If the companion evolved faster, then the RR Lyrae component could possibly be contaminated with heavier elements originated form the ejected envelope during the last stages of the more massive companion (e.g. Kennedy et al. 2014).

Concerning a low-mass companion, it could be in any evolutionary stage. The radius and the luminosity of the companion influence to what extent it manifests itself observationally:

- *Main sequence star* – the amplitude of eclipses would be negligible, the manifestations of the companion almost undetectable in spectra.
- *Asymptotic- and red-giant branch star* – significant eclipses will take place, colour would be shifted to red, the amplitude of light variations of the binary caused by pulsations would be significantly lower than in a separate RR Lyrae, enrichment with heavier elements would be possible with an AGB companion.
- *Horizontal branch star* – significant eclipses will take place, possible colour excess should be detectable, lower amplitude of light changes than in separate RR Lyrae will be observed.

In all these cases the confirmation of the binarity via spectroscopy would be difficult because of the low amplitudes in the RV domain. Long-term tiny changes in RV can only be revealed using accurate template curves which are still missing (see Guggenberger et al. 2016). Without them it is very difficult to find the zero points of the systemic velocities from various measurements which are often based on different spectral lines. In the case of unavailable template curve there is also an indirect method through analysis of the scatter of the pulsation-phased RV curves. After removing the orbital motion, the scatter should significantly decrease (see Fig. 7 in Liska et al. 2015a).

3. Current situation in binary candidates

The first candidate for an RR Lyrae in a binary system was proposed in the 1960s. However, the majority of the candidates have been revealed only recently (Hajdu et al. 2015; Liska et al. 2015b). The number of discovered candidates

can be seen in the left panel of Fig. 1. The mean-magnitude distribution of the candidates is bimodal due to a selection effect (most of stars are coming either from the Galactic bulge, or are bright stars from the Galactic field, see the right panel of Fig. 1).

Except for a few candidates for short-period eclipsing binaries, all other stars have periods longer than a year (left panel of Fig. 2). Longer orbital periods mean that the semi-major axes are also large, on the order of a few astronomical units or larger. When the orbital periods are plotted against the metallicity (right panel of Fig. 2), no apparent dependence is visible except for the splitting which is again an observation bias. About 1/5 of all candidates shows the Blazhko effect. The mass function in systems with models of the orbit ranges from 4×10^{-6} to several tens of solar masses. For detailed statistics see Liška & Skarka (2016).

Due to all discussed problems in Section 2., the most efficient method for revealing the candidates is looking for the variations caused by the orbital motion of the RR Lyrae translating in cyclic period changes known as the light-travel time effect (LiTE). Since this method is indirect and the variations can be misclassified due to other effects (secular erratic changes, long-term Blazhko effect, etc.), an independent confirmation is needed in such objects.

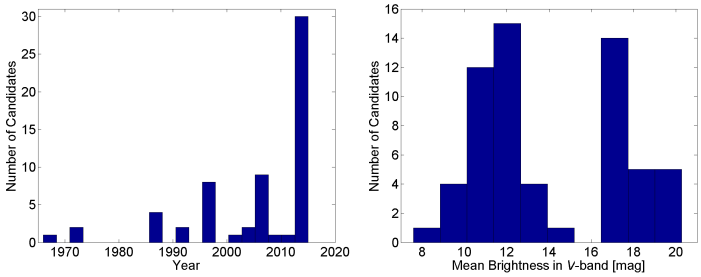

Figure 1. Number of discovered candidates during last 50 years (left panel) and magnitude distribution of known candidates (right panel).

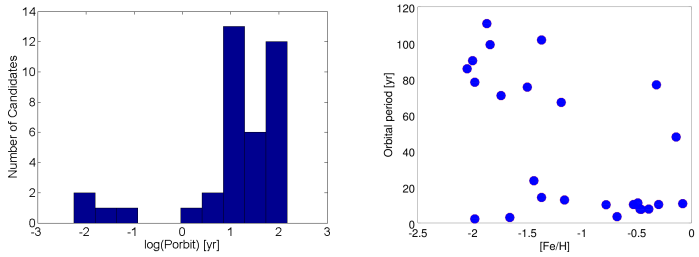

Figure 2. Orbital period distribution (left panel) and orbital period against metallicity (right panel).

4. Interesting cases

Among the Galactic-field candidates, there are several very interesting cases which deserve attention. The first of them is TU UMa with an orbital period of 23 years (Liška et al. 2015b) which is the shortest one among the long-period fraction of candidates. It is bright and therefore an accurate template curve

could be easily accessible. The confirmation of binarity should, therefore, be a task for the near future.

Period variations of two of the candidates indicate possible high mass companion – RZ Cet ($M_{2,\mathrm{min}} = 1.15\,\mathrm{M}_\odot$) and AT Ser ($M_{2,\mathrm{min}} = 1.9\,\mathrm{M}_\odot$), two of the candidates, VX Her and RW Ari, showed suspicious decrease in brightness which might be caused by an unseen body (Fitch et al. 1966; Wiśniewski 1971). However, these events were unique and have never repeated. Assuming the depth of the decrease and colour measured in VX Her by Fitch et al. (1966) the companion would be a horizontal-branch star. When we consider the 83-yr orbital period (Liska et al. 2015b), the eclipse should last for 500 d!

BB Vir and RS Boo were supposed to have an extraordinary colour (Fitch et al. 1966; Bookmyer et al. 1977; Kanyó 1986), and possible LiTE was detected by Liska et al. (2015b).

5. Summary and future prospects

We discussed the status of the research in binary candidates with an RR Lyrae component, their characteristics and problems with their detection. The parameters of the possible component which would have crucial influence on the observable characteristics were discussed. We also highlighted the most interesting candidates.

Only future studies can prove whether the candidates are real binaries. It is proposed to focus on interesting objects with accumulated interesting features, for example eclipses and LiTE, in a systematic and long-term manner to get reliable results being capable to reveal tiny changes.

Acknowledgements

Financial support of grants MUNI/A/1110/2014 and LH14300 is acknowledged.

References

Bookmyer, B. B., Fitch, W. S., Lee, T. A., et al. 1977, RMxAA, 2, 235
Duquennoy, A., Mayor, M. 1991, A&A, 248, 485
Fitch, W. S., Wisniewski, W. Z., Johnson, H. L. 1966, Commun. Lunar and Planetary Laboratory, 5, 3
Guggenberger, E., Barnes, T. G., Kolenberg, K. 2016, these proceedings, p. 145
Hajdu, G., Catelan, M., Jurcsik, J., et al. 2015, MNRAS, 449, L113
Hajdu, G., Catelan, M., Jurcsik, J., et al. 2016, these proceedings, p. 137
Jurcsik, J., Sódor, A., Hajdu, G., et al. 2012, MNRAS, 419, 2173
Kanyó, S. 1986, Commun. Konkoly Observatory, Budapest, Hungary, 87, 1
Kennedy, C. R., Stancliffe, R. J., Kuehn, C., et al. 2014, ApJ, 787:6
Lada, C. 2006, ApJ, 640, L63
Liakos, A., Niarchos, P., Soydugan, E., Zasche, P. 2012, MNRAS, 422, 1250
Liska, J., Skarka, M., Mikulasek, Z., et al. 2015a, arXiv:1502.03331
Liska, J., Skarka, M., Zejda, M., Mikulasek, Z. 2015b, arXiv:1504.05246
Liška, J., Skarka, M. 2016, these proceedings, p. 209
Pietrzyński, G., Thompson, I. B., Gieren, W., et al. 2012, Nature, 484, 75
Sana, H., Evans, Ch. J. 2011, IAUS, 272, 474
Szabados, L. 2003, IBVS, 5394, 1
Wiśniewski, W. Z. 1971, AcA, 21, 307
Zhou, A.-Y. 2014, arXiv:1002.2729v5

RRL2015 – High-Precision Studies of RR Lyrae Stars
L. Szabados, R. Szabó, K. Kinemuchi (Eds.) 2016

New systemic radial velocities of suspected RR Lyrae binary stars

Elisabeth Guggenberger[1,2], Thomas G. Barnes[3], & Katrien Kolenberg[4,5,6]

[1] *Max Planck Institute for Solar System Research, Göttingen, Germany*
[2] *Stellar Astrophysics Centre, Aarhus University, Denmark*
[3] *McDonald Observatory, University of Texas at Austin, Texas, USA*
[4] *University of Antwerp, Belgium*
[5] *KU Leuven, Belgium*
[6] *Harvard-Smithsonian Center for Astrophysics, Cambridge MA, USA*

Abstract. Among the tens of thousands of known RR Lyrae stars there are only a handful that show indications of possible binarity. The question why this is the case is still unsolved, and has recently sparked several studies dedicated to the search for additional RR Lyraes in binary systems. Such systems are particularly valuable because they might allow to constrain the stellar mass.

Most of the recent studies, however, are based on photometry by finding a light time effect in the timings of maximum light. This approach is a very promising and successful one, but it has a major drawback: by itself, it cannot serve as a definite proof of binarity, because other phenomena such as the Blazhko effect or intrinsic period changes could lead to similar results. Spectroscopic radial velocity measurements, on the other hand, can serve as definite proof of binarity.

We have therefore started a project to study spectroscopically RR Lyrae stars that are suspected to be binaries. We have obtained radial velocity (RV) curves with the 2.1 m telescope at McDonald observatory. From these we derive systemic RVs which we will compare to previous measurements in order to find changes induced by orbital motions. We also construct templates of the RV curves that can facilitate future studies.

We also observed the most promising RR Lyrae binary candidate, TU UMa, as no recent spectroscopic measurements were available. We present a densely covered pulsational RV curve, which will be used to test the predictions of the orbit models that are based on the $O-C$ variations.

1. Introduction

So far our knowledge of the masses of RR Lyrae stars mainly relies on models of stellar evolution and pulsation. Having an independent measure of the mass such as the one derived from a binary orbit would be a valuable test case for our understanding of stellar pulsation. The only RR Lyrae star for which this was achieved so far turned out to be a surprise: OGLE-BLG-RRLYR-02792 turned out to have a mass of only 0.26 $M_\odot$ (Pietrzynski et al. 2012) and is now known as an RR Lyrae impostor which mimics the pulsation typical of RR Lyrae stars. The only other RR Lyrae star that can be considered a confirmed candidate is TU UMa with photometric and spectroscopic measurements pointing consis-

tently towards binary motion with a period longer than 20 years (Wade et al. 1999; Liska et al. 2015).

Concerning the large numbers of known and of well-studied RR Lyrae stars this number is surprisingly low as usually about half of all stars are considered to be part of binary or multiple systems. This lack of binaries might partly be due to the fact that not many studies have yet been dedicated to searching for these objects. Several stars have been mentioned in the literature as possible binary candidates but have not been followed up in dedicated campaigns. There are, for example, stars for which discrepant systemic radial velocities have been measured, which was pointed out by Solano et al. (1997) and Fernley & Barnes (1997). These are the stars that we primarily follow up in this project. Sometimes older measurements of the center-of-mass velocity are based only on a few spectra with phases calculated from ephemeris that have later been improved. These measurements might turn out to be erroneous when revisited. With our new data we aim at verifying or refuting the binary nature of the objects in question. The new accurate center-of-mass velocities can then also be used for other studies, for example on Galactic dynamics.

Another indication of a possible binary orbit is periodic change in the times of maximum light, and stars with suspicious $O - C$ diagrams (observed minus calculated time of maximum) have been included in our target list.

Additionally, TU UMa is one of our targets. With the latest published RV value being more than a decade old, new measurements had become necessary to check the predictions from the orbit models which are based on photometry.

2. Techniques

Measuring the velocity changes introduced by orbital motion is a challenging task in RR Lyrae stars. The signal that we expect to measure is about an order of magnitude smaller than that caused by the pulsation motion of the atmospheric layers which usually amounts to tens of km/s. To derive a reliable center-of-mass velocity, one needs to understand the pulsation signal first, in order to remove it from the data. Hence several measurements, spread over different phases of the pulsation cycle, are necessary. With periods of about half a day, this means that it is usually not possible to cover a full pulsation cycle of a target in one night. Continued observations in the subsequent nights should then not duplicate the phases, which requires careful scheduling.

Often templates, for example that of Liu (1991) are used to model the RV curve of RR Lyrae stars and hence to find the center-of-mass velocity. However, when systemic RVs are derived from only a few measurements of the velocity, phases of the observations need to be known accurately (either directly from the RV measurements or from photometry), as well as the amplitude of the signal. In our project we aim at a number of 10 measurements per star in one orbit epoch, which allows for a check of the phases computed from published ephemeris.

Another challenge is the faintness of the RR Lyrae stars. This cannot be overcome by simply increasing the integration time, as the rapid atmospheric motion would then lead to smeared spectral lines. We therefore kept the integration times below 3% of the pulsation cycle.

3. Observations and reductions

Observations were carried out with the Sandiford Echelle Spectrometer (McCarthy et al. 1993) in the f/13.5 Cassegrain focus of the 2.1 Otto Struve telescope at McDonald Observatory, Texas. We have continuous spectral coverage over the observed range of 4250-4750 Å with a resolving power of $R \approx 55000$. The signal to noise ratios are typically between 20 and 60, depending on the brightness of the star and the limitations on the integrations time (<3% of the pulsation period). Radial velocity standard stars were observed several times during the course of each night, and Th-Ar spectra were taken for wavelength calibration after each stellar spectrum. We used standard IRAF routines for data reduction, and we derived the velocities by cross-correlating with the standard star spectra using the IRAF task `fxcor`. Only metal lines were used in the cross-correlation, as the hydrogen lines are known to have a phase offset and different velocity amplitudes compared to iron lines.

4. Preliminary results and outlook

During four runs between March 2014 and June 2015, 18 science objects were observed (see Table 1). For some of them the desired number of about 10 observations has been reached which allows the construction of an individual template. Example RV curves are shown in Fig. 1. For several others we have already obtained the minimum number of 3 observations, which allows an estimate of the systemic radial velocity based on a general template.

The project is ongoing and we have applied for more observing time to increase the number of spectra of the stars which are not well-covered yet, as well as to observe more targets for which indications of binarity have been reported.

Table 1. Stars observed so far in the project and number of observations.

Target	Number of spectra	Target	Number of spectra
TU UMa	47+8	ST Leo	7
CN Lyr	11	BK And	6
DM Cyg	11	XX Hya	5
Z CVn	9	RR Gem	4
BK Dra	9	RV UMa	4
AO Peg	8	CI And	3
AV Vir	8	U Tri	2
BX Leo	7	TT Lyn	1
SZ Leo	7	SS Leo	1

The derived center-of-mass velocities will soon be published in a forthcoming paper together with the individual velocity templates to facilitate future measurements of the center-of-mass velocity. Long orbits like that of TU UMa might be common, especially as close binaries will most likely have interacted with each other or even have been destroyed during the red giant phase of the RR Lyrae star. Hence further campaigns will be necessary in the future to characterize the orbits in detail. In our study we aim at laying a solid foundation for future

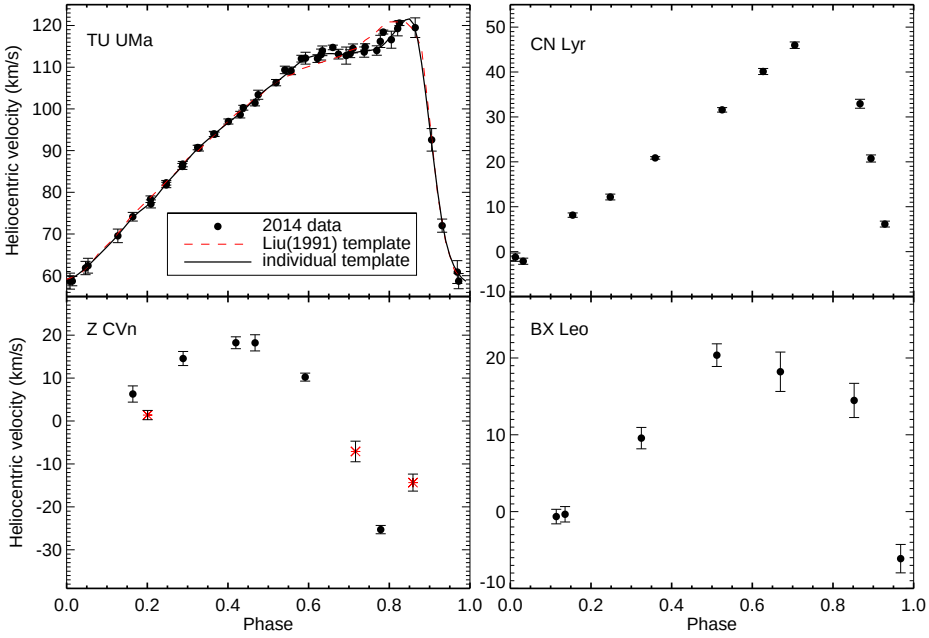

Figure 1. Example RV curves obtained in the McDonald RR Lyrae binary project. TU UMa data of 2014 are shown in the upper left panel, together with the scaled standard template by Liu (1991) (dashed red line) and the individual template created based on our data (solid black line). Other panels show the RRab star CN Lyr (upper right), the RRc star BX Leo (lower right), and the modulated star Z CVn (lower left) which we observed in two different Blazhko phases which are shown as filled circles and red crosses, respectively.

studies of the confirmed candidates. We therefore will also provide individual velocities of each spectrum in order to make direct comparisons possible.

Acknowledgements

The research leading to the presented results has received funding from the European Research Council under the European Community's Seventh Framework Programme (FP7/2007-2013) / ERC grant agreement no 338251 (StellarAges), from FWF grant P19962-N16 (Modulated RR Lyrae Stars) from the Austrian Wissenschaftsfonds (FWF), and from a Marie Curie International Outgoing Fellowship within FP7 (PIOF-255267, SAS-RRL).

References

Fernley, J., Barnes, T. G. 1997, A&AS, 125, 313
Liska, J., Skarka, M., Mikulasek, Z., et al. 2015, arXiv:1502.03331
Liu, T. 1991, PASP, 103, 205
McCarthy, J. K., Sandiford, B. A., Boyd, D., et al. 1993, PASP, 105, 881
Pietrzynski, G., Thompson, I. B., Gieren, W., et al. 2012, Nature, 484, 75
Solano, E., Garrido, R., Fernley, J. et al. 1997, A&AS, 125, 321
Wade R., Donley, J., Fried, R., et al. 1999, AJ, 118, 2442

RRL2015 – High-Precision Studies of RR Lyrae Stars
L. Szabados, R. Szabó, K. Kinemuchi (Eds.) 2016

On the pulsation and evolutionary properties of helium burning radially pulsating variables

G. Bono[1,2], A. Pietrinferni[3], M. Marconi[4], V. F. Braga[1], G. Fiorentino[5], P. B. Stetson[6], R. Buonanno[3], M. Castellani[2], M. Dall'Ora[5], M. Fabrizio[3], I. Ferraro[2], G. Giuffrida[7], G. Iannicola[2], M. Marengo[8], D. Magurno[1], C. E. Martínez-Vázquez[9], N. Matsunaga[10], M. Monelli[9], J. Neeley[8], S. Rastello[11], M. Salaris[12], L. Short[12], R. F. Stellingwerf[13]

[1]*Department of Physics, University of Rome Tor Vergata, Rome, Italy*
[2]*INAF–Osservatorio Astronomico di Roma, Monte Porzio Catone, Italy*
[3]*INAF–Osservatorio Astronomico di Collurania, Teramo, Italy*
[4]*INAF–Osservatorio Astronomico di Capodimonte, Naples, Italy*
[5]*INAF–Osservatorio Astronomico di Bologna, Bologna, Italy*
[6]*Dominion Astrophysical Observatory, Victoria, Canada*
[7]*Agenzia Spaziale Italiana, Data Center, Rome, Italy*
[8]*Iowa State University, Ames, IA, USA*
[9]*Istituto de Astrofisica de Canarias, Tenerife, Spain*
[10]*Institute of Astronomy, University of Tokyo, Tokyo, Japan*
[11]*University of Rome La Sapienza, Rome, Italy*
[12]*Liverpool John Moores University, Liverpool, UK*
[13]*Stellingwerf Consulting, Huntsville, AL, USA*

Abstract. We discuss pulsation and evolutionary properties of low- (RR Lyrae, Type II Cepheids) and intermediate-mass (Anomalous Cepheids) radial variables. We focus our attention on the topology of the instability strip and the distribution of the quoted variables in the Hertzsprung-Russell diagram. We discuss their evolutionary status and the dependence on the metallicity. Moreover, we address the diagnostics (period derivative, difference in luminosity, stellar mass) that can provide solid constraints on their progenitors and on the role that binarity and environment have in shaping their current pulsation characteristics. Finally, we briefly outline their use as standard candles.

1. Theoretical and empirical framework

RR Lyrae (RRL) stars are fundamental tracers of the old ($t > 10$ Gyr) stellar population. Dating back to the seminal investigations by W. Baade that led to the discovery of the difference between young, bluish, thin disk stars (population I) and old, reddish, halo/bulge stars (population II), they have been the crossroad of several long-standing astrophysical problems (Baade 1968).

More than seventy years ago Oosterhoff recognized that RRLs in Galactic globular clusters (GGCs) can be split, according to the mean period of fundamental variables (RRab), in two different groups: the Oosterhoff type I [OoI], with $\langle P_{\rm ab} \rangle \sim 0.56$ days and the Oosterhoff type II [OoII] with longer periods $\langle P_{\rm ab} \rangle \sim 0.66$ days. The mean period of first overtone (RRc) variables displays

a similar dichotomic distribution with $\langle P_c \rangle \sim 0.31$ days and $\langle P_c \rangle \sim 0.36$ days in OoI and OoII GCs, respectively. Further observations demonstrated that the fraction of RRc stars among the total number of RRLs is also smaller in OoI ($N_c/N_{tot} \approx 0.28$) than in OoII ($N_c/N_{tot} \approx 0.50$) GCs. Subsequent spectroscopic investigations enriched the empirical scenario demonstrating that OoI GCs are more metal-rich and cover a broad range in metal abundances, while OoII GCs are more metal-poor stellar systems.

The astronomical community devoted a paramount observational effort in constraining the leading physical parameters affecting the Oosterhoff dichotomy. Large photometric surveys disclosed that Galactic field RRLs display a similar dichotomy in the period distribution (Bono et al. 1997a): ASAS (Pojmanski 2002), LONEOS (Miceli et al. 2008), LINEAR (Sesar et al. 2013). Oddly enough, Local Group galaxies Draco (Kinemuchi et al. 2008), Ursa Minor (Nemec et al. 1988), Carina (Coppola et al. 2013), Leo I (Stetson et al. 2014) and their globulars (Bono et al. 1994) are characterized by mean fundamental periods that fill the so-called 'Oosterhoff gap', i.e. their mean periods range from ∼0.58 to ∼0.62 days (Petroni et al. 2004; Catelan 2009). The lack of Galactic stellar systems with mean periods in the Oosterhoff gap is further supporting the evidence that the Oosterhoff dichotomy is affected by the environment (Coppola et al. 2015; Fiorentino et al. 2015).

We still lack a comprehensive explanation for the above empirical scenario. However, the analysis of this long-standing problem is hampered by several empirical biases.

i) Statistics – The number of GCs with a sizable (more than three dozen) sample of RRLs is limited, 18 out of ≈100 globulars hosting RRLs (Clement et al. 2001). This problem becomes even more severe for ultra faint dwarf galaxies in which the RRL sample never exceeds a dozen (Dall'Ora et al. 2012; Fiorentino et al. 2015).

ii) Completeness – Although, cluster RRLs have been investigated by more than one century (Bailey 1902), the current samples are far from being complete. This limitation applies to objects centrally located and to low amplitude variables. The same problem applies to nearby dwarf galaxies.

iii) Intrinsic properties – There is mounting empirical evidence that old- and intermediate-age stellar populations in nearby dwarf galaxies display different metallicity distributions (Fabrizio et al. 2015). This means that RRLs in dwarf galaxies might be the progeny of stellar populations characterized by a broader age and/or metallicity distribution (Martínez-Vázquez et al. 2015) when compared with cluster RRLs. The same outcome applies to RRLs in ω Centauri, the most massive GGC (Braga et al., these proceedings).

iv) Diagnostics – The Bailey diagram (period vs luminosity amplitude) and the Petersen diagram (period ratio [P_c/P_{ab}] vs fundamental period [P_{ab}]) are solid diagnostics, since they are—together with the period distribution—independent of distance and reddening. To constrain the RRL intrinsic properties, Stetson et al. (2014) and Fiorentino et al. (2015) found that the high amplitude short period (HASP, $P < 0.48$ days, $A_V > 0.75$ mag) variables are not present in dwarf spheroidals, but Sagittarius. Detailed investigation among clusters with sizable sample of RRLs indicate that HASP variables are only present in systems that are more metal–rich than [Fe/H]=−1.5. This finding paves the way to the use

of RRLs to trace the early formation and evolution of the Galactic halo. The period distribution and the Bailey diagram of halo and nearby dwarf galaxy RRLs strongly support the hypothesis that major mergers have been the major players in the halo formation (Fiorentino et al. 2015).

A comprehensive theoretical and empirical analysis of the Petersen diagram clearly indicates that an increase in metal abundance causes a steady decrease in the period ratio of double mode (RRd) pulsators. Interestingly enough, this applies not only to Galactic field, cluster and dwarf galaxy (Magellanic Clouds, Draco, Carina) RRd variables, but also to the bulge RRd variables (Coppola et al. 2015). This evidence further supports the use of the RRd period ratio to constrain the mean metal abundance of old stellar populations. Moreover, accurate mean magnitude and colors soundly indicate that these interesting variables are located in the so-called "OR region", i.e. the region of the instability strip in which variable stars pulsate simultaneously in the fundamental mode and in the first overtone (Bono et al. 1997b). Theoretical arguments dating back to van Albada & Baker (1971, 1973) and more recent developments (Bono & Stellingwerf 1994; Bono et al. 1995, 1997b) indicate that the mode transition in the OR region can explain the Oosterhoff dichotomy (hysteresis mechanism, J. Lub, these proceedings).

To attack the above old open problems and to fully exploit recent findings requires a comprehensive evolutionary and pulsation approach. This means the opportunity to develop a detailed theoretical framework that accounts for both evolutionary and pulsation prescriptions. The approach followed by our group to construct hydrodynamical RR Lyrae pulsation models and to take account of evolutionary prescriptions have already been discussed in a number of previous papers (Bono & Stellingwerf 1994; Bono et al. 1997b, 2001; Marconi & Di Criscienzo 2007; Marconi et al. 2011; Marconi et al., these proceedings].In the following we will focus our attention on their evolutionary properties as a function of the chemical composition. Moreover, we will also address the difference in the evolutionary status when moving from RRLs to Type II Cepheids (TIICs, Bono et al. 1997d) and to Anomalous Cepheids (ACs, Bono et al. 1997d; Fiorentino & Monelli 2012).

2. RR Lyrae stars

Evolutionary properties of the RR Lyrae stars have already been described in many papers (Christy 1966; Iben 1971; Cox 1983; Bono & Stellingwerf 1994). In the following we only mention some key evolutionary properties that are relevant for constraining the difference among RRLs, TIICs and ACs. Note that in dealing with RRLs and TIICs we are assuming that the progenitors are stellar structures approaching the tip of the red giant branch with an age of $\sim$13 Gyrs.

The mass distribution along the Zero-Age Horizontal Branch (ZAHB) is anti-correlated with the effective temperature. This means that hotter HB structures are also characterized by smaller total masses. The decrease in the effective temperature mainly causes the steady increase in the pulsation period when moving from the blue to the red edge of the instability strip. It is also worth mentioning that more metal-rich stellar structures undergo in their off-ZAHB evolution a "blue-hanger", i.e. they attain hotter effective temperatures and

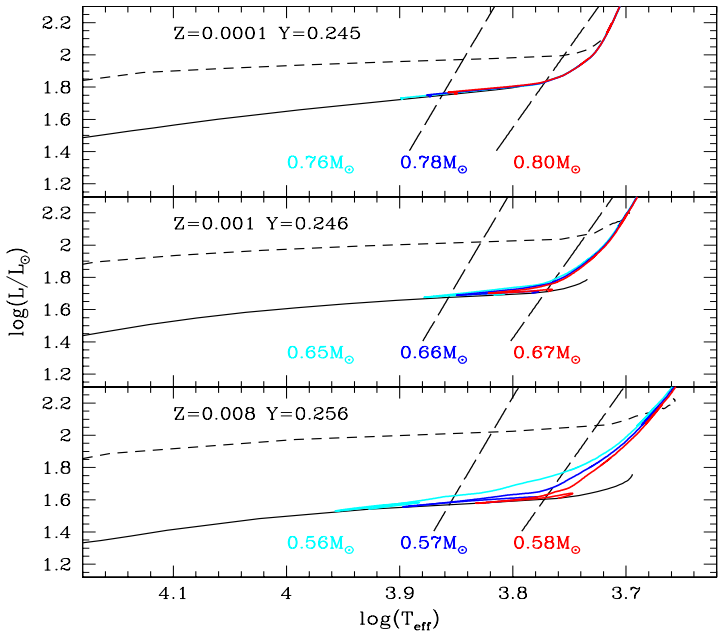

Figure 1. Hertzsprung-Russell diagram of low-mass He burning stellar structures. From top to bottom are plotted theoretical prescriptions for low-mass He burning structures computed (Pietrinferni et al. 2006, see also the BASTI data base: http://basti.oa-teramo.inaf.it/) assuming three different α-enhanced ([α/Fe]=0.4) chemical mixtures (global metallicities, [M/H]=$-$2.27, $-$1.27, $-$0.35). The abundances in mass fraction of both metals (Z) and He (Y) are also labelled. The black solid and dashed lines display the ZAHB and the central He exhaustion. The two almost vertical long-dashed, black lines display the blue (hot) and the red (cool) edge of the RRL instability strip (Marconi et al. 2015). The colored solid lines display HB evolutionary models located inside the RR Lyrae instability strip. The stellar masses are also labelled. Note that the extent toward the blue (blue-hanger) steadily increases when moving from metal-poor to more metal-rich stellar structures.

fainter magnitudes. This "blue-hanger" is the equivalent from the evolutionary point of the "blue loop" experienced by intermediate-mass stars (Bono et al. 2000; Salaris et al. 2008; Prada Moroni et al. 2012; Anderson et al. 2014). Along the blueward evolutionary phases the shell H-burning is more efficient than the core He-burning. On the redward evolution the core He-burning takes over and becomes the main energy source. Note that in spite of these morphological similarities the shell H-burning plays a more fundamental role in intermediate-mass stars than in low-mass stars (Salaris & Cassisi 2008).

In passing, we note that the duration of blue- and redward evolutions play a crucial role in the difference between positive and negative period derivatives. Current theoretical predictions do not match the relative fraction of positive and negative period derivatives observed in OoI and OoII clusters (Kunder et al. 2011; Jurcsik et al. 2012, 2015). The period derivative is a very solid observable to constrain the evolutionary direction. Preliminary evidence indicates that recent homogeneous estimates are significantly less affected by random and

stochastic period changes, thus providing more accurate estimates of secular period changes (Short 2015). The ongoing photometric surveys are providing the accuracy to overcome the long-standing problems in the measurement of these tiny differences. The typical lifetime of an RRL star is, indeed, of the order of 100 Myrs. A more detailed analysis accounting for a wide range of evolutionary and pulsation models is required to properly address this fascinating puzzle.

3. Type II Cepheids

During the last few years Type II Cepheids have been the crossroad of several theoretical and empirical investigations. There is mounting evidence that they do obey optical and NIR period-luminosity relations that are either independent of or minimally affected by metal abundance (Bono et al. 1997c; Di Criscienzo et al. 2007; Matsunaga et al. 2006, 2013; Lemasle et al. 2015). However, their evolutionary status is far from being well established. They typically appear in GCs showing well defined blue HB morphology, this means that the HB is well populated in the so-called blue tail (hot and extreme HB stars). However, they have also been associated to stellar systems in which intermediate-mass stars are also present (LMC, OGLE IV). Thus suggesting that they are the progeny of different evolutionary channels. This working hypothesis is supported by the spectroscopic evidence that some of them are candidate binary systems (Maas et al. 2007; Jurković et al., these proceedings).

The metal-poor HB evolutionary models plotted in Fig. 1 display several interesting features worth being discussed.

The off-ZAHB evolution of low-mass He burning stars shows three different paths. The hottest (lowest total mass, $M/M_{\odot} \leq 0.515$) stellar structures after central He exhaustion become brighter and hotter, they do not experience an asymptotic giant branch (AGB) phase, since their final fate is to evolve into the cooling sequence as a carbon-oxygen (CO) white dwarf (WD, Castellani et al. 2006; Bono et al. 2013; Salaris et al. 2013). These are called AGB-Manqué stellar structures (see the cyan HB evolutionary model in Fig. 2).

More massive HB stellar structures ($0.52 \lesssim M/M_{\odot} \lesssim 0.62$) soon after central He exhaustion evolve toward the red eventually approaching their iso-convective loci, but typically they do not experience a thermal pulsing AGB (TPAGB) phase, since their envelope mass is quite modest (a few hundredths of a solar mass). They climb the AGB and according to the efficiency of the mass loss they will experience a blueward evolution toward their cooling sequence as CO WDs. The red HB evolutionary models plotted in Fig. 2 display three different post-early AGB (PEAGB) stellar structures. Note that these structures cross the instability strip at least twice. The predicted first overtone blue edge (FOBE) and the fundamental red edge (FRE) of the RRL instability strip plotted in Fig. 2 are based on hydrodynamical calculations provided by Marconi et al. (2015). Note that the above boundaries have been extrapolated to brighter luminosities to cover the luminosity range typical of TIICs.

Even more massive stellar structures ($0.62 < M/M_{\odot} \lesssim 0.80$) evolve, after the possible occurrence of the "blue-hanger", toward their iso-convective loci. These stellar structures might have different impact concerning the variable stars. The less massive ones have their ZAHB position bluer than the FOBE, therefore

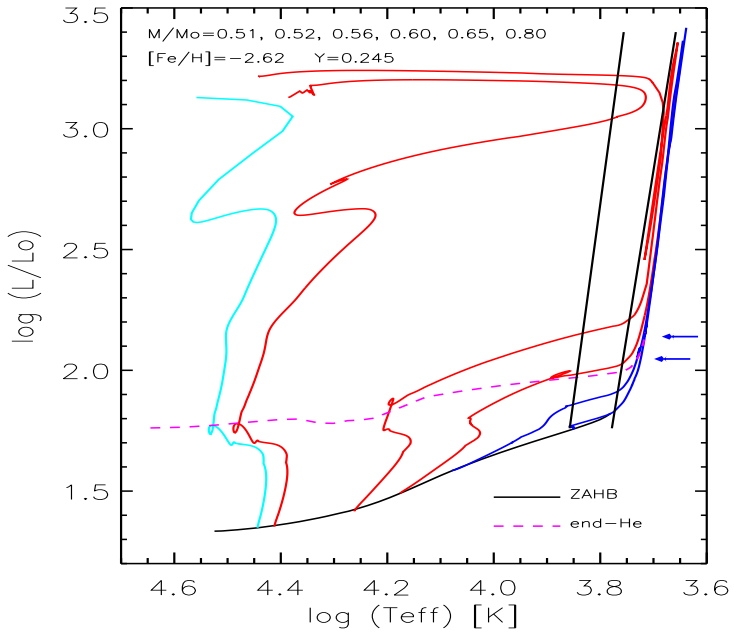

Figure 2. Same as Fig. 1, but only for the most metal-poor chemical composition (see labelled values). The black solid line and the dashed magenta line display the ZAHB and the central He exhaustion. Selected HB evolutionary models are plotted with different colors: cyan, AGB–Manqué; red, PEAGB; blue, TPAGB. The stellar masses are labelled. The almost vertical black lines display the predicted (Marconi et al. 2015) FOBE (hot) and FRE (cool) of the RRL instability strip. The two blue horizontal arrows mark the central He exhaustion for the $M/M_{\odot}$=0.65 (faint) and 0.80 (bright) HB models.

they cross the RRL instability strip, but at luminosities larger than the ZAHB luminosity. The medium mass structures have their ZAHB position inside the instability strip, therefore they are the major contributors in RRLs. The more massive ones have their ZAHB position redder than the FRE, therefore, they typically do not cross the strip in their subsequent evolutionary phases (see also the bottom panel of Fig. 3). These structures evolve along the AGB and after the AGB bump (Salaris 2012) are going to experience a TPAGB phase. The final fate is once again dictated by the efficiency of the mass loss, and in turn by their residual envelope mass.

The above leading physical arguments concerning the final fate of HB stars bring forward interesting astrophysical consequences worth being discussed.

i) RR Lyrae stars. RRL stars are genuine central He-burning stars, since they are the progeny of stellar structures having their ZAHB position inside the instability strip or slightly hotter. Their spread in luminosity is the consequence of their off-ZAHB evolution and of blueward crossings. The range in magnitude covered by RRLs inside the instability strip does depend on the metal abundance (see Fig. 3). This was found ∼30 years ago by Sandage (1981, 1982) and then confirmed by evolutionary calculations (Bono et al. 1995, 1997b).

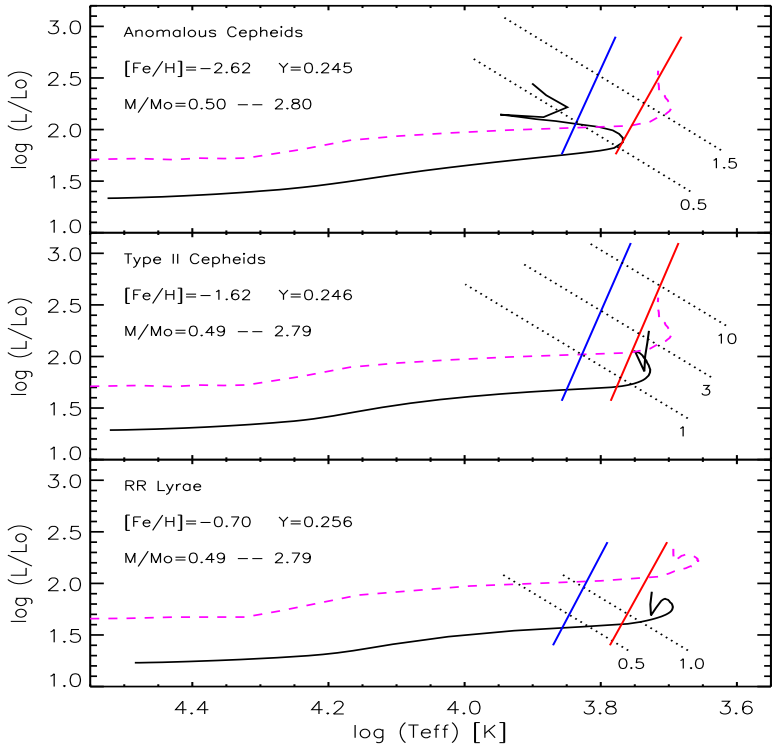

Figure 3. Same as Fig. 1, but for three different groups of pulsators. *Top:* Anomalous Cepheids. The black solid line and the dashed magenta line display the He burning sequence and the central He exhaustion. The chemical compositions and the range in stellar masses covered by the He burning sequence is labelled. The almost vertical blue and red lines display predicted (Marconi et al. 2015) FOBE (hot) and FRE (cool) of the instability strip. The two slant black dotted lines display iso-periodic lines and the periods (days) are also labelled. They were estimated using the pulsation relation for fundamental ACs provided by Fiorentino et al. (2006). *Middle:* Same as the top, but for Type II Cepheids. The iso-periodic lines were estimated using the pulsation relation for fundamental TIICs provided by Di Criscienzo et al. (2007). *Bottom:* Same as the top, but for RR Lyrae stars. The iso-periodic lines were estimated using the pulsation relation for fundamental RRLs provided by Marconi et al. (2015).

ii) Type II Cepheids. TIICs are truly AGB stars. The wiggle performed by PEAGB structures is the equivalent of the AGB-bump, i.e. the beginning of the double shell burning (H and He burning). This means that in spite of the similarity in light curve morphologies and the almost continuous transition between long-period RRLs and short-period TIICs (BL Her) the evolutionary status of the two groups of variable stars is significantly different. A solid argument, at least for cluster variables, to separate them is the difference in luminosity between the lower envelope in the magnitude distribution of RRLs and brighter variables. In passing, we also note that the single evolutionary channel for TIICs would imply the presence of a blue HB morphology. This hypothesis is supported by the fact that dwarf spheroidal galaxies, in which just a limited–if any–number of TIICs have been detected, do not show blue HB morphologies.

The increase in the pulsation period when moving from BL Her to W Vir stars is the consequence of the increase in the luminosity and of the decrease in stellar mass (see the middle panel of Fig. 3). It is worth mentioning that the same structures in their second crossing are also in a different evolutionary phase– post AGB–approaching their WD cooling sequence. They are only supported by the vanishing shell H-burning. The crossing times of the instability strip are roughly 6-7 times shorter than the first crossings (Salaris et al. 2008; Bono et al. 2013). Detailed constraints on the evolutionary status of the RV Tauri stars (Wallerstein 2002; Soszyński et al. 2011), the third subgroup of TIICs, will be addressed in a forthcoming paper.

The evolutionary status of TIIC, was discussed in a series of papers by Gingold (1974, 1976, 1985). The theoretical framework outlined above is relatively similar, but he suggested that blue HB stars after the first crossing of the instability strip experience a "blue nose" (then defined "Gingold's nose") causing two more transits across the instability strip before climbing the AGB. These three crossings could account for the period distribution of BL Herculis variables, while the fourth and final blueward crossing toward the WD cooling sequence could account for W Virginis variables (see also Fig. 2 in Maas et al. 2007). However, recent HB evolutionary models (Lee et al. 1990; Castellani et al. 1991; Dorman et al. 1993; Brown et al. 2001; Pietrinferni et al. 2006; Dotter 2008; VandenBerg et al. 2013) do not show evidence of "Gingold's nose". However, Bono et al. (1997a,b) found evidence that metal-rich stellar structures perform several loops either earlier or during the AGB phase and several of them take place inside the instability strip. The reader interested in a more detailed discussion is referred to the recent investigation by Constantino et al. (2016).

iii) Anomalous Cepheids. The evolutionary status of ACs, has a substantial difference, when compared with the above groups of variable stars. The RRLs are only associated to an old stellar population, the TIICs are mainly associated to an old stellar population, while the ACs are associated to an intermediate-age stellar population (a few Gyrs). Moreover, both RRLs and TIICs cover a broad range in iron abundance ranging from [Fe/H]=−2.5 to super-solar (Maas et al. 2007; For et al. 2011), while the ACs are associated with stellar systems that are more metal-poor than [Fe/H]≈ −1.3 (Fiorentino & Monelli 2012). The difference is mainly caused by the fact that the He-burning sequence does not cross the instability strip for metallicities (scaled solar mixture) larger than $Z = 0.001$ (see Fig. 3 in Fiorentino et al. 2012).

They cover the same region of the HRD covered by TIICs, but their masses are 3-4 times higher. This means that their periods range from a fraction of a day to roughly 2-3 days, while the periods of TIICs range from roughly one day to ≈50 days (see the top and the middle panels of Fig. 3). The above hypothesis concerning the age of the progenitors of ACs is soundly supported by the evidence that only one AC is currently known in a GC (V19 in NGC 5466, Corwin et al. 1999; Szabados et al. 2007). It has also been suggested that they might also be the progeny of blue stragglers (binary hypothesis, McCarthy & Nemec 1997). Finally, let us mention that they are truly core He-burning stellar structures, only partially affected by electron degeneracy (Fiorentino et al. 2012).

4. Discussion and final remarks

The pulsation and evolutionary framework outlined in the above sections are opening the path to several empirical investigations to constrain the evolutionary channel feeding the three groups of variables.

Period derivatives. The period derivative appears as a very promising path not only for RRLs, but also for TIICs and ACs. The evolutionary scenario we outlined in Sect. 2 is suggesting that short-period TIICs should be mainly dominated by positive period derivatives, since they are characterized by a redward evolution. On the other hand, the long-period ones should be characterized by negative period derivatives, since they are evolving blueward in the approach to their WD cooling sequence. The evolutionary scenario for the ACs is more complex, since some of them do perform a sort of loop inside the instability strip. However, the current evolutionary prescriptions suggest that their evolution inside the instability strip is mainly blueward. Therefore, they should be dominated by negative period derivatives. Empirical pieces of evidence are soundly supporting the above theoretical framework, but they are only based on a handful of field (Diethelm 1996; Wallerstein 2002; Templeton 2007) and cluster TIICs (Rabidoux et al. 2010). The period change for ACs has only been investigated for the candidate AC (variable V17) in the very metal-poor GGC M92 (Osborn et al. 2012).

Single vs binary evolution. This is a long-standing problem, since the identification of a variable star in an eclipsing binary system would imply the unique opportunity of a dynamical estimate of the mass. A single RRL has been detected in a binary system, but its mass is significantly smaller than canonical ones, and indeed this new group has also been defined as "impostor variables" (Pietrzyński et al. 2012; Smolec et al. 2013). Several TIICs have been identified in binary systems (Wallerstein 2002; Maas et al. 2007), but their spectroscopic investigation is still in its infancy. In spite of the sizable sample of ACs discovered by OGLE IV in the Magellanic Clouds (Soszyński et al. 2015), the empirical scenario concerning binary identification among ACs is moving towards the first steps (Sipahi et al. 2013a,b).

Evolutionary constraints. Stellar systems hosting different groups of variable stars are fundamental testbenches to constrain their evolutionary properties. However, the above groups of variable stars have simultaneously been identified in massive nearby systems such as the Magellanic Clouds. This means a stellar system with a very complex star formation history and a very broad metallicity distribution that changes as a function of the stellar age. Nearby dwarf spheroidals would be an ideal laboratory, but the current empirical evidence suggests several systems hosting both RRLs and ACs, but we still lack the triplet!

Distance scale. Population II distance indicators (RRL, TIIC) are going to receive special attention from the astronomical community. This is the consequence of the intrinsic accuracy and precision of individual distances based on optical and infrared PL (Braga et al., Neeley et al., J. Lub, these proceedings) and period-Wesenheit (PW) relations. The added value is that theory and observations are suggesting that some of them are independent of metal abundance (Marconi et al. 2015, Martínez-Vázquez et al., these proceedings). The use

of ACs as distance indicators is still an open problem, since we still lack solid observables for their mode identification (Coppola et al. 2015).

It has often been mentioned that the near future promises to be a sort of golden age for stellar astrophysics and resolved stellar populations. This appears a natural consequence of new instruments (HSC and PFS at Subaru; KMOS, MUSE, MOONS at VLT; GEMS at GEMINI; MSE) together with ground-based and space facilities (*JWST, EUCLID, WFIRST*, Extremely Large Telescopes). This opportunity becomes a cornucopia for variability surveys and transient phenomena (LSST, *Gaia, Nano-JASMINE, TESS, CHEOPS, PLATO*).

Acknowledgement

One of us (G.B.) thanks the Japan Society for the Promotion of Science for a research grant (L15518).

References

Anderson, R. I., Ekström, S., Georgy, C., et al. 2014, A&A, 564, A100
Baade, W. 1968, Evolution of Stars and Galaxies. Cambridge, Mass.: Harvard University Press
Bailey, S. I. 1902, Annals of Harvard College Observatory, 38, 1
Bono, G., Caputo, F., Stellingwerf, R. F. 1994, ApJ, 423, 294
Bono, G., Stellingwerf, R. F. 1994, ApJS, 93, 233
Bono, G., Caputo, F., Marconi, M. 1995, AJ, 110, 2365
Bono, G., Caputo, F., Cassisi, S., et al. 1997, ApJ, 483, 811
Bono, G., Caputo, F., Castellani, V., Marconi, M. 1997, A&AS, 121, 327
Bono, G., Caputo, F., Santolamazza, P. 1997, A&A, 317, 171
Bono, G., Caputo, F., Santolamazza, P., et al. 1997, AJ, 113, 2209
Bono, G., Caputo, F., Cassisi, S., et al., A. 2000, ApJ, 543, 955
Bono, G., Caputo, F., Castellani, V., et al. 2001, MNRAS, 326, 1183
Bono, G., Salaris, M., Gilmozzi, R. 2013, A&A, 549, A102
Brown, T. M., Sweigart, A. V., Lanz, T., et al. 2001, ApJ, 562, 368
Castellani, V., Chieffi, A., Pulone, L. 1991, ApJS, 76, 911
Castellani, M., Castellani, V., Prada Moroni, P. G. 2006, A&A, 457, 569
Catelan, M. 2009, Ap&SS, 320, 261
Christy, R. F. 1966, ApJ, 144, 108
Clement, C. M., Muzzin, A., Dufton, Q., et al. 2001, AJ, 122, 2587
Constantino, T., Campbell, S. W., Lattanzio, J. C., van Duijneveldt, A. 2016, MNRAS, 456, 3866
Coppola, G., Stetson, P. B., Marconi, M., et al. 2013, ApJ, 775:6
Coppola, G., Marconi, M., Stetson, P. B., et al. 2015, ApJ, 814:71
Corwin, T. M., Carney, B. W., Nifong, B. G. 1999, AJ, 118, 2875
Cox, A. N., Hodson, S. W., Clancy, S. P. 1983, ApJ, 266, 94
Dall'Ora, M., Kinemuchi, K., Ripepi, V., et al. 2012, ApJ, 752:42
Di Criscienzo, M., Caputo, F., Marconi, M., Cassisi, S. 2007, A&A, 471, 893
Diethelm, R. 1996, A&A, 307, 803
Dorman, B., Rood, R. T., O'Connell, R. W. 1993, ApJ, 419, 596
Dotter, A. 2008, ApJ, 687, L21
Fabrizio, M., Nonino, M., Bono, G., et al. 2015, A&A, 580, A18
Fiorentino, G., Limongi, M., Caputo, F., Marconi, M. 2006, A&A, 460, 155
Fiorentino, G., Monelli, M. 2012, A&A, 540, A102
Fiorentino, G., Stetson, P. B., Monelli, M., et al. 2012, ApJ, 759:L12

Fiorentino, G., Bono, G., Monelli, M., et al. 2015, ApJ, 798:L12
For, B.-Q., Sneden, C., Preston, G. W. 2011, ApJS, 197:29
Gingold, R. A. 1974, ApJ, 193, 177
Gingold, R. A. 1976, ApJ, 204, 116
Gingold, R. A. 1985, MmSAI, 56, 169
Iben, I., Jr. 1971, PASP, 83, 697
Jurcsik, J., Hajdu, G., Szeidl, B., et al. 2012, MNRAS, 419, 2173
Jurcsik, J., Smitola, P., Hajdu, G., et al. 2015, ApJS, 219:25
Kinemuchi, K., Harris, H. C., Smith, H. A., et al. 2008, AJ, 136, 1921
Kunder, A., Walker, A., Stetson, P. B., et al. 2011, AJ, 141:15
Lee, Y.-W., Demarque, P., Zinn, R. 1990, ApJ, 350, 155
Lemasle, B., Kovtyukh, V., Bono, G., et al. 2015, A&A, 579, A47
Maas, T., Giridhar, S., Lambert, D. L. 2007, ApJ, 666, 378
Marconi, M., Di Criscienzo, M. 2007, A&A, 467, 223
Marconi, M., Bono, G., Caputo, F. et al. 2011, ApJ, 738:111
Marconi, M., Coppola, G., Bono, G., et al. 2015, ApJ, 808:50
Martínez-Vázquez, C. E., Monelli, M., Bono, G., et al. 2015, MNRAS, 454, 1509
Matsunaga, N., Fukushi, H., Nakada, Y., et al. 2006, MNRAS, 370, 1979
Matsunaga, N., Feast, M. W., Kawadu, T., et al. 2013, MNRAS, 429, 385
McCarthy, J. K., Nemec, J. M. 1997, ApJ, 482, 203
Miceli, A., Rest, A., Stubbs, C. W., et al. 2008, ApJ, 678, 865
Nemec, J. M., Wehlau, A., Mendes de Oliveira, C. 1988, AJ, 96, 528
Osborn, W., Kopacki, G., Haberstroh, J. 2012, AcA, 62, 377
Petroni, S., Bono, G., Castellani, V, Marconi, M. 2004, in Frontiers of the Universe, Tha Giai Publ., 199
Pietrinferni, A., Cassisi, S., Salaris, M., Castelli, F. 2006, ApJ, 642, 797
Pietrzyński, G., Thompson, I. B., Gieren, W., et al. 2012, Nature, 484, 75
Pojmanski, G. 2002, AcA, 52, 397
Prada Moroni, P. G., Gennaro, M., Bono, G., et al. 2012, ApJ, 749:108
Rabidoux, K., Smith, H. A., Pritzl, B. J., et al. 2010, AJ, 139, 2300
Salaris, M., Cassisi, S. 2008, A&A, 487, 1075
Salaris, M., Cassisi, S., Pietrinferni, A. 2008, ApJ, 678, L25
Salaris, M. 2012, Ap&SS, 341, 65
Salaris, M., Althaus, L. G., García-Berro, E. 2013, A&A, 555, A96
Sandage, A. 1981, ApJ, 248, 161
Sandage, A. 1982, ApJ, 252, 553
Sesar, B., Ivezić, Ž., Stuart, J. S., et al. 2013, AJ, 146:21
Short, L. A. 2015, Master Thesis, Tor Vergata University, Roma
Sipahi, E., Ibanoglu, C., Cakirli, O., Evren, S. 2013a, MNRAS, 429, 757
Sipahi, E., Ibanoglu, C., Cakirli, O., et al. 2013b, RMxAA, 49, 239
Smolec, R., Pietrzyński, G., Graczyk, D., et al. 2013, MNRAS, 428, 3034
Soszyński, I., Udalski, A., Pietrukowicz, P., et al. 2011, AcA, 61, 285
Soszyński, I., Udalski, A., Szymański, M. K., et al. 2015, AcA, 65, 233
Stetson, P. B., Fiorentino, G., Bono, G., et al. 2014, PASP, 126, 616
Szabados, L., Kiss, L. L., Derekas, A. 2007, A&A, 461, 613
Templeton, M. R., Henden, A. A. 2007, AJ, 134, 1999
van Albada, T. S., Baker, N. 1971, ApJ, 169, 311
van Albada, T. S., Baker, N. 1973, ApJ, 185, 477
VandenBerg, D. A., Brogaard, K., Leaman, R., Casagrande, L. 2013, ApJ, 775:134
Wallerstein, G. 2002, PASP, 114, 689

RRL2015 – High-Precision Studies of RR Lyrae Stars
L. Szabados, R. Szabó, K. Kinemuchi (Eds.) 2016

Multiple populations in globular clusters and the origin of the Oosterhoff dichotomy

Sohee Jang & Young-Wook Lee

Center for Galaxy Evolution Research and Department of Astronomy, Yonsei University, Seoul 120-749, Korea

Abstract. The globular cluster community is now facing a new paradigm of multiple stellar populations. In light of this, we have recently proposed a new model to explain the origin of the difference in mean period of type ab RR Lyrae variables between the two Oosterhoff groups. In our model, the instability strip in the metal-poor group II clusters, such as M15, is populated by second-generation stars (G2) with mildly enhanced helium and CNO abundances, while the RR Lyraes in the relatively metal-rich group I clusters such as M3 are produced mostly by first-generation stars (G1) without these enhancements. When these models are extended to all metallicity regimes, the observed dichotomies in the inner and outer halo globular clusters can be naturally reproduced. We found that specific star formation histories are required for the inner and outer halos, which is consistent with the dual origin of the Milky Way halo.

1. Population-shift within the instability strip

The Oosterhoff dichotomy is one of the long-standing problems in modern astronomy. Understanding this phenomenon is intimately related to the Population II distance scale and the formation of the Milky Way halo. Therefore, numerous investigations have been made as to the origin of the Oosterhoff dichotomy. However, a complete understanding of the Oosterhoff dichotomy still requires a more natural solution.

In the multiple population paradigm, we have recently reproduced observed Oosterhoff dichotomy both for the inner and outer halo globular clusters (GCs) (Jang et al. 2014; Jang & Lee 2015). Here we review the most important results from these investigations. In our modeling, first, we have constructed models for M15, which is historically at the heart of the Oosterhoff dichotomy. The photometry of M15 shows three distinct subgroups on the horizontal branch (HB): RR Lyraes, the blue HB, and the blue tail (Buonanno et al. 1985). We assume that they were originated from three distinct subpopulations G1, G2 and G3 (third generation stars) in this GC. At the metallicity and age of M15, we found that G1 is placed on the normal blue HB. For the G2, we assume that they are mildly enhanced in He and CNO ($\Delta Y = 0.015$, $\Delta Z_{\rm CNO} = 0.00026$), and at the same time 1.1 Gyr younger. There are some theoretical and observational support for this assumption, such as theories for AGB stars and spectroscopy (Karakas 2010; Gratton et al. 2012; Marino et al. 2014). These helium and CNO enhancements play a role in increasing the period of RR Lyrae variables. For the blue tail, we assign super helium-rich G3 (Y = 0.30 - 0.33) as their progenitor.

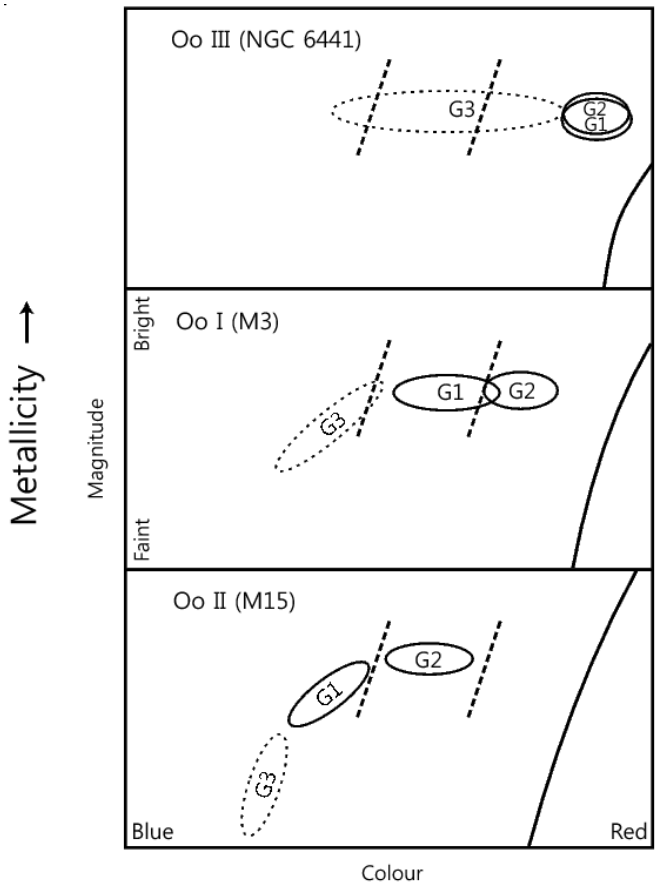

Figure 1. Schematic diagram illustrating the "population shift" within the instability strip (thick dashed lines) with increasing metallicity. In our models, most of the RR Lyraes are produced by G1, G2 (mildly enhanced in helium & CNO abundances), and G3 (most helium-rich), respectively, for the Oosterhoff groups I, II, and III (adapted from Figure 4 of Jang et al. 2014).

When the metallicity is increased from [Fe/H]=~ -2.2 (for M15) to -1.7 (for M3), the HB morphology is shifted to a redder color, and produces a morphology very similar to that for M3. As illustrated in Figure 1, G1, that was on the blue horizontal branch in M15, is now placed within the instability strip (IS) in M3, producing RR Lyrae variables. The G2, that was in the IS in M15 is now shifted to red HB. When the metallicity is increased further to -0.7, our models produces the HB morphology that is similar to the case of NGC 6441. In this case, super helium rich G3 is placed in the IS, producing RR Lyraes with the longest period. This population shift within the IS can naturally reproduce the observed period shift between GCs.

2. Reproducing the Oosterhoff dichotomy

As shown in Jang & Lee (2015), when our models are extended to all metallicity regimes, our models can reproduce the observed Oosterhoff dichotomy both for

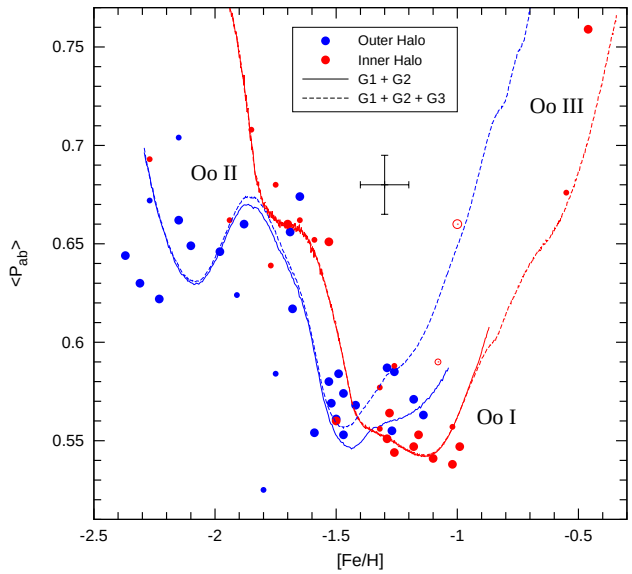

Figure 2. Comparison of the inner and outer halo GCs with our models in the $\langle P_{\rm ab}\rangle$ versus [Fe/H] diagram. The best matches are obtained when Δt(G1 − G2) = 1.4 Gyr for the outer halo, and Δt(G1 − G2) = 0.5 Gyr for the inner halo. $\langle P_{\rm ab}\rangle$ is in days (adapted from Figure 11 of Jang & Lee 2015).

the inner and outer halo GCs. In order to achieve this, however, we found that specific star formation histories are required for the inner and outer halos. In the inner halo GCs, the star formation commenced and ceased earlier with a smaller age difference between G1 and G2, while in the outer halo, the formation of G1 was delayed by ∼0.8 Gyr with a more extended time scale between G1 and G2 (∼1.4 Gyr). This is consistent with the dual origin of the Milky Way halo. Interestingly, in the Milky Way bulge, our models can also reproduce two populations of RR Lyrae stars recently discovered from OGLE survey (Pietrukowicz et al. 2015). Our models can reproduce this observation by a small difference in helium abundance ($\Delta Y \approx 0.01$) between G1 and G2 (Lee & Jang 2016, in preparation).

References

Buonanno, R., Corsi, C. E., Fusi Pecci, F. 1985, A&A, 145, 97
Gratton, R. G., Carretta, E., Bragaglia, A. 2012, A&A Rev., 20, 50
Jang, S., Lee, Y.-W., Joo, S.-J., Na, C. 2014, MNRAS, 443, L15
Jang, S., Lee, Y.-W. 2015, ApJS, 218:31
Karakas, A. I. 2010, MNRAS, 403, 1413
Lee, Y.-W., Jang, S. 2016, in preparation
Marino, A. F., Milone, A. P., Przybilla, N., et al. 2014, MNRAS, 437, 1609
Pietrukowicz P., Kozlowski, S., Skowron, J., et al. 2015, ApJ, 811:113

RRL2015 – High-Precision Studies of RR Lyrae Stars
L. Szabados, R. Szabó, K. Kinemuchi (Eds.) 2016

RR Lyrae stars in the Andromeda satellite galaxies

Felice Cusano[1], Alessia Garofalo[1,2], & Gisella Clementini[1]

[1]*INAF-Osservatorio Astronomico di Bologna, via Ranzani 1, 40127, Bologna, Italy*
[2]*Dipartimento di Fisica e Astronomia-Universitá di Bologna, Viale Berti Pichat 6/2, I-40127 Bologna, Italy*

Abstract. In this contribution we summarize results on the search for variable stars and the study of the resolved stellar populations in four dwarf spheroidal satellites of the Andromeda galaxy that we have observed with the Large Binocular Cameras (LBC) at the Large Binocular Telescope (LBT).

1. Introduction

In the context of the Λ-CMD theory massive galaxies like the Milky Way (MW) and Andromeda (M31) form by accretion and merging of smaller structures (e.g. Bullock & Johnston 2005). Candidates to be the possible residual building blocks of this accretion process are the satellite galaxies observed nowadays around the MW and M31. However, some issues challenge this scenario, like, for instance, the missing satellite problem (Moore et al. 1999) or the observed alignment of a large fraction of the satellite galaxies in planar structures (see e.g. Ibata et al. 2013). In this framework, we have obtained multi-band photometric observations with the Large Binocular Cameras (LBC) at the Large Binocular Telescope (LBT) of a sample of M31 satellites (see Cusano et al. 2013) to characterize both their variable and constant star populations. The final aim of our survey is to derive hints on the formation history of the M31's satellites and relate it to the global context of merging and accretion episodes occurring in M31.

2. Observations and data reduction

Time series photometry in the B and V bands was obtained with the LBC at the foci of the LBT for four M31 satellites, namely, And XIX (Cusano et al. 2013), And XXI (Cusano et al. 2015), And XXV (Cusano et al. 2016) and And XXVII (Cusano et al., in preparation). Observations in the B band were obtained with the Blue camera of the LBC, whereas the V images were acquired with the Red camera. PSF photometry of the pre-reduced images was performed using the `DAOPHOT-ALLSTAR-ALLFRAME` package (Stetson 1987, 1994). Variable stars were identified using the variability index computed in `DAOMASTER` (Stetson 1994), then the light curves of the candidate variables were analyzed with the Graphical Analyzer of Time Series (GRATIS), custom software developed at the Bologna Observatory (see e.g. Clementini et al. 2000). Examples of light curves for two RR Lyrae stars (a fundamental-mode − RRab and a first-overtone −

RRc) and an Anomalous Cepheid (AC) that we detected in And XXV are shown in Figure 1.

Table 1. Summary of number and properties of the variable stars identified in M31 satellite galaxies

Name	N (RRab+RRc)	$\langle P_{\rm ab} \rangle$	N(AC)	$E(B-V)$	$(m-M)_0$	GpoS member	Ref
And I	72+26	0.57	1?	0.05 ± 0.01	24.49 ± 0.06	yes	1
And II	64+8	0.57	1	0.06 ± 0.01	24.11 ± 0.06	no	2
And III	39+12	0.66	4	0.05 ± 0.01	24.38 ± 0.06	yes	1
And VI	91+20	0.59	6	0.06 ± 0.01	24.55 ± 0.07	no	3
And XI	10+5	0.62	0	0.11	24.33 ± 0.05	yes	4
And XIII	12+5	0.66	0	0.15	24.62 ± 0.05	yes	4
And XIX	23+8	0.62	8	0.11 ± 0.06	24.52 ± 0.23	no	5
And XXI	37+4	0.63	9	0.15 ± 0.04	24.40 ± 0.17	no	6
And XXV	41+11	0.60	1	0.06 ± 0.04	24.62 ± 0.16	yes	7
And XXVII	55+36	0.59	1	0.09 ± 0.05	24.57 ± 0.25	yes	8

[1] Pritzl et al. (2005); [2] Pritzl et al. (2004); [3] Pritzl et al. (2002);
[4] Yang & Sarajedini (2012); [5] Cusano et al. (2013); [6] Cusano et al. (2015);
[7] Cusano et al. (2016); [8] Cusano et al., in preparation

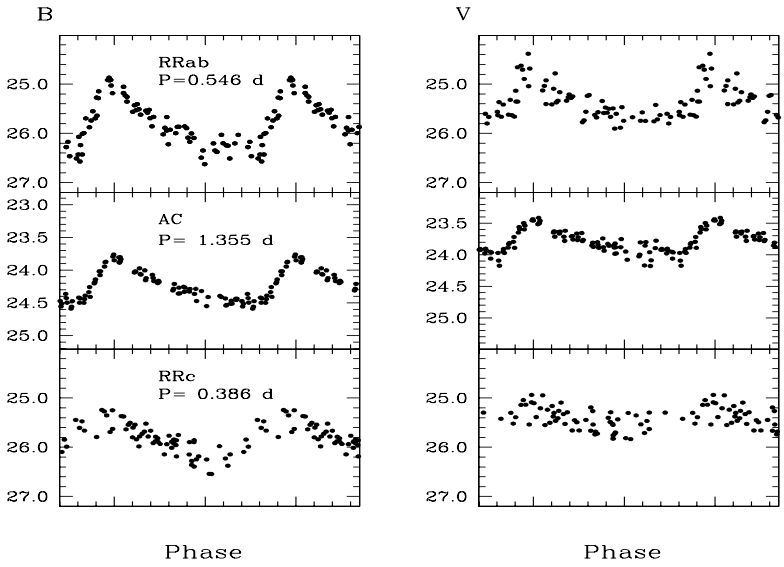

Figure 1. Light curves of a fundamental-mode (upper panel) and first-overtone (lower panel) RR Lyrae stars and of an AC (middle panel) in And XXV; *left:* in B band, *right:* in V band.

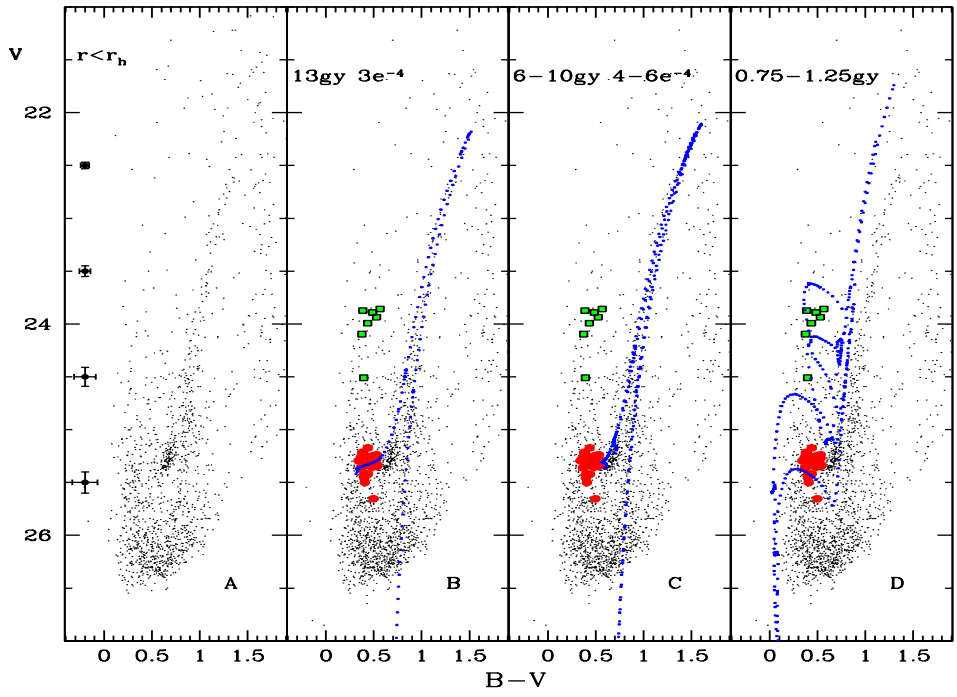

Figure 2. CMD and stellar populations in And XIX. *Panel A*: CMD of the objects in half light radius of the galaxy. *Panel B*: same as *panel A*, but the red filled circles are RR Lyrae stars, while the green filled squares are ACs. The blue dashed line is the isochrone at 13 Gyr and $Z = 0.0003$. *Panel C*: isochrones at 6 and 10 Gyr with $Z = 0.0004$. *Panel D*: isochrones at 0.75 and 1.25 Gyr with $Z = 0.0004$. The isochrones are from Bressan et al. (2012).

3. Results and conclusions

We discovered a total of 215 RR Lyrae stars and 19 Anomalous Cepheids (ACs) in the four M31 satellite galaxies observed with our program. The number and type of variable stars found in each galaxy are summarized in the last four rows of Table 1, whereas the six upper rows report the census and properties of the variable stars detected in other M31 satellite galaxies analysed so far for variability. In particular, the average period of the fundamental-mode RR Lyrae stars ($\langle P_{\rm ab} \rangle$) is given in column 3.

The M31 satellite galaxies that we have observed with the LBT can be classified as Oosterhoff Intermediate (Oo-Int) systems (see Oosterhoff 1939; Catelan 2009, for a description of the different Oosterhoff types). A comparison of the $\langle P_{\rm ab} \rangle$ values reported in Table 1, shows that the majority of the M31 satellites have Oo-Int properties, with only And III and And XIII being Oosterhoff type II (Oo II) systems. In column 7 of Table 1 we report also the membership of each galaxy to the Great plane of satellites (GpoS) discovered by Ibata et al.

(2013). The average period of the RRab stars for galaxies on and off the plane is $\langle P_{\rm ab}\rangle = 0.62 \pm 0.07$ d and $\langle P_{\rm ab}\rangle = 0.60 \pm 0.06$ d, respectively. Both populations are thus compatible with an Oo-Int classification. The number of ACs instead differs significantly among satellites and galaxies on the GpoS have very few ACs when compared to the galaxies off the plane.

Using the RR Lyrae stars we also derived independent estimates of the reddening and distance to the galaxies investigated by us. These values are summarized in columns 5 and 6 of Table 1, respectively.

Besides identifying the variable stars we also built colour-magnitude diagrams (CMDs) to characterize the stellar populations of these four satellite galaxies. We found evidence for three different stellar generations in And XIX and And XXI (see Fig. 2) and of a single old star formation burst in And XXV and And XXVII. We note that And XIX and And XXI do not belong to Ibata et al.'s GpoS, while And XXV and And XXVII lie on it. This and the different number of ACs led us to speculate on whether there might be a connection between star formation complexity/simplicity and GpoS membership.

The large field of view of the LBC allowed to accommodate in just one pointing the half light radius of each of the four galaxies we have observed with the LBT and thus study the spatial distribution of the different stellar components in each galaxy. The location of the RR Lyrae stars along with the isodensity contours of stars in selected regions of the CMD helped us to trace signatures of past and/or ongoing gravitational interactions with M31 or other dwarf galaxies. In particular, we found evidence for And XXI to be the result of a past minor merger between two dwarf galaxies.

References

Bressan, A., Marigo, P., Girardi, L., et al. 2012, MNRAS, 427, 127
Bullock, J. S., Johnston, K. V. 2005, ApJ, 635, 931
Catelan, M. 2009, Ap&SS, 320, 261
Clementini, G., Di Tomaso, S., Di Fabrizio, L., et al. 2000, AJ, 120, 2054
Cusano, F., Clementini, G., Garofalo, A., et al. 2013, ApJ, 779, 7
Cusano, F., Garofalo, A., Clementini, G., et al. 2015, ApJ, 806, 200
Cusano, F., Garofalo, A., Clementini, G., et al. 2016, submitted to ApJ
Ibata, R. A., Lewis, G. F., Conn, A. R., et al. 2013, Nature, 493, 62
Moore, B., Ghigna, S., Governato, F., et al. 1999, ApJ, 524, L19
Oosterhoff, P. T. 1939, The Observatory, 62, 104
Pritzl, B. J., Armandroff, T. E., Jacoby, G. H., et al. 2002, AJ, 124, 1464
Pritzl, B. J., Armandroff, T. E., Jacoby, G. H., et al. 2004, AJ, 127, 318
Pritzl, B. J., Armandroff, T. E., Jacoby, G. H., et al. 2005, AJ, 129, 2232
Stetson, P. B. 1987, PASP, 99, 191
Stetson, P. B. 1994, PASP, 106, 250
Yang, S.-C., Sarajedini, A. 2012, MNRAS, 419, 1362

RRL2015 – High-Precision Studies of RR Lyrae Stars
L. Szabados, R. Szabó, K. Kinemuchi (Eds.) 2016

A comprehensive photometric study of the RR Lyrae variables of the globular cluster M3

Johanna Jurcsik & Péter Smitola

Konkoly Observatory, Research Centre for Astronomy and Earth Sciences, Hungarian Academy of Sciences, H-1121, Budapest, Konkoly Thege Miklós út 15-17, Hungary

Abstract. A new, extended CCD photometry of the variables in M3 is analyzed. The light-curve coverage and the accuracy of the data make it possible to detect small-amplitude signals in the Fourier spectra, and to determine the modulation properties of most of the Blazhko stars. This is the first photometric survey of a homogeneous sample (metallicity, distance) of RR Lyrae stars, which yields accurate parameters of a large population of Blazhko stars, thus making the comparison of Blazhko and non-Blazhko stars of similar parameters possible.

1. Introduction

The observations were obtained with the 60/90 Schmidt telescope of the Konkoly Observatory (Jurcsik et al. 2014). About 1000 measurements were obtained in each of the $B, V, I_{\rm C}$ colours between January and July 2012. Standard photometric data of 147 variables, and flux time-series of other 65 stars from the most crowded regions have been derived. The intensity-averaged mean V magnitudes and B amplitudes of the variables are shown in Fig. 1.

About half of the variables are multiperiodic: 10 RRd, 89 Blazhko stars and 18 $\rm RR_{0.61}$ stars (RRc stars showing a frequency component at $f_{\rm 1O}/f_{\rm x} = 0.61$ frequency ratio) are detected.

2. Most important results on RRc/RRd stars

The results on overtone and double-mode stars were published in Jurcsik et al. (2014, 2015). The special properties of Galactic bulge RRc/RRd stars, revealed by the data of the OGLE IV project (Smolec et al. 2015; Netzel et al. 2015), are in accordance with most of our findings. However, the M3 data show some unique features as well.

The 18 $\rm RR_{0.61}$ stars occupy special regions in the P (period)–brightness, P–amplitude and P–colour diagrams of M3. No $\rm RR_{0.61}$ star is detected at shorter periods, i.e., at hotter temperatures. The light curves of $\rm RR_{0.61}$ stars are more sinusoidal than the light curves of normal RRc stars.

It was first proposed by Clementini et al. (2004) that the Blazhko effect might be the explanation for the peculiarities of some RRd stars in M3. The 2012 data show that, indeed, both radial modes of the anomalous period-ratio RRd stars are Blazhko modulated. The modulation properties of V13 are similar to those of Blazhko double-mode Cepheids (Moskalik & Kołaczkowski 2009), namely, the fundamental and overtone modes are modulated with the same period, and their amplitude- and phase-modulations are anti-correlated. On the contrary, no connection between the modulations of the modes are found in the other

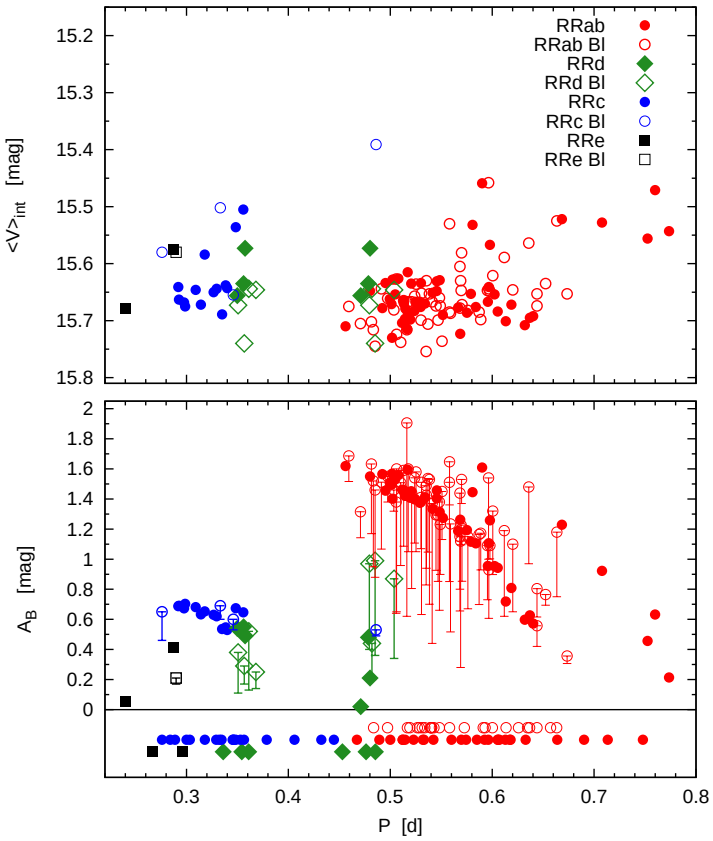

Figure 1. Intensity-averaged mean V magnitudes and B amplitudes of the RR Lyrae stars in M3. The period distribution of variables with uncertain magnitude calibration is indicated in the bottom of the figure.

Blazhko RRd stars (V44, V99, and V166). Large period shifts ($0.010 - 0.015$ d) of the fundamental-mode are detected in some Blazhko RRd stars, which are connected to changes in the modal content of the pulsation.

3. Some special stars

The light curves of some interesting stars are shown in the *a*-*d* panels of Fig. 2.
a) The Blazhko cycle of V144 is longer than 25 years. Its light curve is stable within an observing season.
b) V123, an RRab star with an anomalous light-curve shape, was discussed in Jurcsik et al. (2013). There are two non-Blazhko RRab stars (V123 and V215) with similar, peculiar-shape light curves (shown in panel *b* of Fig. 2) in the total sample of 160 fundamental-mode variables of M3. These light curves look like the mean light curve of a strongly amplitude- and phase-modulated Blazhko star. The mean light curve of the Blazhko RRab star, V119, and of a normal RRab star, V9, are also shown for comparison in panel *b* of Fig. 2.
c) The light-curve modulation of V28 is nearly pure phase modulation. The pulsation amplitudes at the smallest and largest phase offsets differ only slightly.

Its amplitude is smaller than normal by $0.2-0.3$ mag (in V) and the light-curve shape is distorted at any Blazhko phases. Most probably, the phase modulation of the Blazhko effect are always combined with changes of the amplitude and of the light-curve shape. Therefore, phase modulation cannot mimic the light-time effect (as proposed in Guggenberger & Steixner 2015). They are distinguishable if good quality full light curves are available.

d) V119 had been a normal, stable RRab star prior to 2009 (shown by blue line in panel *d* of Fig. 2). The 2009 (Jurcsik et al. 2012) and 2012 data show strong Blazhko modulation. The amplitude is larger than the amplitude of the non-modulated data at the largest-amplitude phase of the modulation. The shapes of the modulated and non-modulated light curves are different around minimum light and at the beginning of the rising branch when their amplitudes equal.

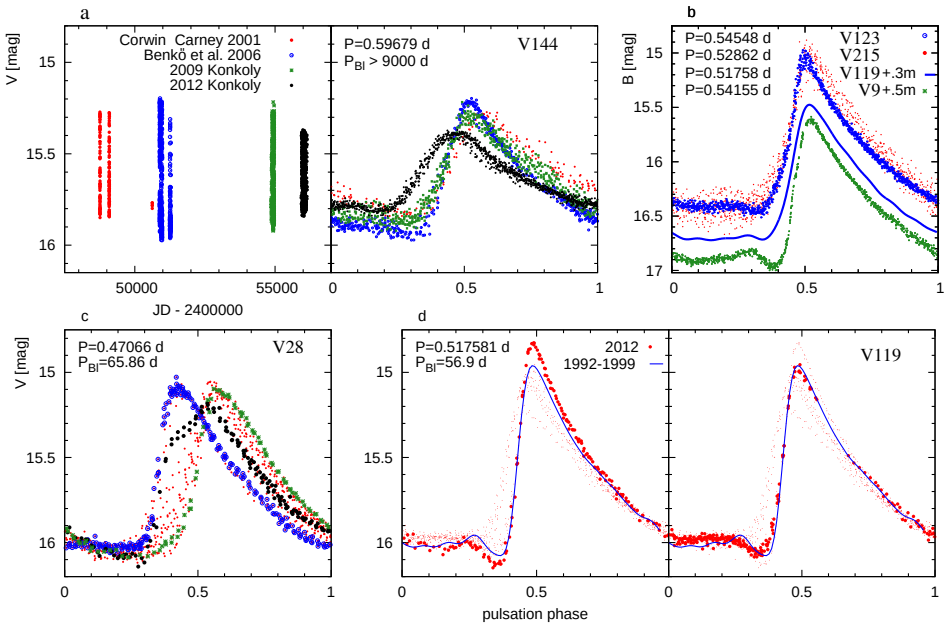

Figure 2. Light curves of some special RRab stars in M3.

4. The Blazhko effect

The Blazhko statistics of fundamental- and double-mode variables are 47% and 45%. This is in high contrast with the 11% Blazhko rate of the overtones. The Blazhko percentage of the Oosterhoff type II overtones is, however, 50% again. It seems that the Blazhko effect is rare or missing exclusively in OoI type overtones of M3, i.e., among the hottest, smallest-mass, not-evolved variables.

The amplitude at around Blazhko maximum is the same as the amplitude of a counterpart, stable RRab star (similar period, brightness and colour) for most of the Blazhko stars. However, the maximum amplitude is larger or smaller than normal in $10-20$% of the Blazhko stars.

No differences have been found between the physical parameters ($L, T_{\rm eff}, R$, derived using the Inverse Photometric Method, Sódor et al. 2008) of Blazhko and non-Blazhko stars.

Pure amplitude modulation is not detected in RRc and RRd stars and it is rare in short-period RRab stars (Fig. 3, left panel). In contrast, each OoII type Blazhko RRab star shows amplitude modulation with no or marginal sign of phase variation. Strong phase modulation characterizes Blazhko RRc stars, the overtone mode of Blazhko RRd stars, and about half of Blazhko RRab stars close to their zero-age horizontal-branch position.

The most frequent Blazhko period value is at around 50 d, but secondary peaks might also be suspected at around 25, 100 and 150 d in the histogram of the Blazhko periods (Fig. 3, right panel). These secondary peaks might be 'alias' signals, as a result of that, from time to time, different components of the multiplet frequencies appearing in the Fourier spectra of Blazhko stars may become dominant (Jurcsik et al. 2011).

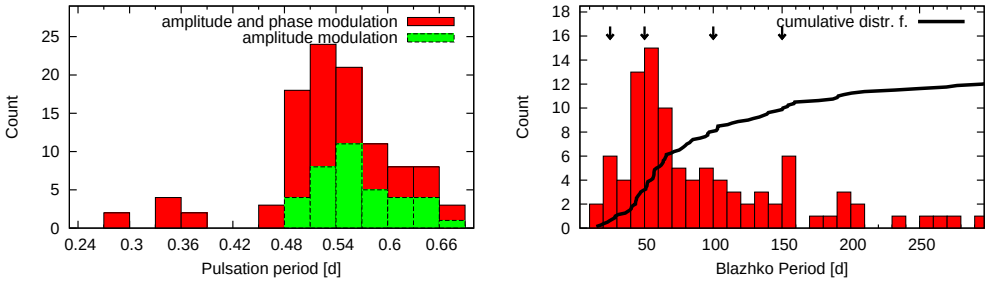

Figure 3. *Left panel:* Period distribution of the Blazhko stars. *Right panel:* Histogram of the Blazhko periods.

Acknowledgments

The first photographic exposure of M3 at Konkoly Observatory was taken in 1938, in the year when Béla Szeidl (1938-2013) was born. He published a comprehensive study of the period changes of RR Lyrae stars of M3 fifty years ago (Szeidl 1965). His impact on the variable-star studies at the Konkoly Observatory is invaluable. This contribution is dedicated to the memory of Béla. JJ would like to thank the organizers for making possible her participation in the meeting.

References

Benkő, J., Bakos, G., Nuspl, J. 2006, MNRAS, 372, 1657
Clementini, G., Corwin, T. M., Carney, B. W., et al. 2004, AJ, 127, 938
Corwin, T. M., Carney, B. W. 2001, AJ, 122, 3183
Guggenberger, E., Steixner, J. 2015, EPJ Web of Conferences, Vol. 101, 06030
Jurcsik, J., Szeidl, B., Clement, C., et al. 2011, MNRAS, 411, 1763
Jurcsik, J., Hajdu, G., Szeidl, B., et al. 2012, MNRAS, 419, 2173
Jurcsik, J., Smitola, P., Hajdu, G., et al. 2013, ApJL, 776:L1
Jurcsik, J., Smitola, P., Hajdu, G., et al. 2014, ApJL, 797:L3
Jurcsik, J., Smitola, P., Hajdu, G., et al. 2015, ApJS, 219:25
Moskalik, P., Kołaczkowski, Z. 2009, MNRAS, 394, 1649
Netzel, H., Smolec, R., Moskalik, P. 2015, MNRAS, 453, 2022
Smolec, R., Soszyński, I., Udalski, A., et al. 2015, MNRAS, 447, 3756
Sódor, Á., Jurcsik, J., Szeidl, B. 2008, MNRAS, 394, 261
Szeidl, B. 1965, Comm. Konkoly Obs., Budapest, No. 58

RRL2015 – High-Precision Studies of RR Lyrae Stars
L. Szabados, R. Szabó, K. Kinemuchi (Eds.) 2016

On the RR Lyrae stars in ω Centauri

V. F. Braga[1], P. B. Stetson[2], G. Bono[1], M. Dall'Ora[3], L. M. Freyhammer[4], I. Ferraro[5], G. Iannicola[5], J. Lub[6], N. Matsunaga[7], J. Neeley[8], & M. Marengo[8]

[1]*Department of Physics, University Tor Vergata, Rome, Italy*
[2]*Dominion Astrophysical Observatory, Victoria, Canada*
[3]*INAF–Osservatorio Astronomico di Capodimonte, Naples, Italy*
[4]*Royal Observatory of Belgium, Brussels, Belgium*
[5]*INAF–Osservatorio Astronomico di Roma, Monte Porzio Catone, Italy*
[6]*Sterrewacht Leiden, Leiden University, Leiden, the Netherlands*
[7]*Institute of Astronomy, University of Tokyo, Tokyo, Japan*
[8]*Iowa State University, Ames, IA, USA*

Abstract. We present new optical ($UBVRI$) photometry of RR Lyrae (RRL) stars in ω Centauri. The images were mainly collected with ESO/Danish 1.54 m telescope, plus various other 1–8 m class telescopes. The data set spans an area of $\approx$20×20 arcmin across the cluster center and a time interval of 21 years. We provide new homogeneous estimates of RRL pulsation properties (periods, mean magnitudes, amplitudes, epochs) and new distance determination. Using the metal-independent $V, B-I$ period-Wesenheit relation we find a distance modulus of 13.70±0.01±0.09 mag. Finally, we also provide new constraints on the metallicity distribution of RRL stars using the I-band period-luminosity-metallicity relation.

1. Empirical scenario

The Galactic globular cluster (GGC) ω Centauri is at the crossroads of several open astrophysical problems. It is the most massive GGC (D'Souza & Rix 2013) and shows a well defined spread in iron abundance (Johnson & Pilachowski 2010), in α-elements and in s- and r-process elements (Johnson et al. 2009). These are the reasons why ω Cen might also be the core of a pristine dwarf galaxy (Zinnecker et al. 1988; Freeman 1993; Bekki & Freeman 2003).

The detailed first investigation of RRLs in ω Cen was performed more than one century ago by Bailey (1902). A detailed and almost complete census, based on CCD photometry, came with the OGLE project (Kaluzny et al. 1997, 2004). More recently, optical (Weldrake et al. 2007) and NIR analyses were performed by Del Principe et al. (2006) using time series data collected with SOFI at NTT and by Navarrete et al. (2015) using images collected with VISTA.

We collected ∼7600 CCD images that had been taken over 21 years, and performed PSF photometry with the DAOPHOT/DAOMASTER/ALLFRAME suite of programs. We ended up with an astrometric catalog including more than 700,000 stars covering a sky area of $40' \times 40'$. The absolute calibration was performed using 4,180 local standards and was applied to ∼584,000 stars

with calibrated photometry in BVI and ∼202,000 in $UBVRI$. The calibrated photometry covers an area of $\sim 20' \times 20'$.

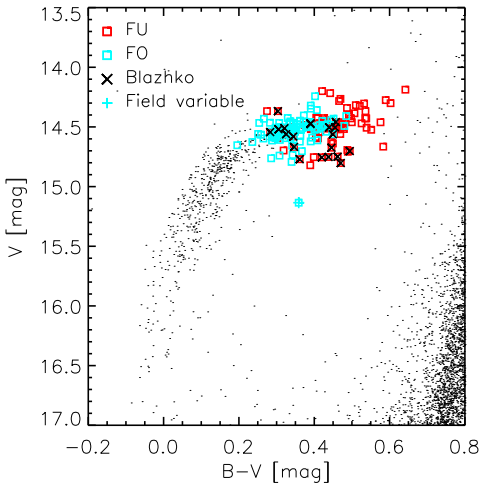

Figure 1. $V, B-V$ CMD of ω Cen, zoomed on the horizontal branch. Fundamental (FU) and first overtone (FO) RRLs appear as red and cyan squares; crosses represent candidate Blazhko stars, while pluses are for field variables.

2. RR Lyrae stars

We provide new calibrated photometry for 176 RRLs, plus new Walraven $VBLUW$ photometry, performed by J. Lub in 1980-81 for two external RRLs. We also collected optical photometry available in the literature (Sturch 1978; Kaluzny et al. 1997; Weldrake et al. 2007; Drake et al. 2009; Torrealba et al. 2015) for nine RRLs. This means that we can provide homogeneous pulsation properties for 187 RRLs. Figure 1 shows their distribution in the $V, B-V$ color-magnitude diagram (CMD).

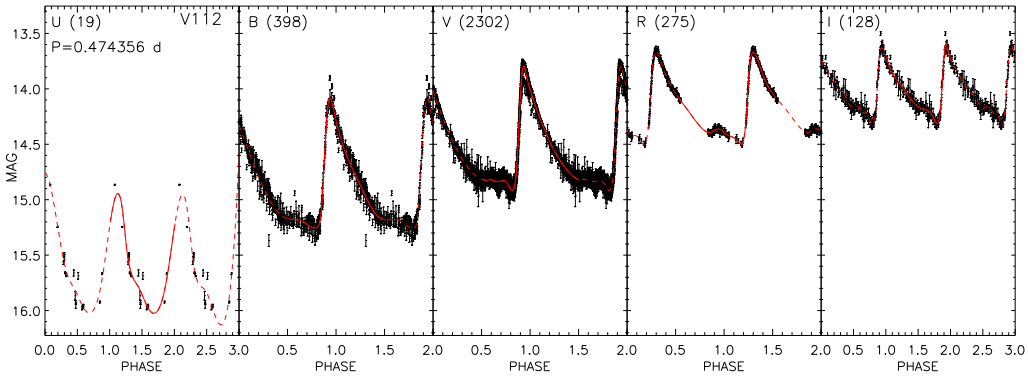

Figure 2. $UBVRI$ light curves of the fundamental-mode pulsator RRL V112. Red lines are the spline fits adopted to calculate their pulsation properties. The numbers of phase points are in parentheses. The periods are also indicated.

The RRL periods were determined using a modified Lomb-Scargle method and they typically agree, within 0.001 d, with literature estimates (Clement et al. 2001, updated 2015, and references therein). We also confirm the pulsation modes of all the RRLs in our sample. We have supplemented this sample with periods from literature, ending up with periods for 192 RRLs. Among them, 187 are candidate cluster variables, in particular 87 fundamental (FU) and 100 first overtone (FO) variables. The fraction of FOs ($N_c/N_{tot} = 0.53$) and the mean period of FUs ($\langle P_{ab} \rangle = 0.66$ days) support the Oosterhoff II classification suggested by Clement & Rowe (2000) and Navarrete et al. (2015).

To derive the mean magnitudes, we have fitted the phased light curves with splines and calculated intensity averages. The same splines have been used to evaluate amplitudes and the epochs of maximum and minimum. Figure 2 shows the optical light curves of the FU RRL V112. The vertical bars represent the measurement uncertainties.

3. Empirical *PL* and *PW* relations, distance and metallicities

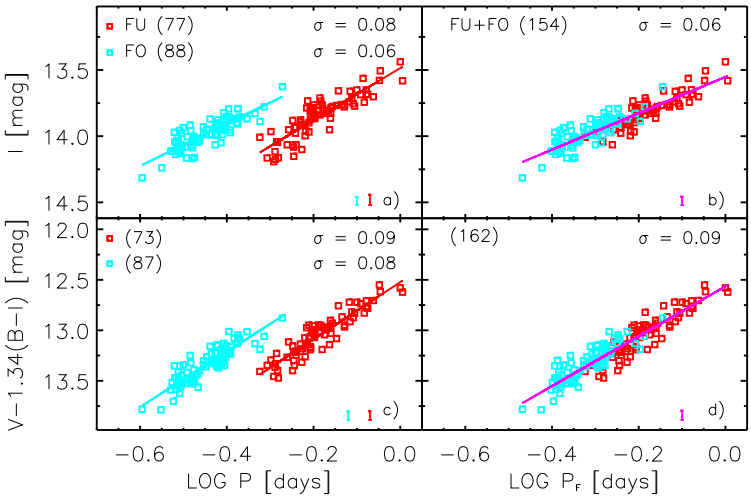

Figure 3. Panel a): Empirical PL_I relation for FU and FO variables; Panel b): The same, but for FU+FO variables. Panels c) and d): The same as a) and b), but for the $V, B-I$ PW relation.

We present empirical I-band period–luminosity (PL) and optical period–Wesenheit (PW) relations using cluster RRLs. RRLs in ω Cen display a well known spread in metallicity (Rey et al. 2000; Sollima et al. 2006a), therefore, we estimate its true distance modulus (μ_0) on the basis of the predicted PW (V,$B-I$) relation (Marconi et al. 2015), that is minimally dependent on metallicity. Using the FU+FO PW relation (162 RRLs) we find $\mu_0 = 13.70 \pm 0.01$ (standard error on the mean) ± 0.09 (standard deviation) mag.

Our estimate is consistent, within 1σ, with the geometrical distance derived on the basis of photometric and spectroscopic observations of the eclipsing binary V209 ($\mu_0 = 13.48 \pm 0.13$, Kaluzny et al. 2007). The agreement is better than 1σ with both estimates based on the PL_K relation of RRLs ($\mu_0 = 13.61$, Longmore et al. 1990 and $\mu_0 = 13.72$, Sollima et al. 2006b). Finally, there is

also an agreement better than 1σ with Bono et al. (2008), who obtained $\mu_0 = 13.65 \pm 0.09$ mag on the basis of the Tip of the Red Giant Branch luminosity.

4. Metallicity of RR Lyrae stars

To further constrain the properties of RRLs we provide their metal abundances using the above distance, a mean reddening of $E(B-V) = 0.11$ mag (Thompson et al. 2001; Lub 2002), $R_V = 3.06$ and $A_I/A_V = 0.590$ (Cardelli et al. 1989; Marconi et al. 2015) to constrain their absolute I-band magnitude (M_I). Finally, we invert the theoretical I-band PLZ relation (Marconi et al. 2015) to evaluate the metallicities. We find that the metallicity distribution peaks at [Fe/H] $= -1.87$ which is ~ 0.27 dex more metal-poor than similar estimates of the RRLs in ω Cen in the literature (Rey et al. 2000; Sollima et al. 2006a). We also find a σ that is larger than similar distributions for giant stars (Calamida et al. 2009; Johnson & Pilachowski 2010). In passing we note that the current approach to constrain individual metal abundances is prone to uncertainties in the estimated distance. A systematic difference of ± 0.05 mag in distance modulus means a shift of ∓ 0.29 dex in metallicity. New distance estimates based on near-infrared photometry are required to improve the accuracy of the metallicity distribution.

References

Bailey, S. I. 1902, Annals of Harvard College Observatory, 38, 1
Bekki, K., Freeman, K. C. 2003, MNRAS, 346, L11
Bono, G., Stetson, P. B., Sanna, N., et al. 2008, ApJ, 686, L87
Calamida, A., Bono, G., Stetson, P. B., et al. 2009, ApJ, 706, 1277
Cardelli, J. A., Clayton, G. C., Mathis, J. S. 1989, ApJ, 345, 245
Clement, C. M., Rowe, J. 2000, AJ, 120, 2579
Clement, C. M., Muzzin, A., Dufton, Q., et al. 2001, AJ, 122, 2587
Del Principe, M., Piersimoni, A. M., Storm, J., et al. 2006, ApJ, 652, 362
Drake, A. J., Djorgovski, S. G., Mahabal, A. A., et al. 2009, ApJ, 696, 870
D'Souza, R., Rix, H.-W. 2013, MNRAS, 429, 1887
Freeman, K. C. 1993, in The Globular Cluster-Galaxy Connection, ASPC 48, 608
Johnson, C. I., Pilachowski, C. A., Michael Rich, R., et al. 2009, ApJ, 698, 2048
Johnson, C. I., Pilachowski, C. A. 2010, ApJ, 722, 1373
Kaluzny, J., Olech, A., Thompson, I. B., et al. 2004, A&A, 424, 1101
Kaluzny, J., Rucinski, S. M., Thompson, I. B., et al. 2007, AJ, 133, 2457
Kaluzny, J., Kubiak, M., Szymanski, M., et al. 1997, A&AS, 125, 343
Longmore, A. J., Dixon, R., Skillen, I. et al. 1990, MNRAS, 247, 684
Lub, J. 2002, in Omega Centauri, A Unique Window into Astrophysics, ASPC 265, 95
Marconi, M., Coppola, G., Bono, G., et al. 2015, ApJ, 808, 50
Navarrete, C., Contreras Ramos, R., Catelan, M., et al. 2015, A&A, 577, A99
Rey, S.-C., Lee, Y.-W., Joo, J.-M., et al. 2000, AJ, 119, 1824
Sollima, A., Borissova, J., Catelan, M., et al. 2006a, ApJ, 640, L43
Sollima, A., Cacciari, C., Valenti, E. 2006b, MNRAS, 372, 1675
Sturch, C. R. 1978, PASP, 90, 264
Thompson, I. B., Kaluzny, J., Pych, W., et al. 2001, AJ, 121, 3089
Torrealba, G., Catelan, M., Drake, A. J., et al. 2015, MNRAS, 446, 2251
Weldrake, D. T. F., Sackett, P. D., Bridges, T. J. 2007, AJ, 133, 1447
Zinnecker, H., Keable, C. J., Dunlop, J. S., et al. 1988, IAUS, 126, 603

RRL2015 – High-Precision Studies of RR Lyrae Stars
L. Szabados, R. Szabó, K. Kinemuchi (Eds.) 2016

Galactic membership of BL Her type variable stars

Monika I. Jurkovic, Milan Stojanović, & Slobodan Ninković

Astronomical Observatory of Belgrade, Belgrade, Serbia

Abstract. As the RR Lyrae stars evolve on the Hertzsprung-Russell diagram they are believed to become short period Type II Cepheids, known as BL Her type (with a pulsation period from 1 to $3-8$ days). Assuming that their mass is around $0.5-0.6\mathrm{M}_{\odot}$, and that they are low metallicity objects, they were thought to belong to the halo of the Milky Way. We investigated seven Galactic short period Type II Cepheids (BL Her, SW Tau, V553 Cen, DQ And, BD Cas, V383 Cyg, and KT Com) in order to establish their membership within the Galactic structure using the kinematic approach. *Gaia* should provide us with more data needed to conduct the study of the whole sample.

1. Introduction

The evolution of low mass stars, such as RR Lyrae, can be followed up in the Type II Cepheids. Wallerstein (2002) gives an overview of Type II Cepheids (T2C). The papers by Harris (1984, 1985) discuss the classification of T2Cs according to their distances from the Galactic plane, while the papers by Diethelm (1986, 1990) address the question of the relation of the metallicities and the position of these stars. By investigating the Galactic membership based on the kinematic approach we are able to reconstruct (within the limits of the model) the movement of an individual star in the Galaxy, which helps us to answer the question of the origin of metal-rich Type II Cepheids. The General Catalogue of Variable Stars[1] (GCVS) in 2012 contained 71 short period T2Cs, which were expanded in the time that has passed, but we stick to that sample, because they were relatively bright objects for which there was a chance to find all the data we needed (the distance or parallax, proper motion, and radial velocity).

2. Method

There are a few approaches for indicating the membership of stars of the Galactic components. Here, we shall use the kinematic approach. We start by converting the distance and position on the sky to the Galactocentric Cartesian system of Galactic coordinates (X, Y, Z). For this we use the well-known formulas:

[1] http://www.sai.msu.su/gcvs/gcvs/

$$\begin{aligned} X &= D\cos b\cos l - R_{\odot} \\ Y &= D\cos b\sin l \\ Z &= D\sin b \end{aligned} \tag{1}$$

In order to obtain the 3-D position vector and velocity vector of a star in space one needs the following data: two celestial coordinates, distance, two proper-motion components, and the radial velocity. Since these are pulsating variable stars they change their radial velocity due to pulsation too, so that one should be cautious when applying the radial velocity values.

In our original sample these necessary data were not available for all stars. For some stars we do not have the parallax or radial velocity, or both. All the data necessary for calculating the velocity components are available for seven stars in total. All the input data should be transformed into the heliocentric Cartesian system; for this purpose we use the procedure described in Johnson & Soderblom (1987). Then we correct velocity values for the solar motion. The obtained velocity components U, V, W are with respect to the local standard of rest (LSR).

The magnitude of the LSR velocity v,

$$v = \sqrt{U_{\rm LSR}^2 + V_{\rm LSR}^2 + W_{\rm LSR}^2} \tag{2}$$

is indicative of the star membership, to the thin disc, thick disc, or halo. If for a star the magnitude of the LSR velocity is very high (say, exceeds 250 $\mathrm{km\,s^{-1}}$), then the probability that this star belongs to the thin or thick disc is very low. If it exceeds, say 100 $\mathrm{km\,s^{-1}}$, then only the probability of belonging to the thin disc is very low.

3. Results

The stars which had all the required data are listed in Table 1.

Table 1. Stars examined for their Galactic membership (in the order of increasing period).

Name	RA (J2000) [h : m : s]	Dec (J2000) [° : ′ : ″]	Proper motion [mas/yr]		Radial velocity [km/s]	Parallax [mas]
BL Her	18:01:09.22	+19:14:56.68	−2.94	−12.94	18.0	1.27
SW Tau	04:24:32.97	+04:07:24.05	4.05	−11.17	10.9	2.8
V553 Cen	14:46:33.63	−32:10:15.25	5.01	−0.71	−6.00	1.84
DQ And	00:59:34.47	+45:24:24.22	5.16	1.92	−230.91	0.67
BD Cas	00:09:51.39	+61:30:50.54	−1.1	−0.9	−49.30	2.13
V383 Cyg	20:28:58.15	+34:08:06.36	−1.99	−2.64	−24.4	4.44
KT Com	13:33:50.22	+17:25:30.37	−15.93	−24.76	−13.0	5.50

Note: All the data were collected from: http://simbad.u-strasbg.fr/simbad/, and from the references within van Leeuwen (2002) for the Hipparcos data.

Figures 1 and 2 show the cross-section of the path of each star in our sample in the past 12 Gyrs from the model calculations. All the stars in Figure 1 are members of the thin disc. DQ Andromedae (see Figure 2) is a halo star, but with a mean metallicity of [Fe/H] = −0.17 (Schmidt et al. 2011). Since the distances to almost all the stars are probably not precise enough, the results could change, but not too much.

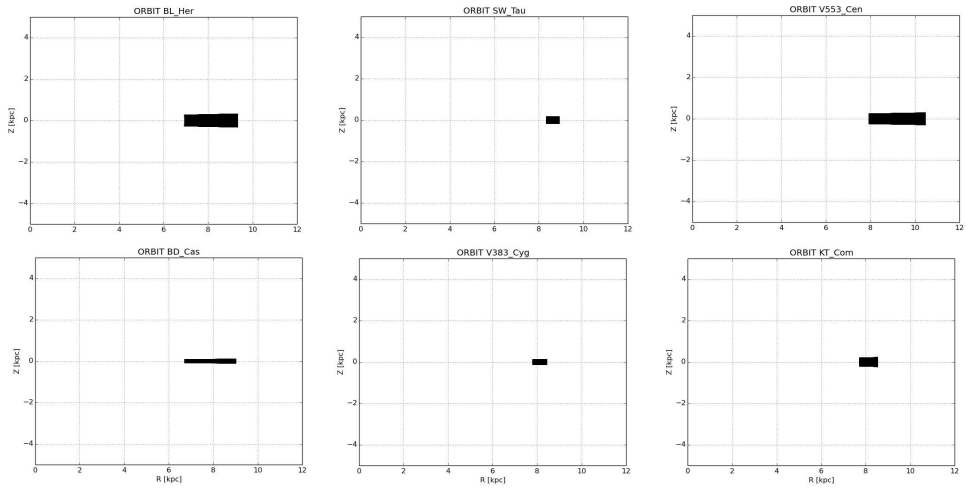

Figure 1. The meridional plots of star orbits for: BL Her, SW Tau, V553 Cen, BD Cas, V383 Cyg and KT Com in the order of their increasing periods. R is the distance from the Galactic rotation axis, z is the distance from the Galactic plane.

The Toomre diagram in Figure 3 shows the distribution of the examined stars in the calculated velocity planes. The lines show the approximate limits between the subsystems in the Galaxy: the innermost part being the thin disc, then the thick disc, and finally the halo.

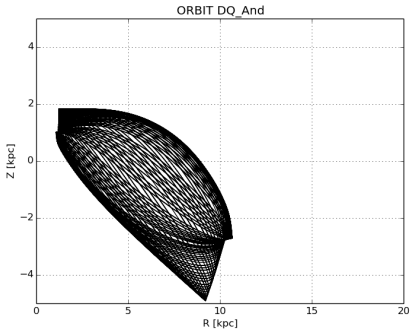

Figure 2. The meridional plot of DQ And. R and z are the same as in Figure 1.

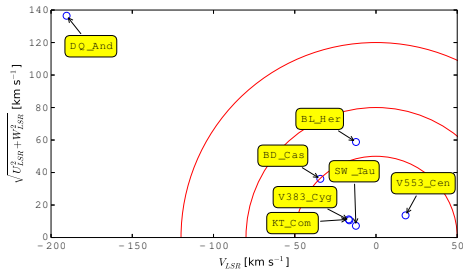

Figure 3. The Toomre diagram of the examined stars.

4. Conclusion

Out of the 71 stars we have studied, only 7 had enough data available to be examined in our model. Even though we are aware of a substantial error influence in the input data, we are still comfortable with stating that the model results do give us the Galactic membership of the stars.

Kinematically BL Her, SW Tau, V553 Cen, BD Cas, V383 Cyg, and KT Com could be thin disk stars, but by examining their light curve shapes it might happen that they turn out to be some other type of variable stars, not Type II Cepheids.

DQ And is the only star which shows evidence of being a member of the halo of the Milky Way, but the asymmetry of its calculated orbit is peculiar. If we consider that the Milky Way has experienced collisions with neighbouring dwarf galaxies, this asymmetry could be due to the capture of this star by our Galaxy or its motion around the centre of the Milky Way might have been perturbed.

In the following years the astrometric measurements from the *Gaia* satellite should give us much more insight into the understanding of the Galactic membership of Type II Cepheids.

Acknowledgements

The authors thank for the financial support from the Ministry of Education, Science and Technological Development of the Republic of Serbia through the projects 176004 and 176011 and the Hungarian National Research, Development and Innovation Office through NKFIH K-115709. This research has made use of NASA's Astrophysics Data System. This research has made use of the VizieR catalogue access tool, CDS, Strasbourg, France. The original description of the VizieR service was published in Ochsenbein et al. (2000).

References

Diethelm, R. 1986, A&AS, 64, 264
Diethelm, R. 1990, A&A, 239, 196
Harris, H. C. 1984, in IAU Colloq. 82, Cepheids, Theory and Observations, ed. B. Madore (Cambridge: Cambridge Univ. Press), 232
Harris, H. C. 1985, AJ, 90, 756
Johnson, D. R. H., Soderblom, D. R. 1987, AJ, 93, 864
Ochsenbein, F., Bauer, P., Marcout, J. 2000, A&AS, 143, 23
Schmidt, E. G., Rogalla, D., Thacker-Lynn, L. 2011, AJ, 141:53
van Leeuwen, F. 2002, A&A, 474, 2, 653
Wallerstein, G. 2002, PASP, 114, 689

RRL2015 – High-Precision Studies of RR Lyrae Stars
L. Szabados, R. Szabó, K. Kinemuchi (Eds.) 2016

Lighthouses in the fog: Locating the faintest Milky Way satellites with RR Lyrae stars

Branimir Sesar

Max Planck Institute for Astronomy, Königstuhl 17, 69117 Heidelberg, Germany

Abstract. Almost every known low-luminosity Milky Way dwarf spheroidal (dSph) satellite galaxy contains at least one RR Lyrae star. Assuming that a fraction of distant ($60 < d_{\rm helio} < 100$ kpc) Galactic halo RR Lyrae stars are members of yet to be discovered low-luminosity dSph galaxies, we perform a *guided* search for these low-luminosity dSph galaxies. In order to detect the presence of dSph galaxies, we combine stars selected from more than 123 sightlines centered on RR Lyrae stars identified by the Palomar Transient Factory. We find that this method is sensitive enough to detect the presence of Segue 1-like galaxies ($M_V = -1.5^{+0.6}_{-0.8}$, $r_h = 30$ pc) even if only ~ 20 sightlines were occupied by such dSph galaxies. Yet, when our method is applied to the SDSS DR10 imaging catalog, no signal is detected. An application of our method to sightlines occupied by pairs of close (< 200 pc) horizontal branch stars, also did not yield a detection. Thus, we place upper limits on the number of low-luminosity dSph galaxies with half-light radii from 30 pc to 120 pc, and in the probed volume of the halo. Stronger constraints on the luminosity function may be obtained by applying our method to sightlines centered on RR Lyrae stars selected from the Pan-STARRS1 survey, and eventually, from LSST.

1. Hundreds of Milky Way satellites?

One of the predictions of the Λ Cold Dark Matter (ΛCDM) model is an abundance of low-mass dark matter subhalos orbiting their host galaxies at the present epoch. Taking into account sensitivity limits of searches based on the Sloan Digital Sky Survey data, Tollerud et al. (2008) predict "that there should be between $\sim$ 300 and $\sim$ 600 satellites within 400 kpc of the Sun that are brighter than the faintest known dwarf galaxies". While Milky Way satellites brighter than $M_{\rm V} \sim -4$ have all likely been discovered in the SDSS footprint within ~ 100 kpc, less luminous satellites ($M_{\rm V} > -4$) may exist beyond 45 kpc from the Sun, just below the detection limit of current surveys.

2. RR Lyrae stars as tracers of faintest Milky Way satellites

While low-luminosity Milky Way satellites may not be detectable in current *blind* searches until surveys such as the Large Synoptic Survey Telescope provide deeper multi-color imaging covering large areas on the sky, these satellites may be detectable in *guided* searches, where potential locations of satellites are known in advance. Since *almost every known low-luminosity Milky Way dwarf satellite galaxy has at least one RR Lyrae star*, positions of RR Lyrae stars in the outer

halo (i.e., beyond 30 kpc from the Galactic center) may indicate locations of undiscovered satellites.

3. Properties of RR Lyrae stars

First, RR Lyrae stars are bright stars ($M_{\rm V} = 0\overset{\rm m}{.}6$) that can be detected at large distances ($5 - 120$ kpc for $14 < V < 21$ mag) with modern imaging surveys. Second, they are standard candles and their distances measured from optical data are precise to $\sim 6\%$. And finally, RR Lyrae stars are variable stars with distinct, saw-tooth shaped light curves which make them easy to identify given multi-epoch observations (peak-to-peak amplitudes of $\sim 1^{\rm m}$ in the Johnson V band and periods of pulsation of ~ 0.6 days).

4. Stacking analysis of sightlines centered on PTF RR Lyrae stars

Using multi-epoch photometry obtained by the Palomar Transient Factory (PTF) survey, we have selected a sample of 123 distant RR Lyrae stars that may indicate potential locations of faint Milky Way satellites. These RR Lyrae stars spread over 10,000 square degrees of sky and are located between 60 to 100 kpc from the Galactic center.

Assuming that RR Lyrae stars trace the positions of unknown satellites, we use a color-magnitude diagram to select all SDSS stars that are at the distance of an RR Lyrae star from our sample, and within $30'$ of its position on the sky. The angular positions of selected SDSS stars are converted to projected physical distances (using distances of RR Lyrae stars), and stars from multiple sightlines are combined into a single map.

If RR Lyrae stars trace locations of unknown Milky Way satellites, the above stacking of stars should produce an overdensity of sources in the center of the combined map. We have developed a probabilistic method that measures the statistical significance of this overdensity of sources, and by testing on mock catalogs, have found that our method can detect the presence of Segue 1-like satellites even if only 20 (out of 123) sightlines truly contain a dwarf satellite galaxy (i.e., even if the majority of sightlines contain an RR Lyrae star, but not a dwarf galaxy; Sesar et al. 2014).

5. Upper limit on the number of faintest satellites

The main results of our work are summarized in Figure 1. Using our stacking analysis we did not detect the presence of low-luminosity satellites, but were able to provide upper limits on their number in the probed volume of the Galactic halo (10,000 square degrees and between 60 to 100 kpc from the Sun). We find that the number of Segue 1-like satellites has to be smaller than 20, which is in slight tension with the predictions by Sesar et al. (2014). If the satellites have larger half-light radii, then their number could be as high as 120.

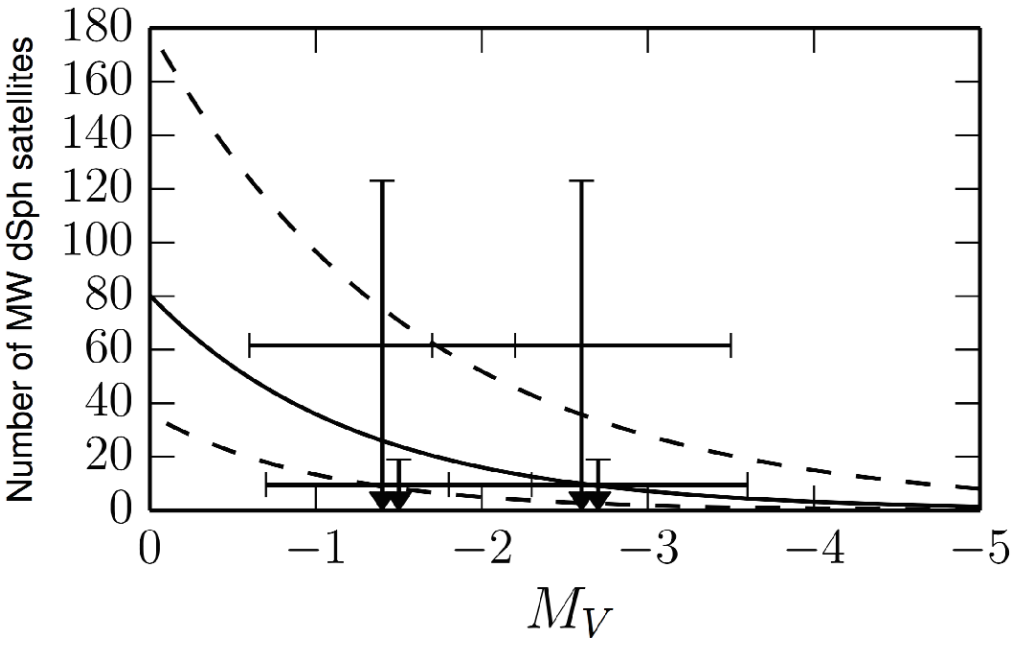

Figure 1. The small down-facing arrows indicate that the number of Segue 1-like ($M_{\rm V} = -1.5 \pm 0.8$) and Boötes 2-like galaxies (i.e., $M_V = -2.7 \pm 0.9$) in the probed volume of the halo has to be smaller than 20, otherwise our method would have detected a signal (i.e., the arrows show upper limits). The horizontal bars indicate the uncertainty in the luminosity of these galaxies. If the satellites are as luminous as Segue 1 or Boötes 2, but have much larger half-light radii (i.e., of 120 pc), then our analysis indicates that there could be as many as 120 such galaxies in the probed volume of the halo (large down-facing arrows). In comparison, the solid line shows the number of satellites predicted by Tollerud et al. (2008), and the dashed lines show the 1σ range. As evident from this comparison, our work provides a strong constraint on the number of Segue 1-like satellites in the Milky Way.

References

Sesar, B., Banholzer, S. R., Cohen, J. G., et al. 2014, ApJ, 793:135
Tollerud, E. J., Bullock, J. S., Strigari, L. E., Willman, B. 2008, ApJ, 688, 277

Gisella Clementini and Michael Feast

RRL2015 – High-Precision Studies of RR Lyrae Stars
L. Szabados, R. Szabó, K. Kinemuchi (Eds.) 2016

Detailed chemical abundances of distant RR Lyrae stars in the Virgo Stellar Stream

S. Duffau[1,2], L. Sbordone[1,2], A. K. Vivas[3], C. J. Hansen[4], M. Zoccali[2,1], M. Catelan[2,1], D. Minniti[5], & E. K. Grebel[6]

[1] *Millennium Institute of Astrophysics, Santiago, Chile*
[2] *Instituto de Astrofísica, Pontificia Universidad Católica de Chile, Santiago, Chile*
[3] *Cerro Tololo Inter-American Observatory, La Serena, Chile*
[4] *Dark Cosmology centre, Niels Bohr Institute, University of Copenhagen, Denmark*
[5] *UNAB, Santiago, Chile*
[6] *ARI, ZAH, Heidelberg University, Heidelberg, Germany*

Abstract. We present the first detailed chemical abundances for distant RR Lyrae stars members of the Virgo Stellar Stream (VSS), derived from X-Shooter medium-resolution spectra. Sixteen elements from carbon to barium have been measured in six VSS RR Lyrae stars, sampling all main nucleosynthetic channels. For the first time we will be able to compare in detail the chemical evolution of the VSS progenitor with those of Local Group dwarf spheroidal galaxies (LG dSph) as well as the one of the smooth halo.

1. Project presentation

Numerous substructures have been found so far in the halo of our galaxy, and although their census is far from complete, the main challenge now seems to be finding the connections between them, characterising their intrinsic properties, and identifying their origin. Following several photometric and spectroscopic studies, it is now clear that a large overdensity of stars containing several density peaks and velocity signatures is present in the direction of the Virgo constellation, its most prominent velocity feature being the VSS RR Lyrae (RRL) stellar stream (Duffau et al. 2014 and references therein). In order to investigate its nature we started a spectroscopic campaign to obtain medium-resolution spectra of some of its constituent RRL members to obtain the first detailed abundance analysis of this kind performed on an RRL stellar stream. RRL stars have proven to be excellent tracers of halo substructures, due to the quality of the distances that can be derived from them, and the relatively straightforward techniques that lead to their identification. However, they have so far never been used to determine the detailed chemistry of the substructures they reveal, since detailed abundance analysis is difficult for these pulsating variables. This is unfortunate, since the crucial chemical assessment of the substructures must then be derived from other stellar populations whose membership in the same substructure is less certain.

The VSS is located at ∼20 kpc from the Sun and its core is at RA ∼ 187° and Dec ∼ −1°. We have selected 7 targets in the area and obtained X-Shooter@VLT spectra at a high signal to noise (80 or higher) and a resolution of ∼6000 for the UVB arm and ∼10000 for the VIS arm, covering altogether approximately from 2900 to 10000 Å. The data were obtained in service mode. In addition to our target stars, we obtained spectra for two comparison RRL stars from the For et al. (2011) sample as well. Six of the targets had been found in a coherent structure in phase-space (heliocentric distance - radial velocity space) using a group finding algorithm developed in Duffau et al. (2014) and one is a kinematical member from the first spectroscopic study in Duffau et al. (2006). All RRL stars selected are of type ab, which is more easily identified and less affected by contaminants than the type c members.

2. Preliminary results

We have conducted a first 1D LTE atmospheric parameters determination and chemical analysis using the MyGIsFOS code (Sbordone et al. 2014). An example of a spectrum section is shown in Figure 1. We found numerous Fe I and Fe II lines allowing for the determination of the stellar parameters directly from the spectra. In only one case we had to fix the effective temperature to determine the abundances.

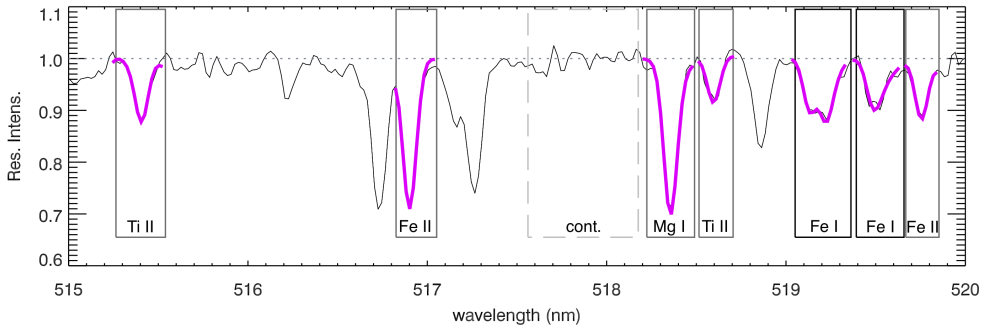

Figure 1. Sample section of spectra (thin line) displaying some of the selected line and continuum features defined for analysis (solid and dashed line boxes), as well as the best fits for abundance determination using MyGIsFOS (thick line within box) and the continuum (dotted horizontal line). The elements under study are marked in each box.

The observations were performed attempting to constrain the phase range away from the rising branch of the light curve to where the effective temperatures are cooler and the abundance analysis is more reliable. Regrettably, the ephemerides we originally used to plan the observations proved outdated and the observations ended up spanning a larger range in phase than intended. As a result, one of our target stars could not be analysed due to unfavourable phase (at 0.97) coupled with a very low metallicity. Of the remaining six targets, four lie close or within the safest phase range (at 0.25, 0.34, 0.51, and 0.82), and parameters and abundances could be obtained for them, while two lie outside of it (at 0.10 and 0.14) and a few of the lines of some of the elements were lost.

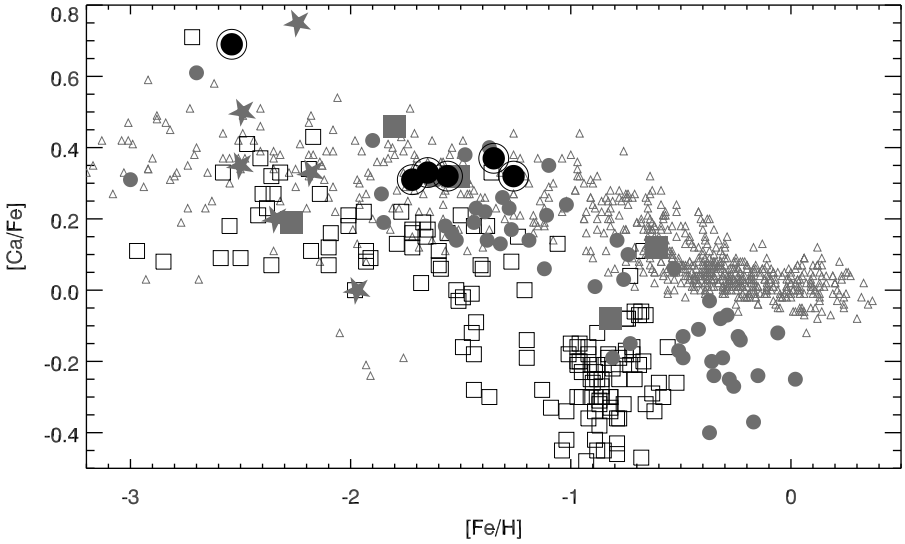

Figure 2. [Ca/Fe] ratio as a proxy for the α-abundance of the VSS sample (large circles) as compared to LG dSph galaxy data (Classical; open squares, Sgr; small circles), MC RRL (stars), and Milky Way data (open triangles).

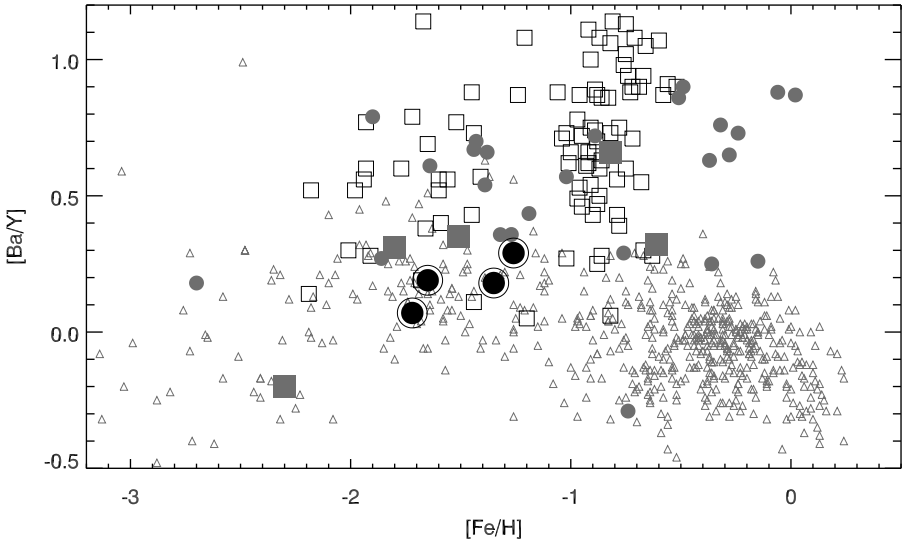

Figure 3. [Ba/Y] ratio for the VSS sample, same symbols as Fig. 2.

Figure 2 shows the results for the six RRLs in our sample and their measured calcium abundance versus metallicity. The calcium abundance is taken here as a representative of the α-elements abundance of the system. The value for

the observed stars is compared with those for a selection of "classical" dwarf spheroidal galaxies (dSph; including Fornax, Sculptor, Carina, Leo, Ursa Minor, Sextans and Draco), for stars and clusters belonging to the Sagittarius dwarf spheroidal galaxy (Sgr dSph; including Terzan 8, Arp 2, M54, Terzan 7 and Palomar 12), for a sample of Milky Way stars from the literature (see Sbordone et al. 2015 and references therein), and for six RRL stars in the Magellanic Clouds (MC; Haschke et al. 2012).

Figure 3 displays the results for four of our RRL stars that had both barium and yttrium measured. For the other two only one of those elements was measurable. The barium over yttrium ratio as a function of metallicity is compared to the value for the same systems as in Fig. 2, except for the MC RRLs whose data for these elements was not available. In the case of the calcium abundance, we see that the value for the bulk of the VSS stars compares better to larger systems like the Sgr dSph and the Milky Way sample, than to the lower-mass classical dSph. This suggests a progenitor with a high star formation efficiency, hence likely a massive one, as massive as the Sgr dSph or maybe even larger. In the case of the barium over yttrium ratio, this ratio is taken as an indication of the efficiency of the s-process of the system under study. It is an observational fact that this ratio remains high for both the Sgr dSph and the classical dSph galaxies when compared to the Milky Way sample in the metallicity range covered by the VSS targets. In this case the value for the VSS is more compatible with the Milky Way sample than with any other sample, again probably also indicating a massive progenitor.

To confirm our results, we will add the information from more elements and other nucleosynthetic channels and study the impact of NLTE/3D effects in our preliminary conclusions. Up until now, these preliminary results show, first of all, that X-Shooter is a very effective instrument for determining detailed chemistry of distant halo RRL stars, as far as 20 kpc. They also suggest that we might have found a case of an accretion event as significant as the Sgr dSph system, that has contributed stars to the Galaxy with the typical chemistry of the smooth halo component.

Acknowledgments

This project is supported by the Ministry for the Economy, Development, and Tourism's Iniciativa Científica Milenio through grant IC 120009, awarded to the Millennium Institute of Astrophysics; by CONICYT's PCI program through grant DPI 20140066; by Proyecto Fondecyt Regular #1141141; and by Proyecto Basal PFB-06/2007.

References

Duffau, S., Zinn, R., Vivas, A. K., et al. 2006, ApJ, 636, 97
Duffau, S., Vivas, A. K., Zinn, R., et al. 2014, A&A, 566, A118
For, B.-Q., Sneden, C., Preston, G. 2011, ApJS, 197:29
Haschke, R., Grebel, A. K., Frebel, A., et al. 2012, AJ, 144:88
Sbordone, L., Caffau, E., Bonifacio, P., et al. 2014, A&A, 564, A109
Sbordone, L., Monaco, L., Moni Bidin, C., et al. 2015, A&A, 579, A104

RRL2015 – High-Precision Studies of RR Lyrae Stars
L. Szabados, R. Szabó, K. Kinemuchi (Eds.) 2016

Conference summary – Personal views

J. Lub

Sterrewacht Leiden, Leiden University, Leiden, the Netherlands

Abstract. This is a collection of remarks on the three and a half days of the RR Lyrae 2015 Conference, limited only by my own lack of attention and understanding. I end with some personal recollections on my complete failure, even though doing the necessary calculations, to spot the importance and the possible application of Fourier amplitudes and phases of the RR Lyrae light curves.

1. Introduction

When the organizer(s) asked me to do the summary talk of the conference, I realized that this is one of those things one cannot refuse. It probably also is a sign of respectability and seniority, I hope.

But let me start first by complimenting the organizers, in particular Róbert Szabó, for the excellent idea to bring researchers from all corners of the research into RR Lyrae stars together. They have provided us with a congenial and relaxed environment in which it was great to pick up new ideas and developments in our field of preference. Well done, thank you, and we should do this more often!

The introductory talk by Prof. Lajos G. Balázs on the career of Prof. László Detre (Dunst), who established the reputation of the Konkoly Observatory in the field of long-term studies of RR Lyrae variables, reminded us all of the fact that by pure perseverance important scientific conclusions can be harvested. It does not have to be just 'stamp collecting'.

His remarks on the early introduction of UBV photometry through smuggling a 1P21 photomultiplier provided by Shapley at the Zurich IAU to Hungary, and Dr. Walraven's delivery of an amplifier and integrating electronics resounded with me. After all I call myself a photometrist, succeeding Dr. Walraven at the Leiden Observatory after his retirement in 1981.

2. What was not discussed (in detail)

Any conference will not cover all possible subjects and angles of the subject, for example there was no real discussion on M_V and (statistical) parallax. Obvious subjects of importance to study the evolutionary status of RR Lyrae stars and their impact on the (nearby) distance scale, in particular the LMC/SMC distance. But then again *Gaia* is expected soon (mid 2017) and we are all eagerly awaiting the first results.

Fundamental photometry has gone out of fashion, so their impact on the derivation of physical parameters, $T_{\rm eff}$, $\log g$, [Fe/H] and in close connection therewith of reddening $E(B-V)$ and mean colours. For a review of the power of these methods I refer to my Los Alamos review (Lub 1987).

Little was also mentioned on spectroscopic abundances and high-resolution spectroscopy for e.g. Baade-Wesselink (B-W) solutions. There was a large effort over two decades ago, but the discrepancy between absolute magnitudes based upon stellar pulsation and horizontal branch models and on the B-W approach has never been resolved in a fully satisfactory way.

3. The conference

Here follows an admittedly biased and selective choice from the different sessions:

(Future) space missions Space has provided and will provide us with many new insights. *Gaia* is our hope to solve the (statistical) parallax problems and with RR Lyrae stars almost the whole Galaxy is accessible. Long term monitoring by *MOST* of the double mode RRab AQ Leo and especially by *Kepler* gave us a treasure trove of new and surprising effects: Long term RRab Blazhko observations and the discovery of period doubling, RRc amplitude variations often suspected but all too often at the limit of detectability from the ground ..., and something nobody asked for: f_X, a mode with no explanation up till now, but it is found literally everywhere (!). Plans for the use of the extended *Kepler* mission were presented, and finally the discovery of Blazhko effect in Cepheids was announced.

Dynamical phenomena Wojciech Dziembowski provided a tutorial on nonradial pulsations, emphasizing the possible implication of nonradial modes of $\ell = 8$ or 9 in the case of the Blazhko effect. The f_X mode with the 0.613 ratio in RRc stars shows three parallel sequences, stars appear to move between those, and moreover an additional mode at a ratio of 0.685 shows up. Who asked for this? Dynamical phenomena can be studied by two methods: amplitude equations or hydrocodes, which are of course two approaches to the same physical problem. Kolláth e.g. investigates the 9:2 resonance using amplitude equations in the Florida-Budapest code.

Period-colour-luminosity relations ω Centauri is always, starting with Christian Martin's (1937) thesis under the guidance of Ejnar Hertzsprung in Leiden, a welcome object for study thanks to its large RR Lyrae population. Navarrete established the near-IR amplitude relations and concluded that the overluminous stars are mainly double. The Carnegie RR Lyrae program extends the period-magnitude relations to even further into the IR to 3.6 μm and 4.3 μm, but is this necessary? K (2.2 μm) is already OK, as I concluded in my talk. Actually the *WISE W1* and *W2* magnitudes add no information which is not already available through K, but can be used if no K observations are available (my own unpublished research). Martínez-Vázquez extends the calibration of [Fe/H] vs. P and ϕ_{31} by combining field and globular clusters to cover the interval and extremes not (well) covered up till now.

The Blazhko enigma It fell to Géza Kovács to review the Konkoly speciality: the Blazhko effect. In the discussion of the various populations it is very striking that the incidence rate in the Galactic field is twice the rate in LMC/SMC. I would have appreciated if his talk were followed by Johanna Jurcsik's presentation of the study of the RR Lyrae in M3, another one of our emblematic 'standard' globular clusters. All the wild and outrageous Blazhko behaviour imaginable is found in just this one cluster. A gold mine is of course the OGLE

survey, where the first single period Blazhko star has been found and additionally 1O+2O stars with a period ratio $P_2/P_1 = 0.805$. In this context Smolec also mentioned the proposed 'Golden' stars where the f_X is 'explained' as the reciprocal of the Golden Ratio: 0.618034. However not a single star shows this value! And just to put the cherry on the cake: RR Lyrae itself, detected by Williamina P. Fleming in 1899, has shown a jump of $P_{\rm Blazhko}$ from 41 to 39 days, and at this moment it hardly shows any amplitude variations.

Deep large area surveys and detection methods We are approaching the era of Pan-STARRS and the like, not to mention LSST. But we should not forget OGLE, DECAM, VST, VISTA, etc. They all promise or provide already exquisite photometric accuracy, improving even with time because the same fields are visited over and over again and all hour angle (right ascension) dependent variations in the absolute photometric calibration can be solved. Maybe the photometric passbands chosen are not always optimal for a broad range of stellar intensity distributions, but this is amply offset by long-term stability (OGLE is reaching now 2 decades).

However who in his or her right mind would then also sample randomly in time and colour? This problem can fortunately be approached by ingenious statistical methods. RR Lyrae stars are harvested as a by-product of other searches deemed more important: SNe, QSO, etc. (Flewelling: Pan-STARRS, Hernitschek: LSST, Medina: VISTA/VST) and are easily found to distances of up till 200 kpc.

Several approaches to derive variability from such (random) multicolour observations were presented: Hernitschek solves sparse sampled surveys with multiband structure functions, Ivezić has extended the time-honoured Lomb-Scargle method and achieves accurate periods at magnitude 24 already after 1 year instead of 10 years. Finally there was an interesting approach by Bellinger, who made fitting a sparse light curve an optimisation problem.

Hydro calculations of RR Lyrae stars and Cepheids Bob Deupree, who could not attend, spoke to us from his office in Canada about his 2D and 3D RR Lyrae calculations. I remember that he started on this essentially almost 40 years ago, with an intermezzo working 'behind the fence' as so many other pulsation theoreticians and hydrodynamicists. Similarly the same can be said for Herbert Muthsam's development of the Cepheid code: few people, long time scales, and slow progress. The 2D RR Lyrae light curves actually look more like 'reality' than the 3D calculations. Marcella Marconi reported on an extension of the Framework Survey of RR Lyrae pulsators into the realm of enhanced helium abundances, such as now required in the study of globular clusters. Not surprisingly this has resulted in a shift to higher luminosities and consequently longer periods. The Bailey (period-amplitude) diagram shifts to the right. But note: relations between photometric parameters such as $W = V - 3.06(B - V)$ and the period remain unchanged (because helium does not influence the opacity in the atmosphere).

OGLE and binarity The surveys for microlensing in V and I turned out to be an even more effective source of RR Lyrae stars and Cepheids, as Udalski told us, since 1992 through many upgrades from OGLE I to OGLE IV. The very high precision from OGLE made many studies possible on populations of Cepheids and RR Lyrae stars and the structure of the Magellanic Clouds. Another as-

pect of OGLE was presented in more detail by Pietrukowicz: the amounts of data amassed on the Galactic bulge now give very detailed information on the structure of the bulge and the inner halo of the Galaxy and on the physical properties of the RR Lyrae population. The Bailey diagram of the bulge now shows two distinct populations. Ideally this survey should offer some hope of finding RR Lyraes in (eclipsing) binaries, but the only one found was a strange star of (pulsation) mass 0.26 $M_{\odot}$. Several further approaches using LTE (light-time effect) or $O-C$ diagrams were described, for the moment with little reward for the tremendous observing effort. In particular Hajdu in a program to determine masses for RR Lyrae stars, discussed several promising candidates from these timing efforts: 20 candidates (out of 1952 stars) from OGLE-III became 12 good candidates after combining with OGLE-IV. Periods are (several) years and follow up is needed. The best other candidate remains TU UMa (mainly from $O-C$).

Pulsation and evolution How to populate the instability strip was reviewed by Giuseppe Bono: the Cepheids have a blue loop, whereas the RR Lyrae perform a blue hook, driven by hydrogen burning with a dependence on [Fe/H]. The redward evolution is driven by helium burning. An attempt was made by Jang to explain the Oosterhoff effect using the now common multiple populations in globular clusters.

Sixty years ago we barely knew RR Lyrae stars in the Magellanic Clouds, the first were discovered by Thackeray & Wesselink (1953, 1954). But now as shown by Cusano, RR Lyrae stars in small faint and disturbed dwarf galaxies close to M31 are followed with the LBT almost without effort. They have an average period of 0.60 days (neither OI nor OII?).

Finally a warning: Jurković wanted to investigate BL Her stars as a Galactic population, but she had to conclude after making a selection from the GCVS and SIMBAD, that without restudying each object anew in detail, she was left with essentially an empty sample.

RR Lyrae: Galactic structure tracers In this session I was struck by a valiant effort by Branimir Sesar: using single RR Lyrae stars as lighthouses to detect low luminosity structures in the halo. Around the position of the variable he could then start looking for K giants or stars around the turn-off. This brought back to my memory the controversy at the end of the 1960's with the 'Stellar Rings'. Near every B star there 'should' be a dissolving cluster of young stars and, lo and behold, A stars were found, selected by photometry, at the expected magnitudes. It was hypothesized that such 'rings' had a standard size. Most likely this was a case of biasing the statistics, a danger which is also might be present in Sesar's approach. So extreme care has to be taken in making the selection of stars, not only photometric, but also using radial velocities and/or proper motions to make sure that one is not fooling oneself. Again, as I used to think sometimes, a single well studied RR Lyrae star might well be as good as a whole globular cluster?

4. Conclusion and a personal recollection

RR Lyrae stars, though being the little brothers of their supergiant relatives, the classical Cepheids, have many well-established applications in astronomy,

within our Galaxy and the Local Group. This conference has once again shown that this classical field of investigation time and again develops new usage.

I would like to end this summary with a personal recollection (confession). In February 1973 I arrived from Amsterdam in Leiden. My thesis supervisor Bruno van Albada had died all of a sudden in December 1972 and Pik Sin The, who overnight had become the caretaker of our small institute in Amsterdam, had asked senior old statesman Jan Oort for advice on what to do with his two orphan PhD students. The other student, Winardi Sutantyo, from Lembang (Indonesia) finally finished his doctorate with Ed van den Heuvel, who arrived in Amsterdam later that year to take the reigns of the institute.

At the suggestion of Prof. Oort, Gijsbert van Herk, probably best known as an astrometrist, see his impressive study of RR Lyrae statistical parallax (van Herk 1965), had started a large survey of precise southern RR Lyrae light curves using the Leiden Lightcollector at Hartebespoortdam equipped with Walraven's five-channel simultaneous $VBLUW$ photometer. In the sixties and before we find many such large programs which were started 'at the suggestion of Professor Oort'. Observations were mostly done between 1968 and 1973 by the resident Leiden observer (over the years they were Willem Wamsteker, Jan W. Pel and mostly Arnout M. van Genderen). From preliminary scarce data taken in previous years it appeared that there might be a relation between 'bumps' at minimum light and metallicity as measured by Preston's ΔS, see van Herk (1971). But van Herk retired at the end of 1972, so there was nobody to reduce and discuss this huge amount of data.

Bruno van Albada's cousin Tjeerd (T. S.) van Albada had just returned to Groningen from a postdoc with Norman Baker at Columbia University and they established the framework for the interpretation of RR Lyrae stars and the horizontal branch in globular clusters, see van Albada & Baker (1971, 1973). He suggested that we took the opportunity to do a thorough study of the variation of the physical parameters over the pulsation cycle and try to establish the 'equilibrium values' – the values the star would have if it were not pulsating – in the instability strip. The Walraven photometry promised to give after all the same or better sensitivity to $T_{\rm eff}$, $\log g$, abundance and reddening as Strömgren's $uvby{\rm H}\beta$ photometric system. He also became my thesis advisor.

My previous education in Amsterdam had given me a solid background in the fields of stellar atmospheres and stellar structure and evolution, so after an interview with the then Leiden Director Harm Habing and Secretary Jan Willem Pel, I was offered the project. Sitting in van Herk's old office in the basement of the Sterrewacht between the dusty volumes of the Carte du Ciel, I set out to calibrate the photometry, extract the light curves, and explore the information in the data.

Somewhere around 1975, an adjunct professor in the field of signal processing was appointed at the Observatory. Cees van Schooneveld came from the Ministry of Defence research organization at TNO-FEL where he had worked on underwater detection by interferometric techniques. This was quite in line with the strong emphasis at Leiden on the Westerbork Synthesis Radio Telescope in those days. He suggested that I read the article by Brault & White (1971) and apply their method of optimal filtering to derive a harmonic Fourier fit to the light curves with sometimes very steep rising branches and bumps close to the

minimum. I remember taking as a start V341 Aql and also V440 Sgr, the first one with a beautiful depression in the falling branch.

I learned that beyond the order $n = 8$ only the noise was being fitted, but I was very pleased with the quality of the fit, with maximally 16 (2 times 8) terms, after correcting these amplitudes (squared) for the noise level (squared). And there I left it, because meanwhile it became clear that the information I was looking for was already available from the measurements of the colour at minimum light, and moreover I did understand the physics behind these measurements. Still I could almost assign by eye a period and a ΔS from the appearance of the light curve, so there must have been useful information in amplitudes and phases. It also was time to write up the thesis (Lub 1977), and find new employment.

A few years later, while I was working at ESO La Silla, I was contacted by Norman Simon and thereafter, after my return to Leiden, by Géza Kovács who as theoreticians had a much deeper understanding of the significance of the amplitudes and phases of the Fourier fits, see Simon & Teays (1982) and Jurcsik & Kovács (1996). But I remember very well that acting as the referee for the second mentioned paper, I remained puzzled and probably still am, by the impact of the Blazhko effect (especially when not recognized) on the application of their relations, especially the beautiful and simple relation giving [Fe/H] in terms of P and ϕ_{31}. (After all their criterion for rejecting stars was rather ad hoc, and moreover as we just heard from Ennio Poretti RR Lyrae itself would at this moment hardly be recognized as a star showing the Blazhko effect!).

My final puzzlement: what is so special about magnitudes in this context? Why does it work so well to fit log(intensity) rather than intensity? Of course taking the logarithm does smooth out/mitigates the steep rise.

Acknowledgements

After the meeting Andrzej Udalski and Pawel Pietrukowicz approached me and showed their beautiful period-amplitude diagram for the Galactic Bulge. Indeed there are RR Lyrae stars on the relation down to amplitudes as low as $0\overset{m}{.}1$, something I had overlooked for a long time. The question remains where are such stars in the local population?

References

Brault, J. W., White, O. R. 1971, A&A, 13, 169
Jurcsik, J., Kovács, G., 1996, A&A, 312, 111
Lub, J. 1977, The Local Population of RR Lyrae Stars, Thesis, Leiden University
Lub, J. 1987, in Stellar Pulsation, Eds: A. N. Cox, W. M. Sparks, S. R. Starrfield, Lecture Notes in Physics, 274, 218
Martin, W. Chr. 1937, Photographische Photometrie van Veranderlijke Sterren in ω Centauri, Thesis, Leiden University
Simon, N. R., Teays, T. J. 1982, ApJ, 261, 586
Thackeray A. D., Wesselink, A. J. 1953, Nature, 711, 693
Thackeray A. D., Wesselink, A. J. 1954, MNASSA, 13, 99
van Albada, T. S., Baker, N. H. 1971, ApJ, 169, 311
van Albada, T. S., Baker, N. H. 1973, ApJ, 185, 477
van Herk, G. 1965, BAN, 18, 7
van Herk, G. 1971, HiA, 2, 781

Poster papers

RRL2015 – High-Precision Studies of RR Lyrae Stars
L. Szabados, R. Szabó, K. Kinemuchi (Eds.) 2016

Constraining RRc candidates using SDSS colours

E. Bányai[1], E. Plachy[2], L. Molnár[2], L. Dobos[1], & R. Szabó[2]

[1]*Dept. of Physics of Complex Systems, Eötvös Loránd University, Pázmány P. sétány 1/A, Budapest, 1117, Hungary*
[2]*Konkoly Observatory, Research Centre for Astronomy and Earth Sciences, Hungarian Academy of Sciences, H-1121, Budapest, Konkoly Thege Miklós út 15-17, Hungary*

Abstract. The light variations of first-overtone RR Lyrae stars and contact eclipsing binaries can be difficult to distinguish. The Catalina Periodic Variable Star catalog contains several misclassified objects, despite the classification efforts by Drake et al. (2014). They used metallicity and surface gravity derived from spectroscopic data (from the SDSS database) to rule out binaries. Our aim is to further constrain the catalog using SDSS colours to estimate physical parameters for stars that did not have spectroscopic data.

1. Method and data

Briefly, Photo-Met estimates the unknown physical parameters of stars by interpolating the known parameters of other stars that have very similar broad-band colours. The method relies on two numerical algorithms:
- efficient k-nearest-neighbour finding in a four-dimensional metric colour-colour space and
- local linear regression.

As with any empirical parameter estimation algorithm, the reliability of the entire process depends much more on the training set than on the actual numerical method. For this study, we used an empirical training set based on SDSS PSF magnitudes of approximately 360 000 stars. The stellar parameters [Fe/H], $T_{\rm eff}$ and $\log g$ are the adopted weighted averages from SSPP (SEGUE Stellar Parameter Pipeline). For further details on the method see Kerekes et al. (2013).

The variable list of the Catalina Sky Survey consists of 5467 stars marked as RRc. The cross-match with the SDSS DR10 Cross-ID tool using an $1\farcs2$ radius search resulted in 2762 stars. For delivering new results we took the stars with photometric measurements only (1732 objects) and applied the Photo-Met method to estimate the surface gravity, the effective temperature and metallicity.

2. Constraining candidates

To distinguish between RRc and contact binary stars we applied two criteria:
- RRc stars are halo giants so they are generally expected to have lower metallicity ([Fe/H] < -1) and surface gravity ($\log g < 3.6$) than disk stars.
- Furthermore according to the work of Drake et al. (2014) the RRc stars are

concentrated between $0.24 < P < 0.42$ and $0.45 < M_{\rm test} < 0.55$ on the $M_{\rm test} - P$ plane, where $M_{\rm test}$ statistic values is a measure of the fraction of time that an object spends below the mean magnitude. We find 236 objects satisfied both, but 636 objects satisfied none of the criteria.

3. Conclusion

We could identify several contact binaries that were originally classified as RRc stars in the CSS Periodic Variable Star Catalog. The PHOTO-MET method, however, clearly placed them outside the RRc domain set by Drake et al. (2014). We plotted in Fig. 1 four light curves where the asymmetry of the minima can be clearly seen when folded with twice the assumed variation period. However, despite our success in finding new contaminating binary stars in the sample, the large errors in the $\log g$ and [Fe/H] determination (up to ± 1.0 dex) and the low quality of the light curves of faint stars make this method uncertain, leaving a lot of ambiguous objects in the catalog.

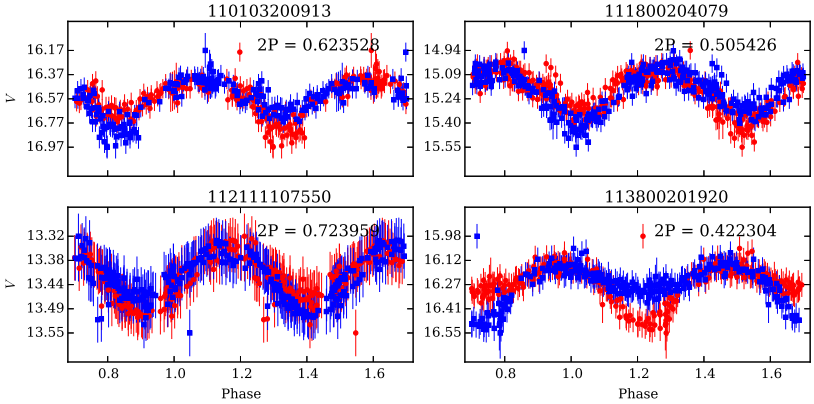

Figure 1. Folded light curves of newly identified eclipsing binaries in the CSS RRc sample. Blue and red points are shifted in phase by 0.5 with respect to each other to highlight the differing minima.

Acknowledgements

This project has been supported by the LP2014-17 Program of the Hungarian Academy of Sciences, the NKFIH K-115709 and the OTKA NN-114560 grants of the Hungarian National Research, Development and Innovation Office. L.M. was supported by the János Bolyai Research Scholarship of the Hungarian Academy of Sciences. The CSS survey is funded by the National Aeronautics and Space Administration under Grant No. NNG05GF22G issued through the Science Mission Directorate Near-Earth Objects Observations Program.

References

Drake, A. J., Graham, M. J., Djorgovski, S. G., et al. 2014, ApJS, 213:9
Kerekes, Gy., Csabai, I., Dobos, L., Trencséni, M. 2013, AN, 334, 9

RRL2015 – High-Precision Studies of RR Lyrae Stars
L. Szabados, R. Szabó, K. Kinemuchi (Eds.) 2016

Describing Blazhko light curves with almost periodic functions

József M. Benkő & Róbert Szabó

Konkoly Observatory, Research Centre for Astronomy and Earth Sciences, Hungarian Academy of Sciences, H-1121 Budapest, Konkoly Thege Miklós út 15-17, Hungary

Abstract. Recent results of photometric space missions such as *CoRoT* and *Kepler* showed that the cycle-to-cycle variations of the Blazhko modulation is very frequent. These variations have either multiperiodic or irregular (chaotic/stochastic) nature. We present a mathematical framework in which all of these variations can be handled. We applied the theory of band-limited almost periodic functions to the modulated RR Lyrae light curves. It yields several interesting results: e.g. the harmonics in the Fourier representation of these functions are not exact multiplets of the base frequency or the modulation function depends on the harmonics. Such phenomena are reported for observed RR Lyrae stars as well showing that the almost periodic functions are promising in the mathematical description of the Blazhko RR Lyrae light curves.

1. Introduction

The Blazhko effect is a periodic amplitude and phase variation in the light curve of RR Lyrae variable stars. It is usually interpreted as a modulation or a beating phenomenon. Benkő et al. (2011) showed that the simultaneous amplitude and frequency modulation could explain most of the observed light curve and Fourier features. The mathematical form of a general (non-sinusoidally) modulated function is given in that paper. Szeidl et al. (2012) showed, however, that this simple modulation picture does not fit well to the observed stars even if they have only one single sinusoidal modulation. Szeidl et al. (2012) suggested a more complicated modulation function which depends on the Fourier harmonics.

The Fourier harmonics are only mathematical representation when we describe non-sinusoidal light curves and have no direct physical meaning. How does the modulation of the star 'know' about the harmonics of the pulsation?

2. Almost periodic functions

$z(t)$ is an *almost periodic function*[1] with the translation number $\tilde{P}$ (which plays the role of the period) corresponding to ε, if

$$z(t) \approx z(t+\tilde{P}), \quad \text{or} \quad |z(t) - z(t+\tilde{P})| < \varepsilon, \tag{1}$$

[1]There are numerous non-equivalent definitions for almost periodic functions in the literature. Here we use a simple definition.

where

$$0 < \varepsilon \ll \|z\| = \sqrt{z^2} = \sqrt{\lim_{\tau\to\infty} \frac{1}{\tau} \int_{-\tau/2}^{\tau/2} z^2(t)dt}.$$

The almost periodic functions have numerous similar features to the periodic ones such as they form a complete orthogonal system, or their Fourier series uniquely determine them (Bohr 1947). Comparing the formulae of the general periodic signal modulated by a general external periodic signal presented by Benkő et al. (2011), the best fit expression for the observed light curves formulated by Szeidl et al. (2012), and the Fourier representation of almost periodic functions, we can conclude that both expressions represent almost periodic functions.

Due to the uniqueness of the almost periodic functions the empirical formula represents an externally modulated signal if and only if it can be transformed to the form of Benkő et al.'s one. According to the observations it is generally not possible. In other words, *the Blazhko effect is not an external modulation on the pulsation.*

An important difference between periodic and almost periodic functions is that the Fourier harmonics are not exactly harmonic, because the instantaneous frequency is $f_n(t) \neq nf_0(t)$, where f_0 means the fundamental mode frequency and n represents the order of Fourier harmonics. This feature might be a natural explanation of the found effect in the Fourier spectrum of V445 Lyr (see Fig. 4 in Guggenberger et al. 2012).

3. Conclusions

If the Blazhko effect was an independent physical modulation on the pulsation signal, the light curves would fit by simple modulation functions as it was done by Benkő et al. (2011). Since this is not possible, the Blazhko effect is an inherent feature of the pulsation. This fact supports the resonant pulsation explanations (e.g. Buchler & Kolláth 2011) of the Blazhko phenomenon. Strictly speaking the Blazhko stars' signal is not a modulated one but a more complicated signal that we can describe by almost periodic functions. The found systematic deviation from the exact harmonic values in the Fourier spectrum of V445 Lyr could be explained by the mathematical consequence of its almost periodic light curve.

Acknowledgement

This project has been supported by the Hungarian National Research, Development and Innovation Office – NKFIH K-115709.

References

Benkő, J. M., Szabó, R., Paparó, M. 2011, MNRAS, 417, 974
Bohr, H. 1947, Almost Periodic Functions, (New York: Chelsea)
Buchler, J. R., Kolláth, Z. 2011, ApJ, 731:24
Guggenberger, E., Kolenberg, K., Nemec, J. M., et al. 2012, MNRAS, 424, 649
Szeidl, B., Jurcsik, J., Sódor, Á., et al. 2012, MNRAS, 424, 3094

RRL2015 – High-Precision Studies of RR Lyrae Stars
L. Szabados, R. Szabó, K. Kinemuchi (Eds.) 2016

Near-field cosmology with RR Lyrae variable stars: A first view of substructure in the southern sky

S. Duffau[1,2], A. K. Vivas[3], C. Navarrete[2,1], M. Catelan[2,1], G. Hajdu[2,1], G. Torrealba[4], C. Cortés[5,1], V. Belokurov[4], S. Koposov[4], & A. J. Drake[6]

[1] *Millennium Institute of Astrophysics, Santiago, Chile*
[2] *Instituto de Astrofísica, Pontificia Universidad Católica de Chile, Santiago, Chile*
[3] *Cerro Tololo Inter-American Observatory, La Serena, Chile*
[4] *Institute of Astronomy, Cambridge CB3 0HA, UK*
[5] *Departamento de Física, Facultad de Ciencias Básicas, Universidad Metropolitana de Ciencias de la Educación, Santiago, Chile*
[6] *California Institute of Technology, Pasadena, CA 91225, USA*

Abstract. We present an update of a spectroscopic follow-up survey at low-resolution of a large number of RR Lyrae halo overdensity candidates found in the southern sky. The substructure candidates were identified in the RR Lyrae catalog of Torrealba et al. (2015) using Catalina Real-time Transient Survey (CRTS) data. Radial velocities and mean metallicities have been estimated for target stars in almost half of the original overdensities to assess their potential membership to coherent halo features.

Surveying the halo for substructure is important to identify the tidal remnants of accretion events that contributed to its formation. The northern sky has seen already a lot of progress towards this goal (see review by Belokurov 2013), but the south remains quite unexplored. The CRTS with the work by Torrealba et al. (2015, from now on T15) has identified 27 overdensity candidates using RR Lyrae (RRL) variables. We started a low-resolution spectroscopic survey ($R \sim 2000$) using primarily the Goodman spectrograph at SOAR and the LDSS3 at Magellan. We obtained spectra to measure radial velocities and mean metallicities for the most promising targets. Radial velocities are used in addition to positional information to search for stream-like features and metallicities for the stream candidate stars are measured to properly characterize the nature of the features found as real substructures.

We have covered so far 11 out of the 27 overdensities listed in T15. We have obtained more than one spectrum for at least 50% of our target RRL stars. Radial velocities for 123 stars have been measured so far using templates from Sesar (2012), and mean metallicities have been estimated using a modified version of the ΔS method developed by Layden (1994) for 99 of our targets. The typical errors in radial velocity and mean metallicity for the sample are $\sim$20 km/s and $\sim$0.2 dex, respectively.

Figure 1 displays the RRLs in the T15 catalog (gray dots) and those observed by us (diamonds or ovals) in each of the surveyed overdensities (shaded polygons), color-coded according to their mean heliocentric distance.

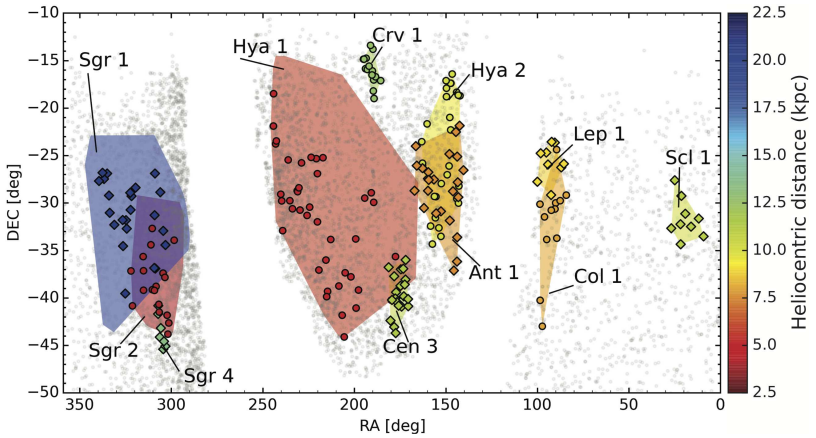

Figure 1. Spatial distribution of the overdensities targeted and the RR Lyrae stars observed within those. See text for more details.

Our most interesting preliminary results indicate that we have probably found the southern extension of the Virgo Stellar Stream velocity complex (Duffau et al. 2014) in Crv 1, while a bimodal radial velocity distribution in Hya 2 suggests there is indeed velocity substructure within the overdensity. Hya 1 is interesting as we have proper motion data available from the literature to combine with our radial velocities, and because in the same direction, albeit at a slightly larger heliocentric distance, a large overdensity has been identified by Casetti-Dinescu et al. (2015) as well. Ant 1 presents an extended radial velocity range with a narrow metallicity distribution, while Cen 3 has a velocity peak like the one expected for thick disk stars in the same direction of the sky. Combining our data with proper motions, information available from other tracers, models of the disruption of the Sagittarius dwarf and the smooth halo component of our Galaxy will allow us to say more about the nature and origin of these overdensities. In particular we will be able to explore the relation between the largest overdensity in T15, Sgr 1, and the tidal tails of the Sgr dwarf galaxy.

Acknowledgments

Support for this project is provided by CONICYT's PCI program through grant DPI 20140066; by the Ministry for the Economy, Development, and Tourism's Iniciativa Científica Milenio through grant IC 120009, awarded to the Millennium Institute of Astrophysics; by Proyecto Fondecyt Regular #1141141; and by Proyecto Basal PFB-06/2007. C.N. and G.H. gratefully acknowledge support from CONICYT-PCHA/Doctorado Nacional grants 2015-21151643 and 2014-63140099, respectively.

References

Belokurov, V. 2013, NewAR, 57, 3, 100
Casetti-Dinescu, D. I., Nusdeo, D. A., Girard, T. M., et al. 2015, ApJ, 810:L4
Duffau, S., Vivas, A. K., Zinn, R., et al. 2014, A&A, 566, A118
Layden, A. C. 1994, AJ, 108, 1016
Sesar, B. 2012, AJ, 144, 114
Torrealba, G., Catelan, M., Drake, A. J., et al. 2015, MNRAS, 446, 2251

RRL2015 – High-Precision Studies of RR Lyrae Stars
L. Szabados, R. Szabó, K. Kinemuchi (Eds.) 2016

Population synthesis of RR Lyrae stars in the original *Kepler* and *K2* fields of view

Ottó Hanyecz[1,2] & Róbert Szabó[1]

[1]*Konkoly Observatory, Research Centre for Astronomy and Earth Sciences, Hungarian Academy of Sciences, H-1121, Budapest, Konkoly Thege Miklós út 15-17, Hungary*
[2]*Eötvös Loránd University, Pázmány P. sétány 1/A, Budapest, 1117, Hungary*

Abstract. It is interesting to ask what fraction of the total available RR Lyrae (RRL) sample that falls in the *Kepler* and *K2* Fields of View (FoV) is known or discovered. In order to answer this question we compared the known RRL sample in the *Kepler* and *K2* fields with synthetic Galactic models. The Catalina Sky Survey RRL sample was used to calibrate our method. We found that a large number of faint RRL stars is missing from *Kepler* and *K2* fields.

1. Simulation of the original *Kepler* and *K2* FoVs

The original *Kepler* mission has been highly successful in providing unprecedented details of the light variation of RR Lyrae stars, as well as in discovering new dynamical phenomena in their pulsation. Almost each object shows unique and novel characteristics, therefore the total number of RR Lyrae stars in the *Kepler* and *K2* fields is of particular interest.

To estimate the expected number of RRL stars we used the TRILEGAL (Girardi et al. 2005) and BESANÇON models (Robin et al. 2003). To get a sense of the uncertainties of the simulated number of RRLs in the instability strip we shifted the original *Kepler* and *K2* FoVs by ± 0.5 degrees in R.A. and DEC directions. We used these standard deviations to check the changes of the simulated numbers of RRLs in slightly different fields.

In order to understand the completeness of the observed *Kepler* and *K2* RRL samples, we moved the original *Kepler* field along the same galactic latitude where the Catalina Sky Survey (CSS) made observations down to $19\overset{\mathrm{m}}{.}5$ (Drake et al. 2013).

Since CSS covered some of the *K2* fields (and discovered a large number of RRL stars), we can use these measurements to compare the simulations with much deeper observational results in the *K2* fields.

2. Results

In Fig. 1 we plot the apparent magnitude distribution of the previously known RRLs and the simulated RRLs from TRILEGAL and BESANÇON simulations for the original *Kepler* FoV and *K2* Campaign 5, respectively.

(1) We found good agreement between the simulated and observed RRL star numbers in a control field covered by CSS, which makes us confident that this method robustly estimates the number of RRL stars.

(2) We found 150 RRLs in the *Kepler* field in total and approximately the same amount in the *K2* fields from TRILEGAL simulations.

(3) We found good agreement between the TRILEGAL sample and the observed RRL stars by CSS between $16^{\rm m}$ and $20^{\rm m}$ in the *K2* fields.

(4) By accepting this calibration and using the predicted TRILEGAL and BESANÇON numbers as a proxy, we predict that approximately three times more RRL stars should lurk in the *Kepler* and *K2* fields, than presently known.

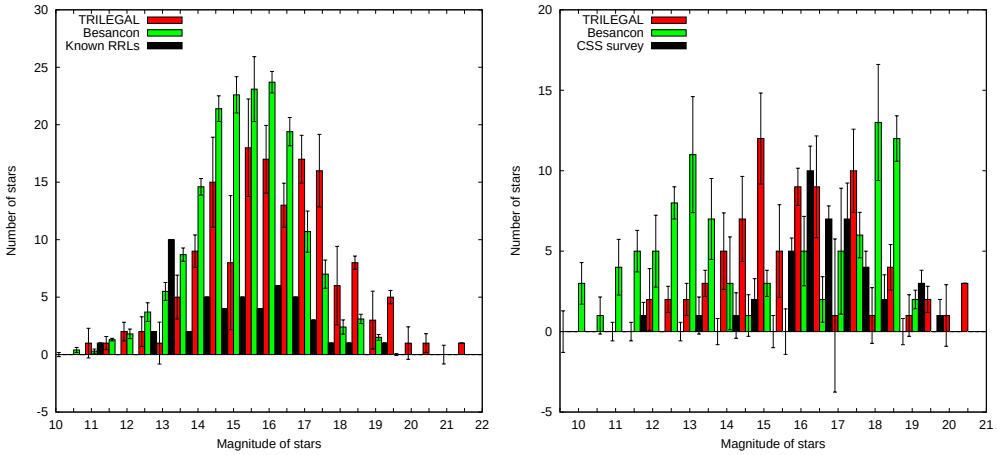

Figure 1. The apparent magnitude distribution of the simulated stars and the known RRL stars in the original *Kepler* FoV (left panel) and in *K2* Campaign 5 (right panel). The red and green boxes show simulated stars from TRILEGAL and BESANÇON, respectively. The black boxes show the 51 and 44 known RRLs in the *Kepler*, and in *K2* Campaign 5, respectively.

These results will help us to better understand the RRL samples of the *Kepler* fields, and motivate us to find the missing faint halo RRL population that could be used for Galactic structure studies.

Acknowledgements

This project has been supported by the NKFIH K-115709, the Lendület-2009 and LP2014-17 Young Researchers' Programs of the Hungarian Academy of Sciences, the ESA PECS Contract No. 4000110889/14/NL/NDe, and the European Community's Seventh Framework Programme (FP7/2007-2013) under grant agreements no. 269194 (IRSES/ASK) and no. 312844 (SPACEINN).

References

Drake, A. J., Catelan, M., Djorgovski, S. G., et al. 2013, ApJ, 763:32
Girardi, L., Groenewegen, M. A. T., Hatziminaoglou, E., et al. 2005, A&A, 436, 895
Robin, A. C., Reylé, C., Derrière, S., et al. 2003, A&A, 409, 523

RRL2015 – High-Precision Studies of RR Lyrae Stars
L. Szabados, R. Szabó, K. Kinemuchi (Eds.) 2016

Observing globular cluster RR Lyraes with the BYU West Mountain Observatory

Elizabeth J. Jeffery, Michael D. Joner, & Ryan S. Walton

Brigham Young University, Provo, UT, USA

Abstract. We have utilized the 0.9-meter telescope of the Brigham Young University West Mountain Observatory to secure data on six northern hemisphere globular clusters. Here we present observations of RR Lyrae stars located in these clusters. We compare light curves produced using both DAOPHOT and ISIS software packages. Light curve fitting is done with FITLC.

1. Introduction

Globular clusters (GCs) provide an important environment for studying RR Lyrae (RRL) variable stars. Our ability to maximize information in these data rests upon our ability to adequately measure photometry for the RRL cluster members. In these proceedings we present representative results of new observations of six northern hemisphere GCs, and compare light curves obtained using point-spread function (PSF) fitting photometry and image subtraction methods.

2. Observations and light curves

We have observed six northern GCs with the 0.9-meter telescope at the West Mountain Observatory (WMO). WMO is located approximately 72 km south of Salt Lake City, Utah, USA, and is owned and operated by Brigham Young University (BYU). The GCs we observed are: M3, M5, M13, M15, M92, and NGC 5466. Observations for five GCs (all but NGC 5466) were taken in the standard $UBVRI$ filter set during the 2012 observing season; NGC 5466 was observed in 2014 in BVR filters. For each cluster we have between 90 and 220 individual observations, resulting in well-sampled light curves.

We measured photometry to construct light curves using two different methods: PSF-fitting methods using DAOPHOT (Stetson 1987), and image subtraction methods employed by the ISIS software suite (Alard 2000). Because ISIS determines differential flux (not magnitude) values, we converted these to differential magnitude values using the method outlined in Székely et al. (2007). We then used FITLC (Sarajedini et al. 2009) to fit an RRL template to determine periods.

In Figure 1 we compare light curves determined from DAOPHOT and ISIS methods for four stars in M3: two are well-separated (V11 and V37) and two are in the crowded cluster core (V190 and V216). As can be seen in this figure, for uncrowded stars, DAOPHOT and ISIS provide comparable results. However, ISIS is more effective at measuring photometry in the crowded cluster core.

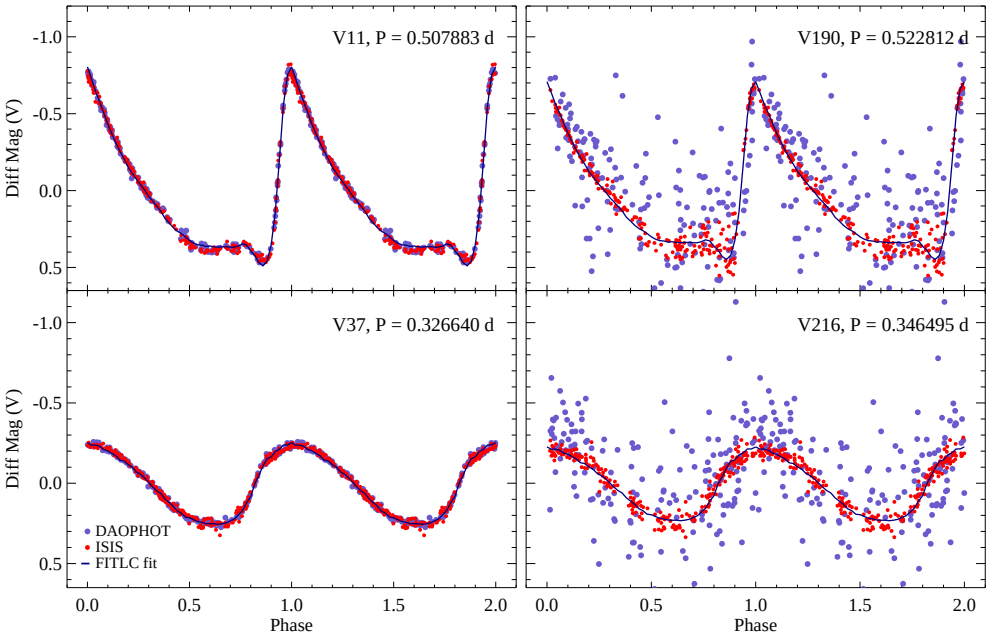

Figure 1. Light curves for four RRL stars in M3. Two stars (V11 and V37) are uncrowded, while two stars (V190 and V216) are in the cluster core. DAOPHOT and ISIS photometry are plotted for comparison, along with the best fit template and period, found by FITLC.

3. Summary

We have presented representative observations of GC RRLs with the WMO 0.9-m telescope. We have constructed light curves using both DAOPHOT PSF-fitting photometry methods, and image subtraction methods employed by the ISIS software package. For stars that are well-separated from other stars, DAOPHOT and ISIS provide comparable results. For stars in the crowded cluster core, the light curves from ISIS are superior. Such methods hold great promise for studying *all* RRL stars in GCs, including those in the crowded core.

Acknowledgments

We acknowledge continued support from the BYU College of Physical and Mathematical Sciences for operation of the West Mountain Observatory. Some of the observations included in this presentation were secured within the term of NSF grant AST-0618209. EJJ acknowledges the BYU Department of Physics and Astronomy and the American Astronomical Society for travel support.

References

Alard, C. 2000, A&AS, 144, 363
Sarajedini, A., Mancone, C. E., Lauer, T. R., et al. 2009, AJ, 138, 184
Stetson, P. B. 1987, PASP, 99, 191
Székely, P., Kiss, L. L., Jackson, R., et al. 2007, A&A, 463, 589

RRL2015 – High-Precision Studies of RR Lyrae Stars
L. Szabados, R. Szabó, K. Kinemuchi (Eds.) 2016

A preliminary study of the RR Lyrae stars observed in *K2* Campaign 3

Áron L. Juhász[1], László Molnár[2], & Emese Plachy[2]

[1]*Eötvös University, Budapest, Hungary*
[2]*Konkoly Observatory, Research Centre for Astronomy and Earth Sciences, Hungarian Academy of Sciences, H-1121, Budapest, Konkoly Thege Miklós út 15-17, Hungary*

Abstract. We have started a comprehensive analysis of the *Kepler K2* Field 3 data set. Our goals are to assess the statistics of the sample, and to search for peculiar stars. We found a candidate triple-mode RRab star, where the first and ninth overtones also seem to be excited.

1. The data sets of *K2* Field 3

The *Kepler K2* mission observed 79 fundamental and 1 first overtone RR Lyrae variables in Field 3 for 69.2 days. Our goals are to investigate the Blazhko periods and examine the properties and occurrences of the various additional modes.

The large number of stars in this sample gives us the opportunity to describe the abundance of each pulsation mode. To do this we need to investigate the reliability of the Field 3 data sets, especially the light curves of faint stars and stars close to the edge of the field of view. We summarize the first results in this paper.

At the release of *K2* Field 3 data, NASA published two kinds of automatically generated light curves for long cadence targets. The first type was created with single aperture photometry. The second type used the same aperture, but the light curves underwent an optimizing and noise reducing method (PDCSAP). In the first part of the investigation we used these latter data.

Within Field 3 there are many PDCSAP light curves which frequently contain large and sudden jumps. The most determinative parameter is the distance of the star from the center of the field of view. The movement of the star's photocenter position is only 0.2-0.3 pixel near the center, but this could be more than 2 pixels at the edge. Therefore in many cases the simple pixel photometry was impractical, because the PSF can move out from the mask or another star could contaminate it (especially in dense fields). This was the reason why we did our own photometry on the stars in many cases, occasionally using more than one aperture. Because of the large number of stars in this sample we hoped for finding some peculiar targets as well. Here we present one such case.

2. The possible FM-O1-O9 triple mode star EPIC 206280713

The Fourier spectrum of the PDCSAP light curve shows one peak slightly above $1.5f_0$. The original light curve does not show Blazhko modulation. We created our own tailor-made pixel photometry for the star with PyKE (Still & Barclay 2012), which suggests that this star is in fact a Blazhko star with a low-amplitude and long-period modulation.

The frequency spectrum of the light curve confirms the peak at $1.5f_0$ and clearly shows peaks on $0.5f_0$ and $2.5f_0$, the signs of period doubling. The most important discovery is the low-amplitude first overtone signal ($f_0/f_1 = 0.7370$; $P_0 = 0.48146$ day, $P_1 = 0.35486$ day) and its linear combinations with the fundamental mode. The frequency spectrum of EPIC 206280713 closely resembles that of RR Lyr itself, and provides another opportunity for comparison with triple-mode non-linear hydrodynamic model calculations (Molnár et al. 2012). These periods put the star in the same region in the Petersen diagram where the modulated double-mode stars are also located (Jurcsik et al. 2015; Smolec et al. 2015).

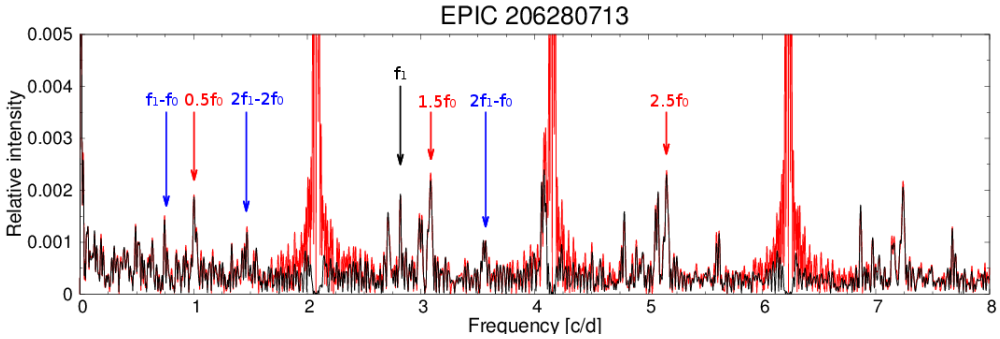

Figure 1. Fourier-spectrum of the tailor-made photometry. Black arrow: the possible first overtone. Red arrows: peaks at $0.5f_0$, $1.5f_0$, $2.5f_0$. Blue arrows: the linear combinations of f_0 and f_1.

Acknowledgements

This work has used *K2* data selected and proposed by the RR Lyrae and Cepheid Working Group of the Kepler Asteroseismic Science Consortium (proposal GO3040). This project has been supported by the Lendület-2009 and LP2014-17 Programs of the Hungarian Academy of Sciences, and by the NKFIH K-115709 and PD-116175 grants of the Hungarian National Research, Development and Innovation Office.

References

Jurcsik, J., Smitola, P., Hajdu, G., et al. 2015, ApJS, 219:25
Molnár, L., Kolláth, Z., Szabó, R., et al. 2012, ApJ, 757:L13
Smolec, R., Soszyński, I., Udalski, A., et al. 2015, MNRAS, 447, 3756
Still, M., Barclay, T. 2012, Astrophysics Source Code Library, ascl:1208.004

RRL2015 – High-Precision Studies of RR Lyrae Stars
L. Szabados, R. Szabó, K. Kinemuchi (Eds.) 2016

Ursa Minor dSph galaxy: Updated census of RR Lyrae stars

Karen Kinemuchi[1,2], Katie Grabowski[1,2], Charles Kuehn[3], & James Nemec[4]

[1] *Apache Point Observatory, Sunspot, NM, USA*
[2] *New Mexico State University, Las Cruces, NM, USA*
[3] *University of Northern Colorado, Greely, CO, USA*
[4] *Camosun College, Victoria, B.C., Canada*

Abstract. We present our observations and photometric results of the Ursa Minor dwarf spheroidal galaxy (UMi dSph). Observations were taken at the Apache Point Observatory 0.5 m ARCSAT telescope in 2014. We identify previously known RR Lyrae stars in the field of view, and also catalog other variable star candidates for which tentative classifications are provided. We have performed a period search for the known and new variable stars. Our ultimate goal is to create an updated catalog of variable stars in the UMi dSph and to compare the RR Lyrae stellar characteristics to other RR Lyrae stars found in Local Group dSph galaxies. The comparisons can give us insights to the near-field cosmology of the Local Group.

1. Introduction

The Ursa Minor dwarf spheroidal (UMi dSph) galaxy has been previously studied for variable star content (Nemec et al. 1988; Kholopov 1971; van Agt 1967), and we present a new, updated photometric survey. Previously, RR Lyrae (RRL) stars and anomalous Cepheids (AC) have been detected in this galaxy. The variable stars provide important information, such as distances and composition of the galaxy, which can lead to a better understanding of the near-field cosmology and formation of our own Galaxy. For this work, our primary goal is to update the number of known variable stars in UMi and confirm previous classifications.

2. Data acquisition and reduction

We collected data on June 2-8 and July 14-20, 2014, at the Astrophysical Research Consortium Small Aperture Telescope (ARCSAT) 0.5 m telescope[1] located at Apache Point Observatory (APO). We used the Survey Cam instrument with a field of view of $31.1' \times 31.1'$ and the Johnson $BVRI$ filters.

Standard data reduction techniques with IRAF were used, and for the photometry, the DAOPHOT packages (Stetson 1987, 1992, 1994) were run. The instrumental magnitudes were converted to the standard system using Landolt field SA 107 (Landolt 1992). In Figure 1, we present our color-magnitude diagram, which verifies that the horizontal branch has been reached, and thus there is a high likelihood of detecting RR Lyrae stars.

[1] http://www.apo.nmsu.edu/Telescopes/ARCSAT/index.html

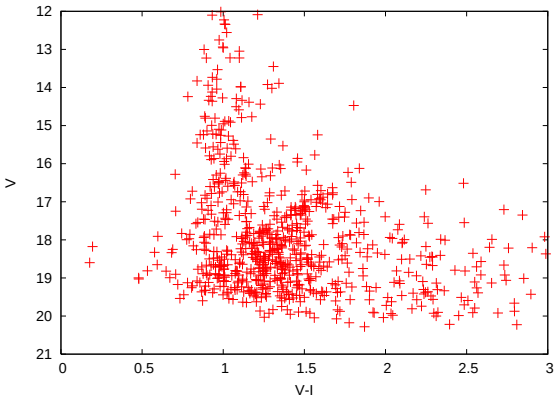

Figure 1. Color-magnitude diagram based on ARCSAT data collected in 2014.

3. Variable star census and results

We identified 166 variable stars from our observations of UMi dSph. Of these detections, we classified 50 RRab, 11 RRc, 2 AC stars and 2 possible eclipsing binaries in our field of view of UMi. Twenty-two RRab and 4 RRc stars from Nemec et al. (1988) were recovered.

For periods, we used our V-band data which consisted of up to 40 observations. We implemented period searching techniques of Supersmoother (Reimann 1994), Lomb-Scargle, Boxed Least Squares methods in VARTOOLS (Hartman 2012), and Period04 (Lenz & Breger 2005). Period aliasing is a major problem in clearly determining the periods due to the cadence of our observations, which produced gaps in the phased light curves. More epochs are needed to break the period aliases, but also to better classify the variable stars.

We determined distances to all the RRL stars, assuming reddening values of Schlafly & Finkbeiner (2011) and $M_V = 0.6$. Based on the RRLs, the distance to UMi dSph was found to be 76 ± 3 kpc. We also investigated the spatial distribution of the RRLs and found no conclusive clustering.

4. Future work

More observations are needed for our period analysis work, and to classify the UMi dSph variable stars. To this end, have obtained additional time at APO in 2016 to continue our photometric survey. We will additionally investigate the period and amplitude modulation of the RRLs once more epochs are on hand.

References

Hartman, J. 2012, Astrophysics Source Code Library, 1208.016
Kholopov, P. N. 1971, Peremennye Zvezdy, 18, 117
Landolt, A. U. 1992, AJ, 104, 340
Lenz, P., Breger, M. 2005, Communications in Asteroseismology, 146, 53
Nemec, J. M., Wehlau, A., Mendes de Oliveira, C. 1988, AJ, 96, 528
Reimann, J. D. 1994, PhD Thesis, University of California-Berkeley
Schlafly, E. F., Finkbeiner, D. P. 2011, ApJ, 737:103
Stetson, P. B. 1987, PASP, 99, 191
Stetson, P. B. 1992, Astronomical Data Analysis Software and Systems I, 25, 297
Stetson, P. B. 1994, PASP, 106, 250
van Agt, S. L. T. J. 1967, Bull. Astron. Inst. of the Netherlands, 19, 275

RRL2015 – High-Precision Studies of RR Lyrae Stars
L. Szabados, R. Szabó, K. Kinemuchi (Eds.) 2016

Database of candidates for RR Lyrae stars in binary systems – RRLyrBinCan

Jiří Liška[1] & Marek Skarka[1,2]

[1]*DTPA, Masaryk University, Brno, Czech Republic*
[2]*Konkoly Observatory, Research Centre for Astronomy and Earth Sciences, Hungarian Academy of Sciences, H-1121, Budapest, Konkoly Thege Miklós út 15-17, Hungary*

Abstract. A new on-line database with RR Lyrae stars bound in binary systems is presented. Its purpose is to give a quick overview about known and suspected RR Lyrae stars in binaries on the basis of available literature. The first released version of the catalogue contains information about 61 double-star candidates, their orbital periods, method of detection, comments and active links to published papers.

1. Introduction

Revealing RR Lyrae stars bound in binary systems is a highly complicated observing task. Since the 1960s several observing groups have tried to succeed. Many objects were marked as candidates for such systems. Unfortunately, only some of them were subsequently studied in detail to prove or disprove their observed behaviour. The rapidly growing number of candidates in the last years (e.g. Li & Qian 2014; Hajdu et al. 2015) has motivated us to prepare a catalogue for candidates of binary systems with an RR Lyrae component – *RRLyrBinCan*[1], which should help with identification of this astrophysically important class of binaries. The list together with the overview is a part of the paper Liska et al. (2015).

2. Structure of the data base

The list with known candidates of binaries, which is included in the main table, was created using the available literature. The table contains the official name of the object, its coordinates, the magnitude range (preferably in V-band), comments on the presence of the Blazhko effect, the type of the pulsator (RRab, RRc), the orbital period, methods which were used for detection, or study of the binarity, a reference with link to NASA ADS web page and, finally, comments. We also give a second table with stars which are blends or other disproved candidates for binarity.

3. Statistics of the candidates

Based on information in the actual version of the *RRLyrBinCan* database (25 September 2015) we give basic statistics. The main table contains 85 records

[1]The *RRLyrBinCan* database is available on a web page http://rrlyrbincan.physics.muni.cz/.

for 61 stars. From this sample 13 stars (21.3%) are confirmed Blazhko stars and 5 of them (8.2%) are suspected in modulation. The majority of stars are of RRab type (59 objects, 96.7%), and only 2 stars are of RRc type.

The listed objects are divided into several classes according to the detection methods/processes with abbreviations: LiTE – possible light-time effect, ED – eclipse(s) detection, RV – systematic shifts in radial velocities, COL – systematic colour discrepancy. The abbreviations with a letter "M" at the end of their mark (LiTEM, EDM, RVM) represent previous detection methods which were additionally used for calculation of orbital model of the binary and its parameters (not only the expected orbital period). It is evident from Fig. 1 that the detection of the LiTE is the most successful way to reveal binarity (48 systems, 78.7%). Orbital parameters of expected binaries of half the sample (28 objects, 45.9%) have not been determined. Binarity was revealed using two or more methods in several cases.

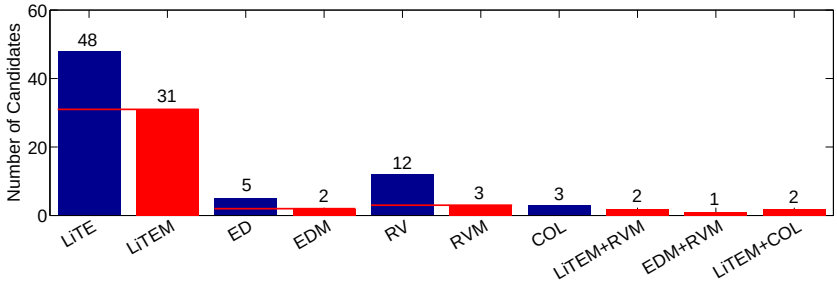

Figure 1. Distribution of candidates according to the detection methods (objects from red columns are included in corresponding blue columns).

4. Conclusions

We introduce the new database of candidates for RR Lyrae stars in binary systems. A short summary of the actual state of the list is presented. Extension of the list with other objects, e.g. from the catalogue of pulsating stars in binary systems (Zhou 2010) or stars from globular clusters, belongs to the future plans.

Acknowledgements

Authors are very grateful to J. Janík, M. Zejda, Z. Mikulášek, and F. Hroch. This research has made use of NASA's Astrophysics Data System and International Variable Star Index (VSX) by the AAVSO. This work has been supported by the grants MUNI/A/1110/2014 and LH14300.

References

Hajdu, G., Catelan, M., Jurcsik, J., et al. 2015, MNRAS, 449, L113
Li, L.-J., Qian, S.-B. 2014, MNRAS, 444, 600
Liska, J., Skarka, M., Zejda, M., Mikulasek, Z. 2015, arXiv:1504.05246
Zhou, A.-Y. 2010, arXiv:1002.2729

RRL2015 – High-Precision Studies of RR Lyrae Stars
L. Szabados, R. Szabó, K. Kinemuchi (Eds.) 2016

RR Lyrae stars in the SDSS Stripe 82 region: period-color and amplitude-color relations

Chow-Choong Ngeow[1], Shashi Kanbur[2], Anupam Bhardwaj[3], & Harinder Singh[3]

[1] *National Central University, Taiwan*
[2] *State University of New York at Oswego, NY, USA*
[3] *University of Delhi, India*

Abstract. Investigation of period-color (PC) and amplitude-color (AC) relations at the maximum and minimum light for RR Lyrae (RRL) stars can be used to probe the interaction of the hydrogen ionization front with photosphere at the atmosphere for this type of pulsating variables. For example, theoretical calculation indicated that such interaction would occur at the minimum light for RRL stars and caused a flat PC relation. In the past, the PC and AC relations have been investigated by using either the $(V-R)$ or $(V-I)$ colors. Here, we extend previous works to multi-bands by analyzing the RRL stars in SDSS (Sloan Digitized Sky Survey) Stripe 82 region, at which multi-epoch data are available for RRL stars located within the footprint of Stripe 82 region in *ugriz* bands. We present the PC and AC relations in four colors after correcting for extinction. We found that the structure of PC and AC relations for this sample of RRL stars is more complicated than a linear regression fit.

1. Data and method

We adopted the periods, extinction and *ugriz* band light curve data from Sesar et al. (2010, hereafter S10) that includes 379 RRab and 104 RRc stars. S10 also provided a set of template light curves in the *ugriz* bands. We fit the RR Lyrae light curve data with these template light curves to derive the g-band amplitude and extinction corrected colors at the g-band maximum and minimum light.

2. Preliminary results

Figure 1 compares the mean light PC relations with the simple relations based on synthetic RR Lyrae calculations presented in Cáceres & Catelan (2008) for two different metallicities. The slopes of the empirical relations (after combining RRab and RRc stars) agreed well with the simple synthetic relations: 0.851 vs. 0.827 ± 0.027 and 0.438 vs. 0.442 ± 0.014 for the $(g-r)_0$ and $(r-i)_0$ colors, respectively. The intercepts of the relations showed a good agreement in $(r-i)_0$ color, but displayed an offset in $(g-r)_0$ color. Note that dependence on metallicity in PC relation is smaller in the $(r-i)_0$ color than in the $(g-r)_0$.

For our preliminary PC and AC relations at maximum and minimum light, we found that the RRab stars only display a flat PC relation at minimum light in $(u-g)_0$ and marginally in $(i-z)_0$, a flat AC relation in all colors at the minimum

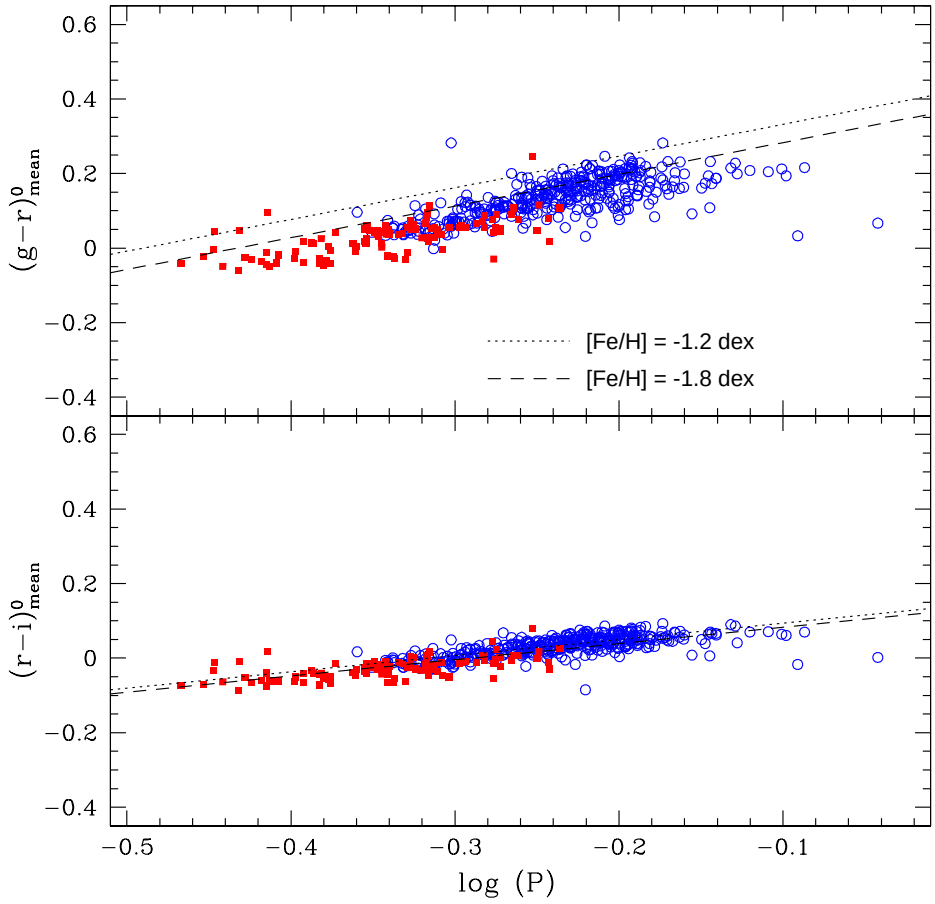

Figure 1. The *PC* relations at mean light for RR Lyrae stars in our sample, at which the mean magnitudes were derived from intensity means of the fitted template light curves. Blue empty circles are for RRab stars and red filled squares are the RRc stars (their pulsation period has been fundamentalized by the formula $\log P_{\rm RRab} = \log P_{\rm RRc} + 0.128$; Cáceres & Catelan 2008). The two lines are the simple relations given in Cáceres & Catelan (2008, their equations 8 & 9), assuming $\log Z = [{\rm Fe/H}] - 1.551$.

light and marginally in $(u-g)_0$ and $(i-z)_0$ colors at maximum light. Other *PC* and *AC* relations show a non-zero slope. The RRc stars display significant slopes in *PC* relation at both maximum and minimum light in all colors. Flat *AC* relations were also seen in $(u-g)_0$, $(r-i)_0$ and $(i-z)_0$ colors at maximum light for these stars, but not in the $(g-r)_0$ color.

References

Cáceres, C., Catelan, M. 2008, ApJS, 179, 242
Sesar, B., Ivezić, Ž., Grammer, S. H., et al. 2010, ApJ, 708, 717

RRL2015 – High-Precision Studies of RR Lyrae Stars
L. Szabados, R. Szabó, K. Kinemuchi (Eds.) 2016

Analysis of light curve of LP Camelopardalis

Zdeněk Prudil, Marek Skarka, & Miloslav Zejda

Department of Theoretical Physics and Astrophysics, Masaryk University, Brno, Czech Republic

Abstract. We present photometric analysis of the RRab type pulsating star LP Cam. The star was observed at Brno Observatory and Planetarium during nine nights. Measurements were calibrated to the Johnson photometric system. Four captured and thirteen previously published maxima timings allowed us to refine the pulsation period and the zero epoch. The light curve was Fourier decomposed to estimate physical parameters using empirical relations. Our results suggest that LP Cam is a common RR Lyrae star with high, almost solar metallicity.

1. Introduction

LP Cam was identified as a variable star by Strohmeier & Knigge (1961). Vidal-Sainz & Garcia-Melendo (2000) classified LP Cam as an RR Lyrae type variable, determined its light ephemeris and calibrated their observation to the standard photometric system. It received identifier NSV 01470. Further observations of LP Cam were rather sparse.

2. Observation

Observation of LP Cam took place at Brno Observatory and Planetarium. During nine nights more than 700 measurements were gathered. Dark frame, flat field corrections and differential aperture photometry were performed using MuniWin software (Motl 2011). UCAC4 763-030005 was used as a comparison star and UCAC4 763-029983, UCAC4 763-030022 served as check stars.

To calibrate measured data to the standard photometric system we observed the SA101 field (Landolt 1992). Conversion was done using the Conv2std.pl program[1]. The standard magnitudes of LP Cam were then estimated using the magnitudes of the comparison star from NOMAD 1 catalogue (Zacharias et al. 2004).

3. Results and conclusions

During our observation we captured brightness maxima four times. The moments of maxima were estimated using fitting with polynomials of third and

[1] http://var2.astro.cz/download.php

fourth order. Our maxima times together with those available in GEOS database[2] allowed us to improve the light ephemeris of LP Cam.

To obtain physical parameters of LP Cam we decomposed its light curve with a sum of trigonometric polynomial functions in CEPHEUS software (Barnacka 2008). Subsequently we gained Fourier coefficients. Using relations from Jurcsik & Kovacs (1996), Jurcsik (1998), and Castellani et al. (1991) we got physical parameters of LP Cam. The distance and the radius of LP Cam were estimated using the Pogson equation and the Stefan–Boltzmann law.

Metallicity value is in good agreement with our expectations. LP Cam lies close to the Galactic plane in a place rich in heavy elements. Because absolute magnitude depends linearly on metallicity (higher metallicity → lower luminosity), LP Cam is less luminous than RR Lyraes with lower metallicity.

Table 1. Physical parameters and light ephemeris obtained from measured data.

P [day]	0.5720232(3)
M_0 [JD]	2454906.509(1)
[Fe/H]	−0.01(6)
M_V [mag]	1.17(5)
T_{eff} [K]	6800(100)
M [$M_\odot$]	0.47(2)
L [$L_\odot$]	29(1)
R [$R_\odot$]	3.9(2)
r [pc]	435(11)

References

Barnacka, A. 2008, *Analiza danych fotometrycznych z przegladow "Pi of the sky" i ASAS*, Master's thesis, Krakow
Castellani, V., Chieffi, A., Pulone, L. 1991, ApJS, 76, 911
Jurcsik, J. 1998, A&A, 333, 571
Jurcsik, J., Kovacs, G. 1996, A&A, 312, 111
Landolt, A. U. 1992, AJ, 104, 340
Le Borgne, J. F., Paschke, A., Vandenbroere, J., et al. 2007, A&A, 476, 307
Motl, D. 2011, MUNIWIN, [Online]. *http://c-munipack.sourceforge.net*
Strohmeier, W., Knigge, R. 1961, Veröffentlichungen der Remeis-Sternwarte Bamberg, 5, 10
Vidal-Sainz, J., Garcia-Melendo, E. 2000, IBVS, 4903, 1
Zacharias, N., Monet, D. G., Levine, S. E., et al. 2004, Bulletin of the American Astronomical Society, 36, 1418

[2]Groupe Européen d'Observations Stellaires, Le Borgne et al. (2007).

RRL2015 – High-Precision Studies of RR Lyrae Stars
L. Szabados, R. Szabó, K. Kinemuchi (Eds.) 2016

Light-curve changes over the Blazhko cycle in RR Lyrae stars

Radosław Smolec[1] & Karolina Bąkowska[1,2]

[1]*Nicolaus Copernicus Astronomical Center, PAS, Warsaw, Poland*
[2]*Fulbright Visiting Scholar, The Ohio State University, OH, USA*

Abstract. We present the on-line gallery of animations illustrating light-curve changes over the Blazhko cycle in RR Lyrae stars.

In an ongoing project we search for the Blazhko effect in fundamental mode RR Lyrae stars (RRab) and analyse its properties. We use the data from the fourth phase of the Optical Gravitational Lensing Experiment (OGLE, Udalski et al. 2015) for the Galactic bulge RR Lyrae stars (Soszyński et al. 2014). Full results of our survey will be presented elsewhere. Here we focus on the light-curve variation over the modulation cycle, which we study with the help of the Fourier decomposition parameters and animations. We first select the stars which show a fairly regular Blazhko cycle and have good coverage of all phases of the modulation[1]. Our analysis is a standard consecutive prewhitening technique, which allows one to find pulsation period, P_0, and modulation period, $P_{\rm B}$, the latter from the separation of multiplet components (Fourier representation of the modulation). We determine some basic properties of the modulation, like parameters characterizing the triplet asymmetry, $R = A_+/A_-$ and $Q = (A_+ - A_-)/(A_+ + A_-)$, where A_+ and A_- refer to the amplitude of the higher and lower frequency triplet components, respectively (see e.g., Guggenberger et al. 2012). These parameters may be calculated at each harmonic order; here we provide their values only for the triplet at the fundamental mode frequency.

Animations are done in the following way. First, we fold the OGLE data with the modulation period. The resulting modulation curve is divided into 40 phase bins, each 0.05-wide (with 0.025 overlap). For each bin, data are folded with the pulsation period and fitted with the Fourier series. The low-order decomposition parameters, R_{21}, R_{31}, φ_{21} and φ_{31}, are calculated. These data form a base for a single frame of the animation. The on-line gallery may be found at the following URL: `http://users.camk.edu.pl/smolec/blazhko/`.

The page starts with a table of the form illustrated in Table 1, with basic data about the stars. Each animation consists of two panels. In the left panel the light curve folded on the pulsation period and its change over the modulation cycle are displayed. The blue curve is a Fourier fit to the extracted fundamental mode light curve, i.e. light curve with all the multiplet components filtered out. Note it is not the same as Fourier fit to the mean light curve (all data folded on the pulsation period). For the right panel one can choose among several options,

[1]It is not easy task. Additional very low amplitude modulation or periodicities may be present in the discussed stars. See 'remarks' column in Table 1. These signals will be discussed elsewhere.

each showing the Fourier parameter variation in different planes, e.g. R_{21}-A_1, φ_{21}-A_1, R_{21}-φ_{21}, etc. The open diamond corresponds to the Fourier parameters of the mean light curve, while filled diamond corresponds to Fourier parameters of the extracted light curve (modulation filtered out). A snapshot from one of the animations is illustrated in Fig. 1.

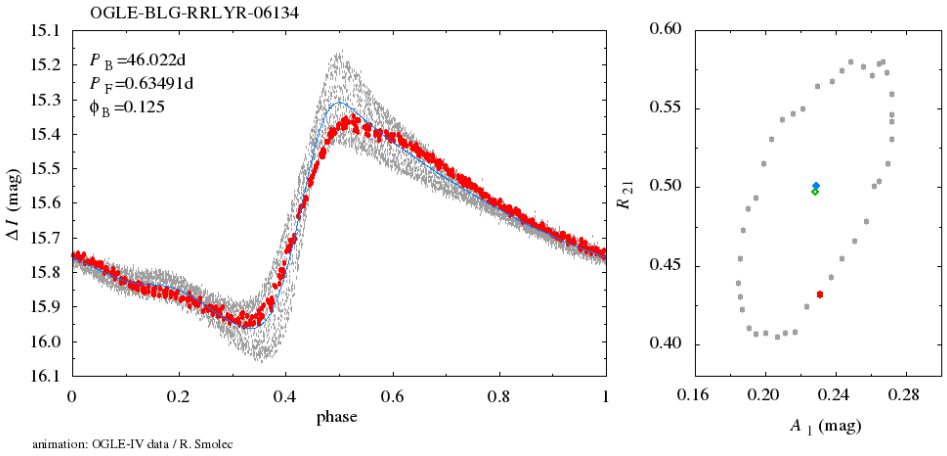

Figure 1. A snapshot from one of the animations, illustrating light-curve changes over the Blazhko cycle.

Table 1. Basic data for analysed stars: star's ID, pulsation and modulation periods, pulsation and modulation amplitudes, A_1 and $\max(A_+, A_-)/A_1$, asymmetry parameters, R and Q, and remarks ('1O' – first overtone detected, 'mod' – other periodicity detected, 'HIF' – periodicity close to half-integer frequency detected, 'BL+' – additional low-amplitude modulation detected). The full table is available on-line.

ID	P_0 (d)	P_B (d)	A_1 (mag)	A_m/A_1	R	Q	remarks
OGLE-BLG-RRLYR-06134	0.634907	46.02	0.229	0.135	0.57	−0.27	
OGLE-BLG-RRLYR-07576	0.618626	121.77	0.127	0.160	2.82	0.48	
OGLE-BLG-RRLYR-09450	0.483470	78.16	0.243	0.154	0.94	−0.03	1O, HIF
...							

We observe a diversity in the light curve changes over the Blazhko cycle. Fourier parameters follow the diverse loop patterns. Detailed analysis and conclusions will be presented elsewhere.

Acknowledgements

The project was supported by the Polish National Science Center grants awarded by decisions DEC-2012/05/B/ST9/03932 (RS) and DEC-2012/07/N/ST9/04172 (KB).

References

Guggenberger, E., Kolenberg, K., Nemec, J. M., et al. 2012, MNRAS, 424, 649
Soszyński, I., Udalski, A., Szymański, M. K., et al. 2014, Acta Astron., 64, 177
Udalski, A., Szymański, M. K., Szymański, G. 2015, Acta Astron., 65, 1

Author Index

Object Index

Bold type numbers mean that the given object is also mentioned on the following page(s) of the same paper.

STARS

STELLAR SYSTEMS